Paleontological Research

Vol. 6 No. 1 April 2002

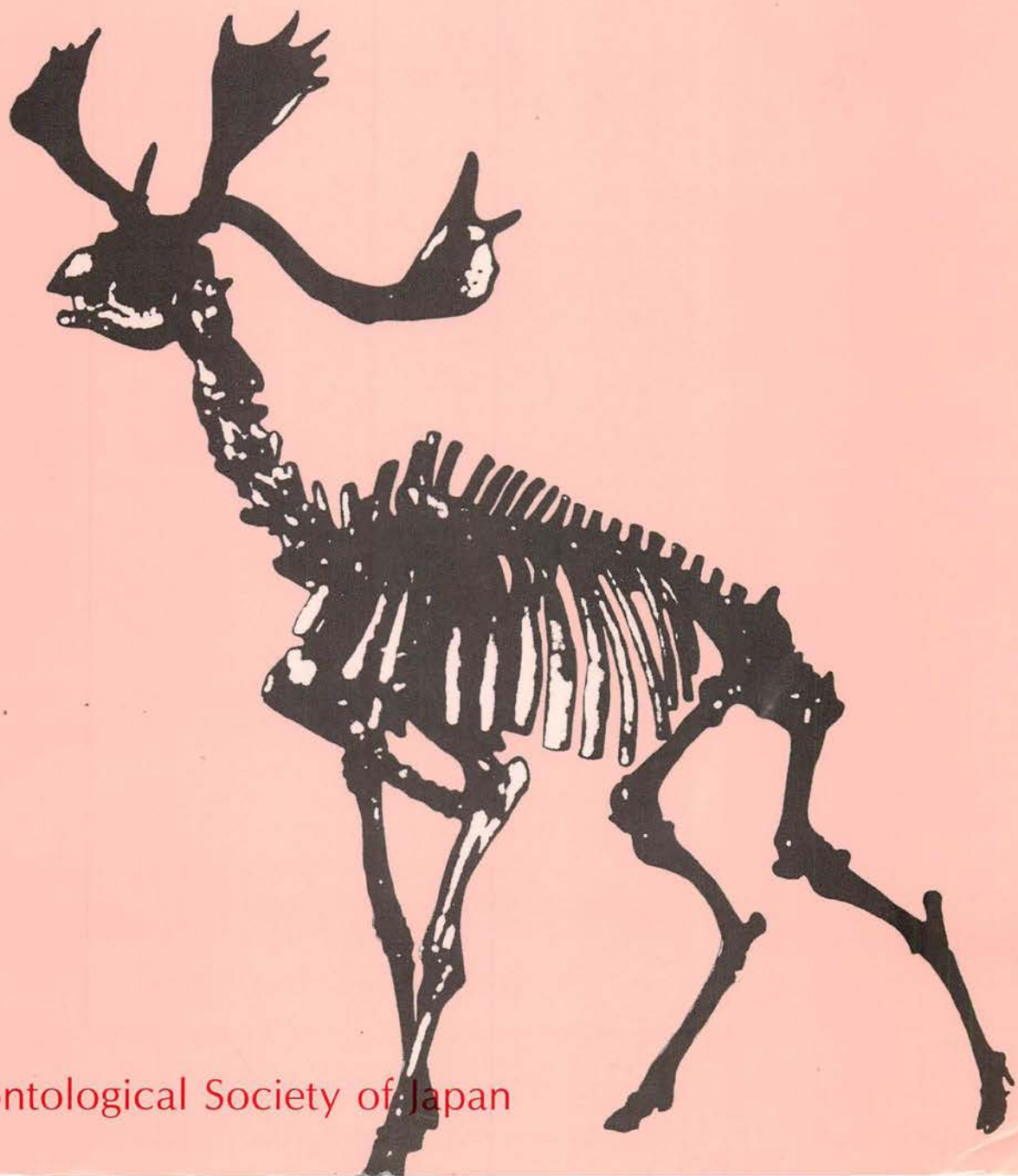

The Palaeontological Society of Japan

Cover: Typical Pleistocene fossils from the Japanese Islands. Front cover: *Sinomegaceros yabei* (Shikama). Back cover: *Paliurus nipponicum* Miki, *Mizuhopecten tokyoensis* (Tokunaga), *Neodenticula seminae* (Simonsen and Kanaya) Akiba and Yanagisawa and *Emiliania huxleyi* (Lohmann) Hay and Mohler.

All communication relating to this journal should be addressed to the
PALAEONTOLOGICAL SOCIETY OF JAPAN
c/o Business Center for Academic Societies,
Honkomagome 5-16-9, Bunkyo-ku, Tokyo 113-8622, Japan
Visit our society website at
http://ammo.kueps.kyoto-u.ac.jp/palaeont/

Paleontological Research, vol. 6, no. 1, pp. 1-22, April 30, 2002

Middle Miocene ostracods from the Fujina Formation, Shimane Prefecture, Southwest Japan and their paleoenvironmental significance

GENGO TANAKA[1], KOJI SETO[2], TAKAO MUKUDA[3] AND YUSUKE NAKANO[4]

[1]*Graduate School of Science and Engineering, Shizuoka University, Shizuoka, 422-8529, Japan*

[2]*Department of Geoscience, Shimane University, Matsue, 690-8504, Japan (e-mail: seto@riko.shimane-u.ac.jp)*

[3]*Graduate School of Integrated Arts and Sciences, Hiroshima University, Higashi-Hiroshima, 739-8521, Japan (e-mail: takaom@hiroshima-u.ac.jp)*

[4]*Okehazama 4-59-226, Arimatsu-cho, Midoriku, Nagoya, 458-0911, Japan (e-mail: y-nakano@chikyumaru.co.jp)*

Received 16 August 2001; Revised manuscript accepted 8 November 2001

Abstract. Thirty-five ostracod species belonging to 18 genera are recognized from the Middle Miocene Fujina Formation (ca. 14-12 Ma), 3 km southwest of Matsue City, Shimane Prefecture, Japan. Most of these species are part of the recent Japan Sea proper water fauna; they are also classified into 4 categories, circumpolar, cryophilic, endemic cool-temperate and temperate species. These ostracod assemblages indicate that the Fujina Formation was deposited under a cold-water environment. Ten new species, *Ambtonia shimanensis*, *A. takayasui*, *Acanthocythereis fujinaensis*, *A. izumoensis*, *Cluthia tamayuensis*, *C. subjaponica*, *Kotoracythere tsukagoshii*, *Laperousecythere ikeyai*, *Palmoconcha irizukii*, and *Robertsonites yatsukanus* are described.

Key words: Fujina Formation, Japan Sea proper water, Middle Miocene, ostracods, paleoenvironment

Introduction

The Japan Sea developed as a result of back-arc spreading prior to 16 Ma and then further expanded by clockwise rotation of the southwestern part of the Japanese islands beginning 15 Ma (Otofuji and Matsuda, 1984). During this short period (ca. 16.5-15 Ma), a tropical to subtropical molluscan fauna, called the Kadonosawa Fauna, spread widely around the Japanese islands. At about 15 Ma, this Kadonosawa fauna was replaced by a cool to temperate molluscan fauna, the Shiobara-Yama type fauna in the Japan Sea region (Chinzei, 1986). According to Chinzei (1986), this drastic faunal change in molluscs was caused by the closure of the Tsushima Straits in the western portion of the Japan Sea. Based on studies of molluscan assemblages in the Middle Miocene of the San'in district along the Japan Sea, the shallow embayment facies (the Shiobara Fauna) appeared after the Omori period (ca. 14.5-15 Ma). During the Fujina period (ca. 14-12 Ma), the molluscan assemblages were accompanied by an offshore facies (the Yama Fauna) and an increase in colder species of the Shiobara Fauna (Takayasu *et al.*, 1992). Thus, it is thought that the Fujina Formation was deposited under a cold-water environment which resulted from the closure of the Tsushima Straits. However, the presence of warm-water cephalopod species (*Aturia* sp. and *Argonauta tokunagai*) in several horizons may suggest the influence of a warm-water current (Sakumoto *et al.*, 1996).

Because benthic ostracods do not have a pelagic life stage, they can be easily isolated by environmental barriers. Although Miocene ostracod assemblages in Japan have been reported from several localities (Ishizaki, 1963, 1966; Yajima, 1988, 1992; Irizuki, 1994; Irizuki and Matsubara, 1994, 1995; Ishizaki *et al.*, 1996; Irizuki *et al.*, 1998), the one report from the marine sediments in the southwest of Japan only covered the early Middle Miocene Bihoku Group (Yajima, 1988). To describe the ostracod assemblages in the Fujina Formation, therefore, it is very important to consider marine paleoenvironments of the Japan Sea coast and to examine their paleoenvironmental significance.

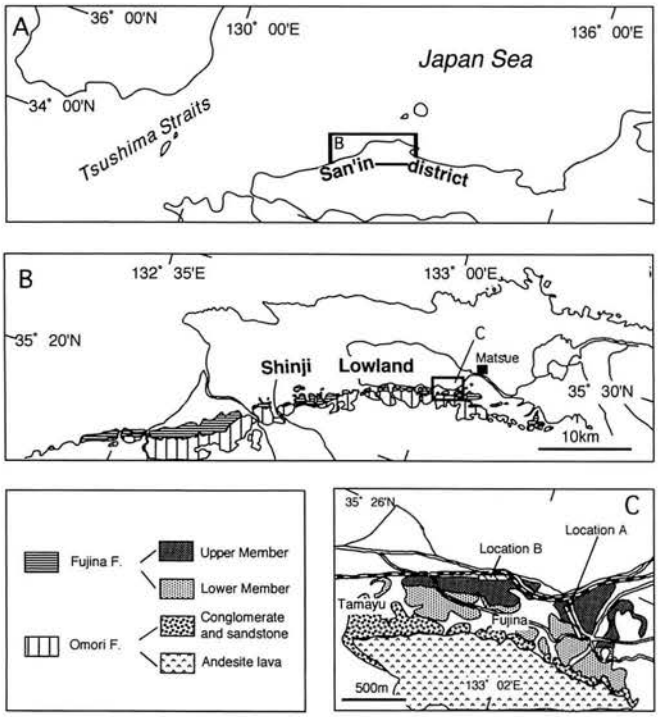

Figure 1. Map of the study area.

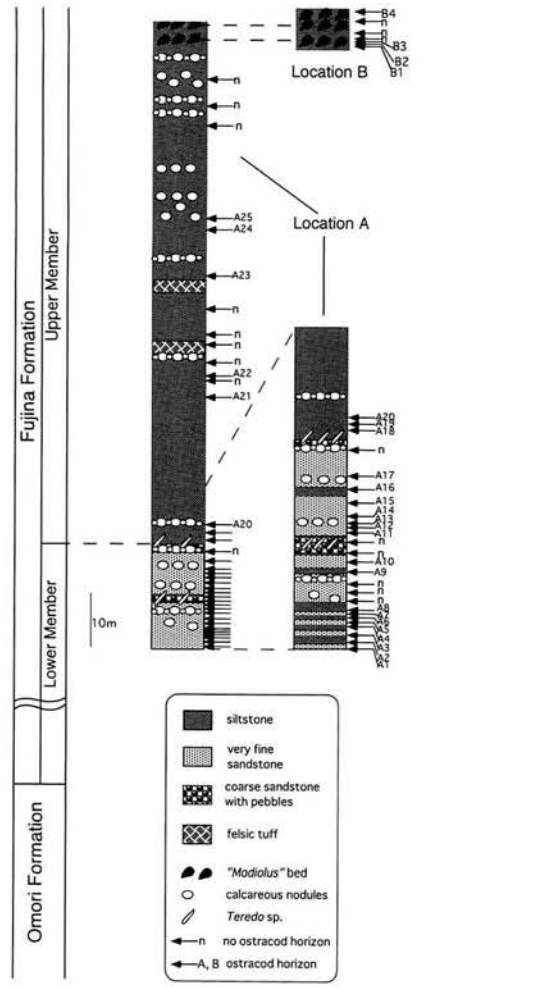

Figure 2. Columnar sections of the Fujina Formation.

Geological setting of Fujina Formation

The Fujina Formation was named by Tomita and Sakai (1937), then redefined by Ogasawara and Nomura (1980) and Takayasu and Nakamura (1984). This formation covers over 50 km, striking approximately EW to NE-SW and dipping about 10°N along the southern part of the Shinji Lowland (Figure 1). It is about 500 m in maximum thickness and conformably overlies the Omori Formation, which is composed of andesite lava in the lower part and shallow marine andesitic conglomerate and sandstone in the upper part (Kano *et al.*, 1994). The Fujina Formation near the type locality (this study area) is divided into the Lower and Upper Members by lithology. The Lower Member is composed of alternating layers of massive, gray, very fine-grained sandstone (0.5–5 m in thickness) containing calcareous nodules, and massive, dark gray siltstone (0.5–1 m in thickness). The sediments of the uppermost part of this member are made of a medium-grained sandstone (0.5 m in thickness) containing pebbles. The Upper Member is mainly composed of a massive, dark gray siltstone which is intercalated with felsic tuff layers (2 m in thickness), calcareous nodule beds, and "*Modiolus*" beds (0.3 m in thickness) in the uppermost part. Many marine molluscs, vertebrates (e.g., *Desmostylus japonicus* and *Carcharodon megalodon*) and decapods occur in all of the Fujina Formation (Kano *et al.*, 1994). Based on the planktonic foraminifers, the Upper Member of the Fujina Formation is assigned to N.10–11 of Blow's zones (14.6/14.8–12.4 Ma) (Nomura and Maiya, 1984).

Materials and methods

Fossiliferous sediment samples used in this study were collected from the upper part of the Lower Member to the Upper Member of the Fujina Formation at two locations (Figure 2). Each of the dried sediment samples (80 g) of a total of 46 collected were disaggregated, making use of naphtha for rock maceration (Maiya and Inoue, 1973), washing through a 235 mesh (63 μ m) sieve, and drying again. This procedure was repeated until the whole sediment sample was disintegrated. A fraction coarser than 120 mesh (125 μm) sieve was sieved and all the ostracod specimens present were picked.

		A1	A2	A3	A4	A5	A6	A7	A8	A9	A10	A11	A12	A13	A14	A15	A16	A17	A18	A19	A20	A21	A22	A23	A24	A25	B1	B2	B3	B4
	Ambtonia shimanensis sp. nov.											4				4	8		1		7									
++	*Ambtonia takayasui* sp. nov.							2				2								4										
--	*Acanthocythereis dunelmensis* (Norman, 1865)																						2	6	1	1	13	1	9	15
	Acanthocythereis fujinaensis sp. nov.								1			4		5																
	Acanthocythereis izumoensis sp. nov.											5			8	10	8			2										
++	*Acanthocythereis koreana* Huh and Whatley, 1997	11							1		2	38	2	2	16	57	29	31	39	11	30									
-	*Acanthocythereis tsurugasakensis* Tabuki, 1986																										8	5		1
	Acanthocythereis sp.1											2									2									
	Acanthocythereis sp.2																				4								2	
+	*Callistocythere japonica uranipponica* Hanai, 1957																1													
+	*Callistocythere kyongjuensis* Huh & Whatley, 1997															2														
	Cluthia subjaponica sp. nov.											1							3		1									
	Cluthia tamayuensis sp. nov.	3						1								2	7		1		1									
	Cluthia sp.																										3			
	Cytheropteron sp.															11											2			
++	*Falsobuntonia taiwanica* Malz, 1982																		2		2									
	Kotoracythere tatsunokuchiensis Ishizaki, 1966											1																		
++	*Kotoracythere tsukagoshii* sp. nov.	44		1	2	6	5	8	13		6	4		2	5	37	13	11	9	3	15									
	Krithe sp.1																		1											
	Krithe sp.2															2	1		2											1
	Laperousecythere ikeyai sp. nov.					2						23	9	5	7	26	1	3	3	11										
	Laperousecythere sp.																													3
	Loxoconcha subkotoraforma Ishizaki, 1966	1																												
	Loxoconchidea sp.								1			2							2											
--	*Munseyella hatatatensis* Ishizaki, 1966																												1	
+	*Paijenborchella* cf. *tsurugasakensis* Tabuki, 1986	62				1				1	1	20		2		21	14	31	39	3	19						4	5	5	7
--	*Palmenella limicola* (Norman, 1865)	1						1				1			2	3	1	1	2	1										
++	*Palmoconcha irizukii* sp. nov.	2										8			1	39	31	31	33	6	52						1			
	Robertsonites japonicus (Ishizaki, 1966)	7	1			2			2			6					2													
-	*Robertsonites reticuliformus* (Ishizaki, 1966)								3			3			2	12		7	1	7	3	1								
--	*Robertsonites* cf. *tuberculatus* (Sars, 1866)																													2
	Robertsonites yatsukanus sp. nov.																							1			18	1	5	
	Robertsonites sp.																							1				3		1
	Semicytherura sp.																	1												
	Urocythereis pohangensis Huh and Whatley, 1997	29										10	5	6	11	22	9	5	8	7	5			3						
	No. of specimens	160	1	1	2	11	5	12	21	1	9	134	16	22	52	248	125	121	146	55	141	1	2	11	1	1	49	15	22	30
	No. of species	9	1	1	1	4	1	4	5	1	3	16	3	6	8	14	14	9	15	10	12	1	1	4	1	1	7	5	5	7
	Weight of Sediments (g)	1520	80	80	80	960	880	1440	1680	80	800	1120	320	320	1040	1680	1440	1440	1120	1040	1040	80	80	240	80	80	2240	1440	1680	1760

Figure 3. List of ostracod species from the Fujina Formation (– –: circumpolar species; –: cryophilic species; +: endemic cool-temperate species; ++: temperate species).

Characteristic ostracods from Fujina Formation

Thirty-five species in 18 genera of ostracods were identified from 29 samples (25 samples from Location A and 4 samples from Location B); (Figure 3). Ostracods from the Fujina Formation can be divided into four different temperature-related categories: 1) circumpolar, 2) cryophilic, 3) endemic cool-temperate and 4) temperate species. Cronin and Ikeya (1987) recognized 26 circumpolar and 21 cryophilic species from several Plio-Pleistocene formations of Japan. They referred to ostracods known from Recent and/or Cenozoic deposits of the North Atlantic and adjacent arctic seas as "circumpolar species", and species that typically occur with circumpolar species in Japanese deposits (in most cases being members of high-latitude genera) as "cryophilic species". Irizuki (1994) selected 13 circumpolar, 9 cryophilic and 4 endemic cold-water species from the Late Miocene Fujikotogawa Formation, Akita Prefecture, northern Japan. Irizuki and Matsubara (1995) described 5 circumpolar and 8 cryophilic species from the early Middle Miocene Suenomatsuyama Formation, Iwate Prefecture, northeastern Japan. They pointed out that circumpolar and cryophilic species preferred living in colder water than other species even during the Miocene. They also recognized 13 temperate species that preferred warmer waters than those mentioned as circumpolar and cryophilic indicators. The following 4 categories concern their (paleo) biogeographic distributions in the northern hemisphere and the relative water temperatures during deposition of the Fujina Formation.

1. Circumpolar species (4 species)

These species were widely distributed from middle- to high-latitude regions in the Miocene (Figure 4; regions 1–10), and dominate the upper horizons of the Fujina Formation. *Acanthocythereis dunelmensis* (Norman), *Munseyella hatatatensis* Ishizaki, *Palmenella limicola* (Norman) and *Robertsonites tuberculatus* (Sars).

2. Cryophilic species (2 species)

Since the Miocene, these species have been distributed around the Japanese islands (Figure 4; regions 5 and 9), and are prominent in the upper horizons of the Fujina Formation with the circumpolar species. *Acanthocythereis tsurugasakensis* Tabuki and *Robertsonites reticuliformus*

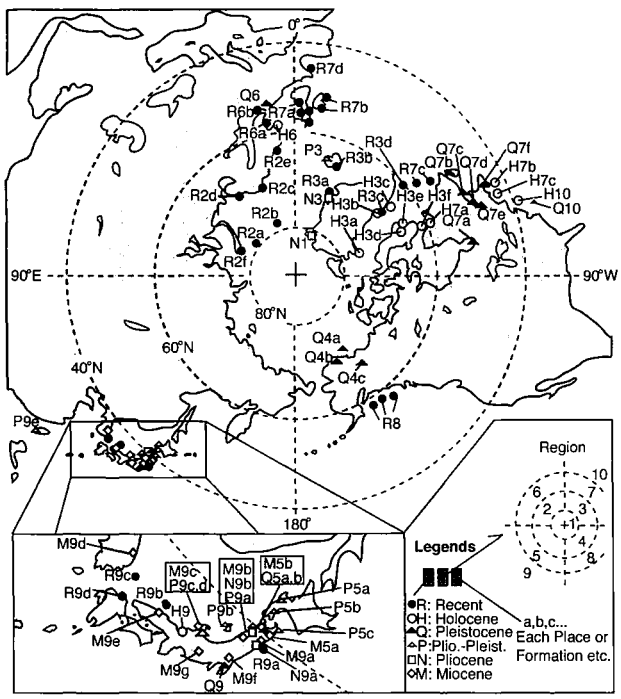

Figure 4. Geographic and stratigraphic distributions of characteristic species of the Fujina Formation. **R** [**2a–e**: Barents Sea (a-e: Elofson, 1941; b: Hartmann, 1992, 1993; c: Freiwald and Mostafawi, 1998); **2f**: Russian Harbour (Neale and Howe, 1975); **3a, b**: Greenland Sea (Elofson, 1941); **3c**: Baffin Bay (Elofson, 1941); **3d**: Labrador Sea (Hulings, 1967); **6a**: North Sea (Elofson, 1941; McKenzie *et al.*, 1989); **6b**: Baltic Sea (Elofson, 1941; Rosenfeld, 1977); **7a**: England (Elofson, 1941); **7b**: Ireland (Elofson, 1941); **7c**: Labrador Sea (Hulings, 1967); **7d**: Bay of Biscay (Caralp *et al.*, 1967; Caralp *et al.*, 1968); **8**: Gulf of Alaska (Brouwers, 1988, 1990); **9a**: Sendai Bay (Ikeya and Itoh, 1991); **9b**:off Shimane (Ikeya and Suzuki, 1992); **9c** : Ulleung Basin (Cheong *et al.*, 1986); **9d**: Fukuoka (Hanai, 1957a)]. **H** [**3a–c**:Baffin Bay (Neale and Howe, 1975); **3d–f** Baffin Island (Neale and Howe, 1975); **6**: Sandnes Clay (Lord, 1980); **7a**: Labrador Sea (Neale and Howe, 1975); **7b, c**: off Nova Scotia (Neale and Howe, 1975); **9**: Takahama shell bed (Kamiya and Nakagawa, 1993); **10**: off NewYork (Neale and Howe, 1975)]. **Q** [4a: Prudhoe Bay Boreholes (McDougall, Brouwers and Smith, 1986); **4b, c**: Gubik F. (Swain, 1961, 1963); **5a**: Wakimoto F. (Cronin and Ikeya, 1987); **5b**: Sasaoka F. (Cronin and Ikeya, 1987); **6**: Esbjerg deposit (Bassiouni, 1965); **7a**: Tyrrel Sea F. (Cronin, 1989); **7b, c**: East Goldthwait Sea F. (Cronin, 1989); **7d, e**: St. Lawrence Lowland (Cronin, 1981); **9**: Shimosa G. (Yajima, 1982; Yajima and Lord, 1990; Ozawa *et al.*, 1995); **10**: off NewYork (Neale and Howe, 1975)]. **P** [**3**: Tjornes Beds (Cronin, 1991); **5a**: Setana F. (Cronin and Ikeya, 1987); **5b**: Tomikawa F. (Cronin and Ikeya, 1987); **5c**: Daishaka F. (Tabuki, 1986); **9a**: Kitaura F. (Cronin and Ikeya, 1987); **9b**: Sawane F.(Cronin and Ikeya, 1987); **9c**: Junicho F. (Cronin and Ikeya, 1987); **9d**: Omma F. (Cronin and Ikeya, 1987; Kamiya *et al.*, 1996); **9e**: Ssukou F. (Malz, 1982)]. **N** [**1**: Kap Kobenhavn F. (Brouwers *et al.*, 1991; Penney, 1993); **3**: Lodin Elv F. (Penney, 1993); **9 a**: Tatsunokuchi F. (Ishizaki, 1966); **9b**: Tentokuji F. (Irizuki, 1996)]. **M** [**5a**: Kadonosawa F. (Irizuki and Matsubara, 1994); **5b**: Kamikoani F. (Yajima, 1988); **9a**: Hatatate F. (Ishizaki, 1966); **9b**: Fujikotogawa F. (Irizuki, 1994); **9c**: Togi Mud F. (Yajima, 1988); **9d**: Yeonil G. (Huh and Paik, 1992a,b; Huh and Whatley, 1997); **9e**: Fujina F. (This study); **9f**: Kobana F. (Irizuki *et al.*, 1998); **9g**: Shukunohora Sandstone (Yajima, 1988)].

(Ishizaki).

3. Endemic cool-temperate species (3 species)

These species are mainly distributed around the Japan Sea area from the Miocene to the Recent (Figure 4; regions 5 and 9), and occur throughout the Fujina Formation. *Callistocythere japonica uranipponica* Hanai, *C. kyongjuensis* Huh and Whatley and *Paijenborchella* cf. *tsurugasakensis* Tabuki. *C. japonica uranipponica* was recognized by Hanai (1957a) as a subspecies of *C. japonica*, and is restricted along the Japan Sea coast and the Pacific side of northern Japan after the Miocene. *C. kyongjuensis* was reported with some cold-water species in the Early Miocene Chunbuk Conglomerate Formation of Korea (Huh and Paik, 1992a,b). *P. tsurugasakensis* occurs in the Omma Formation (Late Pliocene to Early Pleistocene) with many warm- and a few cold-water species (Ozawa, 1996).

4. Temperate species (5 species, including 3 new species)

These have been distributed around the Japanese islands since the Miocene (Figure 4; regions 5 and 9), and dominate into the Lower Member to the lowermost part of the Upper Member of the Fujina Formation. *Acanthocythereis koreana* Huh and Whatley, *A. takayasui* Tanaka sp. nov., *Falsobuntonia taiwanica* Malz and *Kotoracythere tsukagoshii* Tanaka sp. nov. and *Palmoconcha irizukii* Tanaka sp. nov. *A. koreana* was first reported with cold-water species in the Early Miocene Chunbuk Conglomerate Formation of Korea (Huh and Paik, 1992a, b). *A. takayasui* has been reported in the Early Miocene from Mizunami, central Japan with some warm- and shallow-water species (as *F. taiwanica*; Yajima,1988, pl. 1, fig. 7), but this species occurred with some colder species in the Early Miocene of Korea (as *A. obai*; Huh and Paik, 1992a, pl. 2, fig. 14, and *F. taiwanica*; Huh and Paik, 1992b, pl. 2, fig. 14). *F. taiwanica*, *P. irizukii* and *K. tsukagoshii* occurs in horizons deposited under warm-water conditions of the Early-Middle Miocene Kadonosawa Formation, Iwate Prefecture, northeastern Japan (as *K.* sp.; Irizuki and Matsubara, 1994, pl. 1, fig. 3). *K. tsukagoshii* also occurs in the Omma Formation (Late Pliocene to Early Pleistocene) (as *Pectocythere quadrangulata*; Ozawa, 1996, pl. 8, fig. 2). Thus, it is probable that these temperate species adapted to colder environments during the Miocene in the Japan Sea area.

Discussion and conclusion

According to Ikeya and Cronin (1993), the Recent Japan Sea proper water is characterized by the ostracod species *A. dunelmensis*, *Elofsonella concinna*, *P. limicola*, *Robertsonites*, *Cluthia* and *Rabilimis*, and these species suggest cold-water isotherms along the upper slope at depths of

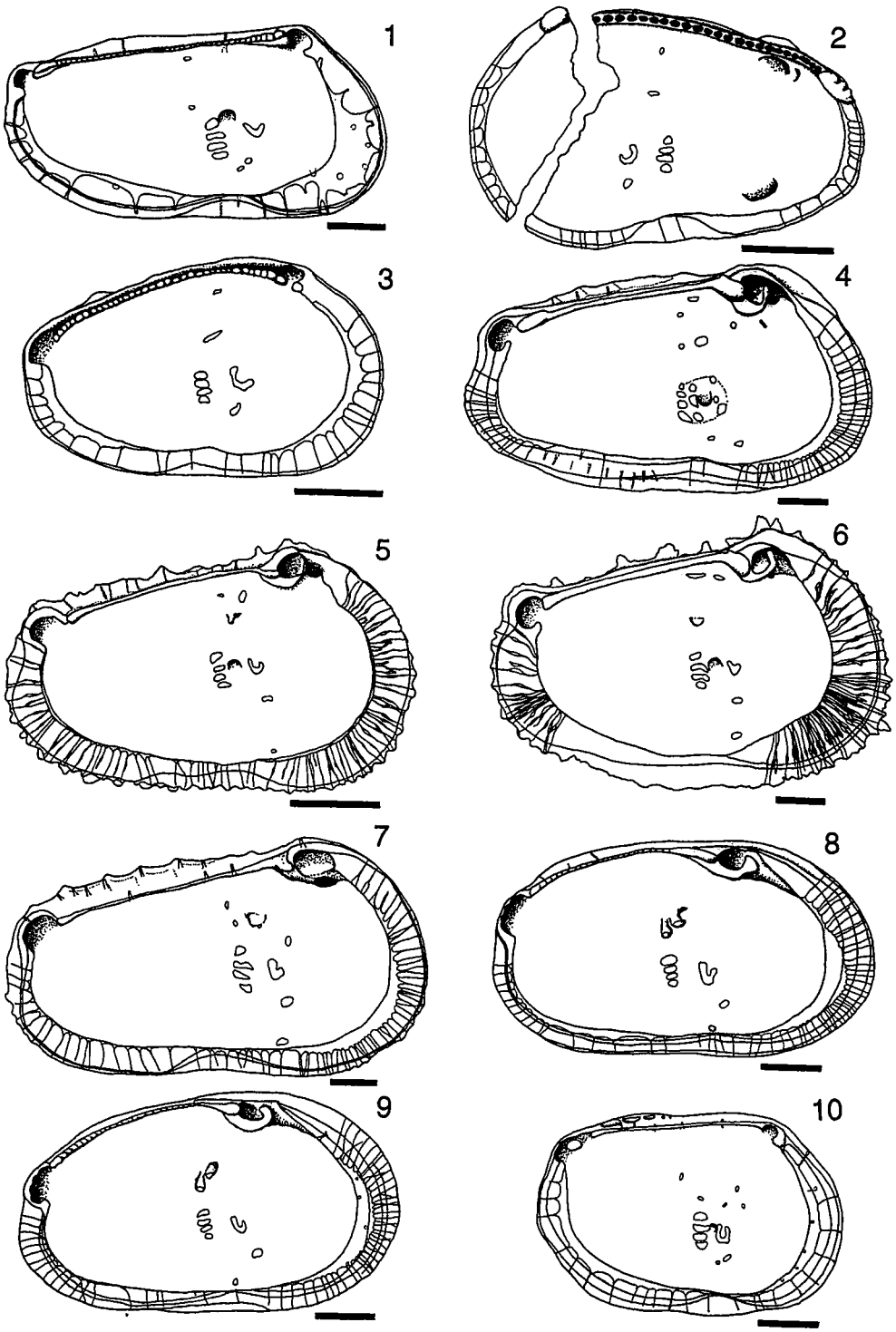

Figure 5. Internal views of each species. **1**: *Kotoracythere tsukagoshii* Tanaka sp. nov., female, LV, paratype, Loc. 1-A15, SUM-CO-1211; **2**: *Cluthia tamayuensis* Tanaka sp. nov., female, RV, paratype, Loc. 1-A1, SUM-CO-1217; **3**: *Cluthia subjaponica* Tanaka sp. nov., female, LV, paratype, Loc. 1-A15, SUM-CO-1220; **4**: *Laperousecythere ikeyai* Tanaka sp. nov., male, LV, paratype, Loc. 1-A11, SUM-CO-1229; **5**: *Acanthocythereis fujinaensis* Tanaka sp. nov.., female, LV, paratype, Loc. 1-A11, SUM-CO-1234; **6**: *Acanthocythereis izumoensis* Tanaka sp. nov., female, LV, paratype, Loc. 1-A17, SUM-CO-1239; **7**: *Robertsonites yatsukanus* Tanaka sp. nov., male, LV, paratype, Loc. 2-B1, SUM-CO-1249; **8**: *Ambtonia shimanensis* Tanaka sp. nov., LV, paratype, Loc. 1-A19, SUM-CO-1252; **9**: *Ambtonia takayasui* Tanaka sp. nov., female, LV, paratype, Loc. 1-A15, SUM-CO-1256; **10**: *Palmoconcha irizukii* Tanaka sp. nov., female, LV, paratype, Loc. 1-A15, SUM-CO-1261. Scale bar is 0.10 mm.

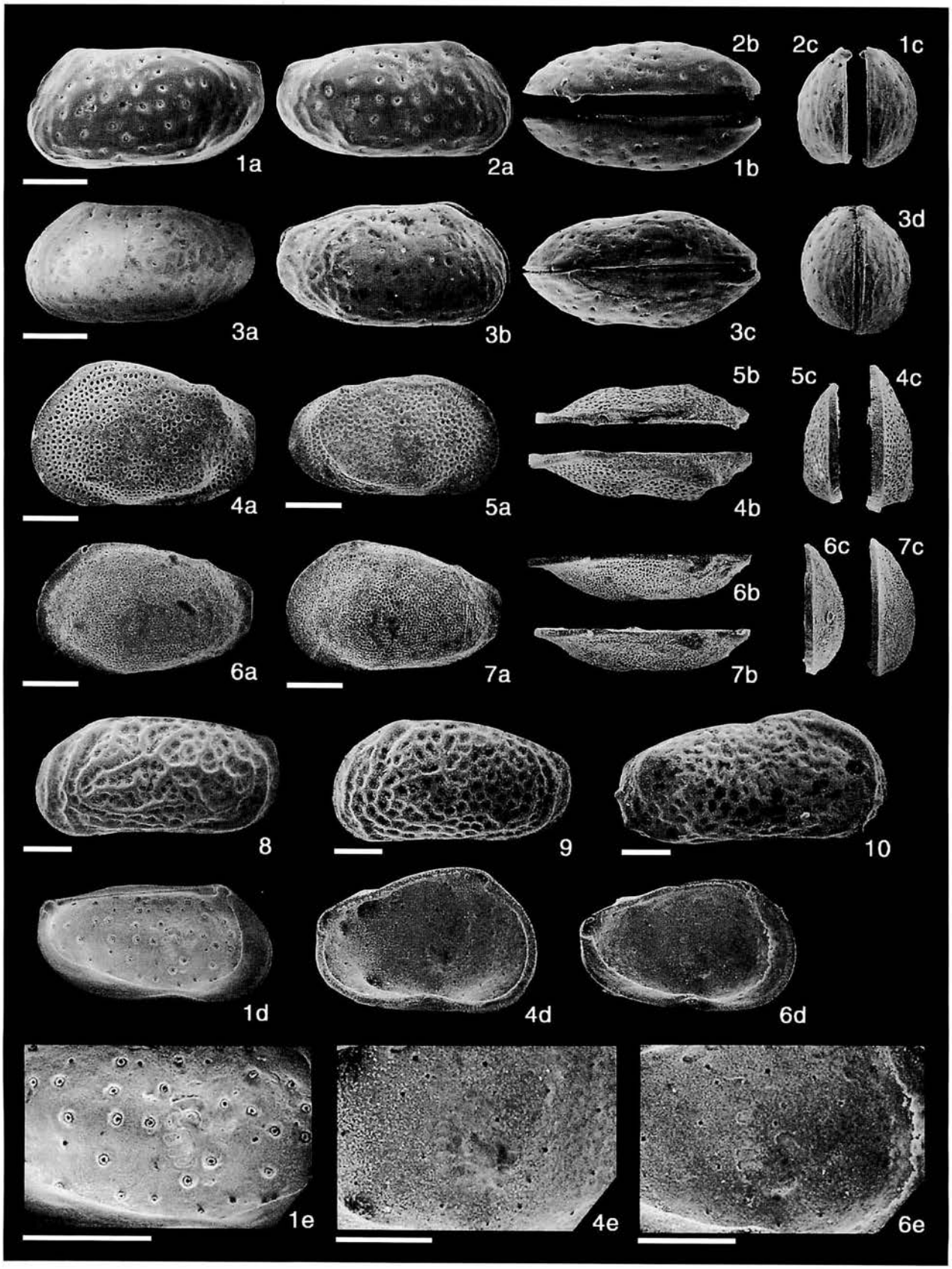
1a
2a
2b
1b
2c
1c
3a
3b
3c
3d
4a
5a
5b
4b
5c
4c
6a
7a
6b
7b
6c
7c
8
9
10
1d
4d
6d
1e
4e
6e

100–300 m. These assemblages resemble the Middle Miocene assemblage from the uppermost part of the Lower Member to the Upper Member of the Fujina Formation. Sakumoto *et al.* (1996) reported some cephalopod species that indicate that the paleo-Tsushima warm-water current flowed in the Proto-Japan Sea. Warmer conditions are indicated by the absence of cool-water ostracodes in part of this formation and the presence of prominent circumpolar and cryophilic species towards the upper horizons of the Fujina Formation, so we think that the Fujina Formation gradually became colder and colder towards the upper horizon, and that the warm-water current did not influence the benthic ostracods. Similar results have also been recognized from the benthic molluscan assemblages (Ogasawara and Nomura, 1980; Takayasu, 1986). Hence, it is concluded that during the early Middle Miocene period, temperate Pacific-side species invaded the coastal and offshore seafloor of the Japan Sea, and afterwards, with the change in marine climate and regional tectonic events, some taxa became isolated in embayments and offshore areas and adapted to cooler conditions.

Systematic descriptions

(by G. Tanaka)

All the illustrated specimens are deposited in the collections of the Shizuoka University Museum (SUM-CO-Number). Type locality of all new species is indicated by the index number: Loc. 1 or 2-horizon number; (Loc. 1: 35° 25.5′N, 133° 02.3′E; Loc. 2: 35° 25.6′N, 133° 01.4′E). Morphological terms follow the usage of Hanai (1961), Scott (1961) and Athersuch *et al.* (1989). The following abbreviations are used in this paper: C, carapace; RV, right valve; LV, left valve; L, length of valve; H, height of valve.

Order Podocopida Sars, 1866
Superfamily Cytheroidea Baird, 1850
Family Eucytheridae Puri, 1954
Subfamily Pectocytherinae Hanai, 1957
Genus ***Kotoracythere*** Ishizaki, 1966

Kotoracythere tsukagoshii Tanaka sp. nov.

Figures 5.1, 6.1–6.3

Kotoracythere sp. Irizuki and Matsubara, 1994, pl. 1, fig. 3.
Pectocythere quadangulata Hanai, Ozawa, 1996, pl. 8, fig. 2.

Etymology.—In honor of A. Tsukagoshi (Shizuoka University, Japan) a specialist in ostracod systematics.

Types.—Holotype, LV of male, SUM-CO-1208 (L = 0.66 mm, H = 0.32 mm). Paratypes, RV of male, SUM-CO-1209 (L = 0.67 mm, H = 0.32 mm); C of female, SUM-CO-1210 (L = 0.64 mm, H = 0.33 mm); LV of female, SUM-CO-1211 (L = 0.64 mm, H = 0.32 mm).

Type locality.—Loc. 1–A15.

Diagnosis.—Valve oblong box-shaped. Surface ornamented by scattered deep pits and very weak reticulations. Vestibule widely developed along anteroventral margin. Radial pore canals few. Anterior and posterior teeth of median element composed of upper and lower elements respectively.

Description.—Valve oblong box-shaped in lateral view. Anterior margin evenly rounded with infracurvature; dorsal margin straight, sloping gently toward posterior; posterior margin truncated dorsally and rounded ventrally; ventral margin nearly straight. Large sexual dimorphism; in lateral view, male forms more elongate; in dorsal view, female forms having inflated carapace in the posteroventral area. Eye spot not observed. Surface ornamented by scattered deep pits, which are the openings of normal pore canals, and very weak reticulation. In dorsal view, carapace is elongate ovate, widest in the posteromedian area, but compressed in the median area in female forms. In anterior view, carapace subovate, broadest at point near mid-height. Marginal zone broad anteriorly, vestibula widely developed in the anteroventral area and narrowly in the posteroventral area. Marginal pore canals few, 7 in anterior. 5 in posterior. Selvage well developed. Hinge pentodont: In LV, anterior and posterior elements are interiorly opened sockets respectively; median element is a crenulate bar with teeth at anterior and posterior terminations which are composed of upper and lower elements respectively. One V-shaped frontal scar. Four elliptical adductor scars are in a vertical row, the middle two are narrow. Two small elliptical mandibular scars. Two dorsal scars (one elliptical, dorsomedial; one elliptical, mid-dorsal). Prominent fulcral point.

Remarks.—This species differs from *K.* sp. widely reported from Plio-Pleistocene formations of north and central Japan (Ishizaki and Matoba, 1985; Tabuki, 1986; Cronin and Ikeya, 1987; Ozawa, 1996), in its very weak reticulation. The present species is distinguished from *Pectocythere tsiuensis* Brouwers, 1990 from the Quaternary

← **Figure 6.** **1–3**, *Kotoracythere tsukagoshii* Tanaka sp. nov. **1a–e**: male LV, holotype, Loc. 1-A15, SUM-CO-1208; **2a–c**: male RV, Loc. 1-A15, SUM-CO-1209; **3a–d**: female carapace, Loc. 1-A15, SUM-CO-1210. **4–5**, *Cluthia tamayuensis* Tanaka sp. nov. **4a–e**: female LV, holotype, Loc. 1-A16, SUM-CO-1215; **5a–c**: male RV, paratype, Loc. 1-A15, SUM-CO-1216. **6–7**, *Cluthia subjaponica* Tanaka sp. nov. **6a–e**: female LV, holotype, Loc. 1-A16, SUM-CO-1218; **7a–c**: male LV, paratype, Loc. 1-A15, SUM-CO-1219. **8**: *Callistocythere japonica uranipponica* Hanai, 1957, male LV, Loc. 1-A16, SUM-CO-1213. **9**: *Callistocythere kyongjuensis* Huh and Whatley, 1997, male LV, Loc. 1-A15, SUM-CO-1214. **10**: *Munseyella hatatatensis* Ishizaki, 1966, male RV, Loc. 2-B3, SUM-CO-1212. Scale bar is 0.10 mm.

sediments of the Gulf of Alaska, North America, in its very weak reticulation and the outline of the anterior margin.

Occurrences.—Early to Middle Miocene and Pleistocene sediments, Honshu, Japan (M5a, M9e and P9d; see Figure 4).

Genus ***Munseyella*** van den Bold, 1957

Munseyella hatatatensis Ishizaki, 1966

Figure 6.10

Munseyella hatatatensis Ishizaki, 1966, p. 153, pl. 19, fig. 2; Cronin and Ikeya, 1987, p. 76, pl. 3, fig. 16; Ikeya and Itoh, 1991, fig. 19A; Huh and Paik, 1992b, pl. 3, fig. 9; Irizuki, 1994, p. 8, pl. 1, fig. 2; Kamiya *et al.*, 1996, pl. 2, fig. 3; Ozawa, 1996, pl. 7, fig. 2.

Munseyella mananensis Hazel and Valentine, 1969, p. 749–751, pl. 97, figs. 19–24, pl. 98, figs. 1, 3, 4, 11, 12, text-figs. 4a, b, 5a, e, g; Cronin, 1989, pl. 2, fig. 8.

Remarks.—Cronin and Ikeya (1987) thought that *M. hatatatensis* was conspecific with *M. mananensis* Hazel and Valentine, 1969. Based on carapace morphology and geographical distribution, I have followed their opinion.

Occurrences.—Miocene to Recent sediments of North Atlantic, Japan and Korea (H3a–c, P5a, b, Q5b, Q7a, b, H7a–c, M9a, b, d, e, P9c, d, R9a, Q10, H10; see Figure 4).

Family Leptocytheridae Hanai, 1957
Genus ***Callistocythere*** Ruggieri, 1953

Callistocythere japonica uranipponica Hanai, 1957

Figure 6.8

Callistocythere japonica uranipponica Hanai, 1957a, p. 457–459, pl. 9, figs. 3a–c; Ishizaki and Matoba, 1985, pl. 2, fig. 8; Kamiya and Nakagawa, 1993, pl. 2, fig. 1.

Callistocythere cf. *japonica uranipponica* Hanai. Ishizaki, 1966, p. 147, pl. 16, fig. 13.

Remarks.—*C. japonica uranipponica* was recognized by Hanai (1957a) as a subspecies of *C. japonica*. *C. japonica uranipponica* is distinguished from *C. japonica* in having a more narrowly rounded posteroventral margin.

Occurrences.—Miocene to Recent sediments along the Japan Sea and the north Pacific areas of Japan (Q5b, M9e, N9a, H9, R9d; see Figure 4).

Callistocythere kyongjuensis Huh and Whatley, 1997

Figure 6.9

Callistocythere kyongjuensis Huh and Whatley, 1997, p. 32, 34, pl. 1, figs. 1–6.

Callistocythere sp. A Huh and Paik, 1992b, pl. 3, fig. 11.

Remarks.—This is the first reporting of *C. kyongjuensis* from Japan.

Occurrences.—Miocene sediments of the south Japan Sea side areas (M9d, e; see Figure 4).

Genus ***Cluthia*** Neale, 1973

Cluthia tamayuensis Tanaka sp. nov.

Figures 5.2, 6.4, 6.5

Etymology.—For the type locality in the town of Tamayu.

Types.—Holotype, LV, SUM-CO-1215 (L = 0.41 mm, H = 0.26 mm). Paratypes, RV of male, SUM-CO-1216 (L = 0.39 mm, H = 0.24 mm); RV of female, SUM-CO-1217 (L = 0.41 mm, H = 0.24 mm).

Type locality.—Loc. 1–A16.

Diagnosis.—alve subreniform. Anterior margin evenly rounded. Surface densely pitted with small, deep, polygonal pits. A mid-ventral carinal ridge runs toward the mid-posterior area. Radial pore canals (10 anteriorly; 10 posteriorly). Significant sexual dimorphism.

Description.—Valve subreniform in lateral view. Anterior margin evenly rounded; dorsal margin straight, sloping toward posterior; posterior margin straight (LV), truncate (RV); ventral margin concave. Large sexual dimorphism; in lateral view, male forms more elongate; in dorsal view, female forms inflated laterally. Eye spot not observed. Surface densely pitted with small, deep, polygonal pits. A carinal ridge occupies the mid-ventral area, runs toward the mid-posterior area. One tubercle developed in the posterodorsal area. In dorsal view, carapace appears compressed and subhexagonal; lateral outline sinuate, anterior end more pointed than posterior. In anterior view, carapace subpentagonal, broadest at the carinal ridge; anterior marginal rim strong. Marginal zone narrow, with narrow anterior and posterior vestibula. Marginal pore canals are straight and number 10 anteriorly; 12 ventrally; 10 posteriorly. Selvage well developed. Hinge entomodont: In RV, anterior element is an elliptical tooth; a crernulated median socket lies just below the smooth bar; posterior element is a well-developed toothplate. One very large U-shaped frontal scar. Four adductor scars in a vertical row (the uppermost and lowermost are semicircular, the middle two are elliptical). One semicircular mandibular scar. Two dorsal scars (one elongate dorsomedial; one semicircular mid-dorsal).

Remarks.—his species differs from *C. japonica* Tabuki, 1986 from the Plio-Pleistocene Daishaka Formation, northern Japan, in its posterior outline,deep polygonal pits and the carinal ridge toward mid-posterior. The present spe-

cies is distinguished from *C. ishizakii* Zhao, 1988 (MS) from the Late Pleistocene and Holocene drilling cores of the Okinawa Trough, East China Sea (in Ruan and Hao, 1988), in its lateral outline and deep polygonal pits.

Occurrence.—nly from the Fujina Formation (M9e; see Figure 4).

Cluthia subjaponica Tanaka sp. nov.

Figures 5.3, 6.6, 6.7

Etymology.—For its close resemblance with *Cluthia japonica* Tabuki.

Types.—olotype, LV of female, SUM-CO-1218 (L = 0.40 mm, H = 0.24 mm). Paratypes, LV of male, SUM-CO-1219 (L = 0.40 mm, H = 0.23mm); LV of female, SUM-CO-1220 (L = 0.40 mm, H = 0.24 mm).

Type locality.—Loc. 1-A16.

Diagnosis.—Valve subreniform. Anterior margin evenly rounded. Surface densely pitted with small, deep, round pits. Radial pore canals (23 anteriorly; 16 posteriorly). Prominent fulcral point. Sexual dimorphism weak.

Description.—Valve subreniform in lateral view. Anterior margin evenly rounded; dorsal margin straight, sloping toward posterior; posterior margin straight; ventral margin nearly straight to slightly convex. Sexual dimorphism weak. Eye spot not observed. Surface densely pitted with small, deep, round pits. One tubercle developed in the posterodorsal area. In dorsal view, lateral outline nearly straight; anterior end more pointed than posterior. In anterior view, LV arched, broadest at point near mid-height; anterior marginal rim strong. Marginal zone relatively broad, with narrow anterior and posterior vestibula. Marginal pore canals are straight, numbering 23 in anterior, 5 in ventral, 16 in posterior. Selvage well developed. Hinge entomodont: in LV, anterior and posterior elements are elongate sockets connected by a containant respectively; a crenulated median bar lies just below the containant. One very large U-shaped frontal scar. Four adductor scars in a vertical row (the uppermost one is semicircular, the lower three are elliptical). One circle mandibular scar. One elliptical dorsal scar mid-dorsally. Prominent fulcral point.

Remarks.—This species differs from *C. japonica* Tabuki, 1986 from the Plio-Pleistocene Daishaka Formation, the north Japan, in its lateral outline, small round pits and lack of tubercles in the posterodorsal and posteroventral areas.

Occurrence.—Only from the Fujina Formation (M9e; see Figure 4).

Subfamily Schizocytherinae Mandelstam, 1960
Tribe Paijenborchellini Deroo, 1966
Genus ***Paijenborchella*** Kingma, 1948

Paijenborchella cf. ***tsurugasakensis*** Tabuki, 1986

Figure 7.1, 7.2

Paijenborchella tsurugasakensis Tabuki, 1986, p.65-67, pl. 2, figs. 12-19, text-fig. 18-3; Kamiya *et al.*, 1996, pl. 3, fig. 3; Ozawa, 1996, pl. 7, fig. 8.

Remarks.—This species was first described from the Plio-Pleistocene Daishaka Formation, the north Japan by Tabuki (1986). Specimens from the Fujina Formation differ slightly from the type specimen, in the shape of posteroventral area.

Occurrence.—Miocene to Pleistocene sediments of Japan Sea side areas and northern Honshu, Japan (P5c, M9e and P9d; see Figure 4).

Genus ***Palmenella*** Hirschmann, 1916

Palmenella limicola (Norman, 1865)

Figure 7.3

Cythere limicola Norman, 1865a, p. 193; Norman, 1865b, p. 20, pl. 6, figs. 1-4.

Palmenella limicola (Norman). Hirschmann, 1916, p. 582-594, text-figs.8-27; Elofson, 1941, p.277, 278, text-fig. 21; Triebel, 1949, p.189, 190, pl. 2, figs. 5, 6; Swain, 1963, p.830, 831, pl.99, figs. 3a-d, text-fig.9d; Ishizaki, 1966, p.156, pl.19, fig. 8; Hanai, 1970, p. 704, text-figs. 6B (solid line), 7G, H; Neale and Howe, 1975, pl. 5, figs. 7, 8; Rosenfeld, 1977, p. 15, 16, pl. 1, figs. 3-6; Lord, 1980, pl. 3, fig. 6; Cronin, 1981, p. 412, pl. 11, figs. 1, 2, 4; Cheong *et al.*, 1986, pl. 2, fig. 1; McDougall *et al.*, 1986, pl. 13, fig. 8; Cronin and Ikeya, 1987, p. 86, pl. 2, fig. 17; Brouwers, 1988, figs. 5, 6; Yajima, 1988, pl. 2, fig. 8; Athersuch *et al.*, 1989, p. 82, 83, pl. 1 (2), fig. 28; Brouwers, 1990, pl. 1, fig. 15, pl. 4, figs. 9, 12, 17, pl. 6, fig. 1; Brouwers *et al.*, 1991, pl. 1, fig. 7; Cronin, 1991, fig. 7-11; Huh and Paik, 1992a, pl. 1, fig. 10; Huh and Paik, 1992b, pl. 1, fig. 10; Hartmann, 1993, p.241, pl. 1, figs. 2-4; Irizuki, 1994, p. 8, pl. 1, fig. 4; Irizuki and Matsubara, 1994, pl. 1, fig. 7; Ozawa *et al.*, 1995, pl. 1, fig. 4; Kamiya *et al.*, 1996, pl. 2, fig. 1; Ozawa, 1996, pl. 7, fig. 9; Irizuki *et al.*, 1998, fig. 5-8; Freiwald and Mostafawi, 1998, pl. 59, fig. 4; (not) Wagner, 1970, pl. 4, fig. 14.

Kyphocythere limnicola (Norman). Swain, 1961, fig. 2-20.

Palmenella sp. Hanai, 1961, p. 369, text-fig.11, figs. 4a, b.

Occurrences.—Miocene to Recent sediments of high-latitude areas (N1, P1a, b, Q1a, b, R2a-e, P3, R3a, c, Q4a, b, M5a, b, P5a, b, H6a, R6a, b, R7a, b, R8, M9b-f, P9d, Q9, R9c; see Figure 4).

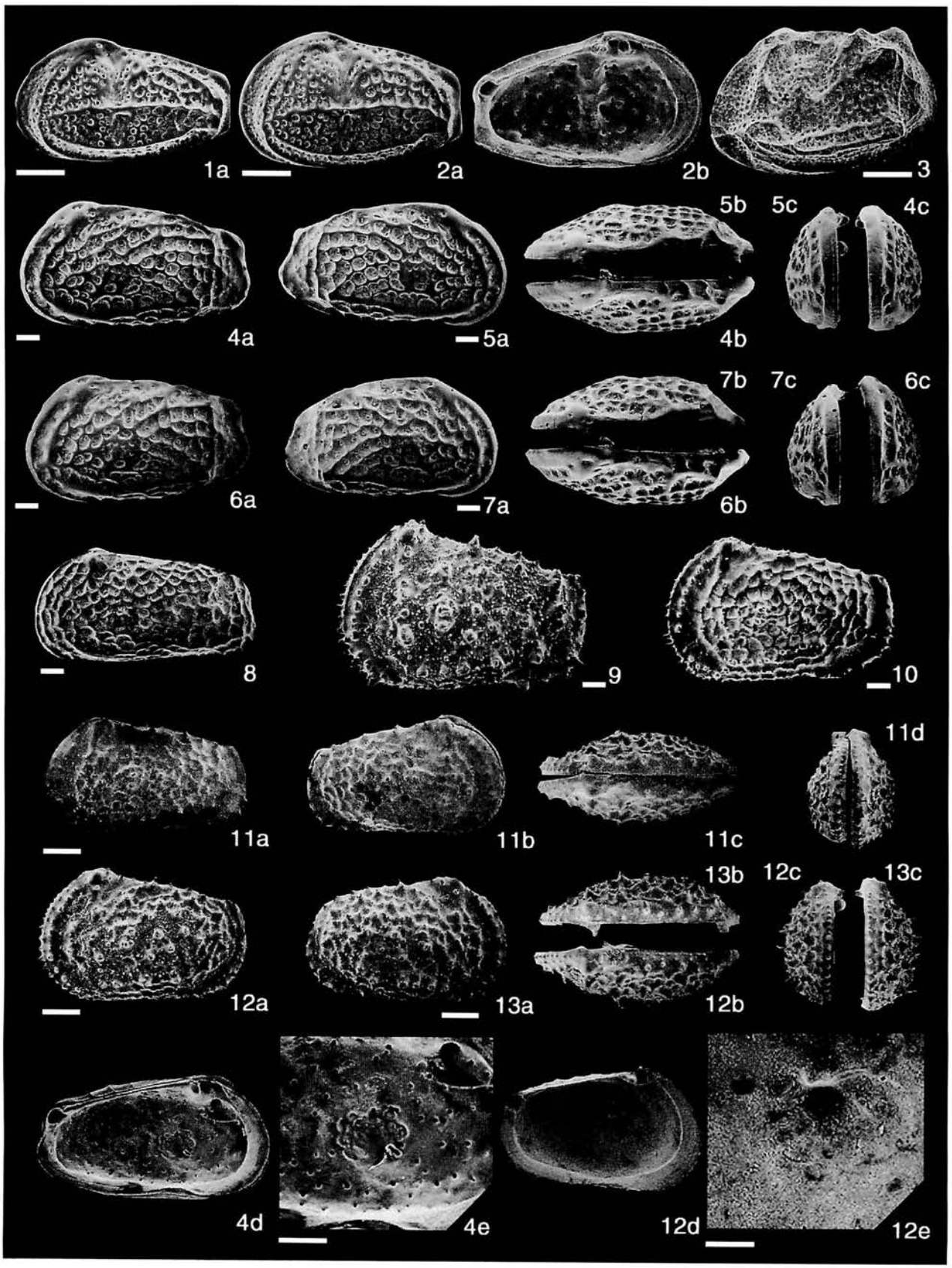
1a
2a
2b
3
4a
5a
5b
5c
4c
4b
6a
7a
7b
7c
6c
6b
8
9
10
11a
11b
11c
11d
12a
13a
13b
12c
13c
12b
4d
4e
12d
12e

Family Hemicytheridae Puri, 1953
Subfamily Urocythereidinae Hartmann and Puri, 1974
Genus ***Urocythereis*** Ruggieri, 1950

Urocythereis pohangensis Huh and Whatley, 1997

Figure 7.8

Urocythereis pohangensis Huh and Whatley, 1997, p. 36, 37, pl. 2, figs. 3-9.

Urocythereis sp. Huh and Paik, 1992a, pl. 1, figs. 17, 18; Huh and Paik, 1992b, pl. 1, figs. 17, 18.

Remarks.—This is the first report of *U. pohangensis* from Japan.

Occurrences.—Miocene sediments of the south Japan Sea side areas (M9d,e; see Figure 4).

Genus ***Laperousecythere*** Brouwers, 1993

Laperousecythere ikeyai Tanaka sp. nov.

Figures 5.4, 7.4-7.7

Etymology.—In honor of N. Ikeya (Shizuoka University, Japan), who is a specialist in the taxonomy and biogeography of the Cenozoic and Recent marine ostracods of the western Pacific region.

Types.—Holotype, LV of male, SUM-CO-1225(L = 0.95 mm, H = 0.51 mm). Paratypes, RV of male, SUM-CO-1226 (L = 0.95 mm, H = 0.49 mm); LV of female, SUM-CO-227 (L = 0.92 mm, H = 0.55 mm); RV of female, SUM-CO-1228 (L = 0.89 mm, H = 0.49 mm); LV of male, SUM-CO-1229 (L = 0.91 mm, H = 0.52 mm).

Type locality.—Loc. 1-A15.

Diagnosis.—Valve subquadrate. Surface ornamented by polygonal reticulations and a carinal ridge runs nearly parallel to anterior and ventral margin. Vestibule narrow. Four circular/elliptical adductor scars, in three of these the ventral side is subdivided.

Description.—Valve subquadrate in lateral view. Anterior margin evenly rounded with infracurvature; dorsal margin straight, sloping gently toward posterior; posterior margin truncated and caudated ventrally; ventral margin nearly straight to slightly convex. Large sexual dimorphism; in lateral view, male forms more elongate; in dorsal view, the carapaces of female forms are inflated posteroventrally. Eye spot large and flat. Surface ornamented by polygonal reticulations. A strong carinal ridge occurs at base of eye spot, runs nearly parallel to anterior and ventral margin, and ends at posteroventral area. A subcentral tubercle is developed. In dorsal view, lateral outline nearly straight; anterior end more pointed than posterior. On dorsal surface of carapace a V-shaped groove runs along hinge line (in vertical section). In anterior view, carapace subovate, broadest at point near mid-height. Marginal zone relatively broad, with narrow anterior and posterior vestibula. Marginal pore canals are straight and number 35 in anterior, 17 in posterior, and a few mid-ventrally. Selvage and list well developed. Hinge holamphidont: in LV, anterior element has an auxiliary tooth in a large elongate socket; anteromedian element is a smooth tooth, posteromedian element is a bar; posterior element is an elongate socket. Three frontal scars (the upper two are circular, the lowermost one is elliptical). Four circular/elliptical adductor scars; the three at ventral side are subdivided. A deep anteromedian depression between frontal and adductor scars, corresponding to the external subcentral tubercle. One elliptical mandibular scar. Six dorsal scars (two dorsomedially; two mid-dorsally; two anterodorsally); the uppermost one is semicircular, the others are circular/elliptical. Prominent fulcral point. One semicircular ventral scar is below and anterior to the mandibular scar. Ocular sinus conspicuous. *Remarks.*—This species differs from *L. robusta* (Tabuki, 1986) from the Plio-Pleistocene Daishaka Formation, northern Japan, in its slightly convexed ventral margin, polygonal reticulation and lack of secondary reticulations. The present species is distinguished from *L. ishizakii* Irizuki and Matsubara, 1995 from the Early-Middle Miocene Suenomatsuyama Formation, northeast Japan, in its outline and possession of a strong carinal ridge.

Occurrence.—Only from the Fujina Formation (M9e; see Figure 4).

Family Trachyleberididae Sylvester-Bradley, 1948
Subfamily Trachyleberidinae Sylvester-Bradley, 1948
Tribe Trachyleberidini Sylvester-Bradley, 1948
Genus ***Acanthocythereis*** Howe, 1963

← **Figure 7.** **1-2**, *Paijenborchella* cf. *tsurugasakensis* Tabuki, 1986. **1a**: male LV, Loc. 1-A17, SUM-CO-1221; **2a, b**: female LV, Loc. 1-A16, SUM-CO-1222; **3**: *Palmenella limicola* (Norman, 1865), female LV, Loc. 1-A18, SUM-CO-1223. **4-7**, *Laperousecythere ikeyai* Tanaka sp. nov. **4a-e**: male LV, holotype, Loc. 1-A15, SUM-CO-1225; **5a-c**: male RV, paratype, Loc. 1-A15, SUM-CO-1226; **6a-c**: female LV, paratype, Loc. 1-A15, SUM-CO-1227; **7a-c**: female RV, paratype, Loc. 1-A15, SUM-CO-1228. **8**: *Urocythereis pohangensis* Huh and Whatley, 1997, male LV, Loc. 1-A15, SUM-CO-1224. **9**: *Acanthocythereis dunelmensis* (Norman, 1865), female LV, Loc. 2-B4, SUM-CO-1230. **10**: *Acanthocythereis koreana* Huh and Whatley, 1997, female LV, Loc. 1-A13, SUM-CO-1240. **11-13**, *Acanthocythereis fujinaensis* Tanaka sp. nov. **11a-d**: male C, holotype, Loc. 1-A13, SUM-CO-1231; **12a-e**: female LV, paratype, Loc. 1-A11, SUM-CO-1232; **13a-c**: female RV, paratype, Loc. 1-A11, SUM-CO-1233. Scale bar is 0.10 mm.

Acanthocythereis dunelmensis (Norman, 1865)

Figure 7.9

Cythereis dunelmensis Norman, 1865a, p. 193; Norman, 1865b, p. 22, pl. 7, figs. 1-4.

Cythere dunelmensis (Norman). Brady, 1868, p. 416, pl. 30, figs. 1-12.

Cythereis dunelmensis (Norman). Elofson, 1941, p. 296-300, figs. 8-11, text-figs. 29, 30; Elofson, 1943, p. 10; (not) Tressler, 1941, p. 100, pl. 19, fig. 21.

Trachyleberis dunelmensis (Norman). Hulings, 1967, p. 324, figs. 7, 8T, pl.4, figs. 24, 25; Caralp *et al.*, 1967, pl.13, fig. 1; Caralp *et al.*, 1968, pl.10, fig. 1.

Acanthocythereis dunelmensis (Norman). Neale and Howe, 1975, pl. 1, figs. 3, 11, 13-16; Rosenfeld, 1977, p. 23, 24, pl. 5, figs. 65-68; Lord, 1980, pl. 1, figs. 8-13; Cronin, 1981, p. 400, pl. 8, figs. 1, 2; Cronin, 1986, pl. 2, fig. 9; McDougall *et al.*, 1986, pl. 13, figs. 2-4; Cronin and Ikeya, 1987, pl. 1, figs. 1, 4; Brouwers, 1988, figs. 5-7; Athersuch *et al.*, 1989, p. 133, 134, pl. 3 (10), fig. 52; Cronin, 1989, pl. 2, fig. 9; McKenzie *et al.*, 1989, pl. 1, fig. 1; Hartmann, 1992, pl. 5, figs.4-6; Ikeya and Suzuki, 1992, pl. 1, fig. 2; Brouwers, 1993, pl. 1, figs. 1-5, pl. 2, fig. 1, pl. 16, fig. 1, text-fig. 3, 4; Irizuki, 1994, p. 10, pl. 2, fig. 3; Irizuki, 1996, figs. 7-1, 2; Kamiya *et al.*, 1996, pl. 2, figs. 8-10; Ozawa, 1996, pl. 1, fig. 1; Freiwald and Mostafawi, 1998, pl. 59, figs. 1, 2.

Acanthocythereis cf. *A. dunelmensis* (Norman). Penney, 1993, fig. 5-I.

? *Acanthocythereis dunelmensis* (Norman). Cronin and Compton-Gooding, 1987, pl. 2, fig. 4.

? *Acanthocythereis* cf. *A. dunelmensis* (Norman). Cronin, 1991, fig. 8-11.

Cletocythereis dunelmensis dunelmensis (Norman). Bassiouni, 1965, pl. 2, fig. 8.

Cletocythereis dunelmensis minor Bassiouni, 1965, p. 513, 514, pl. 2, fig. 9.

Actinocythereis sp., Swain, 1961, fig. 2-36.

Cletocythereis elofsoni elofsoni Bassiouni, 1965, p. 514-516, pl. 2, figs. 4, 5.

Cletocythereis elofsoni elofsoni abbreviata, Bassiouni, 1965, p. 516, pl. 2, figs. 6, 7.

Cletocythereis noblissimus Swain, 1963, p. 824, 825, pl. 98, fig. 5, pl. 99, figs. 15a, b, text-fig. 10a.

Acanthocythereis ? sp. A Cheong *et al.*, 1986, pl. 2, fig. 17.

Acanthocythereis ? sp. B Cheong *et al.*, 1986, pl. 2, fig. 18.

Acanthocythereis ? sp. C Cheong *et al.*, 1986, pl. 2, fig. 19.

Trachyleberis ? *rastromarginata* (Brady). Swain, 1961, fig. 2-32.

Occurrences.—Miocene to Recent sediments of high-latitude areas (R2a-f, P3, R3a, b, d, Q4a-c, P5a, b, Q5a, b, Q6a, H6a, R6a, b, Q7a-e, R7a-d, R8, M9b, N9b, P9a, b, d, R9b, c; see Figure 4).

Acanthocythereis fujinaensis Tanaka sp. nov.

Figures 5.5, 7.11-7.13

Etymology.—For the type locality.

Types.—Holotype, C of male, SUM-CO-1231 (L = 0.41 mm, H = 0.24 mm). Paratypes, LV of female, SUM-CO-1232 (L = 0.43 mm, H = 0.27 mm); RV of female, SUM-CO-1233 (L = 0.42 mm, H = 0.27 mm); LV of female, SUM-CO-1234 (L = 0.46 mm, H = 0.29 mm).

Type locality.—Loc. 1-A13.

Diagnosis.—Valve subquadrate. Posterior margin evenly rounded. Conical spines developed in the anteroventral margin. Surface ornamented by polygonal reticulations with clavate/conic conjunctive spines.

Description.—Valve subquadrate in lateral view. Anterior margin evenly rounded with conical spines, especially anteroventrally; dorsal margin straight, sloping toward posterior with several spines; posterior margin evenly rounded with conical spines posteroventrally; ventral margin concave in male forms, nearly straight in female forms. Strong sexual dimorphism; in lateral view, male forms more elongate; in dorsal view, carapaces of female forms inflated posteroventrally. Eye spot large and protruding. Surface ornamented by polygonal reticulations with clavate/conical conjunctive spines. A row of clavate/conical spines occurs at base of eye spot, runs parallel to anterior margin. Three parallel carinal ridges occupy the mid-ventral area, the uppermost one with clavate spines. A subcentral tubercle developed. In dorsal view, carapace elongate subovate, pointed in front. In anterior view, carapace subovate, lateral outline nearly straight. Marginal zone relatively broad, with very narrow anterior and posterior vestibula. Marginal pore canals are straight/curved with median swellings and number 42 in anterior, 18 in ventral, 23 in posterior. Selvage developed. Hinge holamphidont: in LV, anterior element has an auxiliary tooth in a large elongate socket; anteromedian element is a smooth tooth, posteromedian element is a bar; posterior element is an elongate socket. One U-shaped frontal scar. Four adductor scars in a vertical row (the uppermost one is semicircular, the lower three are elliptical). One elliptical mandibular scar. Three dorsal scars mid-dorsally; the lowermost one protrudes like a tongue, the upper two are elliptical. Prominent fulcral point. One elliptical ventral scar is below and anterior to the mandibular scar. Ocular sinus conspicuous.

Remarks.—This species differs from *A. koreana* Huh and Whatley, 1997 from the Miocene, Korea, in its evenly rounded posterior margin, developed anteroventral conical spines and prominent clavate conjunctive spines.

Occurrence.—Only from the Fujina Formation (M9e; see Figure 4).

Acanthocythereis izumoensis Tanaka sp. nov.

Figures 5.6, 8.1–8.4

Etymology.—Izumo is the ancient provincial name of the type locality.

Types.—Holotype, LV of male, SUM-CO-1235 (L = 0.92 mm, H = 0.56 mm). Paratypes, RV of male, SUM-CO-1236 (L = 0.91 mm, H = 0.53 mm); LV of female, SUM-CO-1237 (L = 0.90 mm, H = 0.60 mm); RV of female, SUM-CO-1238 (L = 0.92 mm, H = 0.59 mm); LV of female, SUM-CO-1239 (L = 0.90mm, H = 0.61 mm).

Type locality.—Loc. 1-A16.

Diagnosis.—Valve subquadrate. In male forms, a large conical spine at the posteroventral corner is prominent. Surface smooth with scattered clavate/conical spines. A row of clavate spines runs parallel to mid-ventral margin. In anterior view, carapace subtrapezoidal, broadest at about one-fifth height from the ventral side. No vestibule.

Description. — Valve subquadrate in lateral view. Anterior margin evenly rounded with conical spines, especially anteroventrally; dorsal margin straight, sloping toward posterior with several clavate/conical spines; posterior margin evenly rounded with several conical spines, a large conical spine at the posteroventral corner is more prominent in male forms; ventral margin convex. Strong sexual dimorphism; in lateral view, male forms more elongate; in dorsal view, female forms having inflated carapace in the mid-posterior area. Eye spot large and protruding. Surface smooth with scattered clavate/conical spines. A row of clavate/conical spines occurs at base of the eye spot, runs parallel to anterior margin. A row of clavate spines runs parallel to mid-ventral margin. In dorsal view, carapace elongate subovate, pointed in front. In anterior view, carapace subtrapezoidal, broadest at about one-fifth height from the ventral side. Marginal zone broad; vestibule not developed. Marginal pore canals are straight/curved with median swellings and number 40 in anterior and 20 in posterior. Selvage developed. Hinge holamphidont: in LV, anterior element has an auxiliary tooth in a large elongate socket; anteromedian element is a smooth tooth, posteromedian element is a bar; posterior element is an elongate socket. One V-shaped frontal scar. Four adductor scars in a vertical row (the uppermost and lowermost are semicircular, the middle two are elliptical). One elliptical mandibular scar. Three dorsal scars; the dorsomedian one protrudes like a tongue, the mid-dorsal two are elongate. Prominent fulcral point. One elliptical ventral scar is below and posterior to the mandibular scar. Ocular sinus conspicuous.

Remarks. — This species differs from *A. mutsuensis* Ishizaki, 1971 from the Recent sediments of Mutsu Bay in northern Japan, in its row of clavate spines running parallel to the mid-ventral margin. The present species is distinguished from *A. koreana* Huh and Whatley, 1997 from the Miocene, Korea, by its smooth surface with scattered clavate/conical spines.

Occurrence.—Only from the Fujina Formation (M9e; see Figure 4).

Acanthocythereis koreana Huh and Whatley, 1997

Figure 7.10

Acanthocythereis koreana Huh and Whatley, 1997, p. 39, pl. 3, figs. 6–12.

Acanthocythereis mutsuensis Ishizaki. Huh and Paik, 1992a, pl. 2, figs. 8, 9; Huh and Paik, 1992b, pl. 2, figs. 8, 9.

Acanthocythereis dunelmensis (Norman). Irizuki and Matsubara, 1994, pl. 1, fig. 13.

Occurrences.—Miocene sediments of the south Japan Sea side areas (M9d, e; see Figure 4).

Acanthocythereis tsurugasakensis Tabuki, 1986

Figure 8.5

Acanthocythereis tsurugasakensis Tabuki, 1986, p. 85, 86, pl. 11, figs. 2–10, text-fig. 20-2; Ozawa, 1996, pl. 1, fig. 3.

Occurrences.—Miocene to Pleistocene sediments along the Japan Sea and Northern Pacific areas of Japan (P5c, M9e and P9d; see Figure 4).

Genus ***Robertsonites*** Swain, 1963

Robertsonites japonicus (Ishizaki, 1966)

Figure 8.6

Buntonia japonica Ishizaki, 1966, p. 156, 157, pl. 19, figs. 6, 7, text-fig.1, figs. 1, 5.

Occurrences.—Miocene sediments of Honshu, Japan (M9a, e; see Figure 4).

Robertsonites reticuliformus (Ishizaki, 1966)

Figure 8.7

Buntonia reticuliforma Ishizaki, 1966, p. 157, 158, pl. 16, fig. 7, text-fig.1, fig. 1; Tabuki, 1986, p. 91–93, pl. 14, figs. 1–12, text-figs. 17-1, 2; Cronin and Ikeya, 1987, p. 84, pl. 2, fig. 15; Yajima and Lord, 1990, fig. 4–9; Huh and Paik, 1992a, b, pl. 2, fig. 13; Irizuki, 1994, p. 10, pl. 2, figs. 4–6; Irizuki, 1996, figs. 7–3, 4; Kamiya *et al.*, 1996, pl. 3, fig. 6; Ozawa, 1996, pl. 8, fig. 6.

Robertsonites ? *reticuliforma* (Ishizaki) [*sic*]. Yajima, 1982, p. 205, pl. 12, fig. 13.

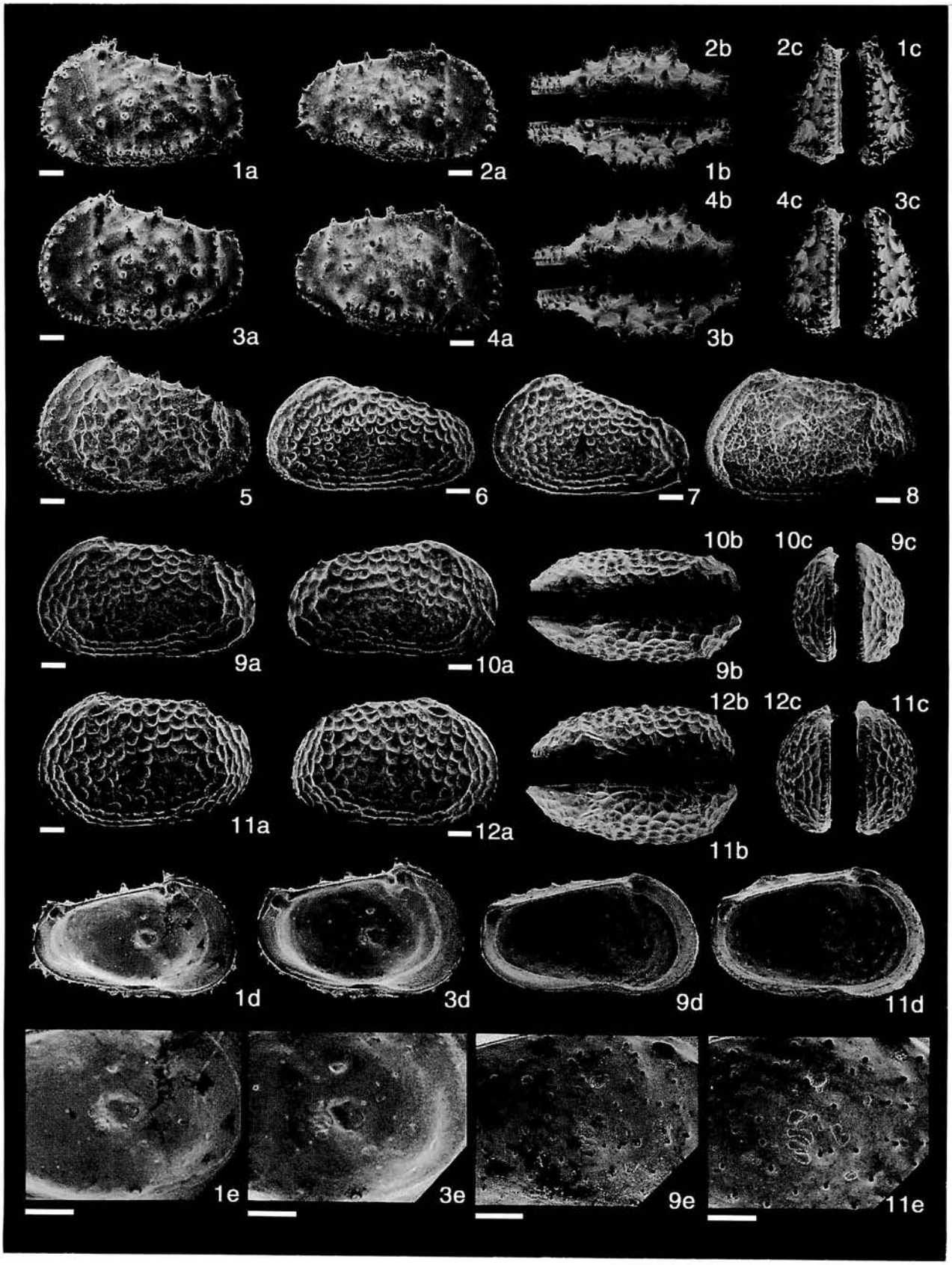
1a
2a
2b
1b
2c
1c
3a
4a
4b
3b
4c
3c
5
6
7
8
9a
10a
10b
9b
10c
9c
11a
12a
12b
11b
12c
11c
1d
3d
9d
11d
1e
3e
9e
11e

Remarks.—This species was first described by Ishizaki (1966) from the Middle Miocene Hatatate Formation in northern Japan. Specimens in Tabuki (1986), Irizuki (1994, 1996), Kamiya *et al.* (1996) and Ozawa (1996) have a prominent posterodorsal subvertical ridge.

Occurrences.—Miocene to Pleistocene sediments of Honshu, Japan (P5c, Q5a, b, M9a, b, d, N9b, P9a, c, d, Q9a; see Figure 4).

Robertsonites cf. ***tuberculatus*** (Sars, 1866)

Figure 8.8

Cythereis tuberculata Sars, 1866, p. 37.

Cythere tuberculata (Sars). Brady, 1868, p. 406, 407, pl. 30, figs. 25–39.

Robertsonites tuberculata (Sars) [*sic*]. Hulings, 1967, p. 324, pl. 4, figs. 21–23; text-figs. 4e, 8p–8s; Neale and Howe, 1975, p. 419, pl. 1, fig. 1; Rosenfeld, 1977, p. 24, 25, pl. 5, figs. 61–64.

Robertsonites tuberculatus (Sars). Cronin, 1981, p. 400, 402, pl. 8, fig. 5; Horne, 1983, p. 39–52, pls. 1–14; Athersuch *et al.*, 1989, p. 148, 149, pl. 4 (7), fig. 59; Cronin, 1989, p. 133, pl. 2, fig. 10; McKenzie *et al.*, 1989, pl. 1, fig. 12; Cronin, 1991, p. 779, fig. 8–2; Hartmann, 1992, p. 187, 188, pl. 5, figs. 7–12; pl. 6, figs. 1–6; Penney, 1993, fig. 5h.

Robertsonites gubikensis Swain, 1963, p. 821, 822, pl. 98, figs. 8a, b; pl. 99, fig. 12; text-fig. 9b.

Robertsonites logani (Brady and Crosskey). Swain, 1963, p. 823, pl. 97, fig. 13.

Robertsonites tuberculatina [*sic*] Swain, 1963, p. 822, 823, pl. 98, fig. 10; pl. 99, fig. 1; text-fig. 9c.

Remarks.—This species exhibits considerable variation in outline and ornament, with variable development of nodes and reticulation (Brouwers, 1993).

Occurrences.—Miocene to Recent sediments of high-latitude areas (N1, R2b, f, N3, P3, R3d, Q4b, c, R6a, b, Q7b–e, R7c; see Figure 4).

Robertsonites yatsukanus Tanaka sp. nov.

Figures 5.7, 8.9–8.12

Etymology.—The district name of the type locality.

Types.—Holotype, LV of male, SUM-CO-1245 (L = 0.95 mm, H = 0.53 mm). Paratypes, RV of male, SUM-CO-1246 (L = 0.93 mm, H = 0.51 mm); LV of female, SUM-CO-1247 (L = 0.94 mm, H = 0.59 mm); RV of female, SUM-CO-1248 (L = 0.91 mm, H = 0.55 mm); LV of male, SUM-CO-1249 (L = 0.94 mm, H = 0.54 mm).

Type locality.—Loc. 2–B1.

Diagnosis.—Valve quadrate, tapering posteriorly. Surface ornamented by polygonal reticulations. Vestibula developed in the anteroventral area and very narrow in the posteroventral area. One J-shaped frontal scar.

Description.—Valve quadrate, tapering posteriorly in lateral view. Anterior margin evenly rounded, weakly denticulated anteroventrally; dorsal margin undulate, sloping toward posterior; posterior margin evenly rounded and weakly denticulated anteroventrally; ventral margin nearly straight. Strong sexual dimorphism; in lateral view, male forms are more elongate; in dorsal view female carapaces are inflated posteriorly. Eye spot small and flat. Surface ornamented by polygonal reticulations. Two anterior carinal ridges prominent, one running from the anterior part of eye spot to the anteroventral area, the other starting at base of eye spot, bifurcating in anterodorsal area and running into anteroventral area. Three carinal ridges run nearly parallel to anterior, ventral and posterior margin and end at posterodorsal area. In dorsal view, carapace is elongate ovate. In dorsal surface of carapace a V-shaped groove runs along hinge line (in a vertical section). In anterior view, carapace subovate, broadest at point near mid-height. Marginal zone relatively broad, vestibula developed in the anteroventral area and very narrow in the posteroventral area. Marginal pore canals straight, number 48 anteriorly, 15 ventrally and 14 posteriorly. Selvage developed. Hinge holamphidont: in LV, anterior element is a large elongate socket; anteromedian element is a tongue like tooth, posteromedian element is a bar; posterior element is an elongate socket. One J-shaped frontal scar. Four adductor scars in a vertical row (the uppermost and lowermost are semicircular, the middle two are narrow). One elliptical mandibular scar. Eight dorsal scars (five dorsomedially; two mid-dorsally; one anterodorsally); the dorsomedian one protrude like a tongue, the others are circular/elliptical. Fulcral point not observed. One elliptical ventral scar is below and posterior to the mandibular scar. Ocular sinus conspicuous.

Remarks.—This species differs from *R. hanaii* Tabuki, 1986 from the Plio-Pleistocene Daishaka Formation in

← **Figure 8.** **1–4**, *Acanthocythereis izumoensis* Tanaka sp. nov. **1a–e**: male LV, holotype, Loc. 1–A16, SUM-CO-1235; **2a–e**: male RV, paratype, Loc. 1–A16, SUM-CO-1236; **3a–c**: female LV, paratype, Loc. 1–A16, SUM-CO-1237; **4a–c**: female RV, paratype, Loc. 1–A17, SUM-CO-1238. **5**: *Acanthocythereis tsurugasakensis* Tabuki, 1986, female LV, Loc. 2–B2, SUM-CO-1241. **6**: *Robertsonites japonicus* (Ishizaki, 1966), male LV, Loc. 1–A11, SUM-CO-1242. **7**: *Robertsonites reticuliformus* (Ishizaki, 1966), male LV, Loc. 1–A15, SUM-CO-1243. **8**: *Robertsonites* cf. *tuberculatus* (Sars, 1866), female LV, Loc. 2–B4, SUM-CO-1244. **9–12**, *Robertsonites yatsukanus* Tanaka sp. nov. **9a–e**: male LV, holotype, Loc. 2–B1, SUM-CO-1245; **10a–c**: male RV, paratype, Loc. 2–B1, SUM-CO-1246; **11a–e**: female LV, paratype, Loc. 2–B1, SUM-CO-1247; **12a–c**: female RV, paratype, Loc. 2–B1, SUM-CO-1248. Scale bar is 0.10 mm.

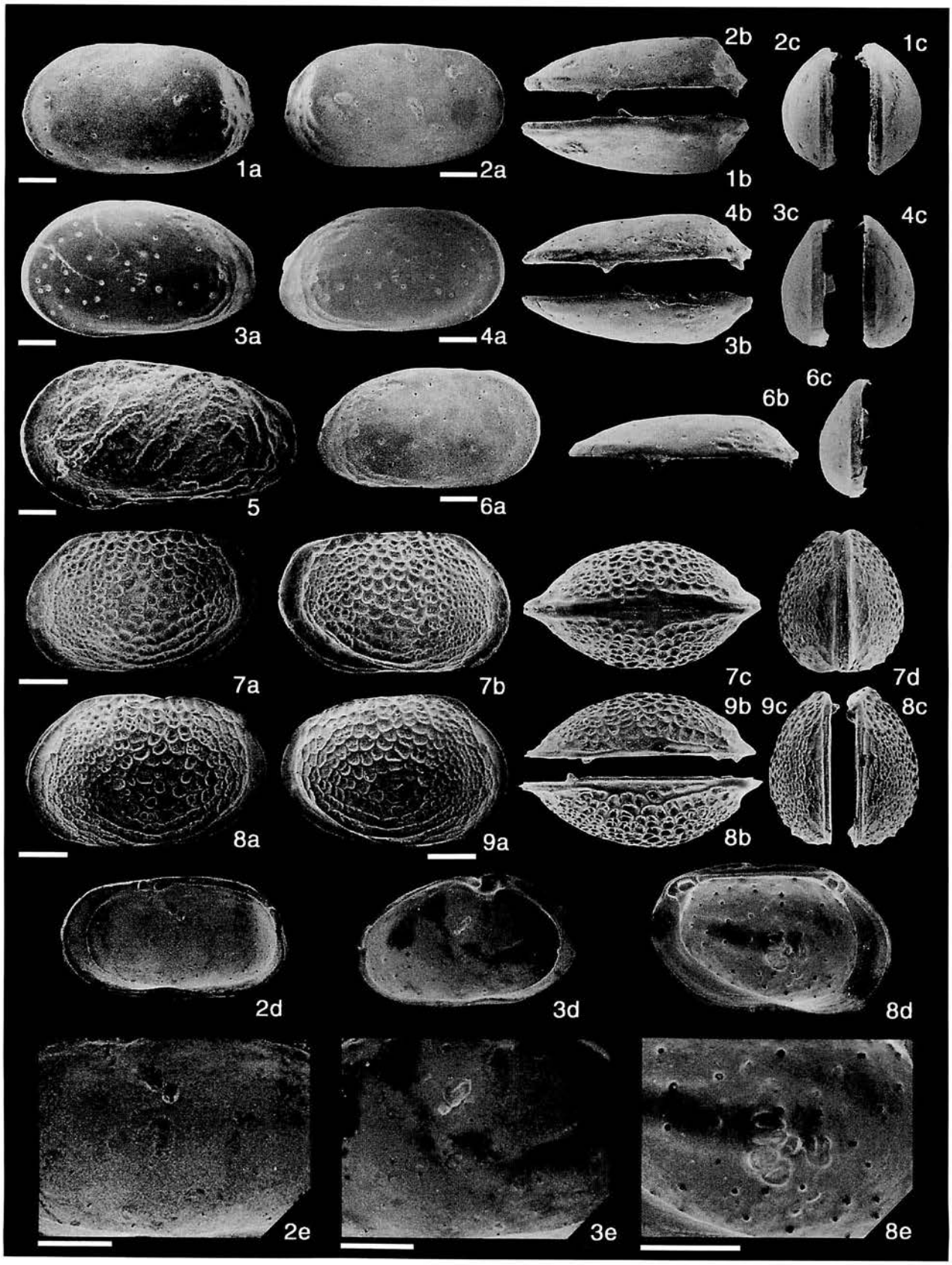
1a
2a
2b
2c
1c
1b
3a
4a
4b
3c
4c
3b
5
6a
6b
6c
7a
7b
7c
7d
8a
9a
9b
9c
8c
8b
2d
3d
8d
2e
3e
8e

northern Japan, in its inflated carapace and three carinal ridges running nearly parallel to anterior, ventral and posterior margins. *R. yatsukanus* is distinguished from *R. tsugaruana* [*sic*] Tabuki, 1986 from the Plio-Pleistocene Daishaka Formation in northern Japan, in lack of secondary reticulations.

Occurrence.—Only from the Fujina Formation (M9e; see Figure 4).

Subfamily Buntoniinae Apostolescu, 1961
Genus ***Ambtonia*** Malz, 1982

Ambtonia shimanensis Tanaka sp. nov.

Figures 5.8, 9.1, 9.2

Etymology.—The prefecture name, Shimane, of the type locality.

Types.—Holotype, RV, SUM-CO-1250 (L = 0.61 mm, H = 0.33 mm). Paratypes, LV, SUM-CO-1251 (L = 0.63 mm, H = 0.35 mm); LV, SUM-CO-1252 (L = 0.65 mm, H = 0.36 mm).

Type locality.—Loc. 1-A11.

Diagnosis. — Valve subcylindrical. Dorsal margin nearly straight. In dorsal view, carapace elongately arrowhead-shaped, tapered in front. Maximum width about one-sixth length from the posterior end. In anterior view, carapace subovate, broadest near mid-height. One V-shaped frontal scar.

Description. — Valve subcylindrical in lateral view. Anterior margin evenly rounded; dorsal margin nearly straight; truncated and caudate ventrally; ventral margin nearly straight to slightly convex. Sexual dimorphism unknown. Eye spot not observed. Surface smooth, scattered deep punctations which are the openings of normal pore canals. Anterior area compressed along the anterior margin. In dorsal view, carapace elongately arrowhead-shaped, tapered in front. Maximum width at about one-sixth length from the posterior end. In anterior view, carapace subovate, broadest at point near mid-height. Marginal zone broad in the anterior area, vestibula developed in the anteroventral area and very narrow in the posteroventral area. Marginal pore canals are straight and number 39 anteriorly, 7 ventrally and 11 posteriorly. Selvage and list well developed. Hinge hemiamphidont: in LV, anterior element has a large elongate socket; anteromedian element is a smooth elongate tooth, posteromedian element is a crenulate bar; posterior element is an elongate socket with several lobes dorsally. One V-shaped frontal scar. Four elliptical adductor scars in a vertical row, the middle two of which are narrow. One elliptical mandibular scar. Two dorsal scars protrude like pivots in the dorsomedian area. Fulcral point not observed. One small round ventral scar is below and posterior to the mandibular scar. No ocular sinus.

Remarks.—This species differs from *A. obai* (Ishizaki, 1971) from the Recent sediments of Mutsu Bay in northern Japan, in its caudate posteroventral margin, slightly convex ventral margin and compressed anterior area. The present species is distinguished from *A. tongassensis* Brouwers, 1993 from the Quaternary sediments of the Gulf of Alaska, North America, in its caudated posteroventral margin, nearly parallel dorsal and ventral margins, and number of marginal pore canals. This species differs from *A. glabra* Malz, 1982 from the Plio-Pleistocene Ssukou Formation of southwest Taiwan, in its straight dorsal margin.

Occurrence.—Only from the Fujina Formation (M9e; see Figure 4).

Ambtonia takayasui Tanaka sp. nov.

Figures 5.9, 9.3, 9.4, 9.6

Falsobuntonia taiwanica Malz. Yajima, 1988, pl. 1, fig. 7; Huh and Paik, 1992b, pl. 2, fig. 14.
Ambtonia obai (Ishizaki). Huh and Paik, 1992a, pl. 2, fig. 14.

Etymology.—In honor of K. Takayasu (Center for Coastal Lagoon Environments of Shimane University, Japan), who is a specialist in the taxonomy and paleoecology of the molluscs of the Fujina Formation.

Types.—Holotype, LV of female, SUM-CO-1253 (L = 0.64 mm, H = 0.37 mm). Paratypes, RV of female, SUM-CO-1254 (L = 0.63 mm, H = 0.33 mm); RV of male, SUM-CO-1255 (L = 0.62 mm, H = 0.33 mm); LV of female, SUM-CO-1256 (L = 0.64 mm, H = 0.37 mm).

Type locality.—Loc. 1-A16.

Diagnosis. — Valve subcylindrical. Dorsal margin arched. In dorsal view, carapace elongately arrowhead-shaped, tapered in front. Maximum width about one-fifth length from the posterior end. In anterior view, carapace subpentagonal, lateral outline nearly straight. One J-shaped frontal scar.

Description. — Valve subcylindrical in lateral view. Anterior margin evenly rounded; dorsal margin arched; posterior margin truncated and caudated ventrally; ventral

Figure 9. **1–2**, *Ambtonia shimanensis* Tanaka sp. nov. **1a–c**: LV, paratype, Loc. 1-A11, SUM-CO-1251; **2a–e**: RV, holotype, Loc. 1-A11, SUM-CO-1250. **3–4, 6**, *Ambtonia takayasui* Tanaka sp. nov. **3a–e**: female LV, holotype, Loc. 1-A16, SUM-CO-1253; **4a–c**: female RV, paratype, Loc. 1-A16, SUM-CO-1254; **6a–c**: male RV, paratype, Loc. 1-A11, SUM-CO-1255. **5**: *Falsobuntonia taiwanica* Malz, 1982, male LV, Loc. 1-A20, SUM-CO-1257. **7–9**, *Palmoconcha irizukii* Tanaka sp. nov. **7a–d**: male C, holotype, Loc. 1-A15, SUM-CO-1258; **8a–e**: female LV, paratype, Loc. 1-A15, SUM-CO-1259; 9a-c: female RV, paratype, Loc. 1-A15, SUM-CO-1260. Scale bar is 0.10 mm.

margin straight. Weak sexual dimorphism. Eye spot not observed. Surface smooth; scattered deep punctations, which are the openings of normal pore canals. Anterior area compressed along the anterior margin. Three weak muri run parallel to posterior margin in the posterior area. In dorsal view, carapace elongately arrowhead-shaped, tapered in front. Maximum width about one-fifth length from the posterior end. In anterior view, carapace subpentagonal, lateral outline nearly straight. Marginal zone broad in the anterior area, vestibula developed in the anteroventral area and very narrow in the posteroventral area. Marginal pore canals straight, number 39 anteriorly, 6 ventrally and 15 posteriorly. Selvage and list well developed. Hinge hemiamphidont: in LV, anterior element has a large elongate socket; anteromedian element is a smooth elongate tooth, posteromedian element is a crenulate bar; posterior element is an elongate socket with several lobes dorsally. One J-shaped frontal scar. Four elliptical adductor scars in a vertical row, the middle two are narrow. One round mandibular scar. Two dorsal scars protrude like pivots in the dorsomedian area. Fulcral point not observed. One small round ventral scar is below and posterior to the mandibular scar. No ocular sinus.

Remarks.—This species differs from *A. tongassensis* Brouwers, 1993 from the Quaternary sediments of the Gulf of Alaska, North America, in its outline in lateral view.

Occurrence.—Miocene formations from Japan and Korea (M9d, e, g; see Figure 4).

Falsobuntonia taiwanica Malz, 1982

Figure 9.5

Falsobuntonia taiwanica Malz, 1982, p. 392, 393, pl. 8, figs. 51-56; Huh and Paik, 1992a, pl. 2, fig. 15; Huh and Paik, 1992b, p. 111, pl. 2, fig 15; (non) Yajima, 1988, pl. 1, fig. 7; Huh and Paik, 1992b, p. 111, pl. 2, fig. 14.

Occurrences.—Miocene to Pleistocene sediments of Japan, Korea and Taiwan (M9d, e and P9e; see Figure 4).

Family Loxoconchidae Sars, 1926
Genus ***Palmoconcha*** Swain and Gilby, 1974

Palmoconcha irizukii Tanaka sp. nov.

Figures 5.10, 9.7-9.9

Palmoconcha sp. Irizuki and Matsubara, 1994, pl. 1, fig. 19.

Etymology.—In honor of T. Irizuki (Aichi University of Education, Japan) who is a specialist in the study of Cenozoic fossil ostracod assemblages of Japan. *Types.*—Holotype, C of male, SUM-CO-1258 (L = 0.47 mm, H = 0.28 mm). Paratypes, LV of female, SUM-CO-1259 (L = 0.49 mm, H = 0.31 mm); RV of female, SUM-CO-1260 (L = 0.46 mm, H = 0.31 mm); LV of female, SUM-CO-1261 (L = 0.51 mm, H = 0.34 mm).

Type locality.—Loc. 1-A15.

Diagnosis.—Valve rhomboidal. Surface ornamented by punctations in the anterior area. Three concentric muri occur in the anteroventral area, convex ventrally in the mid-ventral area, ends in mid-posterior area. One prominent murus runs from the mid-dorsal area to the posterodorsal area, arched dorsally. One large U-shaped frontal scar.

Description.—Valve rhomboidal in lateral view. Anterior margin evenly rounded; dorsal and ventral margins straight in male forms, arched in female forms; posterior margin truncated obliquely in upper half and lower half making blunt angle slightly above mid-height. Strong sexual dimorphism; in lateral view, male forms more elongate; in dorsal view, carapaces of female forms inflated in lateral outline. Eye spot not observed. Surface ornamented by punctations in the anterior area, polygonal reticulations and secondary reticulations in the median and posterior areas. Three concentric muri occur in the anteroventral area, convex ventrally in the mid-ventral area, ends at mid-posterior area. One prominent murus runs from the mid-dorsal area to the posterodorsal area, arched dorsally. In dorsal view, carapace ovate, widest at mid-length, pointed at the anterior and posterior ends. In anterior view, carapace subovate, broadest a little below mid-height. Marginal zone broad anteriorly and posteriorly, with developed vestibula. Marginal pore canals straight, number 6 anteriorly, 11 ventrally, 6 posteriorly. Selvage and list well developed. Hinge gongylodont: In LV, anterior element is a downturned claw-shaped ridge around a socket; median element is a smooth bar; posterior element is a horseshoe-shaped socket around a ball-like knob. One large U-shaped frontal scar. Four adductor scars in a vertical row (the upper three are elliptical, the lowermost one is semicircular). Two elliptical mandibular scars. Five elliptical dorsomedian dorsal scars. Prominent fulcral point.

Remarks.—This species differs from *Loxoconcha* (*Palmoconcha*) *parapontica* Zhou, 1995 from the Recent sediments of Kumano-nada and Hyuga-nada, southwest Japan, in its anterior marginal outline and punctations in the anterior area. *P. irizukii* is distinguished from *P. saboyamensis* (Ishizaki, 1966) from the Middle Miocene Hatatate Formation of northeast Japan, in the outline of the anterior margin and the three concentric muri running toward the mid-posterior area.

Occurrences.—Middle Miocene sediments, Honshu, Japan (M5a and M9e; see Figure 4).

Acknowledgements

The authors express their deep gratitude to N. Ikeya, A.

Tsukagoshi (Shizuoka University) and T. Irizuki (Aichi University of Education) for advice and continuous encouragement throughout the course of the present study. Thanks are also due to R. M. Ross (Paleontological Research Institution, New York), R. J. Smith (Kanazawa University) and K. M. Satish (Shizuoka University) for reading our manuscript. This manuscript was improved by two anonymous referees. We thank K. Tanehira (Shimane), K. Kitakaze (Hiroshima), T. Kosaka (Hiroshima University) and the members of the Cenozoic Environmental Seminar and the Paleontological Seminar (Shimane University) for their fieldwork assistance.

References

Apostolescu, V., 1961: Contribution à l'étude paléontologique (Ostracodes) et stratigraphique des bassins crétacés et tertiaires de l'Afrique Occidentale. *Revue de l'Institut Français du Pétrole et Annales des Combustibles Liquides*, vol. 16, nos. 7/8, p. 779-867.

Athersuch, J., Horne, D. J. and Whittaker, J. E., 1989: Marine and brackish water Ostracods (Superfamilies Cypridacea and Cytheracea). *In*, Kermack, D. M. and Barnes, R. S. K. *eds.*, *Synopses of the British Fauna (New Series)*, no. 43, p. 1-343. The Linnean Society of London and the Estuarine and Brackish-Water Sciences Association.

Baird, W., 1850: *The Natural History of the British Entomostraca*, 364 p. Ray Society, London.

Bassiouni, M. E. A. A., 1965: Über einige Ostracoden aus dem Interglazial von Esbjerg. *Meddelelser fra Dansk Geologisk Forening*, vol. 15, no. 4, p. 507-520.

Bold, W. A. Van den, 1957: Ostracoda from the Paleocene of Trinidad. *Micropaleontology*, vol. 3, no. 1, p. 1-18.

Brady, G. S., 1868: A monograph of the Recent British Ostracoda. *Linnean Society of London Transactions*, vol. 26, no. 2, p. 353-495.

Brouwers, E. M., 1988: Palaeobathymetry on the continental shelf based on examples using ostracods from the Gulf of Alaska. *In*, De Deckker, P., Colin, J. P. and Peypouquet, J. P. *eds.*, *Ostracoda in the Earth Sciences*, p. 55-76. Elsevier, Amsterdam.

Brouwers, E. M., 1990: Systematic paleontology of Quaternary ostracode assemblages from the Gulf of Alaska, Part 1: Families Cytherellidae, Bairdiidae, Cytheridae, Leptocytheridae, Limnocytheridae, Eucytheridae, Krithidae, Cushmanideidae. *U. S. Geological Survey Professional Paper* 1510, p. 1-43.

Brouwers, E. M., 1993: Systematic paleontology of Quaternary ostracode assemblages from the Gulf of Alaska, Part 2: Families Trachyleberididae, Hemicytheridae, Loxoconchidae, Paracytherideidae. *U. S. Geological Survey Professional Paper* 1531, p. 1-47.

Brouwers, E. M., Jørgensen, N. O. and Cronin, T. M., 1991: Climatic significance of the ostracode fauna from the Pliocene Kap København Formation, north Greenland. *Micropaleontology*, vol. 37, no. 2, p. 1-23.

Caralp, M., Klingebiel, A., Lamy, A., Latouche, C., Moyes, J. and Vigneaux, M., 1968: Étude micropaléontologique, sedimentologique et geochimique de quelques carottes de sediments recents du Golfe de Gascogne. *Bulletin de l'Institut de Géol ogie du Bassin d'Aquitaine*, no. 5, p.3-73.

Caralp, M., Moyes, J. and Vigneaux, M., 1967: La microfaune actuelle et subrécente d'une carotte atlantique (golfe de Gascogne): observations écologiques et climatiques. *Bulletin de la Société Géologique de France, Série 7*, vol. 9, p. 418-425.

Cheong, H. K., Lee, E. H., Paik, K. H. and Chang, S. K., 1986: Recent ostracodes from the southwestern slope of the Ulleung Basin, East Sea, Korea. *Journal of the Paleontological Society of Korea*, vol. 2, no. 1, p. 38-53.

Chinzei, K., 1986: Faunal succession and geographic distribution of Neogene molluscan faunas in Japan. *In*, Kotaka, T. *ed.*, *Japanese Cenozoic Molluscs: Their Origin and Migration, Palaeontological Society of Japan, Special Papers*, no. 29, p. 17-32.

Cronin, T. M., 1981: Paleoclimatic implications of Late Pleistocene marine ostracodes from the St. Lawrence Lowlands. *Micropaleontology*, vol. 27, no. 4, p. 384-418.

Cronin, T. M., 1986: Paleozoogeography of Post-glacial Ostracoda from Northeastern North America. *In*, Gadd, N. R. *ed.*, *The Champlain Sea. Geological Survey of Canada, Special Paper*, p. 1-39.

Cronin, T. M., 1989: Paleozoogeography of Postglacial Ostracoda from Northeastern North America. *In*, Gadd, N. R. *ed.*, *The Late Quaternary Development of the Champlain Sea Basin Sea. Geological Association of Canada, Special Paper*, no. 35, p. 125-144.

Cronin, T. M., 1991: Late Neogene marine Ostracoda from Tjörnes, Iceland. *Journal of Paleontology*, vol. 65, no. 5, p. 767-794.

Cronin, T. M. Compton-Gooding, E. E., 1987: 16. Cenozoic Ostracoda from Deep Sea Drilling Project Leg 95 off New Jersey (Sites 612 and 613). *In*, Poag, C. W. *et al.*, *Initial Reports of the Deep Sea Drilling Project*, Volume 95, p. 439-451. U.S. Government Printing Office, Washington, D. C.

Cronin, T. M. and Ikeya, N., 1987: The Omma-Manganji ostracod fauna (Plio-Pleistocene) of Japan and the zoogeography of circumpolar species. *Journal of Micropalaeontology*, vol. 6, no. 2, p. 65-88.

Deroo, G., 1966: Cytheracea (Ostracodes) du Maastrichtien de Maastricht (Pays-Bas), et des régions voisines; résultats stratigraphiques et paléonotologiques de leur étude. *Medelingen Geologische Stichting, Serie C*, vol. 2, no. 2, p. 1-197.

Elofson, O., 1941: Zur Kenntnis der marinen Ostracoden Schwedens mit besonderer Berücksichtigung des Skageraks. *Zoologiska Bidrag från Uppsala*, band. 19, p. 215-534.

Elofson, O., 1943: Neuere Beobachtungen über die Verbreitung der Ostracoden an den skandinavischen Küsten. *Arkiv för zoologie*, vol. 35A, no. 2, p. 1-26.

Freiwald, A. and Mostafawi, N., 1998: Ostracods in a cold-temperate costal environment, Western Troms, Northern Norway: Sedimentary aspects and assemblages. *Facies*, 38, p. 255-274.

Hanai, T. 1957a: Studies on the Ostracoda from Japan, I. Subfamily Leptocytherinae, new subfamily. *Journal of the Faculty of Science, University of Tokyo, Section 2*, vol. 10, pt. 3, p. 431-468.

Hanai, T. 1957b: Studies on the Ostracoda from Japan, II. Subfamily Pectocytherinae, new subfamily. *Journal of the Faculty of Science, University of Tokyo, Section* 2, vol. 10, pt. 3, p. 469-482.

Hanai, T., 1961: Studies on the Ostracoda from Japan: Hingement. *Journal of the Faculty of Science, University of Tokyo, Section* 2, vol. 13, pt. 2, p. 345-377.

Hanai, T., 1970: Studies on the ostracod subfamily Schizocytherinae Mandelstam. *Journal of Paleontology*, vol. 44, no. 4, p. 693-729.

Hartmann, G., 1992: Zur Kenntnis der rezenten und subfossilen Ostracoden des Liefdefjords (Nordspitzbergen, Svålbard). 1. Teil. Mit einer Tabelle subfossil nachgewiesener Fòraminiferen: Ergebnis der Geowissenschftlichen Spitzbergen-Expedition 1990. *Mitteilung aus dem Hamburgischen Zoologischen Museum und Institut*, no. 89, p. 181-225.

Hartmann, G., 1993: Zur Kenntnis der rezenten und subfossilen Ostracoden des Liefdefjords (Nordspitzbergen, Svålbard), 2. Teil: Ergebnisse der Geowissenschaftlichen Spitzbergen Expedition 1991. *Mitteilung aus dem Hamburgischen Zoologischen Museum und Institut*, no. 90, p. 239-250.

Hartmann, G. and Puri, H. S., 1974: Summary of neontological and palaeontological classification of Ostracoda. *Mitteilung aus dem Hamburgischen Zoologischen Museum und Institut*, no. 70, p. 7-73.

Hazel, J. E. and Valentine, P., 1969: Three new ostracodes from off northeast North America. *Journal of Paleontology*, vol. 43, no. 3, p. 741-752.

Hirschmann, N., 1916: Ostracoda of the Baltic Sea collected by N. M. Knipovitch and S. A. Pavlovitch in the Summer of 1908. *St. Petersburg, Ezhegodnik Zoologicheskago Muzeya Imperatorskoy Akademii Nauk (Annuaire du Musée Zoologique de l' Academie Imperiale des Sciences)*, vol. 20, p. 569-597. *(in Russian)*

Horne, D. J., 1983: On *Robertsonites tuberculatus* (Sars). *In*, Bate, R. H., *et al. eds., A Stereo-Atlas of Ostracod Shells*, vol. 10, no. 8, p. 39-52.

Howe, H. V., 1963: Type Saline Bayou Ostracoda of Louisiana. *Louisiana Geological Survey, Geological Bulletin*, vol. 40, p. 1-62.

Huh, M. and Paik, K. H., 1992a: Miocene Ostracoda from the Seojeongri Area, Pohang Basin, Korea. *Journal of the Geological Society of Korea*, vol. 28, no. 3, p. 273-283. *(in Korean with English abstract)*

Huh, M. and Paik, K. H., 1992b: Miocene Ostracoda from the Pohang Basin, Korea. *Paleontological Society of Korea, Special Publication*, no. 1, p. 101-119.

Huh, M. and Whatley, R., 1997: New species of Miocene cytheracean Ostracoda from the Pohang Basin, SE Korea. *Journal of Micropalaeontology*, vol.16, pt. 1, p. 31-40.

Hulings, N. C., 1967: Marine Ostracoda from the western North Atlantic Ocean: Labrador Sea, Gulf of St. Lawrence and off Nova Scotia. *Crustaceana,* vol. 13, part 3, p. 310-328.

Ikeya, N. and Cronin, T. M., 1993: Quantitative analysis of Ostracoda and water masses around Japan: Application to Pliocene and Pleistocene paleoceanography. *Micropaleontology*, vol. 39, no. 3, p. 263-281.

Ikeya, N. and Itoh, H., 1991: Recent Ostracoda from the Sendai Bay region, Pacific coast of northeastern Japan. *Reports of Faculty of Science, Shizuoka University*, vol. 25, p. 93-145.

Ikeya, N. and Suzuki, C., 1992: Distributional patterns of modern ostracodes off Shimane Peninsula, southwestern Japan Sea. *Reports of Faculty of Science, Shizuoka University*, vol. 26, p. 91-137.

Irizuki, T., 1994: Late Miocene ostracods from the Fujikotogawa Formation, northern Japan—with reference to cold water species involved with trans-Arctic interchange. *Journal of Micropalaeontology*, vol. 13, pt. 1, p. 3-15.

Irizuki, T., 1996: Lithology and Ostracoda from the Pliocene Tentokuji Formation along the southern marginal area of Mt. Taiheizan, Akita Prefecture, Northeast Japan. *Bulletin of Aichi University of Education (Natural Science)*, vol. 45, p. 23-32.

Irizuki, T., Ishizaki, K., Takahashi, M. and Usami, M., 1998: Ostracode faunal changes after the mid-Neogene climatic optimum elucidated in the Middle Miocene Kobana Formation, Central Japan. *Paleontological Research*, vol. 2, no. 1, p. 30-46.

Irizuki, T. and Matsubara, T., 1994: Vertical changes of depositional environments in the Lower to Middle Miocene Kadonosawa Formation based on analyses of fossil ostracode faunas. *Journal of the Geological Society of Japan*, vol. 100, no. 2, p. 136-149. *(in Japanese with English abstract)*

Irizuki, T. and Matsubara, T., 1995: Early Middle Miocene ostracodes from the Suenomatsuyama Formation, Ninohe City, Northeast Japan and their paleoenvironmental significance. *Transactions and Proceedings of the Palaeontological Society of Japan, New Series*, no. 177, p. 65-78.

Ishizaki, K., 1963: Japanese Miocene ostracodes from the Sunakosaka Member of the Yatsuo Formation, east of Kanazawa City, Ishikawa Prefecture. *Japanese Journal of the Geology and Geography*, vol. 34, no. 1, p. 19-34.

Ishizaki, K., 1966: Miocene and Pliocene ostracodes from the Sendai Area, Japan. *Science Reports of the Tohoku University, Second Series (Geology)*, vol. 37, no. 2, p. 131-163.

Ishizaki, K., 1971: Ostracodes from Aomori Bay, Aomori Prefecture, Northeast Honshu, Japan. *Science Reports of the Tohoku University, Second Series (Geology)*, vol. 43, no. 1, p. 59-97.

Ishizaki, K., Fujiwara, O. and Irizuki, T., 1996: Ostracod faunas from the Upper Miocene Tsunaki Formation near the southern border of Sendai City, Northeast Japan. *Proceedings of the Second European Ostracodologists Meeting*, p. 113-120.

Ishizaki, K. and Matoba, Y., 1985: Akita (Early Pleistocene cold shallow water Ostracoda). *In*, Organizing Committee of 9th International Symposium on Ostracoda, *9th International Symposium on Ostracoda Guidebook (Excursion 5)*, p. 1-12. Shizuoka University Press, Shizuoka.

Kamiya, T. and Nakagawa, T., 1993: Ostracode fossil assembleges in the Holocene shell bed found in Takahama-cho, Fukui Prefecture, Central Japan. *Bulletin of the Fukui City Natural Museum,* no. 1, p. 115-133.

Kamiya, T., Ozawa, H. and Kitamura, A., 1996: Paleo-water mass structure during the deposition of middle part of the Omma Formation based on the change of ostracode assemblage. *Hokuriku Geology Institute Report*, no. 5, p. 145-165.

Kano, K., Yamauchi, S., Takayasu, K., Matsuura, H. and Bunno, M., 1994: *Geology of the Matsue District. Quadrangle Series Scale 1:50,000, Okayama (12)*, no. 17, p. 1-126. Geological Survey of Japan, Tsukuba. *(in Japanese with English abstract)*

Kingma, J. T., 1948: *Contributions to the Knowledge of the Young-Caenozoic Ostracoda from the Malayan Region*, 119 p. Kemink Printers, Utrecht.

Lord, A. R., 1980: Weichselian (Late Quaternary) ostracods from the Sandnes Clay, Norway. *Geological Magazine*, vol. 117, no. 3, p. 227-242.

Maiya, S. and Inoue, Y., 1973: On the effective treatment of rocks for microfossil analysis. *Fossils (Palaeontological Society of Japan)*, nos. 25/26, p. 87-96. *(in Japanese with English abstract)*

Malz, H., 1982: Plio-/Pleistozäne Buntoniini von SW-Taiwan. *Senckenbergiana Lethaea*, vol. 63, nos. 5/6, p. 377-411.

Mandelstam, M. J., 1960: Ostracoda. *In*, Tschernysheva, E. N. *ed.*, *Fundamentals of Paleontology, Arthropoda Volume*, p. 264-421. State Scientific Technology Publishing House, Moskow. (*in Russian*)

McDougall, K., Brouwers, E.M. and Smith P., 1986: Micropaleontology and sedimentology of the PB Borehole Series, Prudhoe Bay, Alaska. *U.S. Geological Survey Bulletin* 1598, p. 1-62.

McKenzie, K. G., Majoran, S., Emami, V. and Reyment, R. A., 1989: The *Krithe* problem—First test of Peypouquet's hypothesis, with a redescription of *Krithe praetexta praetexta* (Crustacea, Ostracoda). *Palaeogeography, Palaeoclimatology, Palaeoecology*, vol. 74, p. 343-354.

Neale, J. W., 1973: *Cluthia* (Crustacea: Ostracoda), a new Pleistocene and Recent Leptocytherid genus. *Journal of Paleontology*, vol. 47, no. 4, p. 683-688.

Neale, J. W. and Howe, H. V., 1975: The marine Ostracoda of Russian Harbour, Novaya Zemlya and other high latitude faunas. *In*, Swain, F. M. *ed.*, *Biology and Paleobiology of Ostracoda, Bulletins of American Paleontology*, vol. 65, no. 282, p. 381-431.

Nomura, R. and Maiya, S., 1984: Geologic age of the Fujina Formation, Shimane Prefecture, based on planktonic foraminifera. *Memoirs of Natural and Cultural Researches of the San-in Region, Shimane University*, no. 24, p. 1-9. (*in Japanese*)

Norman, A. M., 1865a: Deep-sea dredging on the coasts of Northumberland and Durham in 1864. *British Association for the Advancement of Science Report, 34th Meeting*, p. 189-193.

Norman, A. M., 1865b: Report on the Crustacea. *In*, Brady, G. S. *ed.*, *Reports of the Deep-sea Dredging off the Coasts of Northumberland and Durham*, p. 12-29. *Transactions of the Natural History Society of Northumberland, Durham and Newcastle-upon-Tyne, London.*

Ogasawara, K. and Nomura, R., 1980: Molluscan fossils from the Fujina Formation, Shimane Prefecture, San-in district, Japan. *In*, Igo, H. and Noda, H. *eds.*, *Professor Saburo Kanno Memorial Volume*, p. 79-98. Sasaki Shuppan Co., Sendai.

Otofuji, Y. and Matsuda, T., 1984: Timing of rotational motion of southwest Japan inferred from paleomagnetism. *Earth and Planetary Science Letters*, vol. 70, p. 373-382.

Ozawa, H., 1996: Ostracode fossils from the Late Pliocene to Early Pleistocene Omma Formation in the Hokuriku district, central Japan. *Science Reports of Kanazawa University*, vol.41, no. 2, p. 77-115.

Ozawa, H., Kamiya, T. and Tsukagoshi, A., 1995: Ostracode evidence for the paleoceanographic change of the Middle Pleistocene Jizodo and Yabu Formations in the Boso Peninsula, central Japan. *Science Reports of Kanazawa University*, vol. 40, no. 1, p. 9-37.

Penney, D. N., 1993: Late Pliocene to Early Pleistocene ostracod stratigraphy and palaeoclimate of the Lodin Elv and Kap Køb enhavn formations, East Greenland. *Palaeogeography, Palaeoclimatology, Palaeoecology*, vol. 101, p. 49-66.

Puri, H. S., 1953: The ostracod genus *Hemicythere* and its allies. *Washington Academy of Sciencecs Journal*, vol. 43, no. 6, p. 169-179.

Puri, H. S., 1954: Contribution to the study of the Miocene of the Florida Panhandle. Pt. 3, Ostracoda. *The Florida Geological Survey, Geological Bulletin*, no. 36, p. 215-345.

Rosenfeld, A., 1977: Die rezenten Ostracoden-Arten in der Ostsee. *Meyniana*, vol. 29, p. 11-49.

Ruan, P. and Hao, Y., 1988: 2. Ostracoda. *In*, Research Party of Marine Geology, Ministry of Geology and Mineral Resources, Chinese University of Geoschiences *eds.*, *Quaternary Microbiotas in the Okinawa Trough and their Geological Significance*, p. 227-395. Geological Publishing House, Beijing, China. (*in Chinese with English abstract*)

Ruggieri, G., 1950: Gli Ostracodi delle sabbie grigie quaternarie (Milazziano) di Imola. Parte 1. *Giornale di Geologia, Annali del Museo Geologico di Bologna*, serie 2, vol. 21, p. 1-58.

Ruggieri, G., 1953: Età e fauna di un terrazzo marino sulle costa ioniche della Calabria. *Giornale di Geologia, Annali del Museo Geologico di Bologna, Serie 2a*, vol. 23, p. 17-168.

Sakumoto, T., Seto, K. and Takayasu, K., 1996: Fossil cephalopods from the Middle Miocene Fujina Formation of southwest Japan and its paleoenvironmental significance. *Earth Science (Chikyu Kagaku)*, vol. 50, p. 408-413. (*in Japanese with English abstract*)

Sars, G. O., 1866: Oversigt af Norges marine Ostracoder: Forhandlinger I. *Videnskabs-Selskabet Christiania*, vol. 8, p. 1-130.

Sars, G. O., 1926: *An Account of the Crustacea of Norway, 9 Ostracoda*. Parts 13 and 14, p. 209-240. Bergen Museum, Bergen.

Scott, H. W., 1961: Shell morphology of Ostracoda. *In*, Moore, R. C. *ed.*, *Treatise on Invertebrate Paleontology Part Q. Arthropoda 3 Crustacea, Ostracoda*, Q21-Q37. Geological Society of America and University of Kansas Press.

Swain, F. M., 1961: Ostracoda from the Pleistocene Gubik Formation, Arctic Coastal Plain, Alaska. *In*, Raasch, G. O. *ed.*, *Geology of the Arctic*, vol. 1, p. 600-606. University of Toronto Press, Toronto.

Swain, F. M., 1963: Pleistocene Ostracoda from the Gubik Formation, Arctic Coastal Plain, Alaska. *Journal of Paleontology*, vol. 37, no. 4, p. 798-834.

Swain, F. M. and Gilby, J. M., 1974: Marine Holocene Ostracoda from the Pacific coast of North and Central America. *Micropaleontology*, vol. 20, no. 2, p. 257-352.

Sylvester-Bradley, P. C., 1948: The ostracode genus *Cythereis*. *Journal of Paleontology*, vol. 22, no. 6, p. 792-797.

Tabuki, R., 1986: Plio-Pleistocene Ostracoda from the Tsugaru Basin, North Honshu, Japan. *Bulletin of College of Education, University of the Ryukyus*, no. 29, p. 27-160.

Takayasu, K., 1986: Diversification in the molluscan fauna of the Miocene Izumo Group, San-in district, Southwest Japan. *In*, Kotaka, T. *ed.*, *Japanese Cenozoic Molluscs: Their Origin and Migration, Palaeontological Society of Japan, Special Papers*, no. 29, p. 173-186.

Takayasu, K. and Nakamura, T., 1984: Desmostylia bearing beds in the southern-border of Lake Shinji, West Japan, and their paleoenvironments from the viewpoint of molluscan fossils. *In*, Inuzuka, N. *et al eds.*, *Desmostylians and their Paleoenvironments, Monograph 28, Association for the Geological Collaboration*, p. 91-99. (*in Japanese with English abstract*)

Takayasu, K., Yamasaki, H., Ueda, T., Akagi, S., Matsumoto, T., Nomura, R., Okada, S., Sawada, Y., Yamauchi, S. and Yoshitani, A., 1992: Miocene stratigraphy and paleogeography of San'in district, Southwest Japan. *Memories of the Geological Society of Japan*, no. 37, p. 97-116. (*in Japanese with English abstract*)

Tomita, T. and Sakai, E., 1937: Cenozoic geology of the Huzina-Kimati district, Izumo province, Japan: A contribution to the igneous geology of the East-Asiatic province of Cenozoic alkaline rocks. *Journal of the Shanghai Science Institute, Section 2, Geology, Palaeontology, Mineralogy and Petrology*, vol. 2, 147-204.

Tressler, W. L., 1941: Geology and biology of North Atlantic deep sea cores between Newfoundland and Ireland, part 4, Ostracoda. *U. S. Geological Survey Professional Paper* 196-C, p. 95-103.

Triebel, E., 1949: Mikropaläontologische Kennzeichnung der Ostracoden-Gattungen *Xenocythere* und *Palmenella*. *Senckenbergiana*, vol. 30, nos. 4/6, p. 185-192.

Wagner, F. J. E., 1970: Faunas of the Pleistocene Champlain Sea. *Geological Survey of Canada Bulletin* no. 181, p. 1-104.

Yajima, M., 1982: Late Pleistocene Ostracoda from the Boso Peninsula, central Japan. *In*, Hanai, T. *ed.*, *Studies on Japanese Ostracoda*, *University Museum, University of Tokyo, Bulletin*, no. 20, p. 141-227.

Yajima, M., 1988: Preliminary notes on the Japanese Miocene Ostracoda. *In*, Hanai, T., Ikeya, N. and Ishizaki, K. *eds.*, *Evolutionary Biology of Ostracoda—its Fundamentals and Applications*, p. 1073-1085. Kodansha, Tokyo.

Yajima, M., 1992: Early Miocene Ostracoda from Mizunami, Central Japan. *Bulletin of the Mizunami Fossil Museum*, no. 19, p. 247-268.

Yajima, M. and Lord, A., 1990: The interpretation of Quaternary environments using Ostracoda: an example from Japan. *Proceedings of the Geologists' Association*, vol. 101, no. 2, p. 153-161.

Zhou, B., 1995: Recent ostracode fauna in the Pacific off Southwest Japan. *Memoirs of the Faculty of Science of Kyoto University Series of Geology and Mineralogy*, vol. 57, no. 2, p. 21-98.

Paleontological Research, vol. 6, no. 1, pp. 23-40, April 30, 2002

Stratigraphic and palaeoenvironmental significance of a Pennsylvanian (Upper Carboniferous) palynoflora from the Piauí Formation, Parnaíba Basin, northeastern Brazil

RODOLFO DINO[1] AND GEOFFREY PLAYFORD[2]

[1]*Petrobras/Cenpes, Ilha do Fundão, 21949-900 Rio de Janeiro, Brazil; and Universidade do Estado do Rio de Janeiro (UERJ), Faculdade de Geologia/DEPA, Maracanã, 20559-013 Rio de Janeiro, Brazil (e-mail: dino@cenpes.petrobras.com.br)*

[2]*Department of Earth Sciences, The University of Queensland, Brisbane, Australia 4072 (e-mail: g.playford@earth.uq.edu.au)*

Received 17 September 2001; Revised manuscript accepted 25 November 2001

Abstract. **A well-preserved palynoflora is reported from within a cored interval of a coal-exploratory borehole (1-UN-23-PI of the Geological Survey of Brazil) in the southern part of the Parnaíba Basin, northeastern Brazil. The sample studied is from the lower portion of the Piauí Formation. Its palynoflora is characterized by particular abundance of the trilete cavate/pseudosaccate miospores *Spelaeotriletes triangulus* Neves and Owens, 1966 and *S. arenaceus* Neves and Owens, 1966, together with cingulizonate forms mainly attributable to *Vallatisporites* Hacquebard, 1957 and *Cristatisporites* R. Potonié and Kremp emend. Butterworth *et al.*, 1964. Radially and bilaterally symmetrical monosaccate pollen grains are also well-represented, chiefly by *Plicatipollenites* Lele, 1964 and *Potonieisporites* Bhardwaj, 1954, respectively. Taeniate grains (i.e., monosaccates and bisaccates) are relatively minor constituents of the palynoflora; no marine microplankton were encountered. Several species are described in detail: the trilete apiculate spores *Brevitriletes levis* (Balme and Hennelly) Bharadwaj and Srivastava, 1969 and *Horriditriletes uruguaiensis* (Marques-Toigo) Archangelsky and Gamerro, 1979; and the taeniate pollen grains *Meristocorpus ostentus* sp. nov. and *Lahirites segmentatus* sp. nov. A Pennsylvanian (Late Carboniferous: late Westphalian) age is adduced for the palynoflora via its correlation with part of the Tapajós Group (specifically, the upper Itaituba Formation) of the Amazonas Basin in northern Brazil. The entirely land-derived palynomorphs, associated with abundant plant debris, corroborate previous suggestions that the lower part of the Piauí Formation accumulated in a nonmarine setting under conditions of aridity.**

Key words: biostratigraphy, Brazil, Pennsylvanian, palynology, Parnaíba Basin, Piauí Formation

Introduction

The Carboniferous-Permian rocks of the Palaeozoic basins in north and northeast Brazil provide excellent regional source and reservoir systems for liquid petroleum and gas. Palynology has been applied successfully as a basis for biostratigraphic subdivision of these upper Palaeozoic sequences, although the carbonate and evaporite intervals therein are normally only sparsely, if at all, palyniferous. In the Parnaíba Basin (Figure 1), the Balsas Group, with the Piauí Formation at its base, comprises these younger Palaeozoic deposits. During the Balsas tectonic-depositional cycle, the Parnaíba Basin experienced conditions of severe aridity, and received predominantly continental deposits (Cunha, 1986; Lima Filho, 1991). Lithologies are mainly of sandy, evaporitic, and muddy character and clearly reflect strongly oxidizing conditions of deposition. Such factors obviously tend to militate against their palynostratigraphic potentialities. Accordingly, only a few palynological investigations have been conducted on upper Palaeozoic strata of the Parnaíba Basin. Inferences about age and palaeoenvironment (Müller, 1962) were based on material from exploratory wells drilled by Petrobras. At the beginning of the 1970s, the National Department of Mineral Production (DNPM) initiated research on coal encountered in several wells drilled close to the basin border, but no biostratigraphic analyses were undertaken. The present study concerns the lower part of the Balsas Group, viz., the Piauí Formation, as intersected in one of the DNPM wells. The aims are to determine the chronostratigraphic position of the strata, their possible correlation with other Brazilian Palaeozoic basins, and their environment of deposition.

The section of the 1-UN-23-PI well, investigated herein,

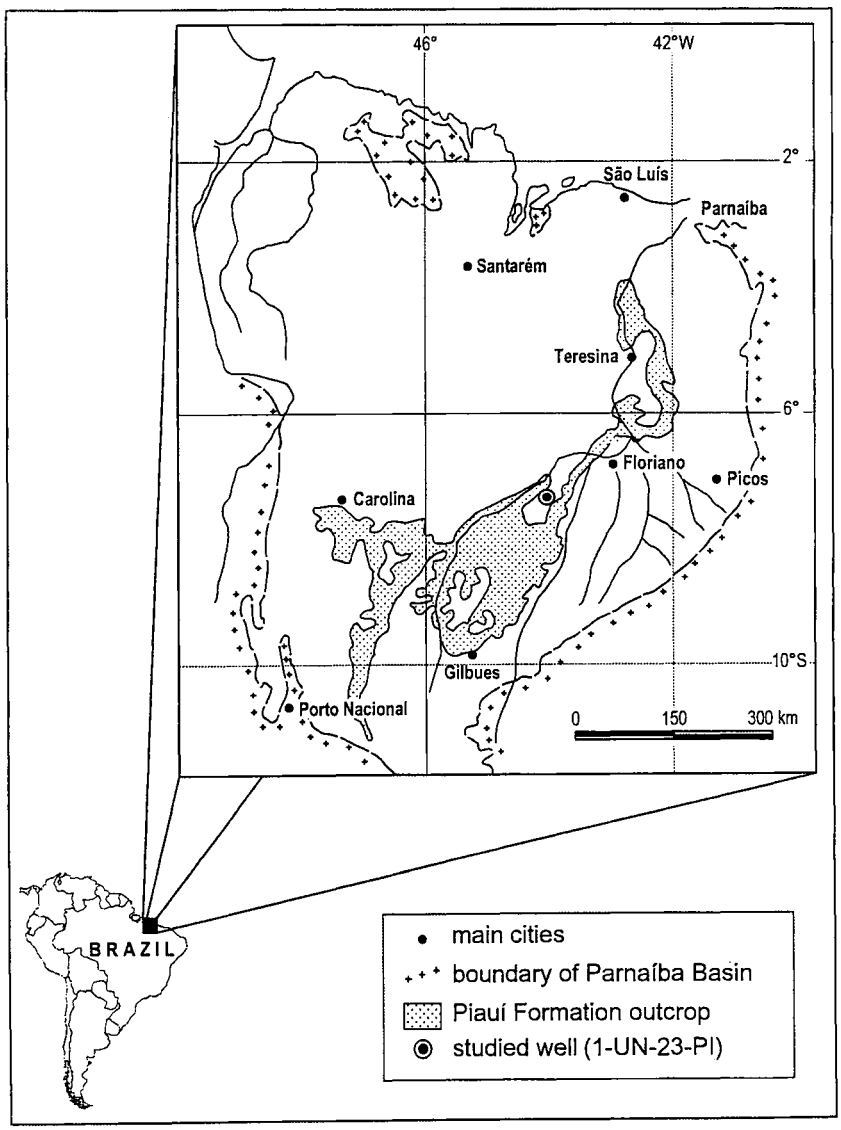

Figure 1. Locality map, Parnaíba Basin, northeastern Brazil, indicating site of borehole (1-UN-23-PI of the Geological Survey of Brazil) sampled for this study.

provides the first spore-pollen inventory for the lower part of the Piauí Formation. Obviously, a comprehensive palynological evaluation of the whole formation would necessarily be based on systematic sampling through the vertical extent of the formation, as developed in the subsurface and in outcrop.

As discussed subsequently, the identified spore-pollen assemblage can be compared, for purposes of stratal correlation, with those that characterize palynostratigraphic units established elsewhere; particularly the Upper Carboniferous-Permian palynozones defined in the Tapajós Group of the Amazonas Basin, northern Brazil (Playford and Dino, 2000b). Palaeoenvironmental implications of the Piauí palynoflora are somewhat limited, and are considered in concert with physical evidence advanced by previous workers.

Outline of stratigraphy

The Parnaíba Basin is essentially a Palaeozoic basin, but includes a cover of younger (Mesozoic and Cenozoic) strata. It is a substantial intracratonic entity, occupying some 600,000 km^2 in the western part of Brazil's northeastern region and positioned among fold belts that border the Guaporé, São Luiz, and San Francisco cratons. Total stratal thickness is *ca.* 3500 m, of which 2900 m comprise Palaeozoic sediments and the remainder are Mesozoic and Cenozoic deposits. The basin's Palaeozoic succession is divi-

sible into three major sedimentary cycles related to different tectonic, structural, and climatic circumstances. In ascending order, these cycles are manifested lithostratigraphically by what are termed the Serra Grande, Canindé, and Balsas Groups.

The initial cycle, of Silurian age, began with the tectonic-thermal development of a large depression in which fluvial, deltaic, and shallow marine sediments of the Serra Grande Group accumulated (Cunha, 1986; Góes and Feijó, 1994). With continuing tectonic evolution, the Canindé Group (of the second cycle) was deposited during Devonian-Early Carboniferous time. This consists of deltaic and shallow marine to paralic deposits at the base, grading upwards into fluvial-deltaics and periglacials, and culminating with fluvial-deltaic and storm-related deposits. The final (Balsas) Palaeozoic cycle in the basin commenced in the Pennsylvanian and extended through the Permian until earliest Triassic time. It followed pronounced uplift that exposed and eroded much of the Brazilian, indeed South American, platform. Accordingly, the Parnaíba Basin experienced strong erosion, as evidenced by its extensive and well-developed pre-Balsas unconformity. Moreover, the climate changed markedly: from the temperate and humid climates of the preceding cycles to conditions characterized by increasing heat and aridity (Mesner and Wooldridge, 1962, 1964). The sediments of this third phase signify dominantly continental conditions, with occasional marine incursions that became increasingly evaporitic.

Piauí Formation

The term Piauí was introduced by Small (1914) to designate—as "Série Piauí"—the entire Palaeozoic section of the Parnaíba Basin. Its application was later restricted (Duarte, 1936) to constitute—as the Piauí Formation—the lowest of four formations that embody the basin's youngest Palaeozoic sedimentary cycle (Balsas Group). This usage is still widely accepted and is adopted herein. The Piauí Formation is a predominantly clastic sedimentary unit, developed widely in the Parnaíba Basin and resting unconformably upon the Canindé Group. The formation crops out in a broad, almost continuous strip along the eastern and southern margins of the basin and discontinuously to the west (Andrade and Daemon, 1974; Suguio and Fulfaro, 1977). Its maximum thickness of *ca.* 350 m is encountered in the subsurface.

Mesner and Wooldridge (1964) proposed a twofold subdivision of the Piauí Formation. The lower part consists of pink to red sandstone; the upper part comprises alternating green and red shales, thin anhydrite beds, pink dolomite, and red or pale grey carbonate beds containing marine fossils. Lima Filho (1991), while maintaining the binary subdivision, modified slightly the Piauí Formation's limits. He recognized several depositional systems in the formation, in particular citing evidence of aeolian and deltaic sedimentation and, towards the top, an episode of shallow marine, carbonate deposition. Accordingly, Lima Filho (1991) concluded that the Piauí Formation accumulated under arid conditions in a setting that included an extensive interior desert and an evaporitic marine basin.

The Piauí Formation consists chiefly of continental redbeds, aeolian sandstones, and fluvial deposits. However, brief marine incursions are attested by the presence of richly fossiliferous carbonate platform or lagoonal sediments, particularly in the formation's upper part as developed in the basin's northeastern sector. Known locally by such names as Mocambo, Contendas, Meruoca, Carimã, Vidalgo, and Boa Esperança, these marine strata become increasingly evaporitic upsection, providing evidence of progressive aridity. The marine faunas, though mostly undescribed, are diverse. They include bivalves, gastropods, cephalopods, brachiopods, trilobites, bryozoans, and echinoderms (crinoids especially), together with conodonts, agglutinated and calcareous Foraminifera, ostracodes, micro-molluscs, and other microfossils (see Duarte, 1936; Kegel, 1951; Kegel and Costa, 1951; Mesner and Wooldridge, 1964; Campanha and Rocha Campos, 1979; Assis, 1980). Faunal affinities between the Piauí Formation and the Itaituba Formation of the Amazonas Basin - as noted by such authors as Mendes (1966), Tengan *et al.* (1976), Campanha and Rocha Campos (1979), and Assis (1980) - support the hypothesis of a marine connection between the Parnaíba and Amazonas Basins during Pennsylvanian time.

Material and methods

This study is based on material from a continuously cored well designated as 1-UN-23-PI and located in the state of Piauí, municipal district of Antonio Almeida, at latitude 7° 15′ 18″ South, longitude 44° 12′ 24″ West, in the southern Parnaíba Basin (Figure 1). Three samples were collected from the depth interval 137.6–145.8 m, representative of the top of the Piauí Formation's lower portion (Figure 2). Of these samples, only one (a grey siltstone, at 145.0 m) proved palyniferous, yielding an abundant and well-preserved palynoflora. The two unproductive samples, collected at depths of 137.6 m and 145.8 m, are both greenish grey shales.

Conventional physico-chemical methods were applied in the laboratory preparation of the samples, specifically those outlined in Playford and Dino (2000a, p. 10–12). Light-microscope photographs of palynomorphs were taken with a Zeiss MC 80 DX camera coupled with a Zeiss Axioplan microscope using Kodak T-Max (100 ASA) film. Scanning electron microscopy assisted in the identification of several species.

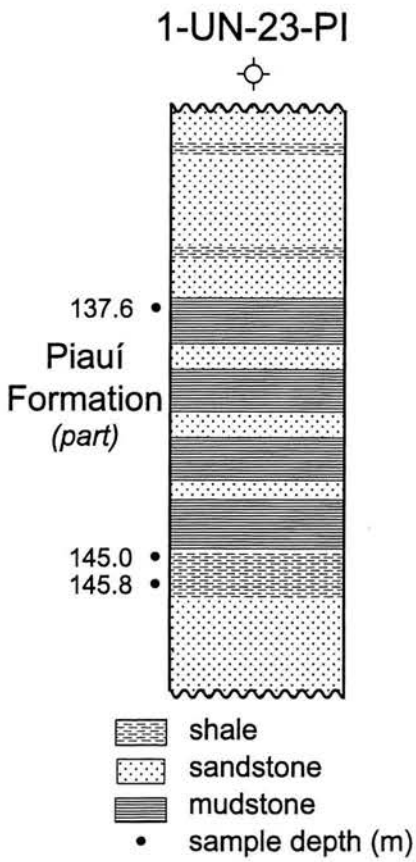

Figure 2. Portion of 1-UN-23-PI litholog showing palynologically sampled interval of Piauí Formation.

Composition of palynoflora

The palynoflora recovered from the productive Piauí sample is dominated by pteridophytic trilete spores and gymnospermous monosaccate pollen grains occurring in almost equal proportions (each accounting for ca. 45% of the total assemblage). Taeniate bisaccate grains are relatively minor constituents (ca. 7%). In addition, fresh or brackish water green algae (*Botryococcus, Brazilea*) have been recovered. No palaeomicroplanktic elements were encountered.

Given below is an inventory of all palynomorph taxa identified. The large majority of these are illustrated by light micrographs (Figures 3, 5–8) and a few also by scanning electron micrographs (Figures 4, 9). In the systematic section, four species (asterisked hereunder) are described in detail, and brief notes are appended on discrimination of the two *Spelaeotriletes* species encountered. Illustrated specimens are listed in relevant figure captions with slide number followed by microscope-stage coordinates (per standard "England Finder" slide). Permanent repository of the specimens is Petrobras/Cenpes/Divex/Sebipe, Cidade Universitária, Quadra 7, Ilha do Fundão, 21949-900 Rio de Janeiro, RJ, Brazil.

Spores

Anteturma Proximegerminantes R. Potonié, 1970
Turma Triletes Reinsch emend. Dettmann, 1963
Suprasubturma Acavatitriletes Dettmann, 1963
Subturma Azonotriletes Luber emend. Dettmann, 1963
Infraturma Laevigati Bennie and Kidston emend. R. Potonié, 1956
Leiotriletes sp. [Figure 3.7]
Calamospora sp. cf. *C. sinuosa* Leschik, 1955 [Figure 3.1]
Punctatisporites gretensis Balme and Hennelly, 1956 [Figure 3.5]
Punctatisporites sp. [Figure 3.6]
Infraturma Apiculati Bennie and Kidston emend. R. Potonié, 1956
Subinfraturma Granulati Dybová and Jachowicz, 1957
Granulatisporites austroamericanus Archangelsky and Gamerro, 1979 [Figures 3.2, 3.3, 4.1]
Cyclogranisporites minutus Bhardwaj, 1957 [Figure 3.4]
Subinfraturma Nodati Dybová and Jachowicz, 1957
"*Acanthotriletes*" *menendezii* Gonzales-Amicon, 1973 [Figure 3.8]
**Brevitriletes levis* (Balme and Hennelly) Bharadwaj and Srivastava, 1969 [Figure 3.9]
Subinfraturma Baculati Dybová and Jachowicz, 1957
Horriditriletes ramosus (Balme and Hennelly) Bharadwaj and Salujha, 1964 [Figures 3.11, 4.2]
**Horriditriletes uruguaiensis* (Marques-Toigo) Archangelsky and Gamerro, 1979 [Figures 3.10, 4.3, 4.4]
Baculatisporites sp.
Raistrickia cephalata Bharadwaj, Kar, and Navale, 1976 [Figures 3.12, 9.3]
Raistrickia sp. cf. *R. saetosa* (Loose) Schopf, Wilson, and Bentall, 1944 [Figure 3.13]
Raistrickia sp.
Subinfraturma Verrucati Dybová and Jachowicz, 1957

➡ **Figure 3.** **1.** *Calamospora* sp. cf. *C. sinuosa*, ×500, 20005916E, K/42. **2, 3.** *Granulatisporites austroamericanus*; **2**, ×750, 20005916/3, Y45/2; **3**, ×750, 20005916/3, R51. **4.** *Cyclogranisporites minutus*, ×750, 20005916D, M36/3. **5.** *Punctatisporites gretensis*, ×750, 20005916E, M49/2. **6.** *Punctatisporites* sp., ×500, 20005916D, P55. **7.** *Leiotriletes* sp., ×750, 20005916B, N39/2. **8.** *"Acanthotriletes" menendezii*, ×1000, 20005916D, H39. **9.** *Brevitriletes levis*, ×750, 20005916/1, A64/3. **10.** *Horriditriletes uruguaiensis*, ×1000, 20005916D, O38/1. **11.** *Horriditriletes ramosus*, ×500, 20005916D, W48/3. **12.** *Raistrickia cephalata*, ×750, 20005916E, V50/3. **13.** *Raistrickia* sp. cf. *R. saetosa*, ×750, 20005916/1, B57. **14.** *Verrucosisporites* sp. cf. *V. morulatus*, ×750, 20005916/2, U66.

Verrucosisporites andersonii Backhouse, 1988 [Figure 5.1, 5.2]

Verrucosisporites sp. cf. *V. morulatus* (Knox) Smith and Butterworth, 1967 [Figure 3.14]

Suprasubturma Laminatitriletes Smith and Butterworth, 1967

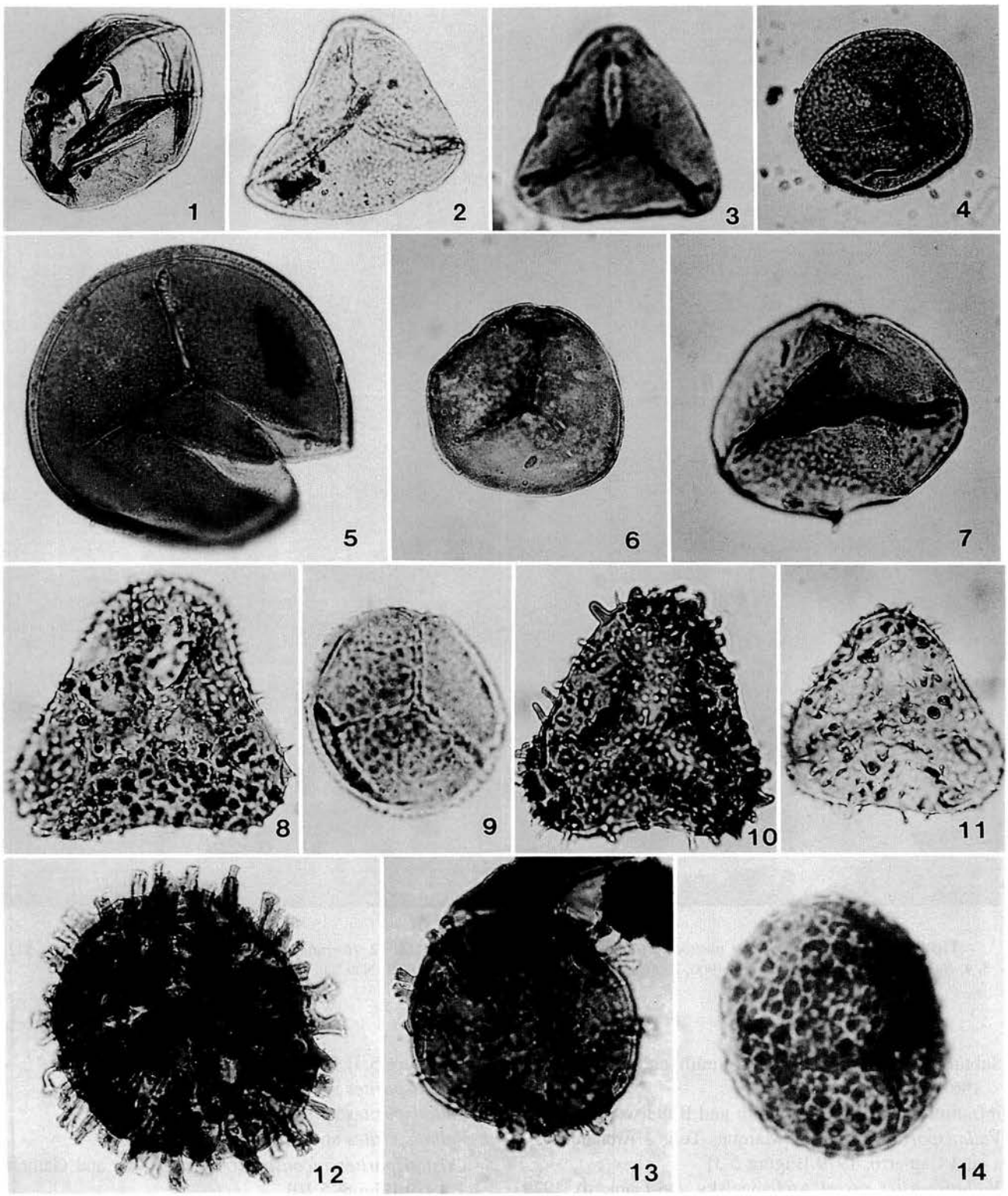

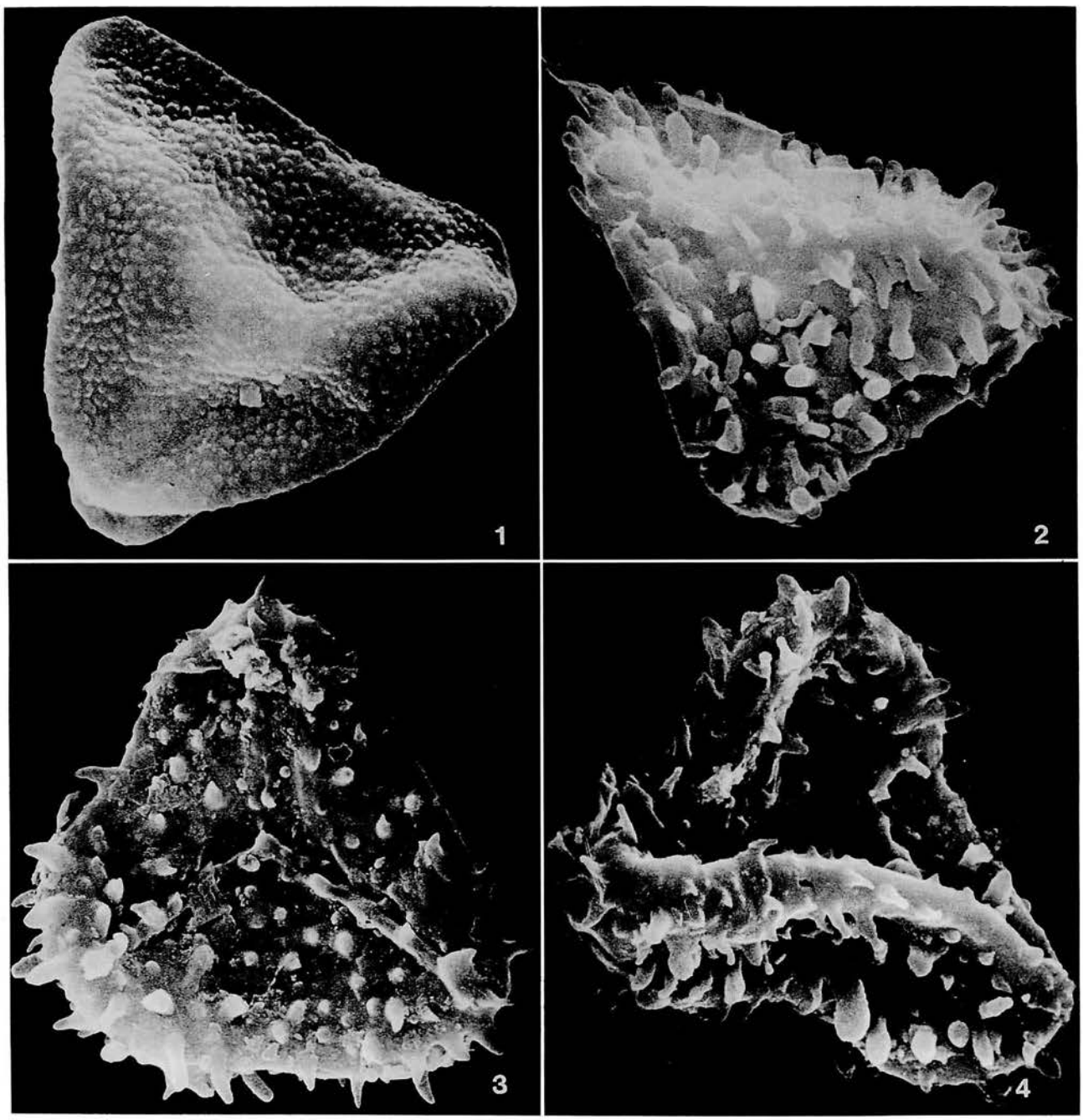

Figure 4. **1.** *Granulatisporites austroamericanus*, ×1900, 20005916/S1, S41/2. **2.** *Horriditriletes ramosus*, ×2000, 20005916/S1, S42. **3, 4.** *Horriditriletes uruguayensis*; **3**, ×1900, 20005916/S1, Q41; **4**, ×2300, 20005916/S1, N39.

Subturma Zonolaminatitriletes Smith and Butterworth, 1967

Infraturma Cingulicavati Smith and Butterworth, 1967

Vallatisporites arcuatus (Marques-Toigo) Archangelsky and Gamerro, 1979 [Figure 5.3]

Vallatisporites russoi Archangelsky and Gamerro, 1979 [Figure 5.4]

Vallatisporites sp. 1 [Figure 5.5]

Vallatisporites sp. 2 [Figure 5.6]

Vallatisporites sp. 3 [Figure 5.7]

Cristatisporites inconstans Archangelsky and Gamerro, 1979 [Figure 5.10]

Suprasubturma Pseudosaccititriletes Richardson, 1965
Infraturma Monopseudosacciti Smith and Butterworth, 1967
Spelaeotriletes arenaceus Neves and Owens, 1966 [Figure 5.9]
Spelaeotriletes triangulus Neves and Owens, 1966 [Figure 5.8]
Turma Monoletes Ibrahim, 1933
Suprasubturma Acavatomonoletes Dettmann, 1963
Subturma Azonomonoletes Luber, 1935
Infraturma Laevigatomonoleti Dybová and Jachowicz, 1957
Laevigatosporites vulgaris (Ibrahim) Ibrahim, 1933 [Figure 5.11]
Infraturma Sculptatomonoleti Dybová and Jachowicz, 1957
Striatosporites heyleri (Doubinger) emend. Playford and Dino, 2000a [Figure 5.12]

Pollen grains

Anteturma Variegerminantes R. Potonié, 1970
Turma Saccites Erdtman, 1947
Subturma Monosaccites Chitaley emend. R. Potonié and Kremp, 1954
Infraturma Aletesacciti Leschik, 1955
Florinites occultus Habib, 1966 [Figure 6.10]
Florinites sp. [Figure 5.13]
Infraturma Vesiculomonoraditi Pant, 1954
Potonieisporites brasiliensis (Nahuys, Alpern, and Ybert) emend. Archangelsky and Gamerro, 1979 [Figure 6.5]
Potonieisporites densus Maheshwari, 1967 [Figure 6.11]
Potonieisporites elegans (Wilson and Kosanke) Wilson and Venkatachala emend. Habib, 1966 [Figure 6.3]
Potonieisporites neglectus Potonié and Lele, 1961
Potonieisporites novicus Bhardwaj, 1954 [Figure 6.2]
Potonieisporites ovatus (Kar) Gutiérrez, 1993 [Figure 6.9]
Potonieisporites simplex Wilson, 1962 [Figure 6.1]
Potonieisporites triangulatus Tiwari, 1965 [Figure 6.8]
Potonieisporites sp. [Figure 7.4]
Peppersites ellipticus Ravn, 1979 [Figure 6.7]
Caheniasaccites ovatus Bose and Kar emend. Gutiérrez, 1993
Costatascyclus crenatus Felix and Burbridge emend. Urban, 1971 [Figure 6.4]
Infraturma Triletesacciti Leschik 1955
Cannanoropollis densus (Lele) Bose and Maheshwari, 1968 [Figure 7.5]
Cannanoropollis korbaensis (Bharadwaj and Tiwari) Foster, 1975 [Figure 6.6]
Plicatipollenites gondwanensis (Balme and Hennelly) Lele, 1964 [Figure 7.6]
Plicatipollenites trigonalis Lele, 1964
Infraturma Striasacciti Bharadwaj, 1962
Striomonosaccites ovatus Bharadwaj, 1962 [Figures 7.9, 9.1]
Meristocorpus explicatus Playford and Dino, 2000 [Figure 8.6]
**Meristocorpus ostentus* sp. nov. [Figure 7.1–7.3]
Subturma Disaccites Cookson, 1947
Infraturma Disaccitrileti Leschik, 1955
Limitisporites sp.
Infraturma Striatiti Pant, 1954
Illinites unicus Kosanke, 1950 [Figure 7.7]
Protohaploxypinus amplus (Balme and Hennelly) Hart, 1964 [Figure 8.4]
Protohaploxypinus bharadwajii Foster, 1979 [Figures 7.8, 8.3]
Protohaploxypinus sp. cf. *Striatopodocarpites magnificus* Bharadwaj and Salujha, 1964 [Figure 8.5]
Striatopodocarpites sp. cf. *S. phaleratus* (Balme and Hennelly) Hart, 1964 [Figure 7.10]
Striatoabieites sp. cf. *S. anaverrucosus* Archangelsky and Gamerro, 1979 [Figure 8.7]
Taeniaesporites sp. [Figure 8.8]
**Lahirites segmentatus* sp. nov. [Figures 8.1, 8.2, 9.2, 9.4]
Striatopodocarpites sp. [Figure 8.9]
Turma Plicates Naumova emend. R. Potonié, 1960
Subturma Monocolpates Iversen and Troels-Smith, 1950
Cycadopites sp.
Sculptured monocolpate form indet. [Figure 7.12]

Green algae (division Chlorophyta)

Class Chlorophyceae, order Chlorococcales
Botryococcus braunii Kützing, 1849
Class Zygnemaphyceae
Brazilea scissa (Balme and Hennelly) Foster, 1975 [Figure 7.11]

Systematic palaeontology

Genus ***Brevitriletes*** Bharadwaj and Srivastava, 1969

Type species.—*Brevitriletes communis* Bharadwaj and Srivastava, 1969; by original designation.

Brevitriletes levis (Balme and Hennelly) Bharadwaj and Srivastava, 1969

Figure 3.9

Apiculatisporites levis Balme and Hennelly, 1956, p. 246–247, pl. 2, figs. 19–21.

Brevitriletes levis (Balme and Hennelly) Bharadwaj and Srivastava, 1969, p. 226–227, pl. 1, figs. 17–20.

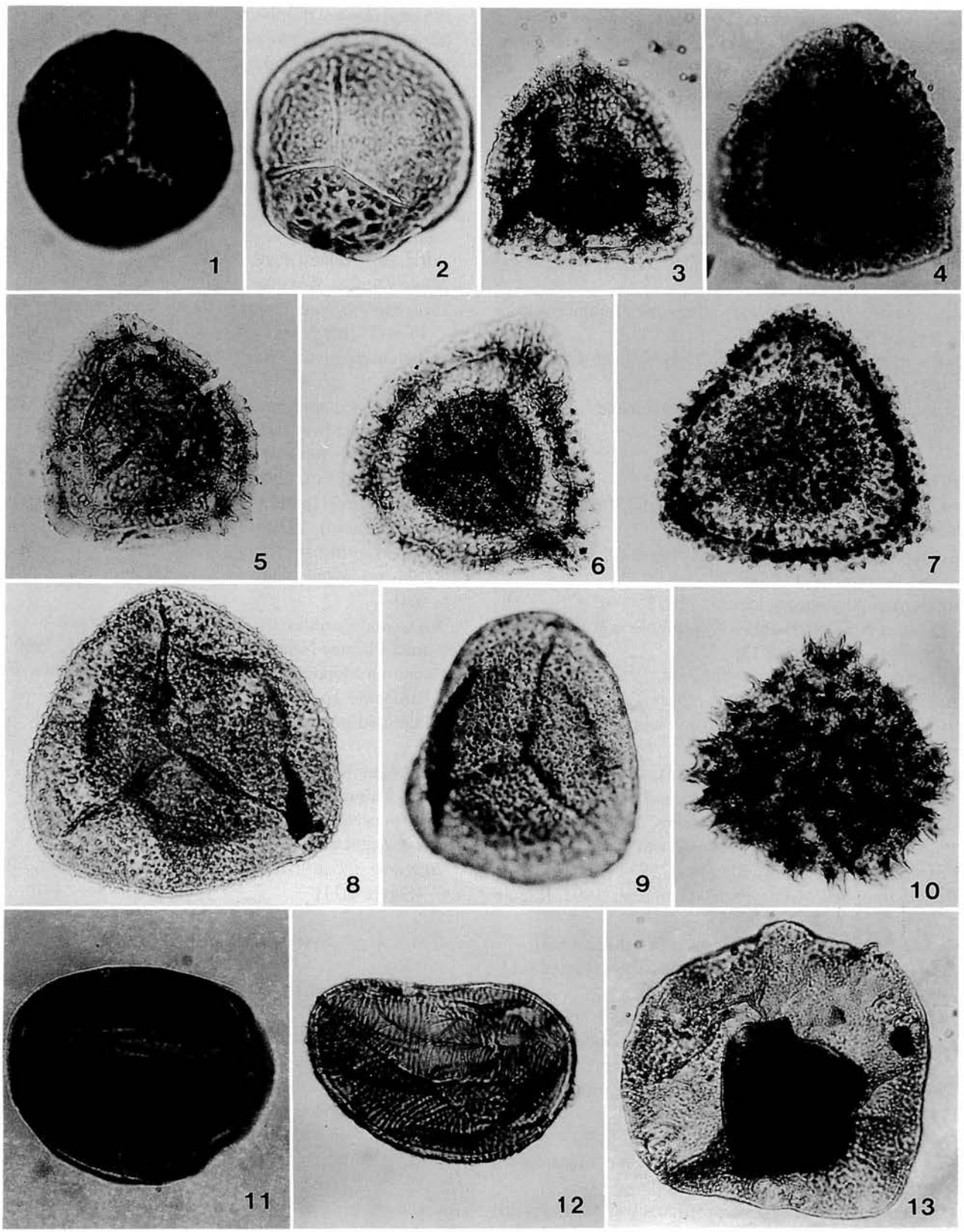
1
2
3
4
5
6
7
8
9
10
11
12
13

Anapiculatisporites ? variornatus Menéndez and Azcuy, 1969, p. 88, 90; pl. 3, figs. A–H.

Apiculiretusispora variornata (Menéndez and Azcuy) Menéndez and Azcuy, 1971, p. 28.

Retusotriletes baculiferus Ybert, 1975, p. 186, pl. 1, figs. 21–23.

non *Apiculatisporis* [sic] *levis* Balme and Hennelly; Césari, Archangelsky, and Seoane, 1995, p. 78; pl. 1, fig. 2.

For further synonymy see Foster (1979, p. 35).

Description.—Spores radial, trilete. Amb circular, subcircular, or very broadly rounded subtriangular. Laesurae distinct, straight, extending almost to equatorial periphery; simple or accompanied by narrow and somewhat irregular lips; frequently terminating in ± distinct curvaturae imperfectae. Exine 1.5–2 μm thick, sculptured distally and equatorially with small, discrete, apiculate elements comprising spinae, coni, and galeae, 1.2–2.5 μm long (usually *ca.* 1.5–2 μm), 0.5–2 μm in basal diameter, spaced 0.5–2 μm apart. Proximal surface laevigate or very sparsely and finely spinose/conate; sometimes polumbrate, with thickened (darkened) interradii emphasizing contact areas or parts thereof.

Dimensions (25 specimens).—Equatorial diameter, excluding sculptural projections, 22 (30) 37 m.

Remarks and comparison.—The specimens described above are in close accord with those described originally (Balme and Hennelly, 1956) and subsequently (Backhouse, 1991, 1993) from the Collie Coal Measures (Permian) of southwestern Australia, and also with Foster's (1979) material from Permian strata of the Bowen Basin, Queensland. In degraded specimens, the apiculate sculptural projections tend to exhibit decapitate or otherwise blunted termini and may thus resemble bacula. In terms of coarseness of sculpture, a morphological continuum exists among specimens belonging to *Brevitriletes levis* (Balme and Hennelly) Bharadwaj and Srivastava, 1969 (cf. Backhouse, 1991, p. 263).

Ybert's (1975) photomicrographs of his species *Retusotriletes baculiferus* leave no doubt as to its synonymy with *Brevitriletes levis*. The same is considered applicable to *Apiculiretusispora variornata* (Menéndez and Azcuy) Menéndez and Azcuy, 1971; see also Césari and Gutiérrez (2001, pl. 2, fig. 6). A specimen recorded by Césari *et al.* (1995, see above synonymy) as *Apiculatisporis* (sic) *levis* differs from the latter in having sparser, essentially rod-like sculpturing elements.

Previous records.—Known widely from the uppermost Carboniferous and Permian of Gondwana. South American reports include those from Argentina (Menéndez and Azcuy, 1969, 1971; Mautino *et al.*, 1998; Vergel, 1998; Césari and Gutiérrez, 2001) and Brazil (Ybert, 1975; Burjack, 1978; Marques-Toigo, 1988).

Genus ***Horriditriletes*** Bharadwaj and Salujha, 1964

Type species.—*Horriditriletes curvibaculosus* Bharadwaj and Salujha, 1964; by original designation.

Discussion.—Foster (1979, p. 38) has clarified the diagnoses and differential diagnoses of *Horriditriletes* Bharadwaj and Salujha, 1964 and its type species.

Horriditriletes uruguaiensis (Marques-Toigo) Archangelsky and Gamerro, 1979

Figures 3.10, 4.3, 4.4

Neoraistrickia uruguaiensis Marques-Toigo, 1974, p. 604, pl. 1, figs. 4, 5.

Neoraistrickia baculicapillosa Pons, 1976, p. 120–121, pl. 2, figs. 14–16.

Horriditriletes uruguaiensis (Marques-Toigo) Archangelsky and Gamerro, 1979, p. 424–426.

Description.—Spores radial, trilete. Amb subtriangular with straight or slightly concave sides and broadly rounded apices. Laesurae more or less distinct, straight, extending at least three-quarters of distance to equator, infrequently with narrow lip development. Exine 1–1.8 μm thick, sculptured irregularly and heterogeneously with bacula (mainly), associated with verrucae, coni, spinae, and clavae of similar dimensions. Sculptural elements discrete and developed comprehensively, but more conspicuous distally and equatorially; length usually 1–4 μm, bases 0.8–2.5 μm in diameter and spaced 0.5–6 μm apart.

Dimensions (20 specimens).—Equatorial diameter, excluding sculptural projections, 33 (43) 60 μm.

Comparison.—*Horriditriletes uruguaiensis* (Marques-Toigo) Archangelsky and Gamerro, 1979 is distinguished from the type species (see Bharadwaj and Salujha, 1964, p. 193–194, pl. 2, figs. 34–39) by its larger size and more densely distributed sculpture; and from *H. ramosus* (Balme and Hennelly) Bharadwaj and Salujha, 1964, which has more uniformly baculate sculpture and subtriangular amb typically with slightly convex sides (Balme and Hennelly, 1956, p. 249, pl. 3, figs. 39–41).

← **Figure 5.** 1, 2. *Verrucosisporites andersonii*; **1**, ×750, 20005916/3, A49; **2**, ×750, 20005916/3, A47. **3**, *Vallatisporites arcuatus*, ×500, 20005916/3, D39. **4**, *Vallatisporites russoi*, ×750, 20005916/3, C54. **5**, *Vallatisporites* sp. 1, ×500, 20005916D, R39/3. **6**, *Vallatisporites* sp. 2, ×500, 20005916D, O36/4. **7**, *Vallatisporites* sp. 3, ×500, 20005916D, E50. **8**, *Spelaeotriletes triangulus*, ×750, 20005916D, F48/4. **9**, *Spelaeotriletes arenaceus*, ×750, 20005916D, O44. **10**, *Cristatisporites inconstans*, ×500, 20005916D, D48/4. **11**, *Laevigatosporites vulgaris*, × 750, 20005916E, H37/2. **12**, *Striatosporites heyleri*, ×500, 20005916D, S52. **13**, *Florinites* sp., ×500, 20005916D, S57.

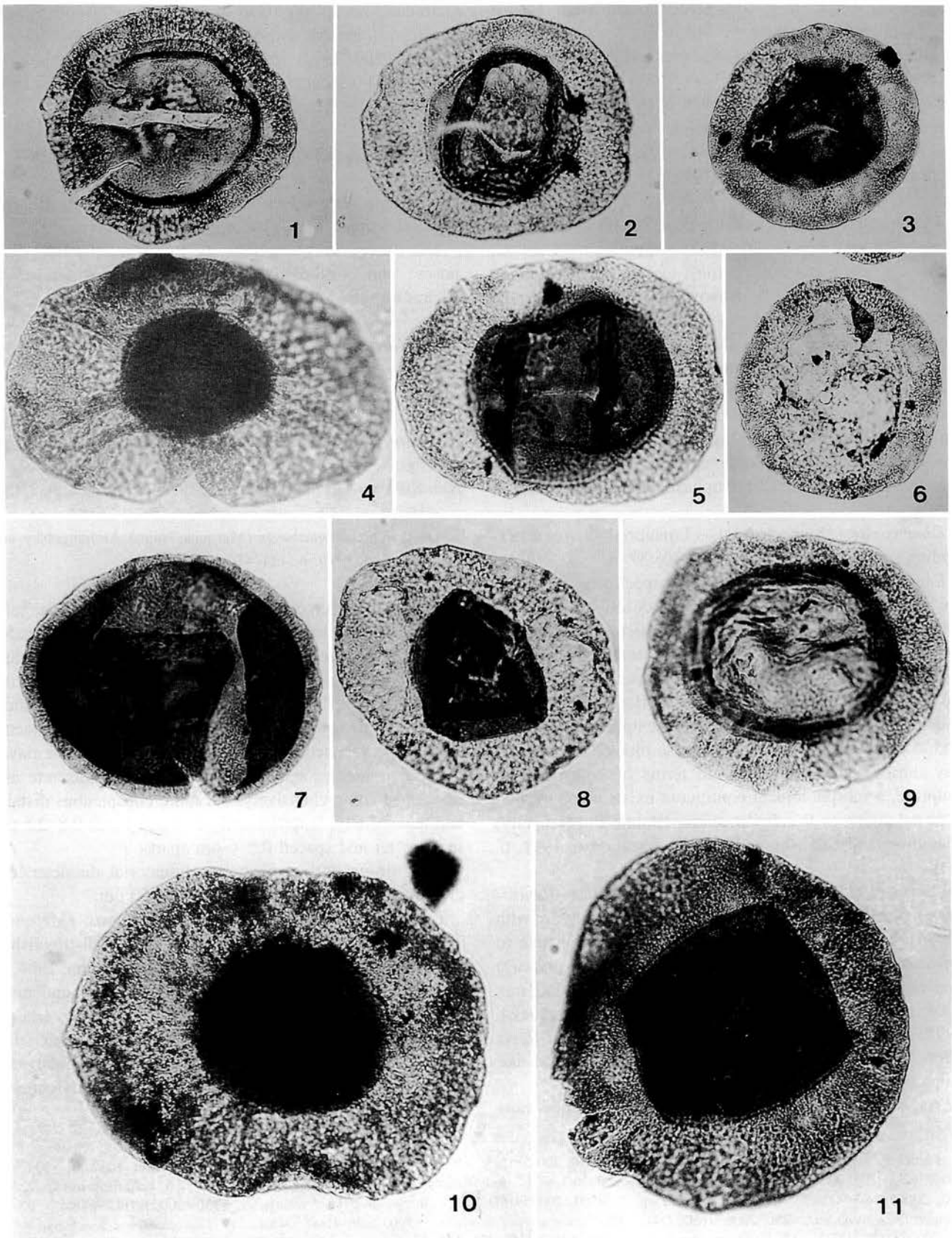
1
2
3
4
5
6
7
8
9
10
11

Previous records. — Originally described (Marques-Toigo, 1974) from the Lower Permian of Uruguay, *Horriditriletes uruguaiensis* has been recorded subsequently in rocks of similar age from there and from Brazil and Argentina (e.g., Pons, 1976; Archangelsky and Gamerro, 1979; Marques-Toigo, 1988; Beri and Goso, 1996; Dias, 1994; Césari *et al.*, 1995; Beri and Aguilar, 1998; Vergel, 1998). According to Césari and Gutiérrez (2001), this species occurs in the Upper Carboniferous-Lower Permian interval of central western Argentina.

Genus ***Spelaeotriletes*** Neves and Owens, 1966

Type species. — *Spelaeotriletes triangulus* Neves and Owens, 1966; by original designation.

Discussion. — Playford *et al.* (2001) have provided a comprehensive review of *Spelaeotriletes* Neves and Owens, 1966 in terms of its diagnosis, differential diagnosis, and Gondwanan representation.

Spelaeotriletes is represented commonly in the Piauí palynoflora by two species that were instituted concurrently by Neves and Owens (1966) and share very similar morphological attributes; *viz.*, the type species *S. triangulus* (Figure 5.8) and *S. arenaceus* (Figure 5.9). Both species were described in detail by Playford and Dino (2000a, p. 21–22, pl. 5, figs. 1–7; pl. 6, figs. 5, 6) on the basis of numerous well-preserved specimens they encountered in the Pennsylvanian portion of the upper Palaeozoic Tapajós Group, Amazonas Basin. The difficulties that may arise in satisfactorily separating these species from each other have been discussed by Playford and Dino (2000a) and Playford *et al.* (2001); see also Spinner and Clayton (1973, p. 161), Playford and Powis (1979, p. 391), and Ravn and Fitzgerald (1982, p. 144). Pending re-examination of the respective type specimens of *S. triangulus* and *S. arenaceus*, and study of possible topotype material, the species are here distinguished - albeit somewhat provisionally as, for instance, in Playford *et al.* (2001)— in accordance with Neves and Owens's (1966, p. 345–346) original criteria (principally sculptural). These are that the exoexine (i.e., outside of the virtually laevigate contact faces) bears sculpturing elements that are generally coarser and more densely and regularly distributed in *S. triangulus* than in *S. arenaceus.*

Previous records.—*S. arenaceus* and *S. triangulus* have been reported widely, either individually or as a single merged specific entity, from upper Palaeozoic (more particularly, lower-middle Pennsylvanian) strata of both northern and southern hemispheres (Playford and Dino, 2000a, p. 21).

Genus ***Meristocorpus*** Playford and Dino, 2000b

Type species.—*Meristocorpus explicatus* Playford and Dino, 2000b; by original designation (monotypic).

Meristocorpus ostentus sp. nov.

Figure 7.1–7.3

Meristocorpus sp. C of Playford and Dino, 2000b, p. 100, pl. 4, figs. 1, 2.

Diagnosis. — Pollen grains bilateral, monosaccate, taeniate, monolete. Amb transversely oval to elongate, ends rounded. Laesura distinct to perceptible, straight or somewhat curved, length variable. Outline of corpus (in polar view) similar to amb, exine 1–1.5 µm thick; proximal surface bearing 5–12 subparallel taeniae, mostly continuous, infrequently bifurcating, each 3–8 µm wide, with intervening clefts 0.5–1.5 µm wide. A pair of straight to broadly curved folds developed marginally across corpus and marking saccus attachments thereto. Saccus relatively narrow where adjoining transverse sides of corpus, with greatest development about longitudinal sides ("ends") of corpus; fine to medium endoreticulum evident in well-preserved specimens.

Dimensions (19 specimens, in polar aspect).—Overall breadth 82 (92) 110 µm; overall length 34 (48) 65 µm. Corpus breadth 55 (70) 82 µm; corpus length 27 (43) 60 µm.

Holotype.—Slide 20005916/3, S38/1; Figure 7.3. Proximal aspect. Amb transversely elongate-oval; overall length 47 µm, width 88 µm; corpus well-defined, 43 µm long, 72 µm wide, outline closely conforming with amb, proximal face modified by 7 subparallel transverse taeniae extending for full corpus breadth, some bifurcation but mainly continuity; longitudinal corpus margins with prominent, straight to outwardly convex folds; maximum sacci development about corpus ends; sacci with fine endoreticulation; laesura perceptible, slightly curved, length 13 µm.

Type locality.—Brazil, Parnaíba Basin, Piauí Formation; 1-UN-23-PI well, core, 145.0 m.

Etymology.— From the Latin, *ostentus*, stretched out.

← **Figure 6.** 1. *Potonieisporites simplex*, ×500, 20005916C, P34/1. **2.** *Potonieisporites novicus*, ×500, 20005916C, G34/4. **3.** *Potonieisporites elegans*, ×500, 20005916C, D44/3. **4.** *Costatascyclus crenatus*, ×500, 20005916/3, T57/3. **5.** *Potonieisporites brasiliensis*, ×750, 20005916A, M37/4. **6.** *Cannanoropollis korbaensis*, ×500, 20005916C, D39/4. **7.** *Peppersites ellipticus*, ×500, 20005916C, A39/2. **8.** *Potonieisporites triangulatus*, ×500, 20005916C, J41/2. **9.** *Potonieisporites ovatus*, ×500, 20005916B, T41/4. **10.** *Florinites occultus*, ×500, 20005916/2, U66. **11.** *Potonieisporites densus*, ×500, 20005916/3, C48/4.

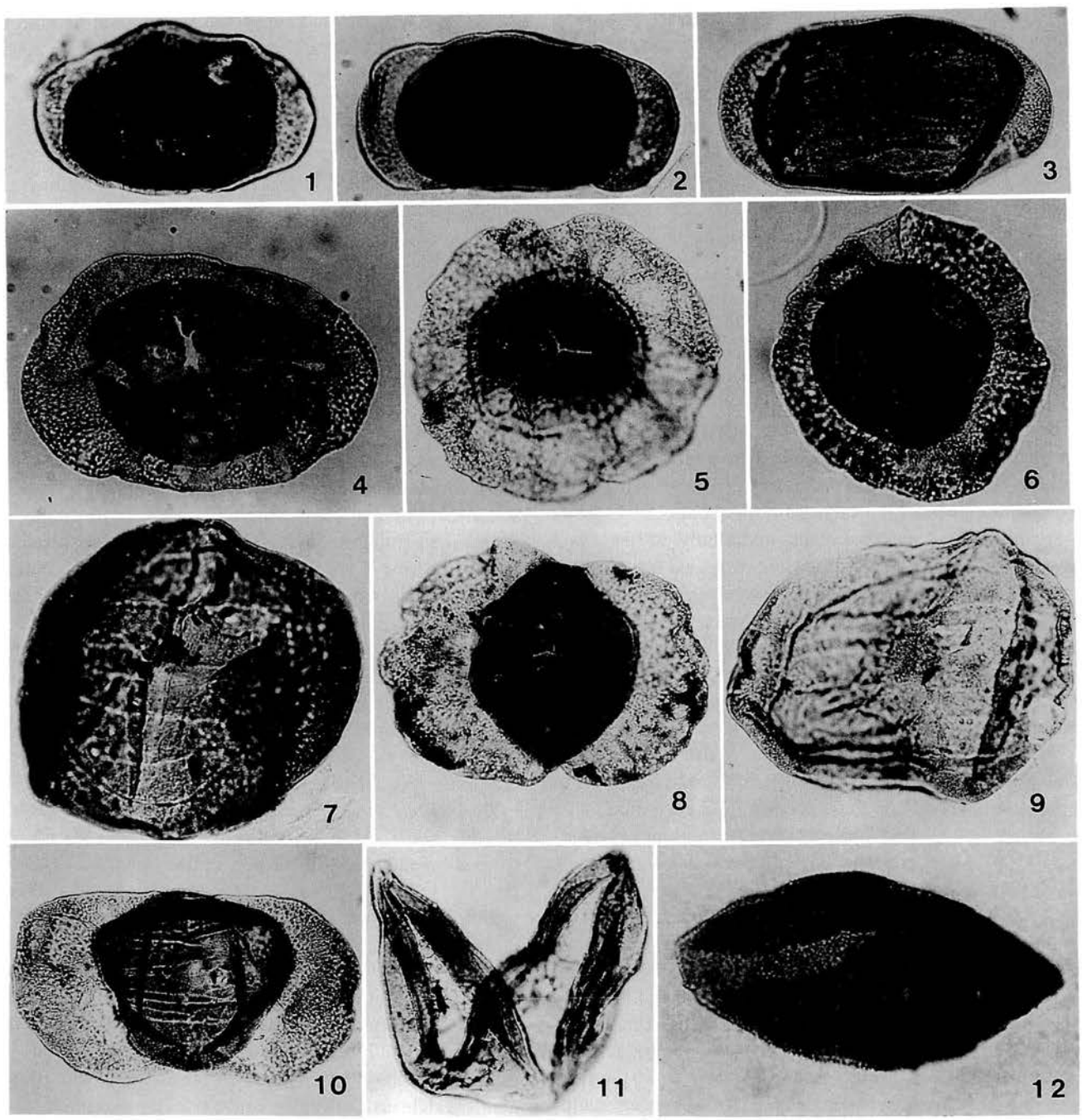

Figure 7. **1–3.** *Meristocorpus ostentus* sp. nov.; **1**, ×750, 20005916/3, G50/3; **2**, ×500, 20005916B, O40/3; **3,** holotype, ×500, 20005916/3, S38/1. **4.** *Potonieisporites* sp., ×500, 20005916D, G33/3. **5.** *Cannanoropollis densus*, ×500, 20005916D, M33. **6.** *Plicatipollenites gondwanensis*, ×500, 20005916F, P35/1. **7.** *Illinites unicus*, ×500, 20005916D, ×50/3. **8.** *Protohaploxypinus bharadwajii*, ×500, 20005916/2, P57/3. **9.** *Striomonosaccites ovatus*, ×500, 20005916E, N/37. **10.** *Striatopodocarpites* sp. cf. *S. phaleratus*, ×500, 20005916C, F33/1. **11.** *Brazilea scissa*, ×750, 20005916/3, K46/2. **12.** Sculptured monocolpate form indet., ×500, 20005916F, S44.

Remarks.—The identification herein of well-preserved specimens of this distinctive form, additional to those reported and designated informally by Playford and Dino (2000b), enables its formal establishment as a new species. *Meristocorpus ostentus* sp. nov. is distinguished from other forms assigned to the genus mainly by the very prominent

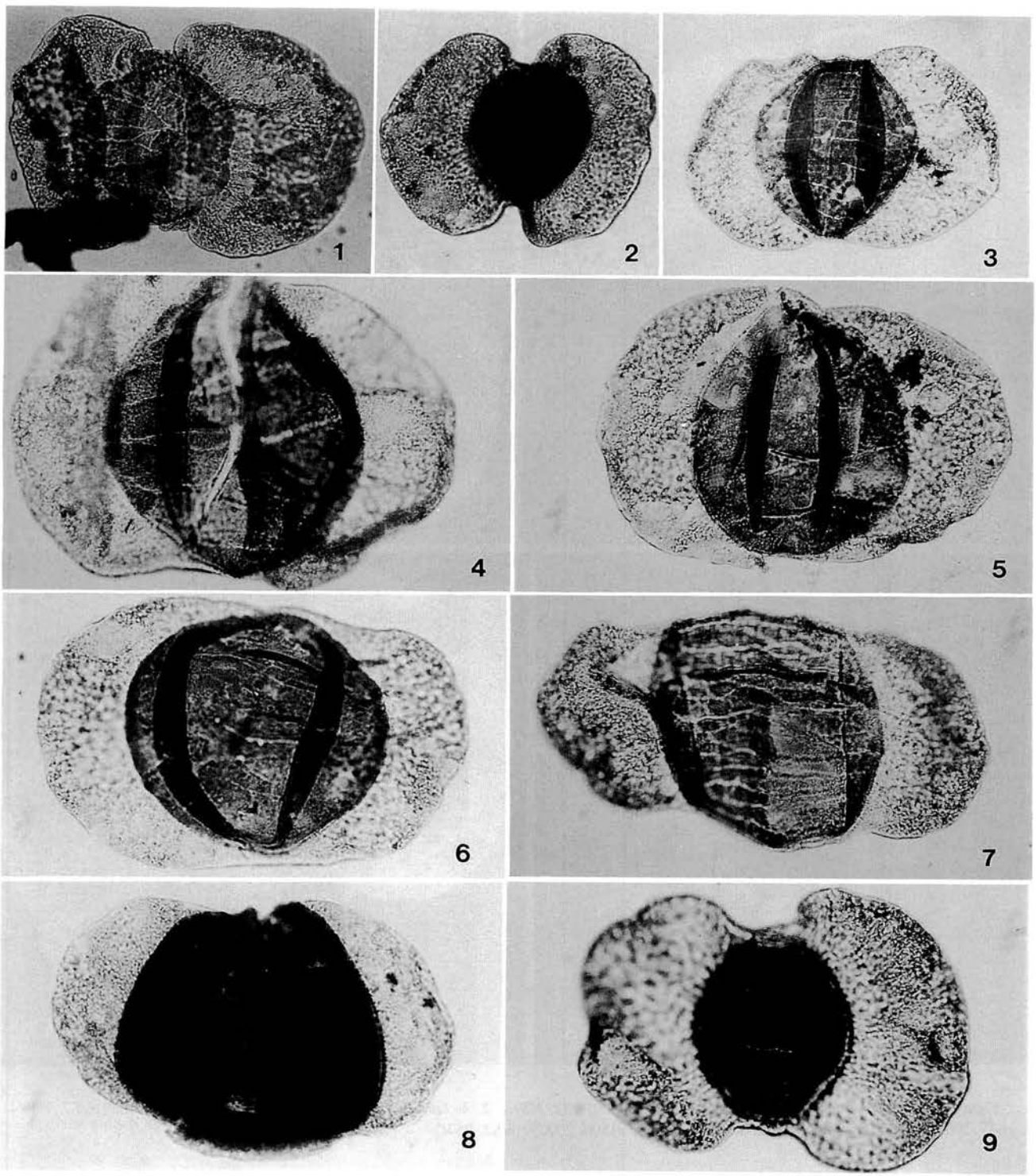

Figure 8. **1**, **2**. *Lahirites segmentatus* sp. nov.; **1**, holotype, ×750, 20005916A, M58/2; **2**, ×500, 20005916A, E39. **3**. *Protohaploxypinus bharadwajii*, ×500, 20005916F, D48/1. **4**. *Protohaploxypinus amplus*, ×750, 20005916/3, C48/2. **5**. *Protohaploxypinus* sp. cf. *Striatopodocarpites magnificus*, ×500, 20005916C, A39/4. **6**. *Meristocorpus explicatus*, ×500, 20005916A, N39/3. **7**. *Striatoabieites* sp. cf. *S. anaverrucosus*, ×500, 20005916C, D35/3. **8**. *Taeniaesporites* sp., ×500, 20005916C, D34/4. **9**. *Striatopodocarpites* sp., ×500, 20005916/3, D41/4.

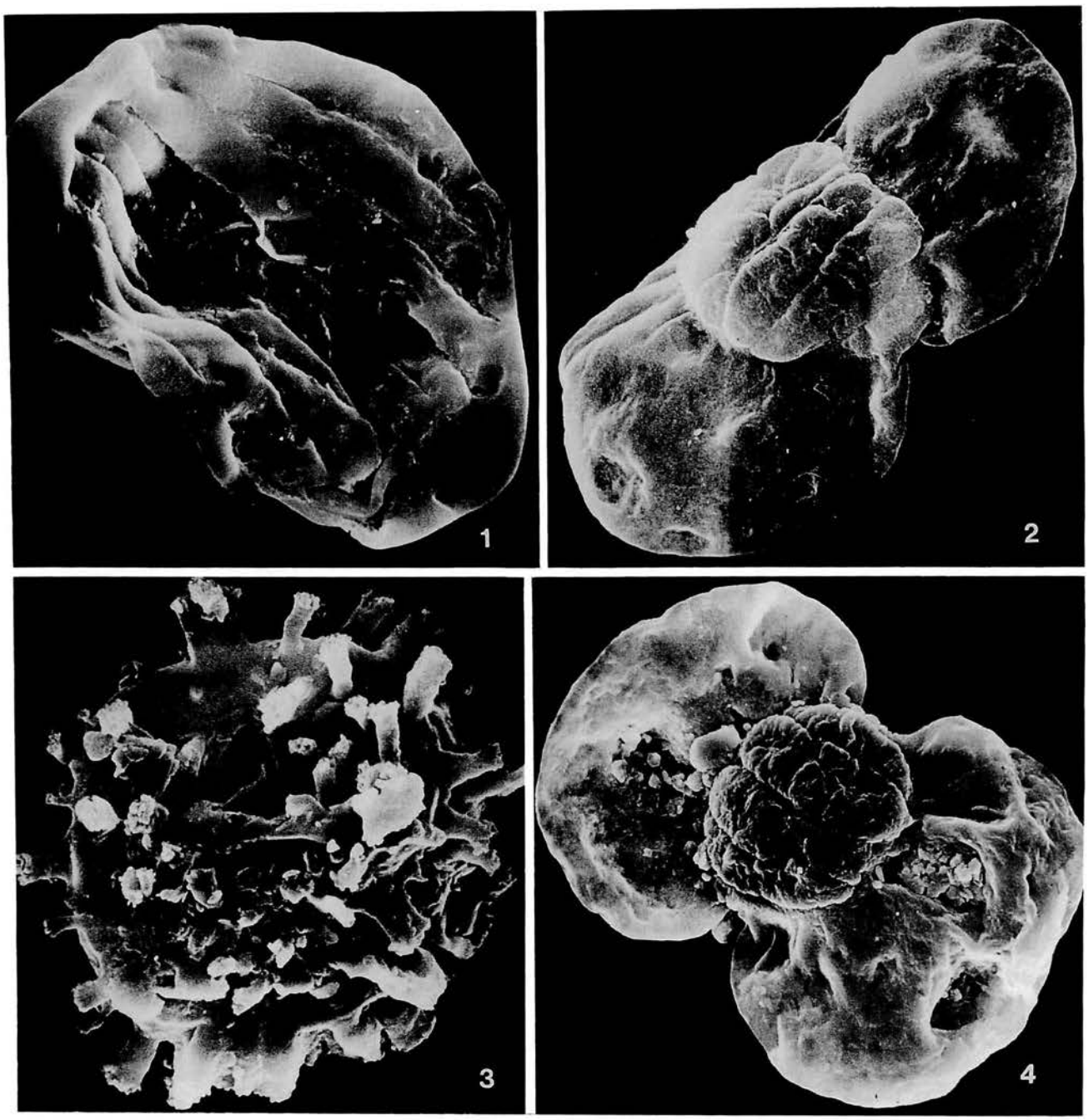

Figure 9. **1**. *Striomonosaccites ovatus*, ×1200, 20005916/S2, N39. **2**, **4**. *Lahirites segmentatus* sp. nov., **2**, ×800, 20005916/S2, N40/4; **4**, ×675, 20005916/S2, N55/4. **3**. *Raistrickia cephalata*, ×1500, 20005916/S2, P57/3.

elongation of its corpus and by relative proportions of the corpus and sacci.

Previous records. — From the Itaituba Formation, Amazonas Basin: *Illinites unicus* Zone, Westphalian C (Playford and Dino, 2000b).

Genus ***Lahirites*** Bharadwaj, 1962

Type species.—*Lahirites raniganjensis* Bharadwaj, 1962; by original designation (monotypic).

Discussion.—The salient attributes of *Lahirites* Bharadwaj, 1962, as exemplified by its type species, are circular

corpus bearing nine proximal transverse ("horizontal") taeniae that have a relatively coarse, segmented ("brick-work-like") appearance resulting from fine ("vertical"), linear, intra-taeniate channels cross-connecting the clefts bounding adjacent taeniae. The well-developed, protrusive sacci impart a distinctly diploxylonoid appearance. As discussed by Playford and Dino (2000b, p. 111), the three genera *Lahirites, Verticipollenites,* and *Hindipollenites,* as established by Bharadwaj (1962), have sufficient common features to render their mutual segregation problematical. Our choice of *Lahirites* as generic repository for the species newly described below is based mainly on its closer similarity to *L. raniganjensis* Bharadwaj, 1962 than to the type species of either of the other genera.

Lahirites segmentatus sp. nov.

Figures 8.1, 8.2, 9.2, 9.4

Diagnosis.— Pollen grains bisaccate, taeniate, strongly diploxylonoid. Corpus circular or near-circular with slight longitudinal elongation (polar orientation); exine 2–3 µm thick, infragranulate. Cappa comprising 7–12 transverse taeniae that are continuous or, more commonly, irregularly furcant. Taeniae 7–10 µm wide, separated by fine clefts 1–2 µm wide; taeniae divided irregularly into broadly rectangular segments by fine channels disposed normally to inter-taeniate clefts, thus producing a brickwork-like negative reticulum. Cappula narrowly rectangular. Sacci > semicircular, with medium to coarse endoreticulum, distal attachment roots producing longitudinal folds near corpus borders.

Dimensions (16 specimens, in polar aspect).—Overall breadth 110 (135) 150 µm; overall length 63 (89) 105 µm. Corpus breadth 35 (55) 65 µm; corpus length 50 (62) 75 µm.

Holotype.—Slide 20005916A, M58/2; Figure 8.1. Proximal aspect. Strongly diploxylonoid; overall breadth 150 µm, overall length 97 µm; corpus subcircular with slight longitudinal elongation (64 µm x 75 µm), exine 2 µm thick, featuring transverse, bifurcating taeniae, 7–10 µm wide, separated by fine clefts and incised (approximately at right angles to the latter) by very narrow, irregular, and less distinct channels; cappula 23 µm x 75 µm; sacci > semicircular, breadth 73 µm, length 97 µm, with medium-coarse endoreticulum.

Type locality.—Brazil, Parnaíba Basin, Piauí Formation; 1-UN-23-PI well, core, 145.0 m.

Etymology.—From the Latin, *segmentum*, partition, segment.

Comparison. — Certain Indian Permian species of *Lahirites* warrant comparison with *L. segmentatus* sp. nov. These species, with their principal morphological distinctions from *L. segmentatus*, are as follows: *L. raniganjensis* Bharadwaj, 1962 (p. 92, pl. 13, fig. 172), taeniae non-furcant; *L. singularis* Bharadwaj and Salujha, 1964 (p. 204–205, pl. 8, figs. 119–121), generally smaller, corpus thin-walled but with distinct marginal ridge, non-furcant taeniae; and *L. rotundus* Bharadwaj and Salujha, 1964 (p. 205–206, pl. 8, fig. 125; pl. 9, figs. 126, 127), corpus with non-furcant taeniae and "laterally prominent marginal ridge".

Correlation and age of palynoflora

Many of the palynomorphs in the present assemblage are identifiable with taxa that are known to have relatively broad stratigraphic ranges within the upper Palaeozoic of South America, and hence do not assist in definitive dating and correlation of the subject stratum. However, certain of the more vertically restricted species can usefully be applied biostratigraphically. These include the following: *Raistrickia cephalata*, *Vallatisporites arcuatus*, *Cristatisporites inconstans*, *Spelaeotriletes arenaceus*, *S. triangulus*, *Striatosporites heyleri*, *Peppersites ellipticus*, *Illinites unicus*, and *Meristocorpus explicatus*. All have been documented previously from the upper Palaeozoic of Brazil (Amazonas Basin principally: Playford and Dino, 2000a, b) and/or of Argentina (e.g., Archangelsky and Gamerro, 1979, Archangelsky *et al.*, 1996, Césari and Gutiérrez, 2001).

Müller's (1962) palynostratigraphic study included analysis of the Piauí Formation as cored in 15 oil exploration wells in the Parnaíba Basin (then termed Maranhão Basin). He recognized, in descending order, zones K, L, and M, covering the Piauí and the overlying Pedro de Fogo Formation and, supposedly (and, we believe, mistakenly), part of the underlying Poti Formation. The zones cannot be regarded, on present standards, as rigorously defined biostratigraphic units; they were ascribed generally to the Pennsylvanian (Westphalian-Stephanian). Zones L-M, represented by the Piauí Formation, include some forms encountered in the present sample; i.e., *Cristatisporites inconstans* (Müller's "Tl-2-I"), *Vallatisporites arcuatus* ("Tl-2-e"); *Verrucosisporites* sp. cf. *morulatus* ("Tl-r-b"), *Raistrickia cephalata* ("Raistr-a"), *Protohaploxypinus bharadwajii* ("V-D-i/st-a1"), and possibly *Spelaeotriletes* sp. ("Tl-z-b"). Accordingly, the sample studied here is compatible with zones L-M (more particularly, the latter) of Müller (1962).

With regard to the Amazonas Basin, no really precise equivalence of the present assemblage can be established vis-à-vis the Playford and Dino (2000b) palynozonation of the upper Palaeozoic Tapajós Group. This may well be a consequence of the current study being based on only one, fortuitously productive sample from within an otherwise non-palyniferous Piauí interval. Moreover, very little is

known of the Parnaíba Basin's overall Carboniferous-Permian palynological sequence. Species considered to be stratigraphically significant in the Tapajós Group, and occurring also in the Piauí sample, include *Illinites unicus*, *Striatosporites heyleri*, and *Raistrickia cephalata*. Prima facie, therefore, the Piauí assemblage could be regarded as falling somewhere within the Amazonas zonal interval defined eponymously and collectively by these three species. However, viewed in more detail, it should be noted that both *S. heyleri* and *R. cephalata* are represented very sparingly, by only one or two specimens, in contrast to their respective zonal abundances in the Amazonas Basin. Correlation with the *Illinites unicus* Zone (Playford and Dino, 2000b, p. 120–121) appears most likely from the presence of *I. unicus* in association with *Meristocorpus explicatus* and *M. ostentus* and with plentiful *Spelaeotriletes triangulus*, *S. arenaceus*, and zonate-cingulizonate forms (*Vallatisporites*, *Cristatisporites*). Additional support for this zonal correlation is provided by the scant representation of taeniate bisaccate pollen grains (which become increasing prevalent in post-*I. unicus* palynozones).

The *Illinites unicus* Zone embraces the upper part of the Itaituba Formation, directly beneath the Nova Olinda Formation, in the Tapajós Group succession of the Amazonas Basin. Hence, zonal attribution of the study sample signifies correlation of at least the subject Piauí stratum with the upper Itaituba Formation. This effectively corroborates other palaeontological evidence (previously cited herein) of faunal affinities between the Itaituba and Piauí Formations, and strengthens the lithostratigraphic correlation between these two formations that was originally advanced by Mesner and Wooldridge (1964). It follows that the upper part of the lower Piauí Formation can be ascribed a mid Pennsylvanian (late Westphalian) age (Playford and Dino, 2000b, p. 131).

Correlation of the present Piauí sample with the Argentinian palynozonation cannot be effected in any satisfactory way owing to the very generalized characteristics promulgated for those zones (Césari and Gutiérrez, 2001, p. 133). The best that can be said is that the Piauí suite would be attributable to the zones DMb or DMc.

Palaeoenvironmental inferences

As discussed previously, sedimentological and palaeontological studies indicate an interplay of several environmental circumstances or settings nonmarine, paralic, marine, evaporitic during accumulation of the Piauí Formation. Many lines of evidence, including data from core descriptions, well logs, remote sensing, lithofacies analyses, and sedimentary petrography, point to the lower part of the formation being predominantly nonmarine and reflecting conditions of aridity.

In the studied sample, the abundant land-derived plant debris in association with wholly terrestrial palynomorphs surely attest to nonmarine conditions. Moreover, the prevalence of monosaccate pollen grains, produced by cordaitalean gymnosperms, suggest arid climatic conditions. Regarding the green algal palynomorphs, the presence of *Botryococcus* permits no unequivocal palaeoenvironmental inferences (e.g., Batten and Grenfell, 1996, p. 210), other than indicating a quiescent aquatic situation; but *Brazilea* is suggestive of an exclusively freshwater habitat (Colbath and Grenfell, 1995).

Conclusions

1. The spore-pollen palynoflora recovered from the single productive sample, representing the upper part of the lower Piauí Formation in the southern Parnaíba Basin, comprises pteridophytic trilete spores associated with a range of gymnospermous pollen grains, principally monosaccates. Taeniate bisaccates are relatively uncommon.

2. In biostratigraphic terms, the assemblage bears closest similarity to the *Illinites unicus* palynozone of the Tapajós succession in the Amazonas Basin.

3. The zonal attribution connotes correlation of the palyniferous Piauí stratum with the upper part of the Itaituba Formation of the Tapajós Group, and dating of the stratum as mid Pennsylvanian (late Westphalian).

4. Such palaeoenvironmental indications that can be gleaned from the palynoflora corroborate the sedimentological, geophysical, and other prior data that imply a nonmarine depositional situation under arid conditions.

Acknowledgements

Sincere appreciation is expressed to the following: Alarico A.F. Mont'Alverne, Chief Geologist of the 4th District of DNPM, in Recife, for granting permission for this study and for facilitating sample collection; Dra. Luzia Antonioli, of Petrobras/Cenpes and Universidade Federal do Rio de Janeiro, for assistance in technical matters; and Professor Geoffrey Clayton (Trinity College, University of Dublin) and another (anonymous) reviewer for their helpful comments on the manuscript. We are most appreciative of a grant awarded by Fundação de Amparo à Pesquisa do Estado do Rio de Janeiro (FAPERJ) in support of this and cognate research-Project nº. E-26/170.127/2001.

References

Andrade, S.M. and Daemon R.F., 1974: Litoestratigrafia e

bioestratigrafia do flanco sudoeste da Bacia do Parnaíba (Devoniano e Carbonífero). *Anais XXVIII Congresso Brasileiro de Geologia*, vol. 2, p. 129-137.

Archangelsky, S., Azcuy, C.L., Césari, S., González, C., Hünicken, M., Mazzoni, A. and Sabattini, N., 1996: Correlación y edad de las biozonas. *In*, Archangelsky, S. *ed.*, *El sistema Pérmico en la República Argentina y en la República Oriental del Uruguay*, p. 203-226. Academia Nacional de Ciencias, Córdoba, República Argentina.

Archangelsky, S. and Gamerro J. C., 1979: Palinología del Paleozoico superior en el subsuelo de la Cuenca Chacoparanense, República Argentina. I. Estudio sistemático de los palinomorfos de tres perforaciones de la provincia de Córdoba. *Revista Española de Micropaleontología*, vol. 11, p. 417-478.

Assis, J.F.P., 1980: Sobre uma fáunula de molusco bivalves do Calcário Mocambo. Carbonífero da Bacia do Maranhão. *Anais da Academia Brasileira de Ciências*, vol. 52, p. 201-202.

Backhouse, J., 1991: Permian palynostratigraphy of the Collie Basin, Western Australia. *Review of Palaeobotany and Palynology*, vol. 67, p. 237-314.

Backhouse, J., 1993: Palynology and correlation of Permian sediments in the Perth, Collie and Officer Basins. *Geological Survey of Western Australia Report*, no. 34, p. 111-128.

Balme, B.E. and Hennelly, J.P.F., 1956: Trilete sporomorphs from Australian Permian sediments. *Australian Journal of Botany*, vol. 4, p. 240-260.

Batten, D.J. and Grenfell, H.R., 1996: *Botryococcus*, chapter 7D. *In*, Jansonius, J. and McGregor, D.C. *eds.*, *Palynology: Principles and Applications*, vol. 1, p. 205-214. American Association of Stratigraphic Palynologists Foundation, Dallas.

Beri, A. and Aguilar, C.G., 1998: Resultados palinológicos y estratigráficos de la Formación San Gregorio (Pérmico Inferior), Uruguay. *Revista Universidade de Guarulhos-Geociências*, vol. 3, p. 108-119.

Beri, A. and Goso, C.A., 1996: Analisis palinologico y estratigrafico de la Fm. San Gregorio (Permico Inferior) en el área de los Cerros Guazunambi, Cerro Largo, Uruguay. *Revista Española Micropaleontologia*, vol. 28, p. 67-79.

Bharadwaj, D.C., 1962: The miospore genera in the coals of Raniganj stage (Upper Permian), India. *The Palaeobotanist*, vol. 9, p. 68-106.

Bharadwaj, D.C. and Salujha, S.K., 1964: Sporological study of seam VIII in Raniganj Coalfield, Bihar (India)-Part 1. Description of sporae dispersae. *The Palaeobotanist*, vol. 12, p. 181-215.

Bharadwaj, D.C. and Srivastava, S.C., 1969: Some new miospores from Barakar stage, Lower Gondwana, India. *The Palaeobotanist*, vol. 17, p. 220-229.

Burjack, M.I.A., 1978: Estudo palinológico da jazida carbonífera de Charqueadas. Dissertação de Mestrado, Universidade Federal de Goiás (UFG), Goiânia, Brasil, 204 p. (unpubl.)

Campanha, V.A. and Rocha Campos, A.C., 1979: Alguns microfósseis da Formação Piauí (Neocarbonífero), Bacia do Parnaíba. *Boletim do Instituto de Geociências, USP*, vol. 10, p. 57-67.

Césari, S., Archangelsky, S. and Seoane, L.V. de, 1995: Palinología del Paleozoico superior de la perforación Las Mochas, provincia de Santa Fe, Argentina. *Ameghiniana*, vol.32, p. 73-106.

Césari, S. and Gutiérrez, P.R., 2001: Palynostratigraphy of upper Paleozoic sequences in central-western Argentina. *Palynology*, vol. 24, p. 113-146.

Colbath, G.K. and Grenfell, H.R., 1995: Review of biological affinities of Paleozoic acid-resistant, organic-walled eukaryotic algal microfossils (including "acritarchs"). *Review of Palaeobotany and Palynology*, vol. 86, p. 287-314.

Cunha, F.M.B., 1986: Evolução Paleozóica da Bacia do Parnaíba e seu arcabouço tectônico. Dissertação de Mestrado, Instituto de Geociências, Universidade Federal do Rio de Janeiro (UFRJ), Rio de Janeiro, Brasil, 107 p. (unpubl.).

Dias, M.E.R., 1994: Palinologia do Grupo Itararé na porção centro-sul do Rio Grande do Sul, Permiano da Bacia do Paraná, Brasil. *Pesquisas*, vol. 20, p. 119-131.

Duarte, A., 1936: Fósseis da sondagem de Teresina-Piauí. *Boletim do Departamento Nacional da Produção Mineral, Notas preliminares e estudos*, vol. 2, p. 1-3.

Foster, C.B., 1979: Permian plant microfossils of the Blair Athol Coal Measures, Baralaba Coal Measures, and basal Rewan Formation of Queensland. *Geological Survey of Queensland, Publication 372, Palaeontological Paper*, no. 45, p. 1-244.

Góes, A.M.O. and Feijó, F.J., 1994: Bacia do Parnaíba. *Boletim de Geociências da Petrobrás*, vol. 8, p. 57-67.

Kegel, W., 1951: Sobre alguns trilobitas carboníferos do Piauí e do Amazonas. *Boletim do Departamento Nacional da Produção Mineral, Divisão de Geologia e Mineralogia*, vol. 135, p. 1-38.

Kegel, W. and Costa, M.T., 1951: Espécies Neopaleozóicas do Brasil, da família Aviculopectinidae, ornamentadas com costelas fasciculadas. *Boletim do Departamento Nacional da Produção Mineral, Divisão de Geologia e Mineralogia*, vol. 137, p. 1-48.

Lima Filho, F.P., 1991: Facies e ambientes deposicionais da Formação Piauí (Pensilvaniano), Bacia do Parnaíba. Dissertação de Mestrado, Instituto de Geociências, Universidade de São Paulo (USP), São Paulo, Brasil, 137 p. (unpubl.)

Marques-Toigo, M., 1974: Some new species of spores and pollens of Lower Permian age from the San Gregorio Formation in Uruguay. *Anais Academia Brasileira de Ciências*, vol. 46, p. 601-616.

Marques-Toigo, M., 1988: Palinologia, bioestratigrafia e paleoecologia do Neopaleozóico da Bacia do Paraná nos Estados do Rio Grande do Sul e Santa Catarina, Brasil. Tese Doutoramento, Insituto de Geociências, Universidade Federal do Rio Grande do Sul (UFRGS), Porto Alegre, Brasil, 259 p. (unpubl.)

Mautino, L.R., Anzótegui, L.M. and Vergel, M.del M., 1998: Palinología de la Formación Melo (Pérmico Inferior) en Arroyo Seco, Departamento Rivera, República Oriental del Uruguay. Parte IV: Esporas. *Ameghiniana*, vol. 35, p. 67-79.

Mendes, J.C., 1966: Moluscos da Formação Itaituba (Neocarbonífero), Estado do Pará, Brasil. *Cadernos da Amazônia*, vol. 9, p. 1-56.

Menéndez, C.A. and Azcuy, C.L., 1969: Microflora carbónica de la localidad de Paganzo, provincia de La Rioja. Parte I. *Ameghiniana*, vol. 6, p. 77-97.

Menéndez, C.A. and Azcuy, C.L., 1971: Microflora carbónica de la localidad de Paganzo, provincia de La Rioja. Parte II. *Ameghiniana*, vol. 8, p. 25-36.

Mesner, J.C. and Wooldridge, L.C.P., 1962: Maranhão basin study revision. *Petrobras Internal Report*, no. 141, Belém, Pará. (unpubl.)

Mesner, J.C. and Wooldridge, L.C.P., 1964: Maranhão Paleozoic Basin and Cretaceous coastal basins, north Brazil. *Bulletin of the American Association of Petroleum Geologists*, vol. 48, p. 1475-1512.

Müller, J., 1962: Report on palynological results of samples exam-

ined from wells in Maranhão. *Petrobrás Internal Report (RPBA)*, Salvador, Bahia, 45 p. (unpubl.)

Neves, R. and Owens, B., 1966: Some Namurian camerate miospores from the English Pennines. *Pollen et Spores*, vol. 8, p. 337-360.

Playford, G. and Dino, R., 2000a: Palynostratigraphy of upper Palaeozoic strata (Tapajós Group), Amazonas Basin, Brazil: part one. *Palaeontographica, Abteilung B*, vol: 255, p. 1-46.

Playford, G. and Dino, R., 2000b: Palynostratigraphy of upper Palaeozoic strata (Tapajós Group), Amazonas Basin, Brazil: part two. *Palaeontographica, Abteilung B*, vol. 255, p. 87-145.

Playford, G., Dino, R. and Marques-Toigo, M., 2001: The upper Paleozoic miospore genus *Spelaeotriletes* Neves and Owens, 1966, and constituent Gondwanan species. *Journal of South American Earth Sciences*, vol. 14, p. 593-608.

Playford, G. and Powis, G.D., 1979: Taxonomy and distribution of some trilete spores in Carboniferous strata of the Canning Basin, Western Australia. *Pollen et Spores*, vol. 21, p. 371-394.

Pons, M.E., 1976: Estudo palinológico do Subgrupo Itararé na "Coluna White", Permiano Inferior, Santa Catarina. Parte I. *Ameghiniana*, vol.13, p. 109-125.

Ravn, R.L. and Fitzgerald, D.J., 1982: A Morrowan (Upper Carboniferous) miospore flora from eastern Iowa, U.S.A. *Palaeontographica, Abteilung B*, vol. 183, p. 108-172.

Small, H., 1914: Geologia e suprimento de água subterrânea no Piauhy e parte do Ceará. *Boletim da Inspetoria de Obras contra as secas. Serie I.D.*, vol. 25, p. 1-80.

Spinner, E. and Clayton, G., 1973: Viséan spore assemblages from Skateraw, East Lothian, Scotland. *Pollen et Spores*, vol. 15, p. 139-165.

Suguio, K. and Fulfaro, V.J., 1977: Geologia da margem ocidental da Bacia do Parnaíba (Estado do Pará). *Boletim do Instituto de Geociências, USP*, vol. 8, p. 31-54.

Tengan, C., Shimabukuro, S. and Rocha Campos, A.C., 1976: Conodontes carboníferos do poço FBst-1-AM, Bacia do Amazonas, Brasil. *XXIX Congresso Brasileiro de Geologia, Ouro Preto, Resumo dos Trabalhos*, p. 305.

Vergel, M. del M., 1998: Palinología del Paleozoico superior (Formación Sachayoj) en tres perforaciones de la subcuenca de Alhuampa, Cuenca Chacoparanense (Argentina). Parte I: esporas. *Ameghiniana*, vol. 35, p. 387-403.

Ybert, J.-P., 1975: Étude des miospores du bassin houiller de Candiota, Hulha Negra, Rio Grande do Sul, Brésil. *Pesquisas*, vol. 5, p. 181-226.

Paleontological Research, vol. 6, no. 1, pp. 41-65, April 30, 2002

Indian metoposaurid amphibians revised

DHURJATI PRASAD SENGUPTA

Indian Statistical Institute, Geological Studies Unit 203 Barrackpore Trunk Road, Calcutta 700035, India (dhurjati@isical.ac.in)

Received 18 August 2000; Revised manuscript accepted 30 November 2001

Abstract. A recent collection of more than a hundred fossil bones belonging to at least six individuals of metoposaurids from the basal part of the Late Triassic, Maleri Formation of the Pranhita-Godavari valley, Gondwana succession, has helped to formulate new ideas. Detailed morphological studies have been used to include all specimens of metoposaurids so far collected from India within a single taxon, *Buettneria maleriensis*, a new combination. A reconstruction of the skeleton of *Buettneria maleriensis* is presented for the first time. *Buettneria maleriensis* remains are common in the continental red beds of India, deposited under fluvial conditions witnessing seasonal climate changes. While some bones of *Buettneria maleriensis* were rolled and transported after death and are now found as sporadic fossils in mudstone (or occasionally in sandstones and calcirudites), the other type of occurrences, the rich accumulation of bones, are present only in mudstones. *Buettneria maleriensis* was replaced by the Chigutisauridae, a temnospondyl family exclusive to Gondwanaland. India is the only place where both metoposaurids and chigutisaurids are found in such close succession. The paleoposition of India during the later part of the Triassic may have been responsible for this.

Key words: *Buettneria*, India, Late Triassic, Maleri Formation

Introduction

The Metoposauridae is a Late Triassic temnospondyl amphibian family known from Europe, North America, North Africa and India. They were quite large (at least 1.5 m in length), essentially aquatic animals (Defauw, 1989), with flat and heavily ornamented skull roofs marked with lateral line canals. Metoposaurids are to some extent morphologicaly similar to the present day crocodiles. However, unlike crocodiles, they had limbs unsuitable for quick movement on land.

The first metoposaurid, *Metoposaurus diagnosticus* (Meyer, 1842), was described from Europe. Subsequently a large number of metoposaurids belonging to several genera and species have also been reported from Europe and North America (Fraas, 1889, 1896, 1913; Lydekker, 1890; Watson, 1919; Romer, 1947; Colbert and Imbrie, 1956 and Werneburg, 1990). Dutuit (1976) carried out a study of another population of metoposaurids from North Africa. The Metoposauridae as a whole was extensively revised by Hunt (1993). However, Indian metoposaurids have not been studied in similar detail. Lydekker (1885) and Huene (1940) were the early workers to report metoposaurid fragments from India and Colbert (1958) discussed the significance of Indian metoposaurids in some detail. Later, Roychowdhury (1965) studied the Indian metoposaurids and recently a partial skull was described by Sengupta (1992). A revision of the Indian metoposaurids has been attempted here in the light of the recovery of more than a hundred fossilised bones belonging to at least six individuals. These remains represent a mass accumulation and were found near Aigerapalli village in the basal part of the Maleri Formation of the Pranhita-Godavari valley of Central India.

Taphonomic and palaeobiogeographic studies of the metoposaurids have also revealed some interesting results. India is the only region where the typically Laurasian metoposaurs are found together with some stereospondyls exclusive to Gondwanaland. The significance of this association will be discussed.

Family Metoposauridae

The family Metoposauridae is morphologically a very compact group which shares a number of character states. They have flat elongate skulls with tapering snouts, dorsolateral and anteriorly placed orbits, a pineal foramen far posterior to the orbits, low skulls with occipital condyles placed in the same line and plane (or a little posterior in certain cases) as the quadrate condyles, large paraquadrate foramina, spoollike intercentra (Romer, 1947; Watson, 1919, 1962; Colbert and Imbrie, 1956; Rouchowdhury, 1965; Dutuit, 1976) and wide cultriform process of the parasphenoid (Coldiron, 1978). In addition, Milner

(1990) noted that the palatine ramus of the pterygoid is rather short with a posteromedial ramus of the ectopterygoid contributing to the strut. Jupp and Warren (1986) stated that, in metoposaurids, the posterior coronoid forms part of the dorsal margin of the posterior Meckelian foramen. Warren and Snell (1991) further noted that the ilium of the metoposaurids has some taxonomic importance since the iliac blade is not "expanded" like other temnospondyls. They also noted that the metoposaurid humerus has well developed ends and prominent areas for muscle insertion, a rare trait among the temnospondyls. Both Werneburg (1990) and Warren and Snell (1991) suggested that the interclavicles of the metoposaurids have some characteristic features.

While the monophyly of the family Metoposauridae is established, the taxonomy at the generic level is somewhat problematic. There are only a few character states which are variable between different populations as well as within the single population of a particular area. The problem of taxonomy of metoposaurids at the generic level thus depends on proper understanding of those limited numbers of character states.

Colbert and Imbrie (1956) used two character states to differentiate the North American from the European populations. In the North American populations the lachrymal enters the orbit margin while in the European forms it does not. The degree of overlap of the clavicles on the interclavicles and the pattern of ornamentation of the clavicles were also different in the North American and European metoposaurids.

Roychowdhury (1965) grouped all the metoposaurid genera into a single genus, *Metoposaurus*. Subsequently Dutuit (1976) erected some new species from North Africa and designated them as *Metoposaurus* at the generic level. Gregory (1980) pointed out that there are at least two metoposaurid genera present in North America; one with an otic notch and the other without. Davidow-Henry (1989) divided the metoposaurids into three generic groups, one with otic notches, one without, and a third having a pineal foramen placed more forward than in the others. This splitting was continued by the recent work on metoposaurid taxonomy by Hunt (1993) and Milner (1994). Hunt (1993) divided the metoposaurids into five genera and six species. They are: *Metoposaurus diagnosticus* (Meyer, 1842), *M. bakeri* (Case, 1931), *Buettneria perfecta* (Case, 1922), *Dutuitosaurus ouazzoui* (Dutuit, 1976, new combination *sensu* Hunt, 1973), *Arganasaurus lyazidi* (Dutuit, 1976, new combination *sensu* Hunt, 1973)and *Apachesaurus gregorii* (Hunt, 1993). Hunt stated that the last-mentioned genus has a very shallow otic notch while in the other genera they are deeper.

The most conspicuous change in the work of Hunt (1993) is the lumping of many taxa found from various places of the world into *Buettneria perfecta,* which also includes the Indian metoposaurid, *Metoposaurus maleriensis* (Roychowdhury, 1965), making it a junior synonym of *B. perfecta.* All the species of *Buettneria* have their lachrymals included within the border of the orbits.

Following a different approach, Milner (1994) grouped the metoposaurids into more than one "grade" which are further divided into certain "clades." He included "*M. maleriensis*" within the clade *Anaschisma.* The latter according to him is a "terminal clade" with the elongate lachrymal entering the orbit margin (a character-state of grade *Buettneria*), large, closely spaced nares and the supraorbital lateral line canals always broken behind the orbits (character states which separate *Anaschisma* from *Buettneria*).

Indian metoposaurids

The history of the work on Indian metoposaurids was discussed in detail by Roychowdhury (1965). Only one more specimen of the family has been described in recent years by Sengupta (1992). Hence only a brief discussion on the Indian metoposaurids is provided below.

In India metoposaurids are known from the Maleri Formation of the Pranhita Godavari (P–G) valley and the Tiki Formation of the Son Mahanadi valley. Initially, the Indian metoposaurids were known from fragmentary surface collections which did not permit diagnosis below family level (Lydekker,1885; Huene,1940). Later, systematic collection of *in situ* specimens from the Maleri Formation yielded a number of well preserved fragments. These fragments were sufficiently diagnostic and included at least two partial skulls, clavicles and interclavicles, and vertebral elements. Roychowdhury (1965) erected *Metoposaurus maleriensis* on the basis of these specimens and also presented a restoration of the skull.

As mentioned earlier Hunt (1993) included *M. maleriensis* as *Buettneria perfecta.* The taxonomic status of the Indian metoposaurids is revised in the present work. All the specimens of the Indian metoposaurids are grouped into a single genus and species, *Buettneria maleriensis,* a new combination.

Systematic paleontology

Order Temnospondyli Zittel, 1888
Family Metoposauridae Watson, 1919
Genus ***Buettneria*** Case, 1922

Buettneria maleriensis (Roychowdhury, 1965)
new combination

Figures 1–16

Metoposaurus maleriensis Roychowdhury, 1965, p. 21, figs. 3–

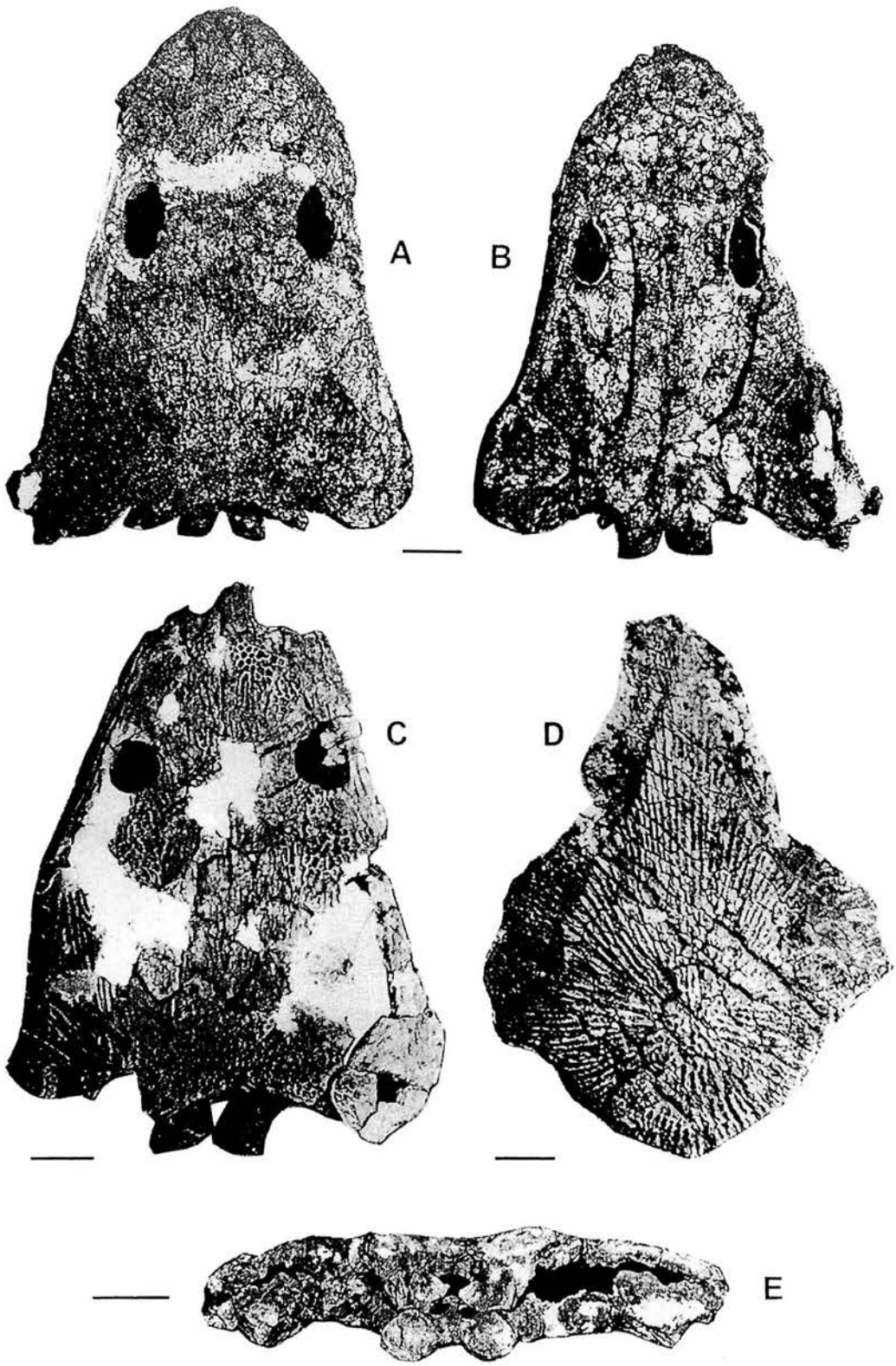

Figure 1. Skull roof (**A** = ISIA 56, **C** = ISIA 59), palate (**B** = ISIA 56), interclavicle (**D** = ISIA 67) and occiput (**E** = ISIA 53) of *Buettneria maleriensis*, new combination. Scale bars = 5 cm.

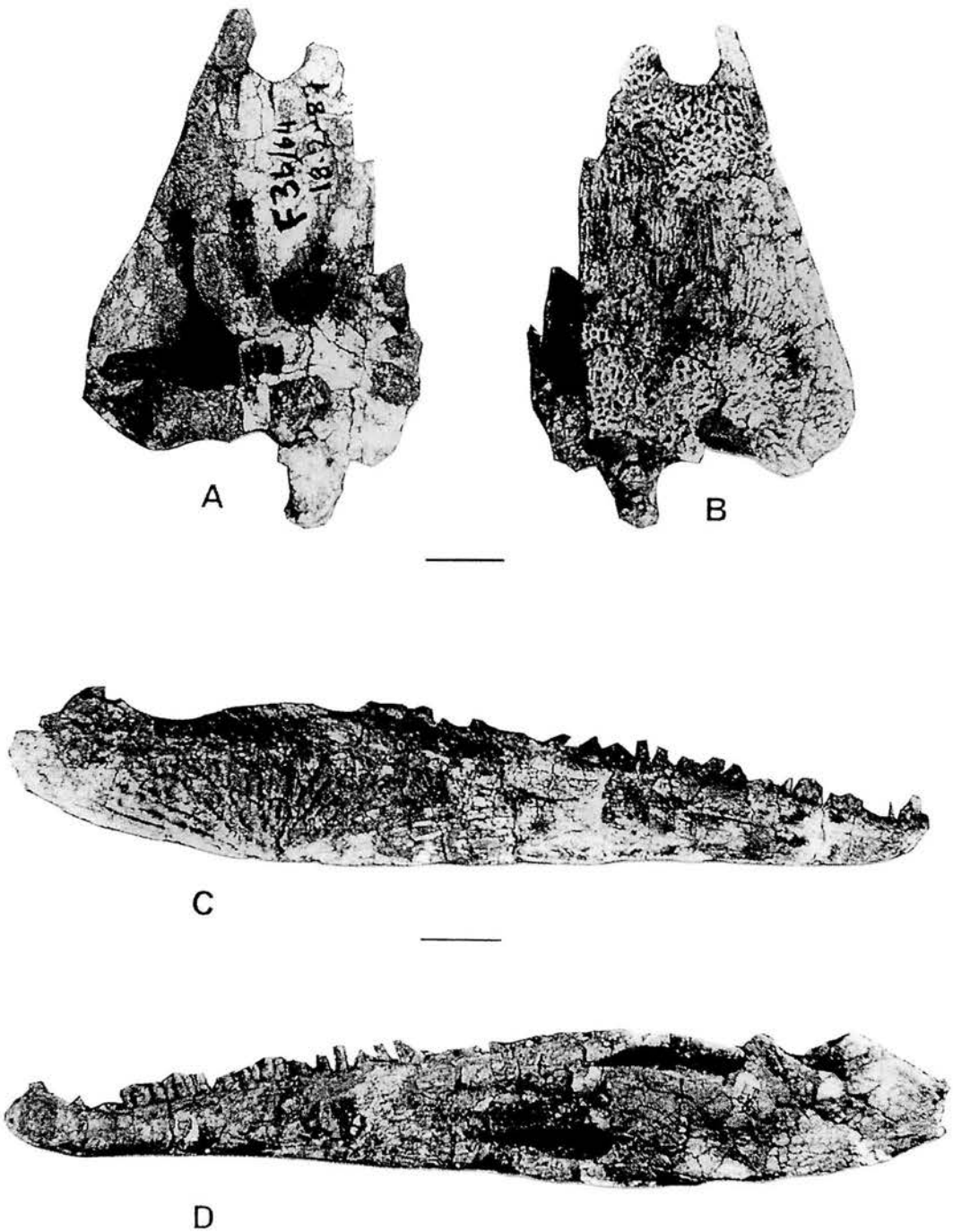

Figure 2. Palate (**A** = ISIA 58), skull roof (**B** = ISIA 58) and mandible (**C**, **D** = labial and lingual view of ISIA 60) of *Buettneria maleriensis*, new combination. Scale bars = 5cm.

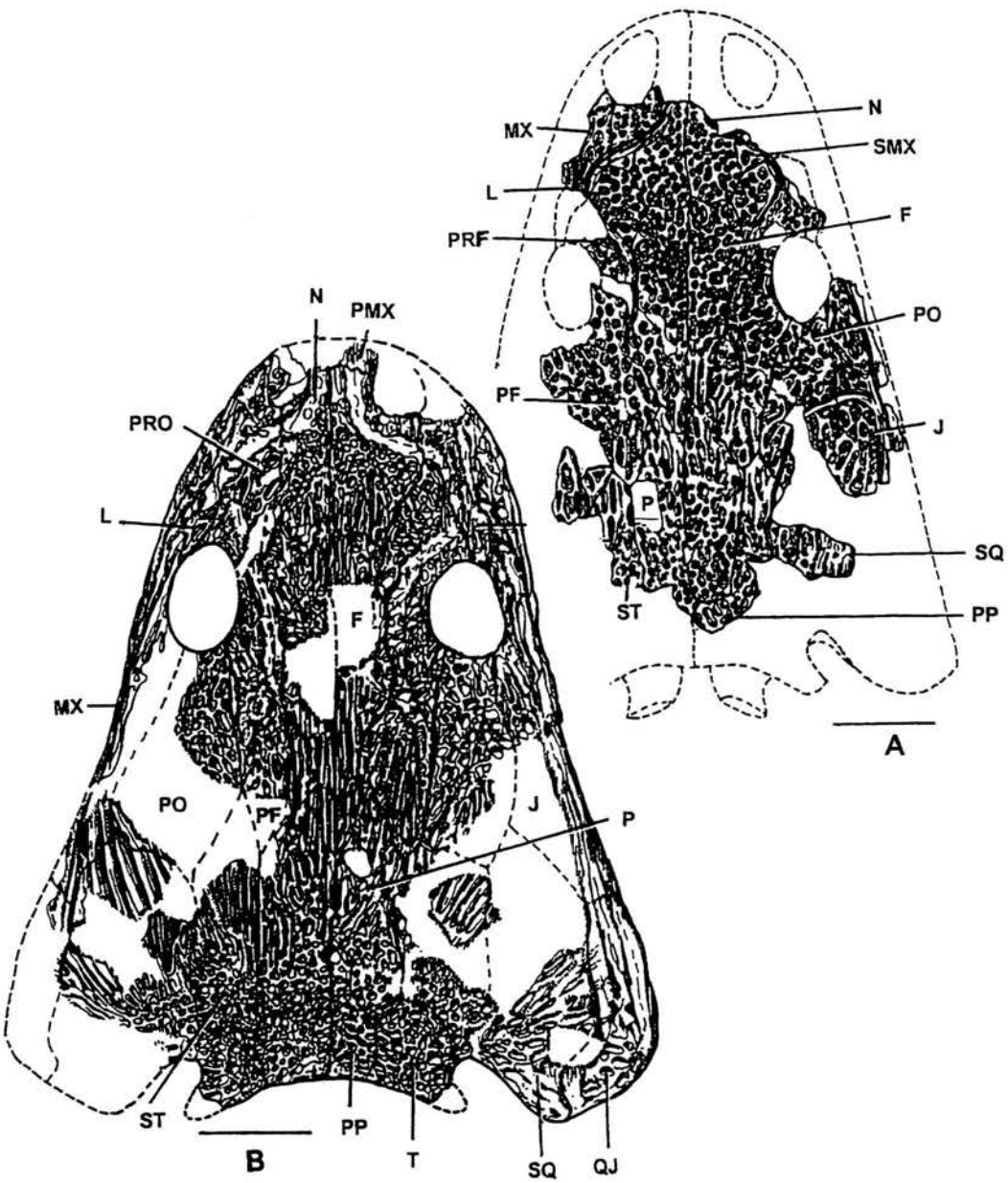

Figure 3. Skull roof of *Buettneria maleriensis*, new combination, **A** = ISI A 4, **B** = ISI A 59. Abbreviations: F= frontal; J = jugal; L = lachrymal; N = nasal; P = parietal; PRF = prefrontal; PMX = premaxilla; PO = postorbital; PP = postparietal; PF = postfrontal; QJ = quadratojugal; SQ = squamosal; ST = supratemporal; T = tabular. Scale bars = 5 cm.

20, pls. 21–41; Sengupta, 1992, p. 300, figs. 1–4, pl. 1.
Buettneria perfecta, Hunt, 1993, p. 78, figs. 7–9 (in part).

Material examined.—GSI 2249, 2254 and 2263 (Lydekker, 1885), K 33/638, 616a, b, 630a, 606a, 611a, 602a (Huene, 1940), ISI A 1 to 17 (Roychowdhury, 1965), ISI A 53 (Sengupta, 1992), ISI A 56, and ISI A 58 to175. The specimens with numbers starting with ISI A are housed in the Geological Museum, Indian Statistical Institute, Calcutta, India (Table 1) and specimens K 33/638, 616a, b, 630a, 606a, 611a, 602a, and GSI 2249, 2254 and 2263 are kept in the Indian Museum, Calcutta, India.

Holotype.—ISI A 4, in the collection of the Geology Museum, Indian Statistical Institute, Calcutta, India.

Paratypes.—ISI A 1 to 3 and ISI A 5 to 17, 53, 56, 58 to 175.

Distribution and age.—*B. maleriensis* occur in the lower part of the Maleri Formation of the Pranhita Godavari val-

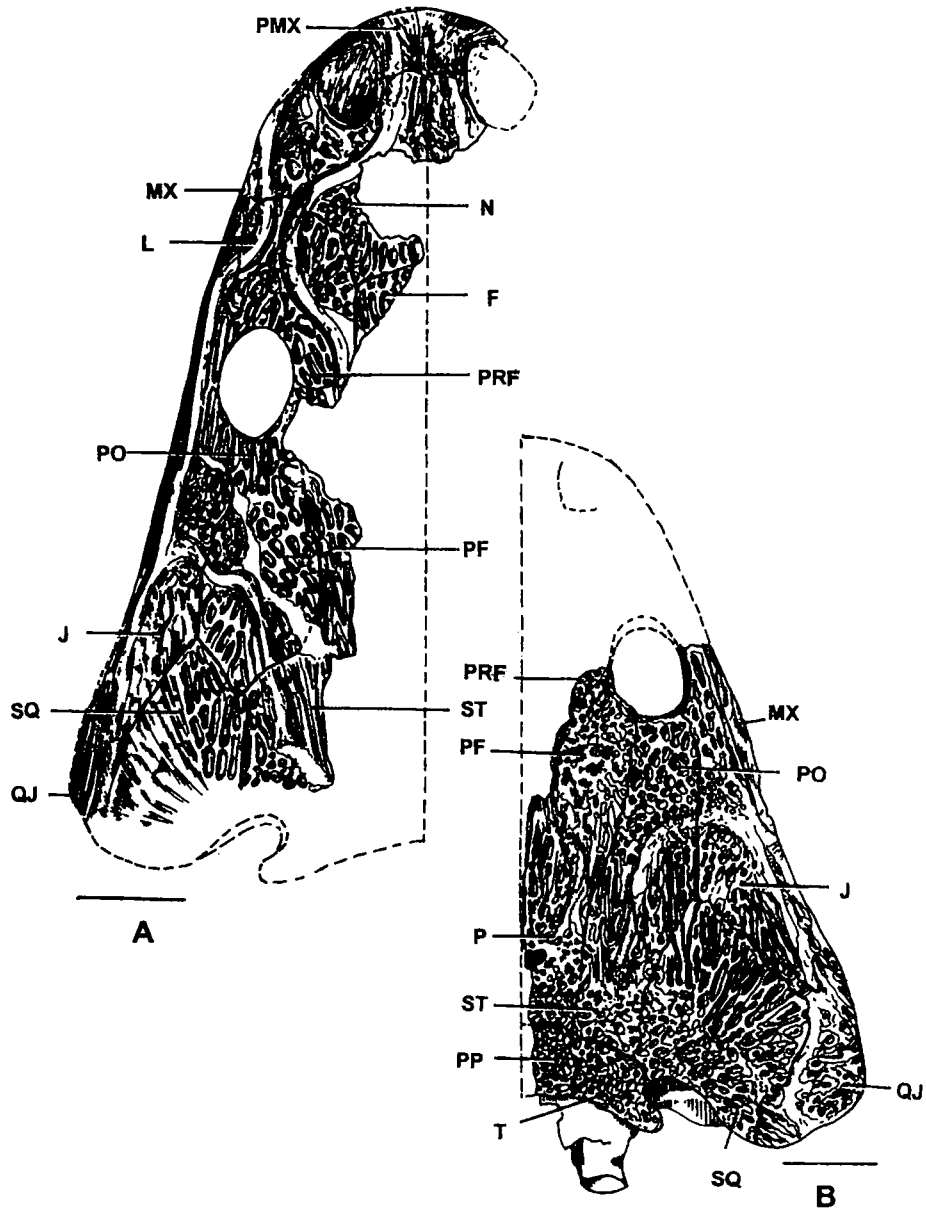

Figure 4. Skull roof of *Buettneria maleriensis*, new combination, **A** = ISI A 8, **B** = ISI A 58. Abbreviations used are same as Figure 3. Scale bars = 5 cm.

ley and also in the Tiki Formation of the Son Mahanadi valley of Central India. Material examined were mostly collected around the villages of Achlapur, Gampalpalli and Aiegarapalli, Adilabad District of Andhra Pradesh, India. The age of *B. maleriensis* is Late Carnian.

Diagnostic characters.—Buettneria maleriensis has the lachrymal in the margin of the orbits and thus it differs from all other metoposaurids except *B. perfecta, sensu* Hunt (1993). *B. maleriensis* differs from most specimens of *B. perfecta* in the presence of large, closely spaced nares and lateral line canals never forming a loop behind the orbits (Milner, 1994). Two specimens (FMNH UC 447 and 448, kept in the Field Museum of Natural History, University College collection, Chicago) designated as "*Anaschisma*" by Branson, 1905 have similarity with *B. maleriensis* in this regard. *B. maleriensis*, however, has a different type of ornament than that of "*Anaschisma*" and has a comparatively larger orbit.

The lachrymal is present as a narrow strip of bone in *B. maleriensis*. The anterior boundary of the lachrymal and that of the prefrontal are at the same level. All the specimens of *B. maleriensis* are unique in having parts of the

Table 1. List of the specimens of *Buettneria maleriensis*, new combination, housed in the Geology Museum, Geological Studies Unit, Indian Statistical Institute (ISI) Calcutta.

Element	ISI no.	Element	ISI no.	Element	ISI no.
Part of skull	ISI A 1	Femur, Right	ISI A 84	Intercentrum (Dorsal)	ISI A 129
Part of skull	ISI A 2	Femur, Right	ISI A 85	Intercentrum (Dorsal)	ISI A 130
Part of skull	ISI A 3	Ilium, Right	ISI A 86	Intercentrum (Dorsal)	ISI A 131
Part of skull	ISI A 4	Ilium, Right	ISI A 87	Intercentrum (Dorsal)	ISI A 132
Left squamosal	ISI A 5	Ilium, Right	ISI A 88	Intercentrum (Dorsal)	ISI A 133
Part of skull	ISI A 6	Scapulacoracoid, Rt	ISI A 89	Atlas	ISI A 134
Part of skull	ISI A 7	Scapulacoracoid, Rt	ISI A 90	Atlas	ISI A 135
Part of skull	ISI A 8	Scapulacoracoid, Rt	ISI A 91	Intercentrum (Caudal)	ISI A 136
Interclavicle	ISI A 9	Scapulacoracoid, Lt	ISI A 92	Intercentrum (Caudal)	ISI A 137
Left clavicle	ISI A 10	Scapulacoracoid, Lt	ISI A 93	Intercentrum (Caudal)	ISI A 138
Left clavicle	ISI A 11	Scapulacoracoid, Lt	ISI A 94	Intercentrum (Caudal)	ISI A 139
Right clavicle	ISI A 12	Ulna, Right	ISI A 95	Intercentrum (Caudal)	ISI A 140
Atlas	ISI A 13	Ulna, Right	ISI A 96	Intercentrum (Caudal)	ISI A 141
Four vertebrae	ISI A 14	Ulna, Left	ISI A 97	Intercentrum (Caudal)	ISI A 142
Three vertebrae	ISI A 15	Tibia, Right	ISI A 98	Intercentrum (Caudal)	ISI A 143
Right ischium	ISI A 16	Tibia, Left	ISI A 99	Intercentrum (Caudal)	ISI A 144
Left humerus	ISI A 17	Radius, Right	ISI A 100	Intercentrum (Caudal)	ISI A 145
Partial skull	ISI A 53	Fibula, Right	ISI A 101	Intercentrum (Caudal)	ISI A 146
Complete skull	ISI A 56	Neural spine	ISI A 102	Intercentrum (Caudal)	ISI A 147
Partial skull	ISI A 58	Neural spine	ISI A 103	Intercentrum (Caudal)	ISI A 148
Complete skull	ISI A 59	Neural spine	ISI A 104	Rib (Dorsal)	ISI A 149
Left msndible	ISI A 60	Neural spine	ISI A 105	Rib (Dorsal)	ISI A 150
Left mandible	ISI A 61	Intercentrum (Dorsal)	ISI A 106	Rib (Dorsal)	ISI A 151
Right mandible	ISI A 62	Intercentrum (Dorsal)	ISI A 107	Rib (Dorsal)	ISI A 152
Right mandible	ISI A 63	Intercentrum (Dorsal)	ISI A 108	Rib (Dorsal)	ISI A 153
Clavicle, left	ISI A 64	Intercentrum (Dorsal)	ISI A 109	Rib (Dorsal)	ISI A 154
Clavicle, left	ISI A 65	Intercentrum (Dorsal)	ISI A 110	Rib (Cervical)	ISI A 155
Interclavicle	ISI A 66	Intercentrum (Dorsal)	ISI A 111	Rib (Dorsal)	ISI A 156
Interclavicle	ISI A 67	Intercentrum (Dorsal)	ISI A 112	Rib (Dorsal)	ISI A 157
Humerus, Right	ISI A 68	Intercentrum (Dorsal)	ISI A 113	Rib (Dorsal)	ISI A 158
Humerus, Left	ISI A 69	Intercentrum (Dorsal)	ISI A 114	Rib (Dorsal)	ISI A 159
Humerus, Right	ISI A 70	Intercentrum (Dorsal)	ISI A 115	Rib (Caudal)	ISI A 160
Humerus, Right	ISI A 71	Intercentrum (Dorsal)	ISI A 116	Rib (Caudal)	ISI A 161
Humerus, Right	ISI A 72	Atlas with spine	ISI A 117	Rib (Dorsal)	ISI A 162
Humerus, Left	ISI A 73	Axis	ISI A 118	Rib (Dorsal)	ISI A 163
Humerus, Right	ISI A 74	Axis	ISI A 119	Rib (Cervical)	ISI A 164
Humerus, Right	ISI A 75	Axis	ISI A 120	Rib (Caudal)	ISI A 165
Humerus, Left	ISI A 76	Intercentrum (Dorsal)	ISI A 121	Rib (caudal)	ISI A 166
Ischium, Left	ISI A 77	Intercentrum (Dorsal)	ISI A 122	Phalange (post.right)	ISI A 167
Ischium, Right	ISI A 78	Intercentrum (Dorsal)	ISI A 123	Phalange (post.right)	ISI A 168
Ischium, Left	ISI A 79	Intercentrum (Dorsal)	ISI A 124	Phalange (post.right)	ISI A 169
Cleithrum, Left	ISI A 80	Intercentrum (Dorsal)	ISI A 125	Phalange (ant.right)	ISI A 170
Cleithrum, Right	ISI A 81	Intercentrum (Dorsal)	ISI A 126	Phalange (ant.right)	ISI A 171
Cleithrum, Left	ISI A 82	Intercentrum (Dorsal)	ISI A 127	Phalange (ant.right)	ISI A 172
Femur, Left	ISI A 83	Intercentrum (Dorsal)	ISI A 128	Phalange (ant.right)	ISI A 173
				Phalange (post.right)	ISI A 174

two main sets of the line canals, lateral and supraorbital, within the lachrymal. They are sinuous and touch each other inside the lachrymal.

The ratio of the width of the lachrymal at the orbit margin and the diameter of the orbit ranges between 0.2588 and 0.3409 in *B. maleriensis*. This ratio ranges from 0.6 to 0.4545 in case of *B. perfecta*. It appears that in *B. perfecta* the lachrymal is more equant and has a wider insertion on the orbit margin (Case, 1922, fig. 1). This is evident also in "*B. howardensis*" (Sawin, 1945, fig. 3) and in "*Eupelor browni*" (Colbert and Imbrie, 1956, fig. 8) which were grouped into *B. perfecta* by Hunt (1993).

The curvature of otic notch, the shape of the tabular horn, the position and size of the orbits and the narial openings with respect to the skull length are also more uniform among the specimens of *B. maleriensis* than they are in *B.*

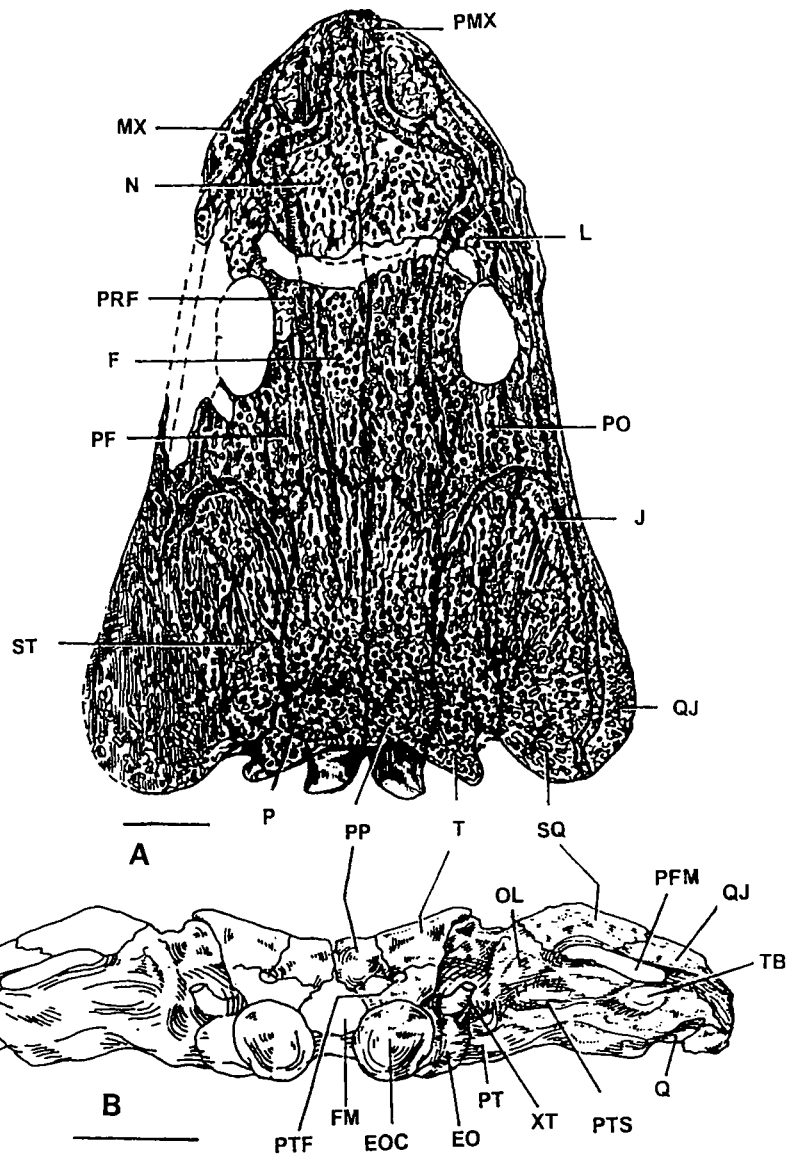

Figure 5. A = ISI A 56, skull roof of *Buettneria maleriensis*, new combination (abbreviations used are same as Figure 3). B = Occiput of *B. maleriensis*, based on the right side of ISIA 58. Abbreviations: EO = exoccipital; EOC = exoccipital condyle; FM = foramen magnum; OL= otic lamellae; PFM = paraquadrate foramen; PP = postparietal; PT = pterygoid; PTF = posttemporal fenestra; PTS = pterygoid sinus; Q = quadrate; QJ = quadratojugal; SQ = squamosal; XT = broken part of the stapes; T = tabular; TB = tubercule. Scale bars = 5 cm.

perfecta.

Remarks.—As discussed earlier, Hunt (1993) differentiated *Buettneria* from all other metoposaurids by the presence of the lachrymal in the orbit border. Other metoposaurids were further divided into several genera and species on the basis of certain synapomorphies and autapomorphies. For example, *Dutuitosaurus* and *Apachesaurus* share the apomorphy of having presacral centra with a diameter length < 0.8 cm and the former has the maxilla entering the orbit margin as an autapomorphy (Hunt 1993, p. 80). For the genera which do not have the lachrymal in the orbit margin, the shape of the lachrymal was considered by Hunt (1993) to separate *Metoposaurus diagnosticus* from *Metoposaurus bakeri*. *Apachesaurus* has been partly characterised by the flexure of the supraorbital canal being separated from the lachrymal (Hunt, 1993, p. 81). However, all metoposaurids having their lachrymal in the orbit were grouped as *B. perfecta* by Hunt. The shape of the lachrymal or the position of the flexure of the supraorbital line canals or any other variations were not

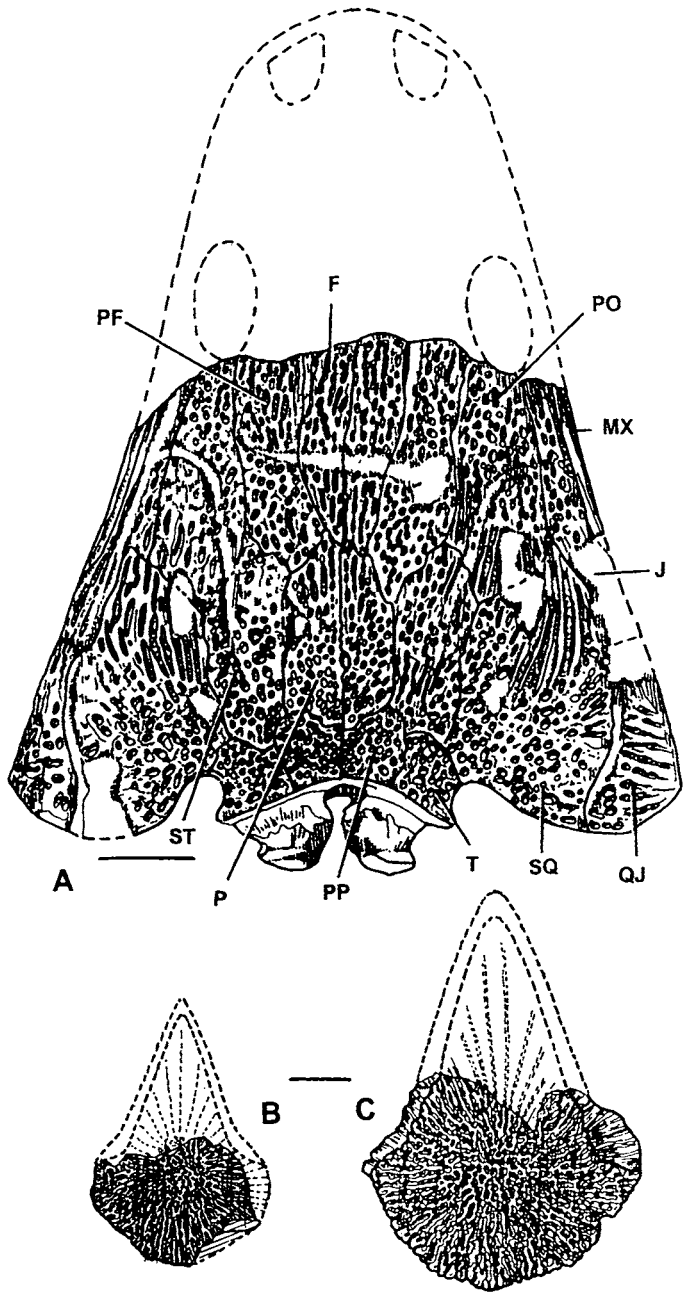

Figure 6. **A** = ISI A 53, skull roof of *Buettneria maleriensis*, new combination (abbreviations used are same as Figure 3). **B, C** = Interclavicles of *B. maleriensis*; **B** = collected from Tiki Formation (G.S.I. 2249, originally described by Lydekker 1885 as a skull roof bone), **C** = from Maleri (K33/638, Huene 1940). A, B and C are after Sengupta 1992. Scale bars = 5cm.

considered. Thus *Buettneria sensu* Hunt (1993) lacks any autapomorphy and results in a metataxon (Smith, 1994). Differentiating *B. maleriensis* from *B. perfecta* (*sensu* Hunt, 1993) on the basis of the width of the lachrymal at the orbit margin and the presence of the flexures of both the lateral and supraorbital line canals on the lachrymal is, therefore, relevant.

The localities yielding *B. perfecta* are restricted to the central and eastern United States, western Europe and northeastern Africa. During Late Triassic times these localities were believed to be very close and probably connected by land (Hunt, 1993, fig. 1). The population of *B. maleriensis* occurs outside that zone. Roychowdhury (1965) also emphasized the geographic isolation of the

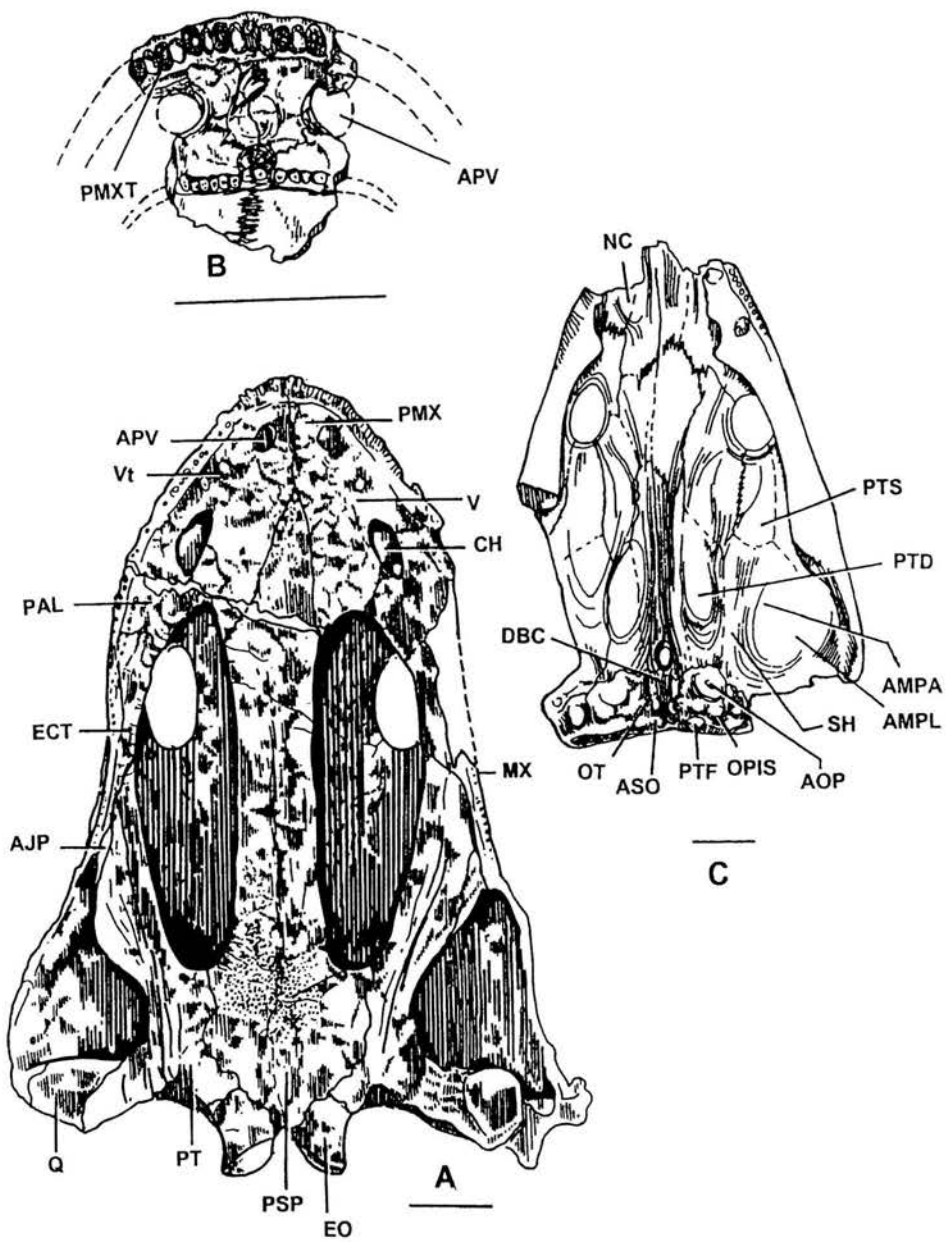

Figure 7. **A** = ventral view of the palate of *Buettneria maleriensis*, new combination based on ISIA 56. **B** = the anterior palatal vacuities and the straight row of teeth behind based on a supplementary fragment ISIA 56a collected from Nalapur. Note the detached tooth, complete and well preserved, cemented later on the vomer. **C** = ventral view of the skull roof of *B. maleriensis* based on ISIA 59. Abbreviations: AJP = alar process of the jugal; AMPA = *adductor mandibulae,* posterior *articularis* (after Wilson, 1941); AMPL = *adductor mandibulae* posterior *longus* (after Wilson, 1941); AOP = attachment for the cartilaginous otic process; APV = anterior palatal vacuity; ASO = attachment for the supraoccipital; CH = choana; DBC = dorsal side of cartilaginous brain case; ECT = ectopterygoid; EO = exoocipital; MX = maxilla; NC = dorsal impression of the nasal capsule (after Wilson, 1941); OT = otic capsule; PAL = palatine; PMX = premaxilla; PMXT = premaxillary teeth; PSP = parasphenoid; PT = pterygoid; PTD = deep portion of *pterygoideus* (after Wilson, 1941); PTF = posttemporal fenestra; PTS = superficial *pterygoideus* (after Wilson, 1941); Q = quadrate; SH = *suspensorius hyoideus* (after Wilson, 1941); V = vomer; Vt = vomerine tusk. Scale bars = 5 cm.

Indian population and suggested that biometric studies could reveal its specific characters. The biometric studies of Indian metoposaurids will be dealt in a separate publication. Meanwhile certain observations are noted below.

Colbert and Imbrie (1956, figs. 13, 14, p. 434–438, table 8) illustrated a technique to plot the bivariate population range diagram of certain skull roof parameters. The field range for *B. maleriensis* has been calculated using similar

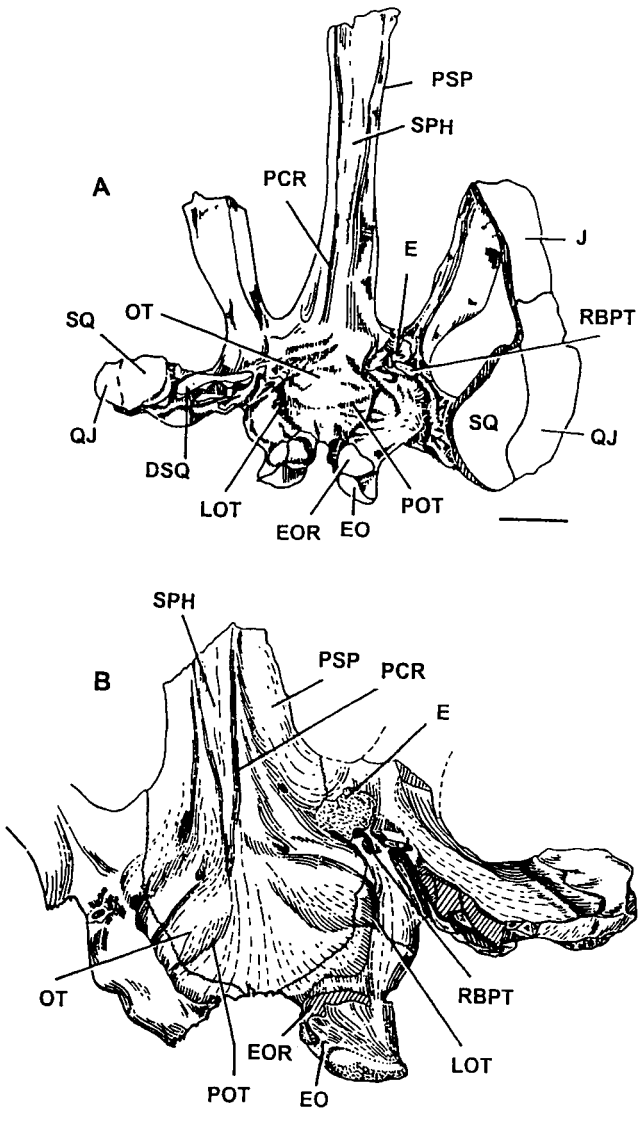

Figure 8. Dorsal view of the palate of *Buettneria maleriensis*, new combination; **A** = ISI A 59; **B** = ISI A 7, after Roychowdhury (1965). Abbreviations: DSQ = descending process of the squamosal; E = epipterygoid; EO = exooccipital; EOR = ascending process of the exoccipital (broken); LOT = lateral ridge bounding otic region; OT = otic capsule; PCR = ridge on the cultriform process of the parasphenoid; POT= posterior ridge bounding otic region; PSP = parashenoid; QJ = quadratojugal; RBPT= rim of the basipterygoid process; SPH= depression for sphenethmoid; SQ= squamosal. Scale bars = 5cm. B.

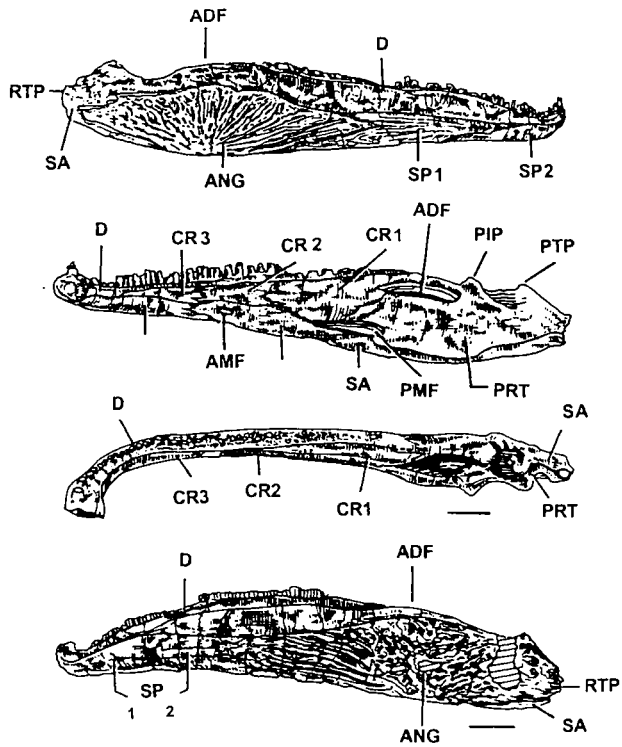

Figure 9. Right mandible of *Buettneria maleriensis*, new combination based on ISIA 60. From top: labial, lingual and dorsal views. Bottom: left mandible of *Buettneria maleriensis* based on ISIA 61. Abbreviations: ADF = adductor fossa; AMF = anterior Meckelian foramen; ANG = angular; CR (1,2,3) = coronoids; **D** = dentary; PIP = preglenoidal internal process; PMF = posterior Meckelian foramen; PRT = prearticular; PTP = postglenoidal process; RTP = retroarticular process; SA = surangular; SP (1,2) = splenials. Scale bar = 5 cm.

techniques. It is found that the range of *B. maleriens* is specific and only partly overlapping with the multigeneric North American species now grouped together as *Buettneria perfecta* by Hunt (1993).

Sengupta and Ghosh (1993) attempted some cephalometric studies of some of the individuals of the North American metoposaurids and *B. maleriensis*. They used several skull roof parameters and extracted three major factors through a principal-component-based factor analysis. They found that the plots of the factor scores on two-dimensional Cartesian coordinates (Sengupta and Ghosh, 1993, fig. 2) indicate a peripheral position of the Indian metoposaurids with respect to the main concentration of the similar plots of the American metoposaurids.

General characters of *Buettneria maleriensis*

Osteology of both the dorsal and ventral sides of the skull roof and of the palate of the metoposaurids have been described in some detail by Cope (1868), Fraas (1889, 1913), Case (1922, 1932), Watson (1919), Sawin (1945), Romer (1947), Colbert and Imbrie (1956), Roychowdhury (1965), Dutuit (1976) and Hunt (1993) among others. Wilson (1941) discussed the soft parts. Hence only the general characters of the skull of *B. maleriensis* are given below.

Skull roof.—Buettneria maleriensis has a very flat skull with short snout and anterolaterally placed orbits (Figures

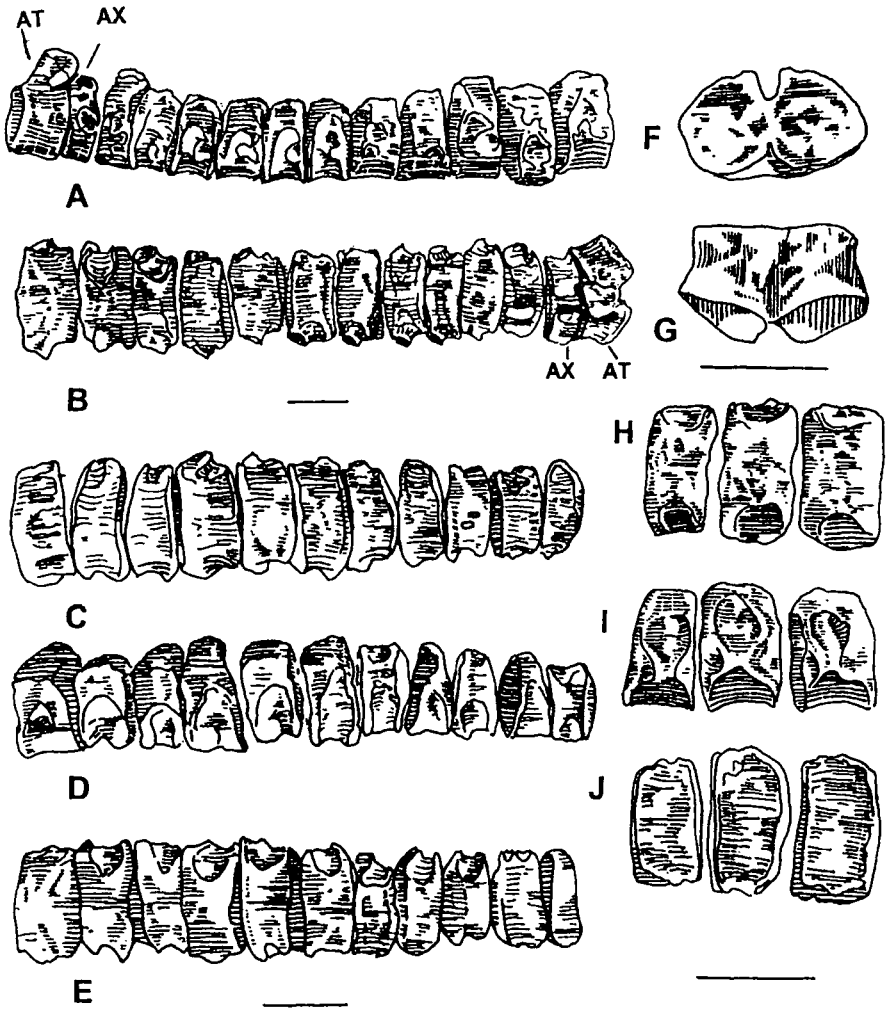

Figure 10. Elements of vertebral columns of *Buettneria maleriensis*, new combination. **A** = lateral and **B** = dorsal views of one possible presacral column; **C** = dorsal, **D** = lateral and **E** = ventral views of second such pre sacral column. AT and AX are the atlas and the axis. Another single atlas with anterior (**F**) and dorsal (**G**) views are also shown. **H**, **I** and **J** are the dorsal, lateral and ventral views of a set of three adjacent caudal intercentra. All the specimens were collected from the Aigerapalli accumulation. Scale bars = 5 cm.

1A–C; 2A, B; 3; 4; 5A; 6A). Skulls have well defined, curved tabular horns and deep otic notches. The pineal foramen is placed well posterior to the orbit. The postparietal is shorter than the parietal.

The posterior part of the skull has rather thick rectangular bones, namely the tabular, postparietal, parietal and supratemporal, which are strongly ornamented with circular pits walled by high ridges.

The snout, with close, large nares, is also well built with a similar type of ornament. Premaxilla and nasal are the two major bones in this area. Roychowdhury (1965) noted the presence of an extra bone in one of the specimens (ISI A 4) of *B. maleriensis* exposed on the dorsal surface of the skull. No such bone has been identified in any of the newly collected specimens. This is probably the extra sutural growth noted in many temnospondyls (Romer, 1947; Welles and Cosgriff, 1965). The floor of the naris is made up of the septomaxilla which is thin and flat.

The middle part of the skull table is flat, thin and has elongate bones, namely, the frontal, postorbital, prefrontal and jugal with elongate ridges and valleys as ornament. The lateral line canals do not form a loop posterior to the orbit. The lachrymal becomes narrow and touches the orbit margin.

Palate.—The ventral side of the palate (Figure 7A, B) has a flat rectangular base composed of parasphenoid from which a triradiating structure emerges with two palatine rami of the pterygoid between sub temporal and interpterygoid vacuities and a wide, flat cultriform process of the parasphenoid in the middle. The latter connects the base

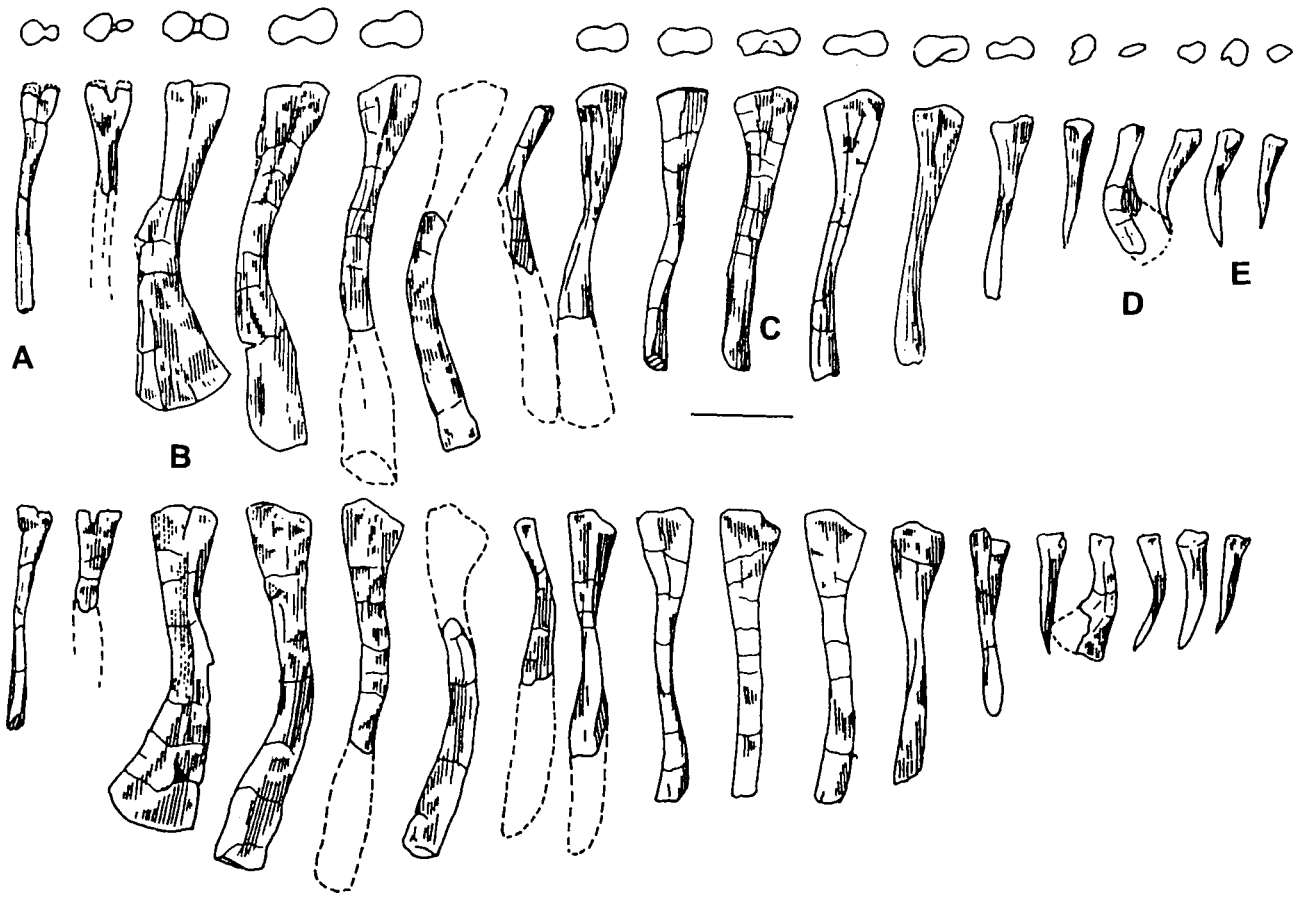

Figure 11. Ribs (left side) of *Buettneria maleriensis*, new combination based on specimens ISIA 149 to ISIA 166. The total number of cervical, thoracic, sacral and caudal ribs are not known. In the diagram, only the preserved specimens are arranged one after another (external view at the top and internal view at the bottom). **A** = one of the two cervical ribs preserved. **B** = a typical anterior thoracic rib; **C** = posterior thoracic rib; **D** = possibly the lone sacral rib and **E** = caudal rib. Scale bar = 5 cm.

of the parasphenoid to the wide vomers. On the ventral side of the skull roof a narrow ridge is present in the midline particularly in the postorbital part (Figure 7C). This tapers towards the anterior and is perforated by the pineal foramen. This ridge corresponds in position to the depression present on the dorsal side of the cultriform process of the parasphenoid. This depression probably housed the cartilaginous sphenethmoid (Figure 8).

The position of the epipterygoid and the foramen of the internal carotids, the recess for the basipterygoid process, the anterior end of the depression for the sphenethmoids and the position of the arcuate ridges bordering the otic region on the dorsal side of the palate of *B. maleriensis* are figured (Figure 8). These features, however, are similar in all the metoposaurids (see Case, 1922, figs. 2, 3; Wilson, 1941, figs. 1, 2; Roychowdhury, 1965, fig. 12; DuTuit, 1976, pls. 11-15).

On the dorsal side of the pterygoid, in ISI A 59, a part of the epipterygoid is preserved (Figure 8A, B). The ascending process of the epipterygoid was previously illustrated by Roychowdhury (1965, p 28). The braincase and associated features, the position of the epipterygoids and adjacent canals shown by Roychowdhury (1965), Case (1922) and Dutuit (1976) are noted in almost all the new specimens of *B. maleriensis*. Similar braincases are partly preserved in ISI A 7 and ISI A 59. The stapes is partly preserved in two individuals, ISI A 56 and ISI A 58 (Figure 5B).

Maxillary and palatal dentitions.—Maxillary and palatal dentitions extend far posterior to the centre of the interpterygoid vacuities. Vomerine and palatine tusks are present. One of the paratypes (ISI A 56a) has two well developed, circular, well separated, anterior palatal vacuities and a series of small vomerine teeth posterior to them (Figure 7A, B).

Occiput.—The occiput has the shape of a triangle with the base made up of postparietal and tabular on the dorsal side (Figure 5B). The exoccipital sutures with the postparietal and tabular housing a small, circular posttem-

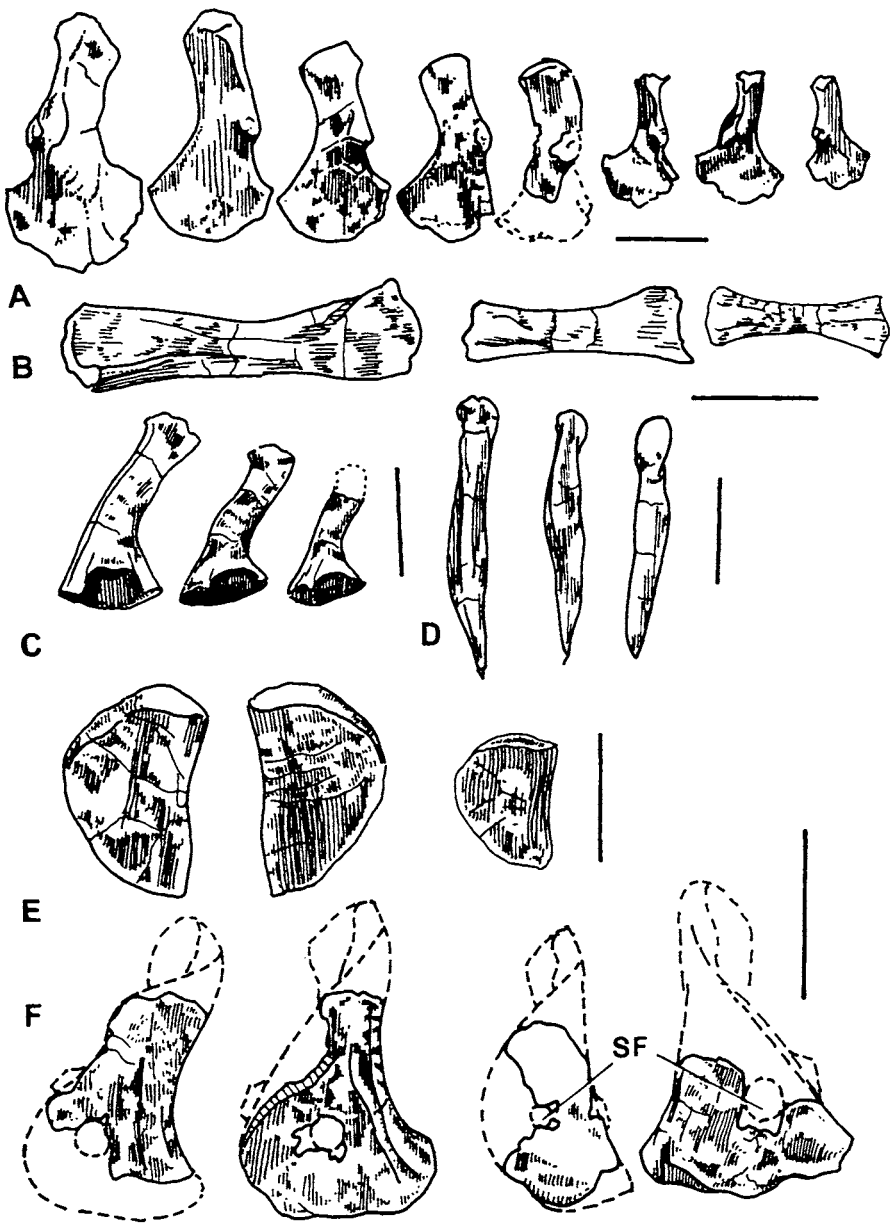

Figure 12. Some of the postcranial bones of *Buettneria maleriensis*, new combination, collected from the Aigerapalli metoposaur graveyard. **A** = Humeri, ventral view (ISIA 69 to 76), **B** = Femora, ventral view (ISIA 83 to 85), **C** = Ilia, lateral view (ISIA 86 to 88), **D** = Cleithra, mesial view (ISIA 80 to 82), **E** = Ischia, dorsal view (ISIA 77 to 79) and **F** = Scapulocoracoids, mesial view (ISIA 89, 90, 92, 94) with supraglenoid foramen (SF). Scale bars = 5 cm.

poral fossa at the junction of the three bones. The foramen magnum is at the centre of the triangle which is terminated by the flat parasphenoid and occipital condyles almost at the same ventral level. There is a little vaulting of the pterygoid and the ascending processes of the bone sutures with the quadratojugal and squamosal. These bones form the dorsal margin of a large, elliptical paraquadrate foramen. Unlike the earlier composite reconstruction of the occiput (Roychowdhury, 1965, fig. 11, p. 21), the specimens described here show a thin insertion of the pterygoid in the lateral part of the paraquadrate foramen.

Mandible.—The mandible of *B. maleriensis* is described here for the first time. Two complete mandibles and a few broken fragments are available for study (Figure 9). The specimens are deepest in the region of the angular and their cross-sections are squared at the midlength. One of the specimens (ISIA 60) is more cylindrical in cross-section and narrow at the region of the spenials. The mandible has

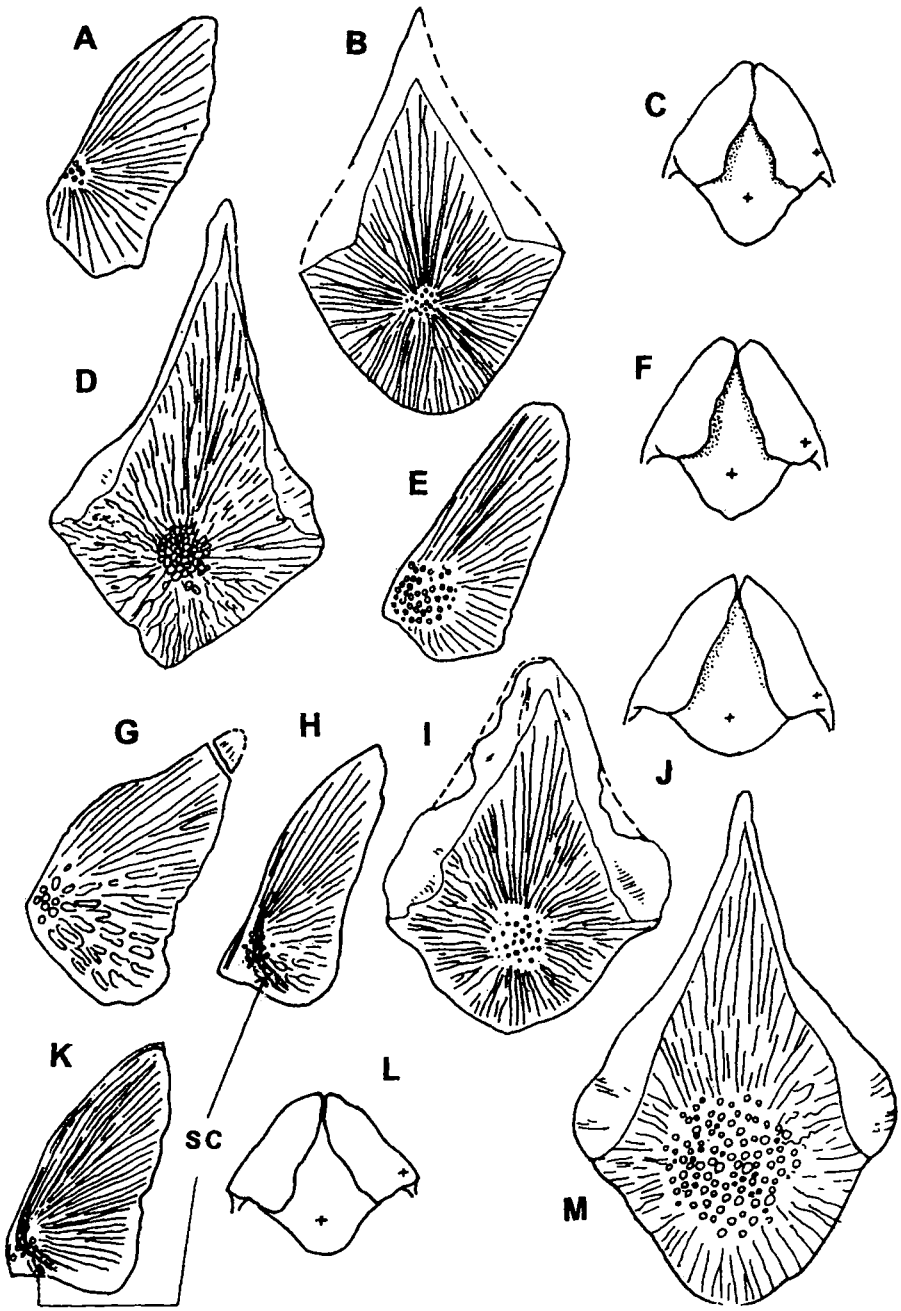

Figure 13. Clavicles and interclavicles of *Metoposaurus diagnosticus* Fraas, 1913 (**A** = clavicle; **B**= interclavicle; **C**= clavicle interclavicle together); "*Buettneria howardensis*" Sawin, 1945 (**D** =clavicle; **E** = interclavicle; **F** = clavicle interclavicle together); *B. maleriensis*, new combination, (**G** = clavicle; **H** = clavicle; **I** = interclavicle; **J** = clavicle interclavicle together); "*M. ouazzouri*" Dutuit, 1976 (**K** = clavicle; **L**= clavicle interclavicle together; **M** = interclavicle); Sc = sensory canal. For *B. maleriensis* two different types of clavicles are shown (**G** and **H**). C; F and L are after Wernerburg (1990). Diagrams are schematic (not in scale) as interclavicles are enlarged (compared to respective clavicles) to illustrate the ornament.

a short retroarticular process with articular, surangular and prearticular exposed on the dorsal surface. Jupp and Warren (1986) described this as the type of postglenoid area noted in some temnospondyls including metoposaurids. The angular is the dominant bone of the labial side. On the lingual side a large, elongate posterior Meckelian foramen is present whose anterior border is formed by the posterior coronoid. The adductor fossa is

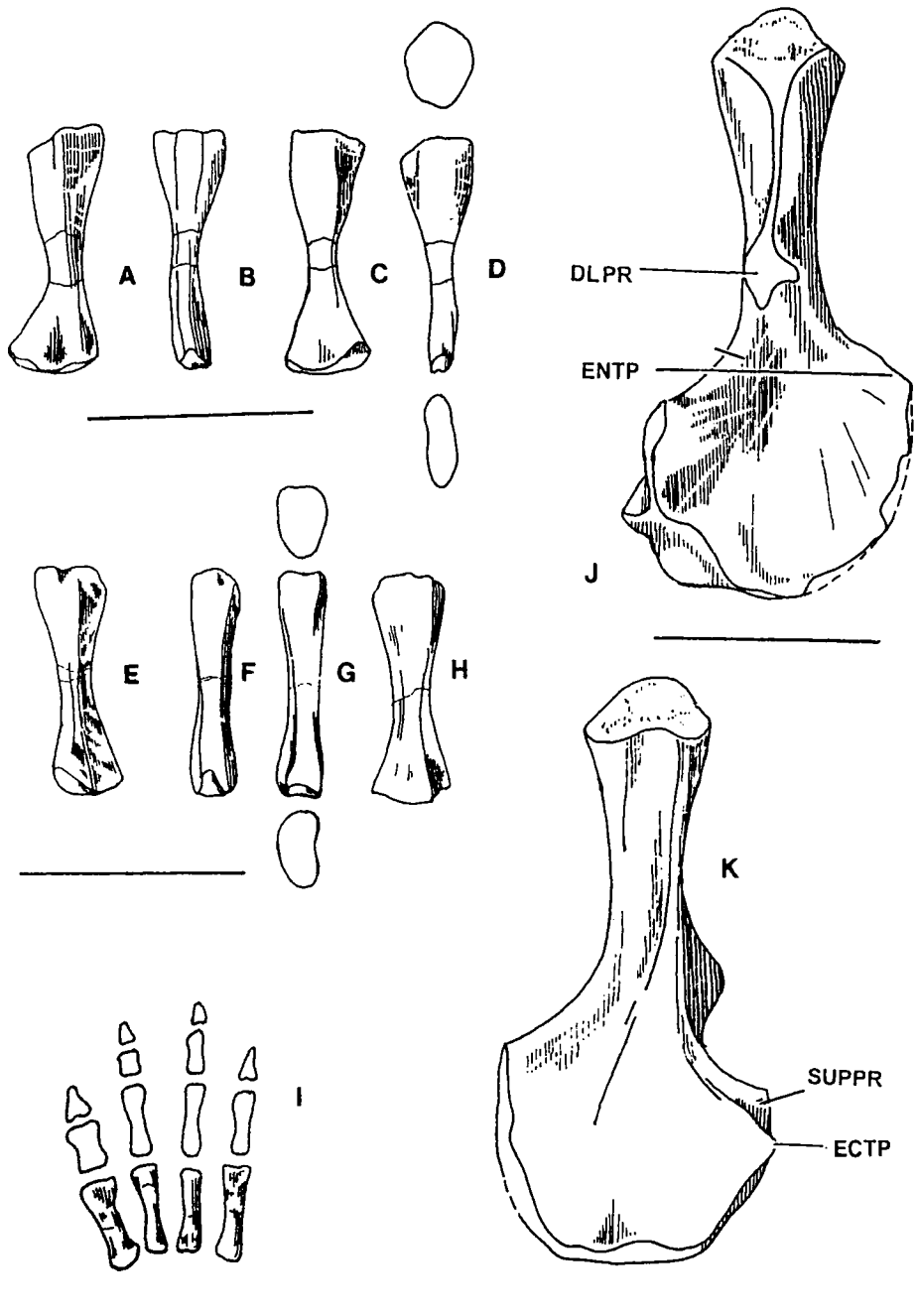

Figure 14. Right radius of *Buettneria maleriensis*, new combination, **A** = external, **B** = anterior, **C** = internal, **D** = posterior views and right ulna **E** = external, **F** = anterior, **G** = internal, **H** = posterior views (based on ISIA 100 and ISIA 95 respectively). **I** = digits of manus of the right side (ISI A 170, to 173, phalangeal formula based on Dutuit , 1976). Right humerus based on ISIA 68; **J** = Ventral, **K** = Dorsal views. DLPR = *Deltoidial* process; ECTP = ectepicondyle; ENTP = entepicondyle; SUPPR = supinater process. Scale bars = 5cm.

large and elliptical. No coronoid process is present. There is a large circular depression around the symphyseal tusk which forms part of the dentary tooth row. A small row of teeth is present on the inner side of the circular depression.

Vertebral elements.—All metoposaurids have typical discoid intercentra of different sizes and shapes (Figure 10). The overall shapes vary from circular to triangular and sometimes these variations are associated with their position in the vertebral column. Variations are also noted

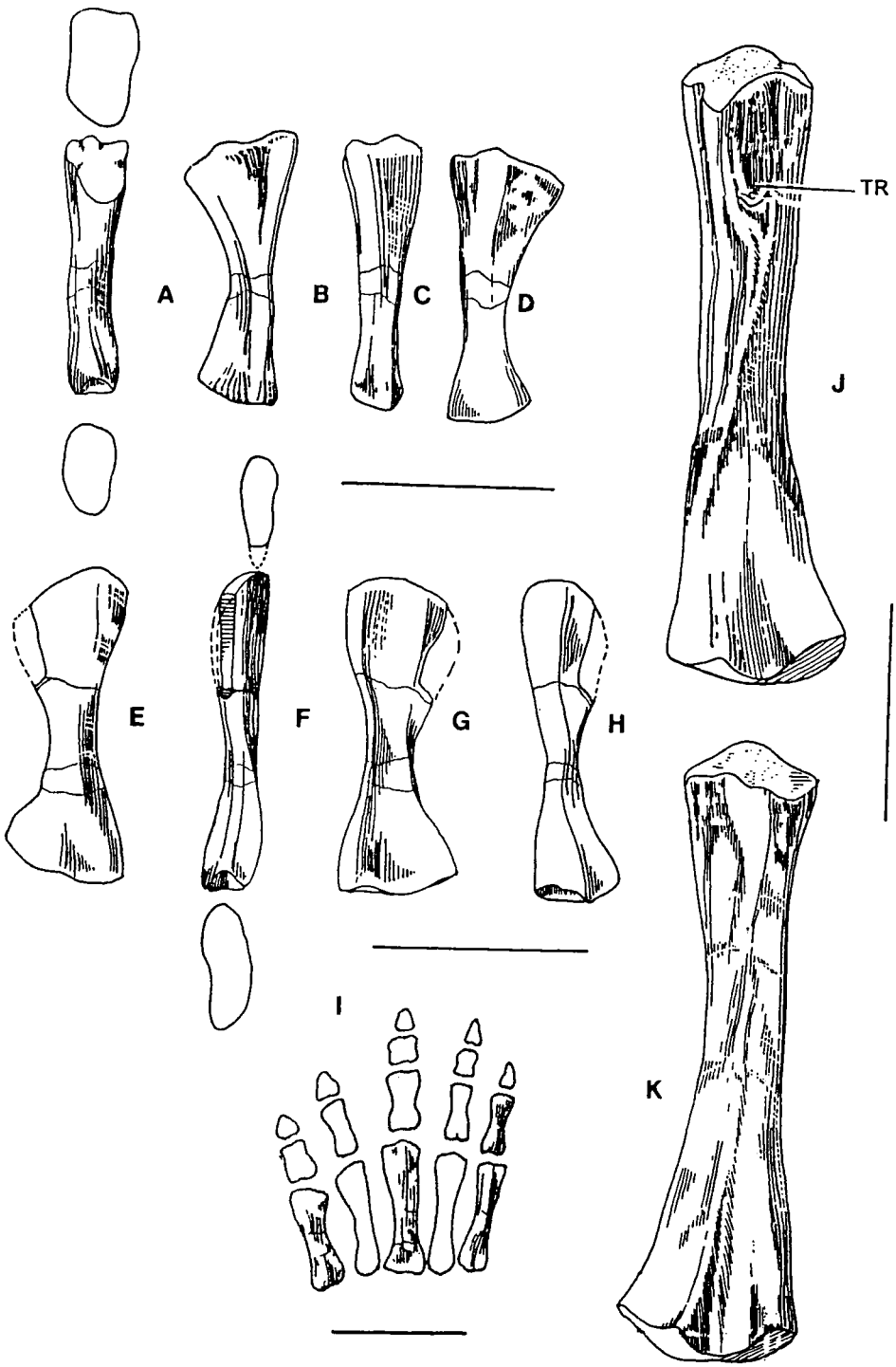

Figure 15. Left tibia of *Buettneria maleriensis*, new combination, **A** = posterior, **B** = internal, **C** = anterior, **D** = external and right fibula, **E** = posterior, **F** = internal, **G** = anterior, **H** = external. (based on ISIA 99 and 101 respectively). Pes of the right side (based on ISI A 167, 168, 169 and 174). Phalageal formula based on Dutuit (1976). Left femur based on ISIA 83; **J** = ventral, **K** = dorsal views; TR = *trochanter*. Scale bars = 5 cm.

among individuals. The vertebral count of an individual of the metoposaurids is uncertain. Sawin (1945) figured 18 presacral intercentra for *Buettneria*. Dutuit (1976) illustrated 22 intercentra for one individual of "*M. ouazzoui*" (XIII /14/66) and 20 for another (XIII /4/66). In the reconstruction of *B. maleriensis* an average of 20 presacral

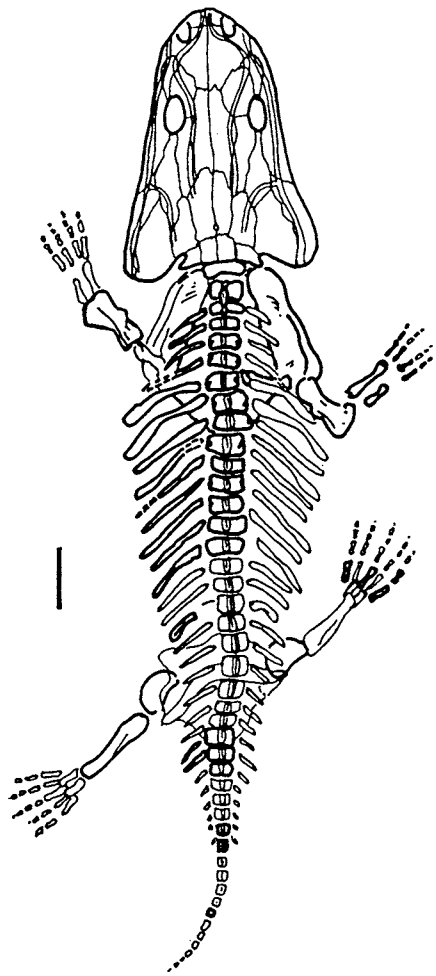

Figure 16. Composite restoration of *Buettneria maleriensis*, new combination. Dark lines represent elements from one individual. Scale bar = 10cm.

intercentra have been figured. The new collection from Aigerapalli includes 23 dorsal and 13 caudal intercentra. From the accumulation of vertebral elements of at least six individuals, parts of two possible columns (Figure 10) are reconstructed from the presacral vertebrae following Sawin (1945) and Dutuit (1976).

The atlas is double faceted at the anterior end to host the double condyles (Figure 10A, B, F, G). In one of the two inferred vertebral columns just mentioned (Figure 10A) the axis and one intercentra (possibly occurring just behind the axis) have two rib facets on the lateral side. In some of the intercentra the facets protrude whereas in larger intercentra (which are possibly further down the trunk), the posterior presacrals have only the facet without the neck. Anterior to the facet there is another curvature. In lateral view these two curvatures form an hourglass-like depression. This is more pronounced in the caudal intercentra (Figure 10I). The caudals are triangular in outline, quite flat on the dorsal side, platyocoelous to opisthocoelous and smaller in size (Figure 10H–J). Sawin (1945) figured a sacral intercentrum which really differs little from some of the presacrals of the Indian taxon.

In one axis, a space created by the underside of the base of the posteriorly depressed neural arch and the scooped posterior dorsolateral part of the intercentrum clearly indicates the shape of the pleurocentrum. In another specimen, parts of the plerocentrum are preserved. Dutuit (1976) described one vertebra of "*M. ouazzoui*" where both the intercentrum and pleurocentrum are preserved and the combined centrum looks like a discoid with a slightly off-centered notochordal perforation. This type of vertebra has also been observed in *Compsocerops cosgriffi*, an Indian chigutisaurid (Sengupta, 1995). However, no such pleurocentral ossification is noted in *B. maleriensis*.

Unfortunately all the specimens in the collection have their neural arches broken. The axis has the base of the neural arch preserved in some specimens. An intervertebral position of the arches has been predicted by some authors (e.g. Roychowdhury, 1965; Dutuit, 1976; Warren and Snell, 1991). However, there is no direct evidence for this in the specimens of *B. maleriensis*.

Ribs.—The total number of ribs present is uncertain. Two cervical, several anterior presacral and some abdominal ribs have been found (Figure 11). One possible sacral and few caudal ribs are also present.

The cervicals have two separate facets or rib heads. The presacral rib heads are elliptical with capitulum and tuberculum connected by a narrow extension. The postsacral ribs have triangular or even squarish heads. The anterior presacral units have flattened distal extensions with uncinate processes. The abdominal ribs are cylindrical and lack the uncinate process. Warren and Snell (1991) noted that temnospondyls possess a single sacral rib which is expanded both proximally and distally and is stout and short. One short, curved and distally expanded rib is figured here as a possible sacral ribs (Figure 11D). It has a rather expanded proximal end but is quite thin. The caudals are shorter, curved and pointed distally.

Elements of the pectoral girdle.— The scapulocoracoid and the cleithrum are new additions to the Indian metoposaurid collections. They have the usual characters of metoposaurids (Dutuit, 1976). The clavicle and interclavicle have already been described (Roychowdhury, 1965). The scapulocoracoid has an enclosed supraglenoid opening (Figure 12F). This was considered as a primitive character (Warren and Snell, 1991). The cleithrum is spoon-shaped with dorsal expansions (Figure 12D).

Clavicle and interclavicle. — Roychowdhury (1965) noted two different types of clavicles in the Indian metoposaurids. He also mentioned that the clavicles of *M. diag-*

nosticus have a long contact anterior to the interclavicle which is not seen in *B. maleriensis*. Sengupta (1992) illustrated two similar-looking interclavicles, one from the Tiki and the other from the Maleri Formation which are redrawn here (Figures 6B, C). Colbert and Imbrie (1956) used the difference in the position of the centre of ossification and the variable nature of the clavicle-interclavicle overlap as taxonomically important characters. This variability was also highlighted by Warren and Snell (1991) and Werneburg (1990). Figure 13 indicates the clavicles and interclavicles of different metoposaurid taxa with variations in the ornament, position of the centre of ossificaton and nature of overlap of the clavicle on the interclavicle. However, ISI A 12 as illustrated by Roychowdhury (1965, figure 18), has a unique shape. A sensory canal is present in the clavicles of the Indian metoposaurids. This was also noted in *M. ouazzoui* (Dutuit, 1976).

Ilium and ischium.—The ischium is a semicircular bone and the ilium is elongate with a dorsal blade which is rather thick (Figure 12C). Warren and Snell (1991) considered this as a character of taxonomic value.

Fore limbs.—The humerus, like all other metoposaurid humeri, is well built, twisted and has pronounced processes for muscle attachments (Figure 14J, K). The ulna (Figure 14A–D) and radius (Figure 14E–H) are similar to the ones described by Dutuit (1976) for the metoposaurids from Morocco. Some digits of the right manus were also found (Figure 14I).

Hind limbs.—The femur, figured for the first time here (Figure 15J, K), is rather long and fully ossified with complete distal and proximal articular surfaces. The areas for *trochanters* are well developed. The tibia (Figure 15A–D), fibula (Figure 15E–H) and some digits of the right pes (Figure 15I) are also figured. The proximal and distal end of the tibia and fibula are less expanded than in "*B. howardensis*" as figured by Sawin (1945).

A composite restoration of *B. maleriensis* is shown in Figure 16.

Aspects of taphonomy

Buettneria maleriensis, as stated earlier, is known from a large number of specimens from the Maleri Formation of the Pranhita-Godavari valley. Its occurrence in the Tiki Formation of the Son Mahanadi valley is rare. Hence emphasis is given here to the geology and the nature of occurrence of *B. maleriensis* in the Maleri Formation.

Geological attributes.—Mudstone, sandstone and peloidal calcarenite/calcirudite of various colours of the Maleri Formation crop out in NW-SE trending linear belts (Figure 17). The overall dip is 12 to 18 degrees towards the NE. The paleocurrent direction is towards the north.

The mudstone is dominantly red in colour and is structureless. Smectite is the major constituent of the clayey part (Sarkar, 1988). Haematite crystals are also common and iron oxide is responsible for the red colour (Robinson, 1970). The mudstones are exceptionally rich in vertebrate fossils. The sandstone is usually calcareous, cross-bedded, fine- to coarse-grained, containing weathered feldspars and infrequent garnets. Rock fragments and clay galls of different size, shape and colours are common. Fining-upward sequences are discernible in the sandstones (Sarkar, 1988). The sand bodies form narrow elongate ridges with mudstone valleys in between.

The peloidal calcarenite/calcirudite occurs either as solitary mounds and/or a string of such mounds within the red mudstone and also at the bottom of the sandstone (Sarkar, 1988, p. 267). The peloidal calcarenite/calcirudites are cross-bedded with overlapping troughs of various magnitudes and comprise calcite-cemented spherical or discoid peloids of micrite or microspary calcite. According to Sarkar (1988) the paucity of broken abraded peloids and other evidences indicate a local pedogenic origin of the peloids.

Sengupta (1970) noted that while the mudstones represent the interchannel facies, the sand bodies are deposited in the channels of a meandering river system flowing north in a large valley trending NW-SE. Maulik and Chaudhuri (1983) described such sandbodies as ephemeral channel fills.

Palaeoclimate. — Pascoe (1959) suggested that the Maleri sediments were deposited in an extremely arid environment. Robinson (1970) first noted that the red mudstones of the Pranhita-Godavari valley were not necessarily deposited in desert like conditions. The Maleri vertebrate fauna indicates a well watered country. The colour of the mudstone is imparted by iron oxides and the high content of ferric oxides and presence of haematite crystals indicate an oxidising environment of deposition. Recent works suggest that the red colour may be remotely linked with climate (Pye, 1983). The absence of many dessication cracks and footprints as well as the occurrence of fewer evaporites indicate that the climate was not arid. This is also supported by the presence of unionids and an array of aquatic or amphibious vertebrates. The paucity of plants was previously considered as an indicator of aridity. However, this is negative evidence and a good number of herbivore remains are found. On the other hand, the high smectite content (Sarkar, 1988) may indicate low rainfall (Singer, 1980). Peloidal calcirudite and arenite are also indicative of reworking of older soil profiles (Sarkar, 1988). To explain the contrasting evidence it is suggested that there was possibly seasonality in the climate. The aquatic members of the Maleri fauna, living in ephemeral rivers, had survived the drier situations by concentrating in the more permanent bodies of water (Robinson, 1971; Chatterjee *et al.*,

1987).

Mode of occurrence. — Animals living in the lowland habitat are mostly found in the floodplain deposits of the Maleri Formation (Kutty, 1971). Though exact proportions are difficult to determine, the number of lowland metoposaurids are always more than those of the robust rhynchosaurs and phytosaurs. The floodplains were well watered with a good drainage as remains of lowland or semiaquatic vertebrates are found there, associated with occasional bivalves, fossil wood and other sporadic plant debris, within thick red-coloured mudstones (Behrensmeyer and Hook, 1992).

Fossils are found as cracked, flaked or distorted bones which are often covered by peloidal calcirudite and calcarenite and calcareous concretions. Various stages of bone weathering (Behrensmeyer, 1982) are also present in the fossilized bones of the Pranhita-Godavari valley (Sengupta, 1990). The transported, disarticulated, abraded bones indicate large time gaps between their death and burial (Behrensmeyer and Hook, 1992)

In most of the red beds of the Maleri Formation vertebrate remains occur chiefly as surface accumulations of stray fragments and also as *in situ* bones in the floodplains. The *in situ* bones, in turn, can be fragmentary or complete. Four taphonomic facies can be identified in the Maleri sediments. The vertebrate bones occur as 1) complete *in situ* material in the mudstone, 2) fragmentary but *in situ* material in mudstone, 3) well preserved but broken bone accumulation in the sandbodies or in the peloids and 4) stray surface accumulation in the mudstones. Types 2 and 3 can be subdivided into i) isolated but broken skeletal parts and ii) fragments of one or more skeletal elements.

Bones belonging to metoposaurids are found in all these types of accumulations. Most of the metoposaurid material described by the early workers like Miall (1875), Lydekker (1885) and Huene (1940) belonged to taphonomic facies 4. Voorhies (1969) noted three major groups of bones according to their potential for dispersal particularly by water. The bulk of the specimens of *B. maleriensis* belong to Voorhies' (1969) group which constitutes an assemblage of skulls and mandibles. This indicates the transported nature of the metoposaurid material from the Maleri Formation. The most common skull fragments are of the tabular area as it is the strongest. The jaws are frequently represented by the symphyses. The skull margins are often preserved, without the thin midskull region. The deposition of peloidal calcirudites of diagenetic origin on the bones indicates various orders of reworking.

The above taphonomic picture indicates that, after death, the semiaquatic and lowland fauna of the Maleri Formation, living in a seasonal climate, were mostly exposed on the flood plains and were fragmented and transported (and even reworked). The lowermost mudstone unit of the Maleri Formation is the thickest (Figure 17) and there the remains of lowland vertebrates are high in number. In that unit, due to some events leading to mass accumulations, finds like Aigerapalli came into being. A closer look at the Aigerapalli site may reveal some more information.

Taphonomy of the Aigerapalli accumulation. — The Aigerapalli site, near the base of the basal mudstone, chiefly comprises mudstones of red colour, with a few streaks of white, calcareous, fine- to medium-grained well-sorted sandstone. The bones were excavated from an area of only 10 m by 5 m which yielded over 100 disarticulated bones of several individuals.

There are 9 humeri (6 from the right side and 3 from the left) from six individuals with three different size ranges (Figure 12A). As indicated by the size ranges, two individuals were larger in size, one intermediate and three were small. The larger humeri come in the size range of 12.6 to 11.5 cm in length. There are three such specimens (a left and two from right) from two individuals. The next size range is a left and a right humerus of around 10 cm length possibly representing another individual. The last size range is around 6 cm length and from 4 specimens (three from left and one right) at least three individuals can be identified. The three size domains are also supported by the length of the three femora (Figure 12B). However, two skulls were recovered of which one is complete.

Though the thickest mudstone unit of the Maleri contains the metoposaur accumulation, sporadic occurrence of peloidal calcarenites/rudites within the unit suggests intermittent exposure to aridity. In fact, it is argued in the section dealing with paleoclimate that contradictory evidence for aridity and humidity are present in the lithology and fauna of the Maleri Formation and a seasonal climate could be a possible explanation. The aquatic fauna survived in small deeper pools at the time of aridity and might have moved away in search of safer places (Robinson, 1971, Chatterjee *et al.*, 1987). While doing so they could be trapped in the thick mud. Their remains were buried after being scattered by various agents. The bones have evidences of some amount of transportation. On the other hand, some of the small postcranial as well as a number of small and delicate teeth are well preserved. Hence, the transportation was possibly not prolonged.

The Aigerapalli type of bone accumulation is not uncommon at other metoposaurid-yielding localities around the world (Romer, 1939; Dutuit, 1976). The absence of articulated individuals is marked in the Aigerapalli and also in the mass accumulation of metoposaurids in the Lamy amphibian quarry in New Mexico (Romer, 1939). The latter has a similar taphonomic background to Aigerapalli where hydrodynamic sorting of bones of dead individuals from a residual pool affected by drought has been thought

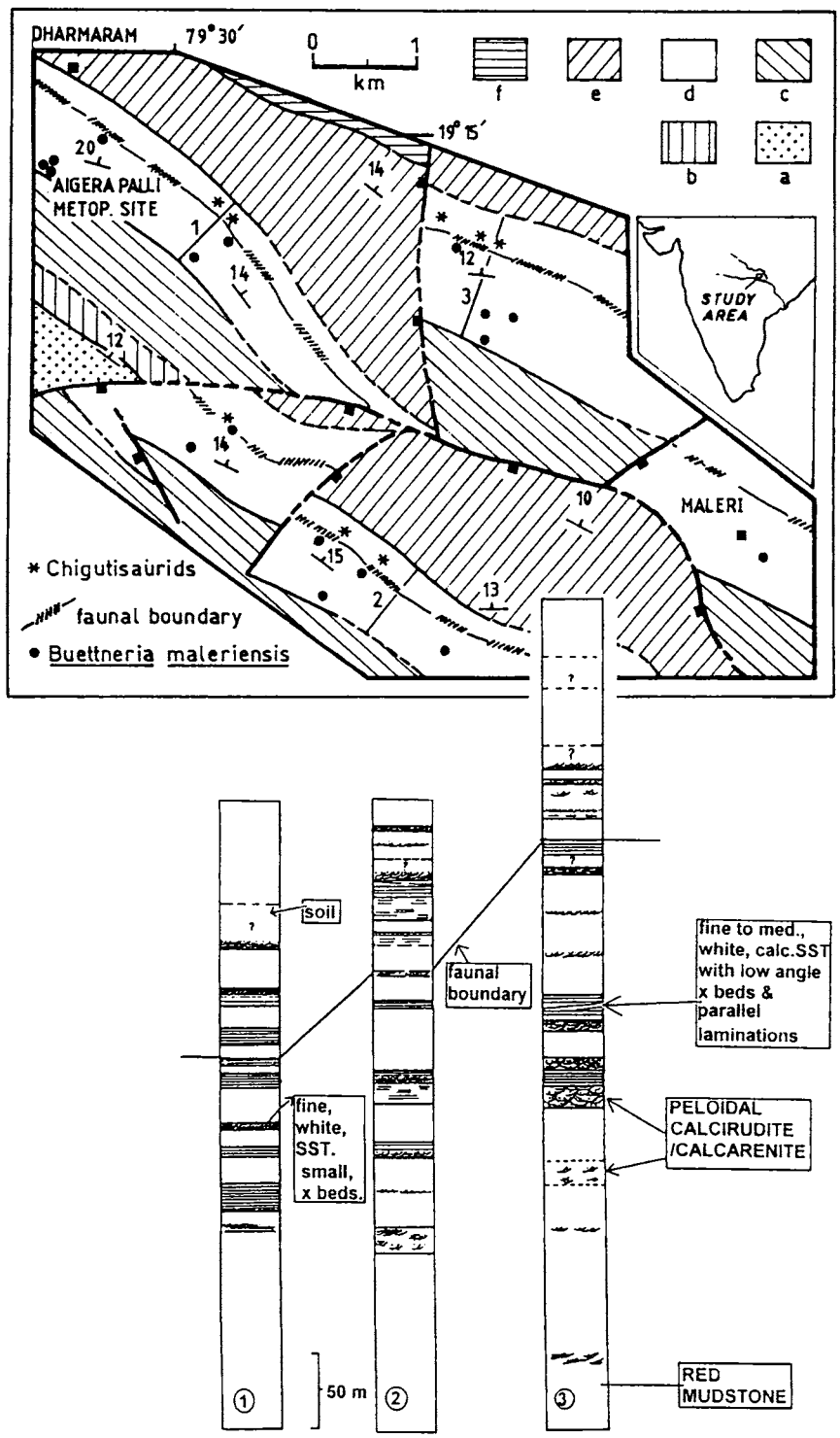

Figure 17. Geological map around the villages of Maleri and Dharmaram. Legends: a = Kamthi Formation, b = Yerrapalli Formation, c = Bhimaram Formation, d = Maleri Formation. Within the Maleri Formation the boundary between the lower and upper Maleri fauna is shown. The lines 1, 2 and 3 represent the positions of the columnar sections shown below the map.

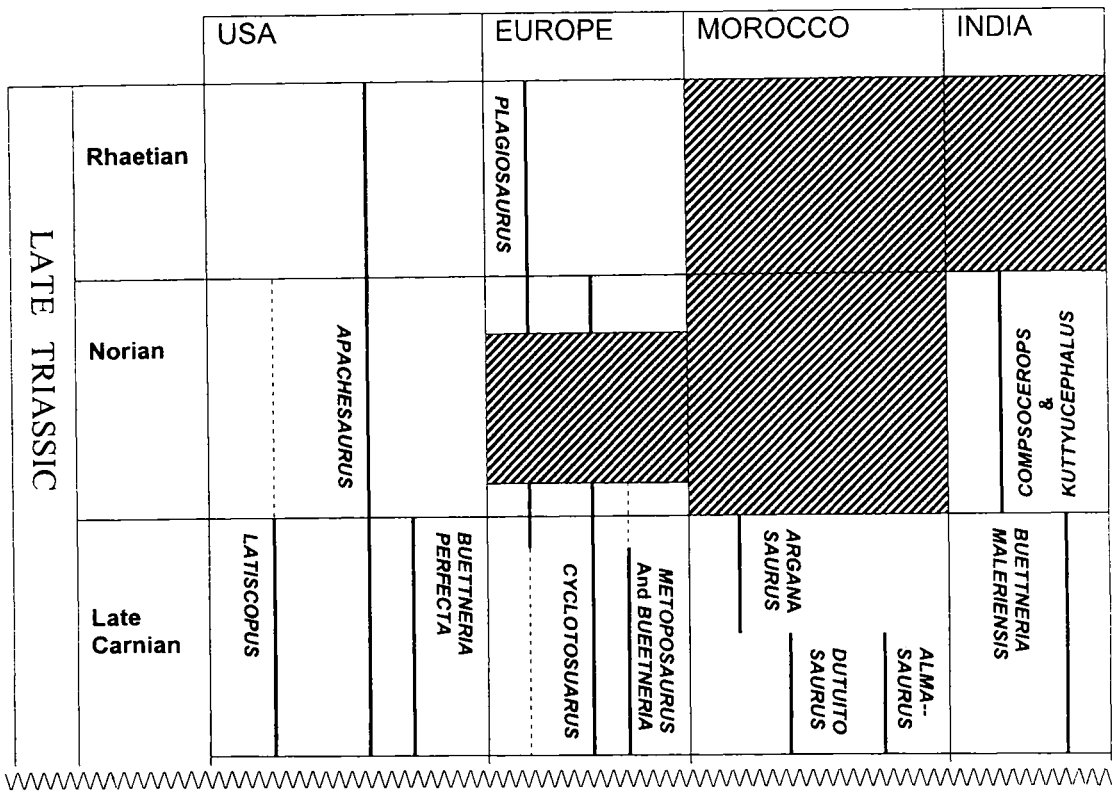

Figure 18. Stratigraphic ranges of metoposaurids and other associated temnospondyls of the Late Triassic Period.

to be the reason behind the accumulation (Romer, 1939; Hunt and Lucas, 1989)

Stratigraphic range of *B. maleriensis*

Roychowdhury (1965) suggested that the Maleri fauna is Carnian or early to middle Norian in age. Subsequently Kutty and Sengupta (1989) divided the Maleri fauna into two groups, a lower and an upper. The age of the lower group, which includes *B. maleriensis*, was stated as Late Carnian. The fauna associated with *B. maleriensis* chiefly consists of the phytosaur *Parasuchus* (*Paleorhinus*), the rhynchosaur *Paradapedon, the* theropod *Alwalkeria*, the protorosaur *Malerisaurus*, the cynodont *Exeraetodon,* an aetosaur and a large dicynodont. Hunt (1993), following the scheme of Lucas and Hunt (1989), put the lower Maleri fauna into the early part of the Late Carnian. The presence of *Paleorhinus* which is found from Tuvulian marine strata of Austria and stands as a good marker fossil in continental deposits, helped to infer this age (Hunt and Lucas, 1991).

Lucas (1998), stated that palynostratigraphy, sequence stratigraphy and magnetostratigraphy of the Chinle Group indicate a Late Carnian age and the principal correlatives are the lower Maleri, Schilfsandstein, Kieselsandstein, and Blasensandstein of the German Keuper and the Argana fauna of Morocco. There is dispute also whether the lower Maleri fauna is early Late Carnian as stated by Hunt (1993) and Hunt and Lucas (1991) or late Late Carnian as stated by Kutty and Sengupta (1989). Hunt and Lucas (1991) predicted the age of the lower and upper Maleri faunas on the basis of phytosaurs. The Upper Maleri phytosaurs are yet to be described in detail. Moreover, immediately above the upper Maleri the Lower Dharmaram fauna (Kutty and Sengupta, 1989) also has an undescribed phytosaur and one or more aetosaurs. Bandyopadhyay and Roychowdhury (1996) noted that *Rutiodon*-like phytosaurs are found only from the upper Maleri and the age of the immediately overlying lower Dharmaram could be Late Norian. This suggests an Early Norian age for the upper Maleri fauna confirming the late Late Carnian age of the lower Maleri fauna occurring immediately below. Hence, it is likely that the last appearance datum of *B. maleriensis* is late Late Carnian.

Except in North America all metoposaurids were restricted to the Carnian. In North America, the Dockum Formation of Western Texas, Bull Canyon and Redonda Formations of Eastern New Mexico, the Painted Desert Member of the Petrified Forest Formation and the Owl

Rock Formation of northeastern Arizona have metoposaurids younger than Carnian in age. The post Carnian metoposaurid, *Apachesaurus,* is not abundant compared to the Carnian occurrences (Hunt, 1993). From the Southwestern United States, Long and Murry (1995) noted "a definite replacement of large metoposaurids by smaller ones" during the Early Norian. No small temnospondyls like *Apachesaurus* (Hunt, 1993) and *Latiscopus* (Wilson, 1948) from North America or *Almasaurus* (Dutuit,1976) from Morocco are found in the Late Triassic deposits of Europe or India. On the other hand, no brachyopid temnospondyl, with parabolic skull and deep palate with downturned pterygoids, has been described from the North American Late Triassic (Figure 18). Such temnospondyls are represented in Europe by the plagiosaurids (Kuhn, 1932; Milner, 1994) and in India by the chigutisaurids (Sengupta, 1995).

Paleoposition of India and aspects of paleogeography, paleoclimate and faunal migration

Metoposaurids are restricted chiefly to latitude 40 to 60 North, with the exceptions being the Indian occurrences. The distance of the latter from the other localities was, however, minimised to some extent by the union of the continents during the Late Triassic. On the other hand, chigutisaurids are thought to have originated in Australia (Warren and Hutchinson, 1983) and are so far found to be restricted to Gondwana. India is the only place where metoposaurids were replaced by the chigutisaurids. This has led to some interesting observations on the paleoposition of India and some aspects of paleoclimate, paleogeography and faunal migration.

The absence of endemism among the Late Triassic Indian tetrapods has long been known (Colbert, 1958; Chatterjee and Hotton, 1986). Cox (1974) noticed that the similarity coefficient of Indian fauna with that of North America and Europe is quite high (59% and 81% respectively). On the other hand that with Africa and South America is also not negligible (75% and 56%).

Smith and Briden (1977; map 13, p. 24) have shown that, during the Triassic, Australia was close to India and so were Europe and North America. The circum-Tethyan shoreline is short and curved and the position of Africa was such that the land distance between India and North America was minimal. The figures shown by Hay *et al.* (1982) indicate the position of India was almost halfway between North America and Australia at the end of the Triassic.

Cox (1974) noted that in the Triassic there were no major climatic barriers. Robinson (1973) postulated a sharply seasonal rainfall in parts of North America, Europe, Africa and India during the Triassic (Robinson,1973, fig.10). Parrish *et al.* (1982, fig. 5, p. 39) have also shown that during Induan time a low pressure belt was located in Africa with an adjacent high in the north of India and another one in Europe causing a similar type of wind flow in the areas close to the Tethys. The entire area had 100 to 200 units of rainfall (Parrish *et al.*, 1982) without any major climatic barrier. The Late Triassic metoposaurids could have come from Laurasia along the circum-Tethyan shoreline to India as a geographically peripheral group (this could also support the contention that the Indian metoposaurid, *B. maleriensis*, is a distinct taxon). Chigutisaurids, on the other hand, arrived later, either from Australia or South America.

Acknowledgements

The work was part of the integrated research programme of the Pranhita -Godavari valley carried out by the Geological Studies Unit, Indian Statistical Institute, Calcutta. The field work was funded by the Institute. The specimens were collected by many workers of the Institute. T. Roychowdhury and T. S. Kutty collected and prepared many of the specimens and so did D. Pradhan and Shiladri Das of the Geological Studies Unit (GSU). I am thankful to T. Roychowdhury for critically going through the manuscript. A. Warren of La Trobe University, Victoria reviewed the manuscript and helped to improve it. She and A. Milner of Birkbeck College, London, also helped in recognizing certain taxonomically important characters of the metoposaurids.

References

Bandyopadhyay, S. and Roychowdhury, T. 1996: Beginning of the continental Jurassic in India: A paleontological approach. *In*, Morales, M. *ed.*, *Continental Jurassic. Museum of Northern Arizona Bulletin* 60, p 371-378.

Behrensmeyer, A. K., 1982: Time resolution in fluvial vertebrate assemblage. *Paleobiology*, vol. 8, p.211-227.

Behrensmeyer, A. K. and Hook, R. S., 1992: Paleoenvironments and taphonomy. *In*, Behrensmeyer, A. K. *et al. eds.*, *Terrestrial Ecosystem through Time, Evolutionary Paleoecology of Terrestrial Plants and Animals*, p. 15-136. The University of Chicago Press, Chicago and London.

Branson, E. B., 1905: Structure and relationship of American Labyrinthodontidae. *Journal of Geology*, vol. 13, p. 568-610.

Case, E. C., 1922: New reptiles and stegocephalians from the Upper Triassic of Western Texas. *Carnegie Institution of Washington Publication*, vol. 321, p. 1-84.

Case, E. C., 1931: Description of a new species of *Buettneria* with a discussion of the brain case. *Contributions from the Museum of Paleontology, University of Michigan*, vol. 3, p. 187-206.

Case, E. C., 1932: A collection of stegocephalians from Scurry County, Texas. *Contributions from the Museum of Paleontology, University of Michigan*, vol. 4, p. 1-56.

Chatterjee, S, and Hotton, N. II, 1986: The paleoposition of India.

Journal of South East Asian Earth Science, vol. 1, pt. 3, p. 145-189.

Chatterjee, S., Jain, S. L., Kutty, T. S. and Roychowdhury, T. K., 1987: Mesozoic Gondwana vertebrates of the Pranhita-Godavari valley, Deccan, India—A review. *Geological Survey of India Special Publication*, vol. 11, no.1, p. 195-212.

Colbert, E. H., 1958: Relationships of the Triassic Maleri Fauna. *Journal of the Palaeontological Society of India*, vol. 3, p. 68-81.

Colbert, E. H. and Imbrie, J., 1956: Triassic metoposaurid amphibians. *Bulletin of the American Museum of Natural History*, vol. 110, p. 403-452.

Coldiron, R. W., 1978: *Acroplous vorax* Hotton (Amphibia, Saurerpetontidae) restudied in the light of new material. *American Museum Novitates*, no. 2662, p. 1-27.

Cope, E. D., 1868: Synopsis of the extinct Batrachia, Reptilia and Aves of North America. *Proceedings of the Academy of Natural Sciences, Philadelphia* 1868, p. 208-221.

Cox, C. B., 1974: Vertebrate paleodistribution pattern and continental drift. *Journal of Biogeography*, vol. 1, p. 75-94.

Davidow-Henry, B., 1989: Small metoposaurid amphibians from the Triassic of Western North America and their significance. *In*, Lucas S. G. and Hunt, A. P. *eds.*, *Dawn of the Age of the Dinosaurs in the American Southwest*, p. 278-292. New Mexico Museum of Natural History, Albuquerque.

DeFauw, S. L., 1989: Temnospondyl amphibians: A new perspective on the last phases in the evolution of the Labyrinthodontia. *Michigan Academician*, vol. 21, p. 7-32.

Dutuit, J. M., 1976: Introduction à l'étude paléontologique du Trias Continental marocain. Descriptions des premiers stegocephales recueillis dans le Couloir d'Argana (Atlas occidental). *Mémoires du Muséum National d'Histoire Naturelle (Sciences de la Terre)*, Paris, vol. 36, p. 1-253.

Fraas, E., 1889: Die Labyrinthodonten der Schwabischen Trias. *Palaeontographica*, vol. 36, p. 1-158, pls. 17.

Fraas, E., 1896: Die schwabischen Triassaurier nach dem Material der Kgl. Naturalien-Sammlung in Stuttgart zusammengestellt. *Mitteilungen desKöniglichen Naturalien-Cabinets in Stuttgart* 5, p.1-18.

Fraas, E., 1913: Neue Labyrinthodonten aus der Schwabischen Trias. *Palaeontographica*, vol. 60, p.275-294, pls. 16-22.

Gregory, J. T., 1980: The otic notch of metoposaurid labyrinthodonts. *In*, Jacobs, L. L. *ed.*, *Aspects of Vertebrate History*: Essays in Honor of Edwin Harris Colbert, p. 25 - 136. Museum of Northern Arizona Press, Flagstaff.

Hay, W. W., Behensky, J. F. Jr., Branson, J. E. and Sloon, J. L. II., 1982: Late Triassic-Liassic paleoclimatology of the proto-central North Atlantic rift system. *Palaeogeography, Palaeoclimatology, Palaeoecology*, vol. 40, p. 13-30.

Huene, F. von, 1940: The tetrapod fauna of the upper Triassic Maleri beds. *Palaeontologica Indica, New Series*. vol. 32, no. 1, p.1-42, pls. 1-10.

Hunt, A. P., 1993: Revision of the Metoposauridae (Amphibia: Temnospobdyli) and description of a new genus from Western North America. *In*, Morales, M. *ed.*, *Aspects of Mesozoic Geology and Paleontology of the Colorado Plateau, Museum of Northern Arizona Bulletin* 59, p. 67-97.

Hunt, A. P. and Lucas, S. G., 1989: Late Triassic vertebrate localities in New Mexico. *In*, Lucas, S. G. and Hunt, A. P. *eds.*, *Dawn of the Age of the Dinosaurs in the American Southwest*, p. 72 - 101. New Mexico Museum of Natural History, Albuquerque.

Hunt, A. P. and Lucas, S. G., 1991: The *Paleorhinus* biochron and the correlation of the nonmarine Upper Triassic of Pangaea. *Palaeontology*, vol. 34, p. 487-501.

Jupp, R. and Warren, A. A., 1986: The mandibles of the Triassic temnospondyl amphibians. *Alcheringa*, vol. 10, p. 99-124.

Kuhn, O., 1932: Labyrinthodonten und Parasuchier aus dem mittleren Keuper von Ebrach in Oberfranken. *Neues Jahrbuch für Mineralogie, Geologie und Paläontologie, Reihe B*, vol. 69, p. 94-144.

Kutty, T. S., 1971: Two faunal associations from the Maleri Formation of the Pranhita-Godavari valley. *Journal of Geological Society of India*, vol.12, no, 1, p. 63-67.

Kutty, T. S. and Sengupta, D. P., 1989: Late Triassic formations of the Pranhita-Godavari valley and their vertebrate faunal sequence—a reappraisal. *Indian Journal of Earth Sciences*, vol. 16, no. 4, p. 189-206.

Long, R. A. and Murry, P. A., 1995. Late Triassic (Carnian and Norian) tetrapods from the Southwestern United States. *New Mexico Museum of Natural History and Science Bulletin* 4, p. 1-254.

Lucas, S. G., 1998: Global Triassic tetrapod biostratigraphy and biochronology. *Palaeogeography, Palaeoclimatology, Palaeoecology*, vol. 143, p. 347-384.

Lucas, S. G. and Hunt, A. P., 1989: Vertebrate biochronology of the Late Triassic. *28th International Geological Congress Abstracts* 2, p. 335-336.

Lydekker, R., 1885: Maleri and Denwa Reptilia and Amphibia. *Palaeontologia Indica, Series 4*, no.1, p. 1-38.

Lydekker, R., 1890: *Catalogue of the Fossil Reptilia and Amphibia in the British Museum of Natural History*, Part IV, 296 p. London.

Maulik, P. and Chaudhuri, A. K., 1983: Trace fossils from continental Triassic red beds of the Gondwana sequence, Pranhita-Godavari valley, South India. *Palaeogeography, Palaeoclimatology, Palaeoecology*, vol. 41, p. 17-34.

Meyer, H. von., 1842: Labyrinthodonten Genera. *Neues Jahrbuch für Mineralogie, Geologie und Paläontologie* 1842, p. 301-304.

Miall, L. C., 1875: Report of the committee, consisting of Professor Huxley, L. D., F. R. S.; Professor Harkness, F. R. S.; Henry Woodward, F.R.S.; James Thomson; John Brigg; and L. C. Miall on the structure and classification of the labyrinthodonts. *Report of the Meeting of the British Association for the Advancement of Science*, vol. 44, p. 149-192.

Milner, A. R., 1990: The radiation of temnospondyl amphibians. *In*, Taylor P. D. and Larwood G. P. *eds.*, *Major Evolutionary Radiations*, p. 321-349. Clarendon Press, Oxford.

Milner, A. R., 1994: Late Triassic and Jurassic amphibians, fossil records and phylogeny. *In*, Fraser, N. and Sues, H.-D. *eds.*, *In the Shadow of the Dinosaurs: Early Mesozoic Tetrapods*, p. 5-22. Cambridge University Press, Cambridge.

Parrish, J. T., Ziegler, A. M. and Scotese, C. R., 1982: Rainfall pattern and the distribution of coal and evaporites in the Mesozoic and Cenozoic. *Palaeogeography, Palaeoclimatology, Palaeoecology*, vol. 40, p. 67-101.

Pascoe, E. H., 1959: *A Mannual of Geology of India and Burma*, vol II, p. 485-1343. Goverment of India Press, Calcutta.

Pye, K., 1983: Red beds. *In*, Goudie, A. S. and Pye, K. *eds.*, *Chemical Sediments and Geomorphology: Precipitates and Residua in the Near Surface Environment*, p 227-264. Academic Press, London, New York.

Robinson, P. L., 1970: The Indian Gondwana formations-a review. *1st International Symposium on Gondwana Stratgraphy*, p. 201-268. I.U.G.S. South America.

Robinson, P. L., 1971: A problem of faunal replacement on Permo-Triassic continents. *Palaeontology,* vol. 14, p. 131-153.

Robinson, P. L., 1973: Paleoclimatology and continental drift. *In,* Tarling, D. H. and Runcorn, S. K. *eds., Implications of Continental Drift to the Earth Sciences,* p. 451-467. Academic Press, New York.

Romer, A. S., 1939: An amphibian graveyard. *Scientific Monthly,* vol. 49, p. 337-339.

Romer , A. S., 1947: Review of the Labyrinthodontia. *Bulletin of the Museum of Comparative Zoology Harvard* 99, p. 1-367.

Roychowdhury, T. K., 1965: A new metoposaurid amphibian from the upper Triassic Maleri Formation of Central India. *Philosophical Transaction of the Royal Society of London, Series B,* no. 250, p. 1-52.

Sarkar, S., 1988 Petrology of caliche derived calcirudite/calcarenites in the Late Triassic Maleri Formation of the Pranhita-Godavari valley, South India. *Sedimentary Geology,* vol. 55, p. 263-282.

Sawin, H. J., 1945: Amphibians from the Dockum Triassic of Howard County, Texas. *University of Texas Publication,* no. 4401, p. 361-399.

Sengupta, D. P., 1990: *New Amphibians (Labyrinthodontia, Temnospondyli) from the Maleri Formation of Deccan, India; their Significance in Geology and Palaeontology,* 152 p. Ph. D. Thesis, (Science, Geology), University of Calcutta.

Sengupta, D. P., 1992: *Metoposaurus maleriensis* Roychowdhury from the Tiki Formation of the Son-Mahanadi valley of central India. *Indian Journal of Geology,* vol. 64, no. 3, p. 300-305.

Sengupta, D. P., 1995: Chigutisaurid temnospondyls from the Late Triassic of India and a review of the family Chigutisauridae. *Palaeontology,* vol. 38, p. 313-339.

Sengupta, D. P. and Ghosh, D. P., 1993: Morphometrics of some Triassic temnospondyls. *In,* Lucas, S. G. and Morales, M. *eds., The Nonmarine Triassic. New Mexico Museum of Natural History and Science Bulletin* 3. p. 423-428.

Sengupta, S., 1970: Gondwana sediments around Bheemaram, Pranhita-Godavari valley, India. *Journal of Sedimentary Petrology,* vol. 40, p. 140-170.

Singer, A., 1980: The paleoclimatic significance of clay minerals in soils and weathering profiles. *Earth Science Reviews,* vol. 15, p. 303-326.

Smith, A. B., 1994: *Systematics and the Fossil Record Documenting Evolutionary Patterns,* 223 p. Blackwell Scietific Publication, Oxford.

Smith, A G. And Briden, J. C., 1977: *Mesozoic and Cenozoic Paleocontinental Maps,* 63 p. Cambridge University Press, London, New York and Melbourne.

Voorhies, M., 1969: Taphonomy and population dynamics of an early Pliocene vertebrate fauna, Knox County, Nebraska, *University of Wyoming, Contribution to Geology, Special Paper,*. no. 1, p. 69.

Warren, A. A. and Hutchinson, M. N., 1983: The last labyrinthodont? A new brachyopoid (Amphibia, Temnospondyli) from the Early Jurassic Evergreen Formation of Queensland, Australia. *Philosophical Transactions of the Royal Society of London, Series B,* no. 303, p.1-62.

Warren, A. A. and Snell, N., 1991: The post cranial skeleton of Mesozoic temnospondyl amphibians: a review. *Alcheringa,* vol. 15, p. 43-64.

Watson, D. M. S., 1919: The structure, evolution and origin of the Amphibia — the orders Rachitomi and Stereospondyli. *Philosophical Transactions of the Royal Society of London, Series B,* no. 209, p.1-73.

Watson, D. M. S., 1958: A new labyrinthodont (Paracyclotosaurus) from the Upper Trias of New South Wales. *Bulletin of the British Museum of Natural History, London (Geology),* vol. 3, p. 233-263.

Watson, D. M. S., 1962: The evolution of the labyrinthodonts. *Philosophical Transactions of the Royal Society of London,* ser. B, no. 245, p. 219-265.

Welles, S. P. and Cosgriff, J. W., 1965: A revision of the labyrinthodont family Capitosauridae and a description of *Parotosaurus peabodyi,* n. sp. from the Wupatki Member of the Moenkopi Formation of Northern Arizona. *University of California Publications in Geological Sciences,* vol. 54, p. 1-148, pl. 1.

Werneburg, R., 1990: Metoposaurier (Amphibia) aus dem Unteren Keuper (Obertrias) Thüringens. *Veröffentlichung Naturhistorischen Museum Schleusingen,* vol. 5, no.1, p. 31-38.

Wilson, J. A., 1941: An interpretation of the skull of *Buettneria* with reference to the cartilages and soft parts. *Contributions from the Museum of Paleontology, University of Michigan* 6, p. 71-111.

Wilson, J. A., 1948: A small amphibian from the Triassic of Howard County, Texas. *Journal of Paleontology,* vol. 22, no. 3, p. 359-361.

Zittel, K. A. von., 1888: *Handbuch der Paläontologie Abteilung 1. Paläozoologie Band III. Vertebrata (Pisces, Amphibia, Reptilia, Aves),* 900 p. R. Oldenbourg, Munich and Leipzig.

Paleontological Research, vol. 6, no. 1, pp. 67–72, April 30, 2002

Permian bivalves from the H. S. Lee Formation, Malaysia

KEIJI NAKAZAWA

28-2 Koyama Shimouchikawara-cho, Kita-ku, Kyoto, 603-8132, Japan

Received 2 July 2001; Revised manuscript accepted 7 December 2001

Abstract. **Three bivalve species collected from the Permian H. S. Lee Formation at the H. S. Lee No. 8 Mine in Perak, Malaysia are described. They are identified as *Sanguinolites ishii* sp. nov., *Megalodon* (*Megalodon*) *yanceyi* sp. nov., and *Myalina* (*Myalina*) cf. *wyomingensis* (Lea). The fossil locality is famous for the abundant occurrence of gastropods together with bivalves, cephalopods, calcareous algae and others, but is flooded and inaccessible now. The new species of *Megalodon* is considered to be the first record of the genus in the Permian.**

Key words: **H. S. Lee Formation, Malaysia, *Megalodon*, Permian bivalves**

Introduction and previous research

The bedrock of open-pit tin mines in the Kampar area, Perak, Malaysia is mostly composed of carbonate rocks, such as limestone, dolomitic limestone, and dolomite. The fossiliferous limestone beds occupying the uppermost interval of this sequence occur in the H. S. Lee and Nam Long Mines, and were named the H. S. Lee Beds by Sunthralingam (1968). The rich Permian fossils collected from the H. S. Lee Mine (mostly No. 8 Mine, the type locality of the formation) are described by various authors. They were first reported by Jones, Gobbett, and Kobayashi in 1966, then by Suntharalingam (1968). In addition to abundant and diverse gastropods, common bivalves, cephalopods, scaphopods, brachiopods, chitons, corals, sponges and calcareous algae were listed. Fusulinids were reported by Ishii (1966), calcareous algae by Elliot (1968), *Prodentalium* by Yancey (1973), one chiton and 91 gastropod species in 52 genera by Batten (1972, 1979, and 1985), and two ammonoid species by Lee (1980).

Concerning the bivalves, the morphology and taxonomic position of large bizarre shells of alatoconchid bivalves were discussed by Runnegar and Gobbett (1975), Boyd and Newell (1979), Yancey (1982), Yancey and Boyd (1983), and Yancey and Ozaki (1986). Ten other bivalve species were described by Yancey (1985). According to Runnegar and Gobbett (1975) and Yancey (1985) molluscan fossils are abundant in the upper 15 m of the formation. A 3–5 m-thick alatoconchid zone is sandwiched between gastropod-rich limestones. Bivalves are mainly contained in the alatoconchid zone and are not common in the gastropod-rich limestones. Ten species of bivalves belonging to eight genera are enumerated in Yancey (1985):

Grammatodon (*Cosmetodon*) *obsoletiformis* (Hayasaka)
Grammatodon (*Cosmetodon*) sp.
Shikamaia perakensis (Runnegar and Gobbett)
Saikraconcha (*Dereconcha*) *kamparensis* Yancey and Boyd
Saikraconcha (*Dereconcha*) sp.
Prospondylus chintongia Yancey
Pernopecten malaysia Yancey
Palaeolima sp.
Lyroschizodus sp.
Permartella quadrata Yancey

The age of the H. S. Lee Formation is confirmed by fusulinids and ammonoids. The upper part of the formation contains the fusulinid *Misellina claudiae* and the lower part contains *Pseudofusulina kraffti* (Ishii, 1966). According to Runnegar and Gobbett (1975), *Pseudofusulina kraffti* is found 10 m below the alatoconchid beds. Ishii correlated both fusulinid intervals to the *Misellina* subzone (the lower subzone of the *Parafusulina* zone) in South China (Sheng, 1963), and the *Misellina claudiae* zone in Japan, which was considered to be equivalent to the *Pseudofusulina ambigua* zone and *P. kraffti* zone by Kanmera (1963). Based on these fusulinids the age of the H. S. Lee Formation is assigned to the late Bolorian in the Tethys or the late Kungurian Stage in the Urals and probably correlates with the late Leonardian in the United States. Lee (1980) identified three ammonoid species in the H. S. Lee Formation, *Adrianites* cf. *insignis* Gemmellaro, *Neocrimites* cf. *guanxiensis* Chao and Liang, and *Prostacheoceras skinneri* Miller, and considered the age of the formation to be Artinskian or early Guadalupian (probably late Artinskian). The fossil evidences of both groups indicates an age of latest Cisuralian (Early Permian) or early Guadalu-

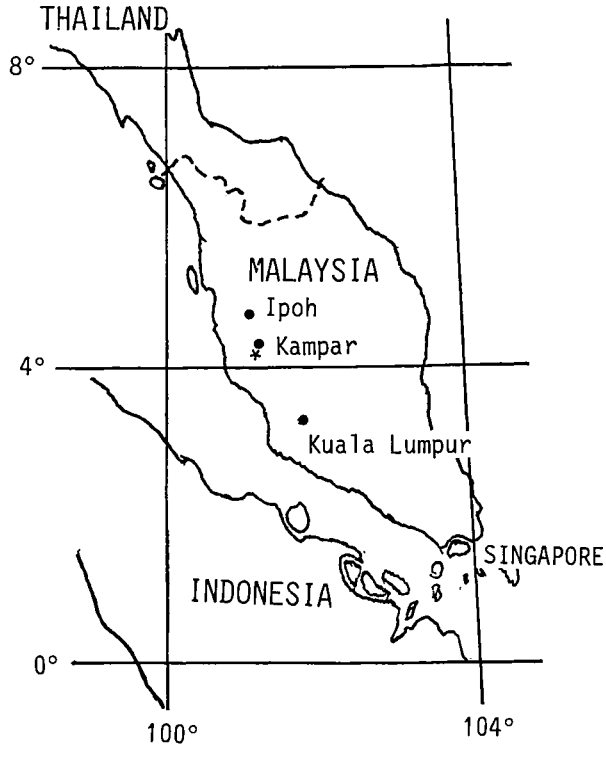

Figure 1. Index map showing the fossil locality (asterisk).

pian (Middle Permian) of the three-fold division of the Permian (Wardlaw, 2000).

Yancey (1985) pointed out the close similarity of the bivalve assemblage to that of the Akasaka Limestone in central Japan, which contain *Shikamaia akasakensis* Ozaki, *Grammatodon obsoletiformis* (Hayasaka), *Lyroschizodus japonicus* (Hayasaka) and others. The Akasaka Limestone is one of the members of the accretionary complex believed to be shifted from the tropical region (Nakazawa, 1991). It ranges from the *Parafusulina* Zone up to the *Codonofusiella-Reichelina* Zone. The above-mentioned bivalves are found in the *Neoschwagerina* Zone (Murgabian). Accordingly, the Malaysian fauna is a little earlier in age than that of the Akasaka Limestone fauna.

The materials examined in the present paper were collected by Ishii from the horizon just above the alatoconchid zone at the H. S. Lee No. 8 Mine (Figure 1). They are part of a collection given to Kyoto University in 1970, which contains the type specimen of *Prospondylus chintongia* described by Yancey (1985). In addition, *Sanguinolites ishii* sp. nov., *Megalodon* (*Megalodon*) *yanceyi* sp. nov., *Myalina* (*Myalina*) cf. *wyomingensis* (Lea), *Permartella quadrata* Yancey, and *Grammatodon* (*Cosmetodon*) *obsoletiformis* (Hayasaka) are identified in the collection. The first three taxa are described below. The occurrence of *Megalodon* is most remarkable, because the genus has not previously been reported in the Permian. Furthermore, the H. S. Lee No. 8 Mine was flooded and the exposures are no longer accessible (Runnegar and Gobbett, 1975). Therefore, the above-mentioned species are worthy of description. All the specimens are kept at the Kyoto University Museum.

Systematic description

Order Pholadomyoida Newell, 1965
Family Grammysiidae S. A. Miller, 1977
Genus ***Sanguinolites*** M'Coy, 1844

Sanguinolites ishii sp. nov.

Figure 2A, B

Materials.—A pair of incomplete right and left valves, holotype HP100027.

Etymology.—Dedicated to Ken-ichi Ishii who collected the fossils and offered them to Kyoto University.

Diagnosis.—Large *Sanguinolites* with posteriorly expanded shape, weak ventral sinus, and relatively weak umbonal ridge.

Description.—Shell large, equivalve, inequilateral, elongate, trapezoidal, more than 115 mm long, 45 mm high, and about 15 mm deep, more than twice as long as high, a little expanded posteriorly; umbo subdued, prosogyrate, slightly projecting above hinge margin, lying at anterior one-fifth of shell length; umbonal ridge weak, rounded, becoming obsolete with growth; hinge line straight, ventral margin weakly sinuous, anterior margin well rounded, and posterior margin truncated with rounded posteroventral corner; lunule deep and narrow; escutcheon probably absent; long, opisthodetic ligament well preserved; hinge edentulous; surface covered with weak, sometimes rugose, growth lines. Anterior and posterior gape of shell uncertain.

Discussion.—A part of the anterior area and the posteroventral area in the left valve are not preserved, and only part of the dorsal margin of the right valve is visible. However, the general shape can be judged by growth lines. The dorsal margin of the shell is thickened and contains a shallow furrow which receives the external ligament. Although the escutcheon is not observed and the concentric sculpture is weak, the present specimen is considered to belong to the genus *Sanguinolites* based on the other characteristics, such as elongate outline, very anteriorly located umbo, presence of umbonal ridge, long opisthodetic ligament, edentulous hinge, and concentric ornament.

This species is similar in shape to *Sanguinolites kamiyassensis* Nakazawa and Newell (1968, p.42, pl. 11, figs. 3, 4) reported from the lower Middle Permian in Japan, but differs in its much larger size, weaker umbonal ridge and the absence of radial ornaments on the posterodorsal area.

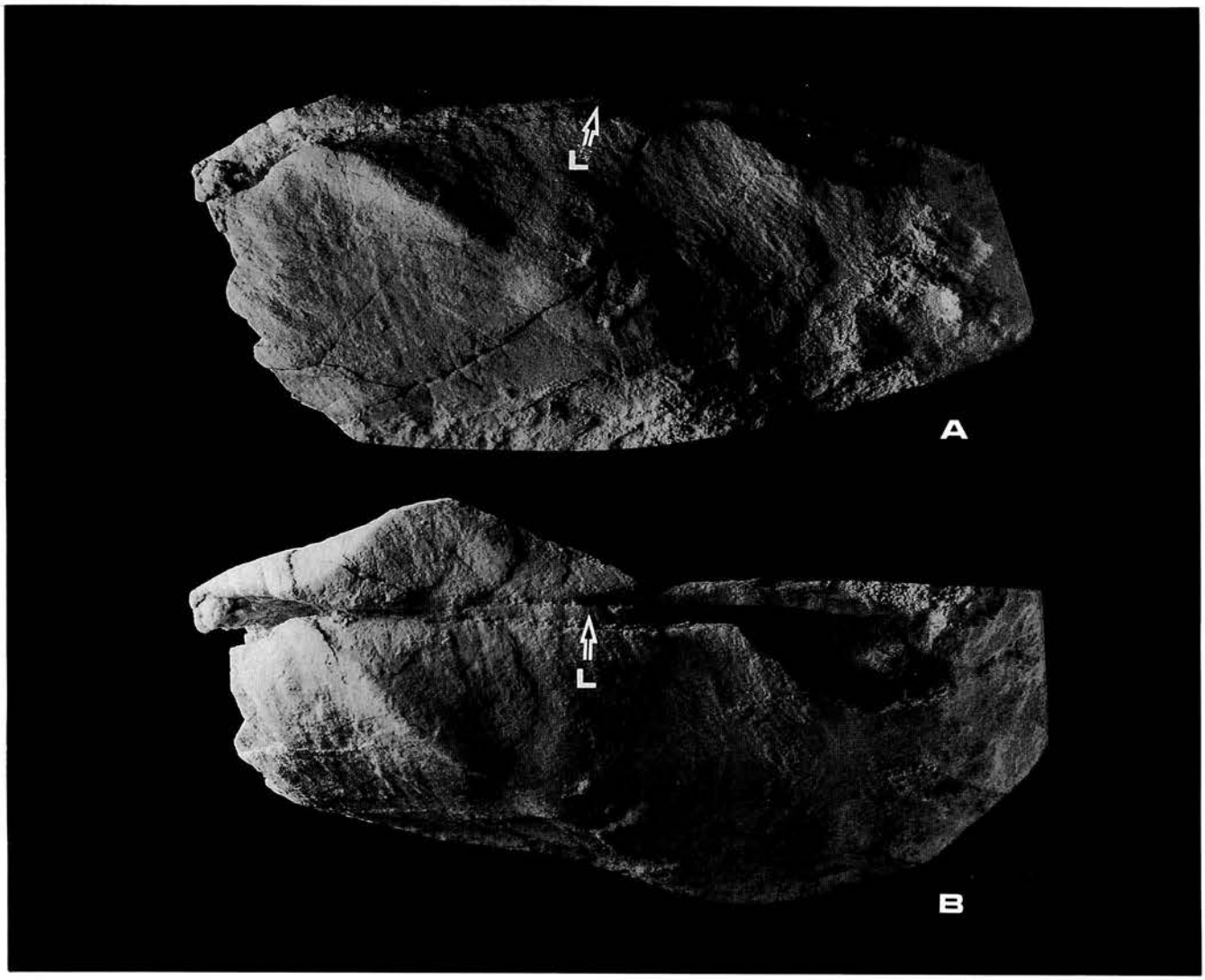

Figure 2. **A, B.** *Sanguinolites ishii* sp. nov., holotype (HP 100027). A. Left valve, lateral view; B. Oblique dorsal view of joined left and right valves, both in natural in size. L = calcified ligament.

The Upper Devonian *Sphenotus* (= *Sanguinolites*) *tiogensis* McAlester (1962, p. 62, pl. 26, figs. 1–14) is more similar to the present species in shape and size, but is distinguished from the latter in its stronger rugose concentric sculpture.

Order Hippuritoida Newell, 1965
Superfamily Megalodontoidea Morris and Lycett 1853
Family Megalodontidae Morris and Lycett, 1853
Genus ***Megalodon*** Sowerby, 1827
Subgenus ***Megalodon*** Sowerby, 1827

Megalodon* (*Megalodon*) *yanceyi sp. nov.

Figures 3A–C, 4A–F

Materials.—Nearly complete, left and right valves. Right valve, holotype HP100025; left valve, paratype HP100026. (After the manuscript was accepted, the posteroventral part of the holotype specimen was accidentally damaged as shown in Figure 4A–C).

Etymology.—Dedicated to Thomas Yancey for his contribution to the study of the molluscs of the H. S. Lee Formation.

Diagnosis.—A Permian species of *Megalodon* characterized by relatively unmodified cardinal hinge, and one poterior lateral tooth in the left and two in the right valve.

Description.—Shell medium in size, equivalve, inequilateral, subtrigonal in shape, inflated, spirogyrate, strongly carinate posteriorly with a sharp umbonal ridge; angle be-

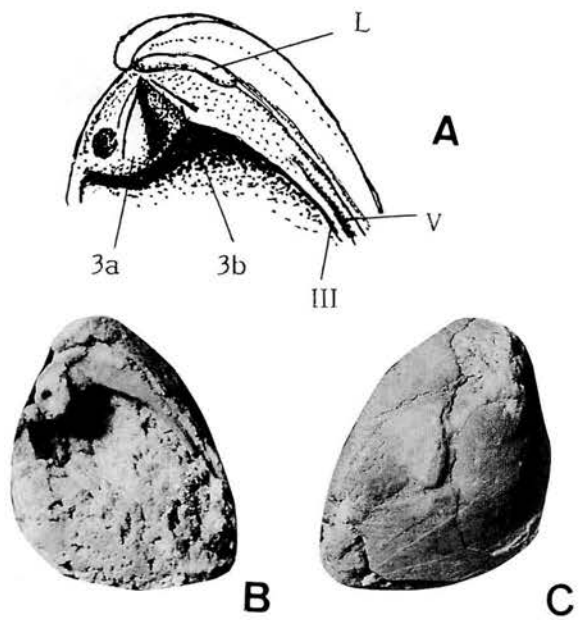

Figure 3. *Megalodon* (*Megalodon*) *yanceyi* sp. nov. **A.** Sketch showing the hinge of right valve, ×1.5, Abbreviations: 3a and 3b, anterior and posterior cardinal teeth; III and V, posterior lateral teeth; L. ligament. **B, C.** Holotype specimen (HP100025) before damage, B, ×1.0, C, ×1.0.

tween posterior area and flank of shell about 90°; posterior area having a weak radial furrow; hinge plate thick, hinge of right valve consisting of a strong, trigonal, anterior cardinal tooth (3a) with a weak radial groove, a very weak, rudimentary, posterior cardinal tooth (3b), and two, long, posterior lateral teeth (III and V) running parallel to posterodorsal margin; cardinal area of left valve poorly preserved, but judging from cardinal sockets of left valve, hinge of right valve consisting of a round, anterior cardinal tooth (4a) and a strong, trigonal, posterior cardinal tooth (2) with uneven surface and a posterior lateral tooth (IV) which is inserted between two posterior lateral teeth of right valve and continues into wide nymph; ligament external, opisthodetic, well preserved; surface of both valves covered with dense growth lines; muscle scars not observed.

Discussion .—The dental formula (Bernard, 1895) of the present species is shown as

3a	3b	III	V
4a	2		IV

The external shape and the dentition indicate that this species belongs to *Megalodon* (*Megalodon*) Sowerby (the type species of the genus is a Devonian species, *M. cucullatus* Sowerby; see Newell, 1969, N743 m, fig. E215-4). The details of dental features of the genus are rather variable. The Malaysian species is especially similar to *Megalodon* (*Megalodon*) *abbreviatus* (von Schlotheim) (= *cucullatus*) described by Haffer (1959, p. 149, fig. 6; p. 150, pl. 12, figs. 13, 14), who discussed the hinge character of the genus in detail. However, the cardinal plate of the described species is less robust and the cardinal hinge is less modified than the latter.

Measurements.—Right valve, HP100025, length 39.0 mm, height 31.0 mm, umbonal length from anterior end of shell 8.0 mm, depth 13.0 mm, height/length ratio 1.26, depth/length ratio 0.26, maximum shell length 41.0 mm; left valve, HP100026, length 40.0 mm, height 32.0 mm, umbonal distance from anterior end of shell 9.0 mm, depth 15.0 mm, height/length ratio 1.25, depth/length ratio 0.23, maximum shell length 42.0 mm.

Order Pterioida Newell, 1965
Suborder Pteriina Newell, 1965
Family Myalinidae Frech, 1891
Genus ***Myalina*** de Koninck, 1842
Subgenus ***Myalina*** de Koninck, 1842

Myalina* (*Myalina*) cf. *wyomingensis (Lea,1853)

Figure 4G, H

Compared with.—
Modiolus wyomingensis Lea, 1853, p. 205, pl. 20, fig. 1a.
Myalina wyomingensis (Lea). Girty, 1903, p. 422, pl. 8, figs. 8–13.
Myalina (*Myalina*) *wyomingensis* (Lea). Newell, 1942, p. 49, pl. 3, figs.1–4, 7, 10; pl. 7, fig. 6.

Material.—One nearly complete left valve, HP100028.

Description.—Shell medium in size, prosocline, changing in shape from *Promytilus* type to *Myalina* type through ontogeny; highly vaulted, umbonal ridge prominent and rounded with umbonal angle increasing from 45° in early growth stage to 75° in adult; 35 mm long, 37 mm high, and 17 mm deep, greatest dimension 43 mm; anterior lobe well developed, anterior margin slightly sinuated, hinge margin straight and nearly equal to shell length; surface covered with close-set growth lines, occasionally developed into lamellae; hinge unknown.

Discussion.—Although the hinge of the shell cannot be observed, the present species is quite similar to *Myalina* (*Myalina*) *wyomingensis* (Lea) found from the Desmoinesian to Wolfcampian in the United States, and it is difficult to separate the two species from each other based on the external shape, but the Malaysian species seems to be less oblique and a little higher than the American *M. wyomingensis*.

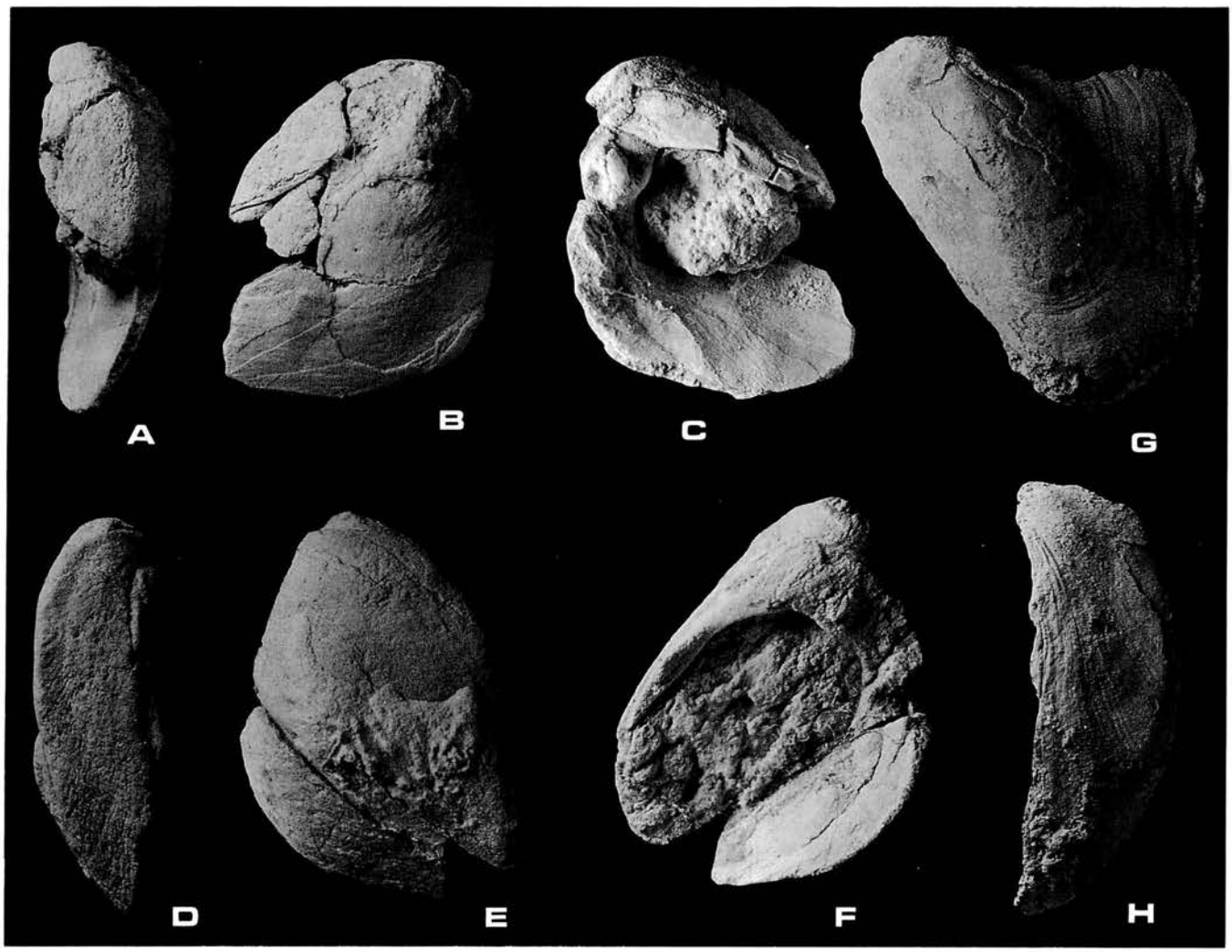

Figure 4. **A–F.** *Megalodon* (*Megalodon*) *yanceyi* sp. nov. Posterior (A), lateral (B), and interior (C) views of right valve of the holotype (HP100025) after damage. Posterior (D), lateral (E), and interior (F) views of left valve of the paratype (HP 100026), cardinal area poorly preserved. Calcified ligament is observed in both balves. **G, H.** *Myalina* (*Myalina*) cf. *wyomingensis* (Lea). Lateral (G) and anterior (H) views of left valve (HP100028). All figures ×1.5.

Acknowledgments

I am very grateful to Ken-ichi Ishii of the Hayashibara Natural Science Museum, who collected the materials and offered them to Kyoto University. Norman D. Newell of the American Museum of Natural History read the draft and gave me instructive comments. Thanks are also extended toTakeshi Irino of Kyoto University and S. Suzuki of the Hayashibara Natural Science Museum, who helped in preparing the photos of the fossils. Ishii gathered many small gastropod shells in addition to bivalves. These were examined and identified by Roger L. Batten (then American Museum of Natural History) and are also kept at the Kyoto University Museum. I wish to take this occasion to my gratitude to him. Lastly, I appreciate reviewers' valuable suggestions and refinement of my English.

References

Batten, R. L., 1972: Permian gastropods and chitons from Perak, Malaysia. Part 1. Chitons, bellerophontids, euomphalids and pleurotomarians. *Bulletin of the American Museum of Natural History*, vol. 147, article 2, p. 1–44, figs. 1–52.

Batten, R. L., 1979: Permian gastropods from Perak, Malaysia. Part 2. The trochids, patellids and neritids. *American Museum Novitates*, no. 2685, p. 1–26, figs. 1–33.

Batten, L. R., 1985: Permian gastropods from Perak, Malaysia. Part 3. The murchisoniids, cerithiids, loxonematids, and subulitids. *American Museum Novitates*, no. 2829, p. 1–40,

figs. 1-62.

Bernard, F., 1895: Premiére note sur le développement et la morphologie de la coquille chez les lamellibranches. *Société Géologique de France, Bulletin*, vol. 23, pt. 3, p. 104-154.

Boyd, D. W. and Newell, N. D., 1979: Permian pelecypods from Tunisia. *American Museum Novitates*, no. 2686, p. 1-22, figs. 1-23.

Elliot, G. F., 1968: Three new Tethyan Dasycladaceae (calcareous algae). *Palaeontology*, vol. 11, pt. 4, p. 491-497.

Girty, G. H., 1903: The Carboniferous formations and faunas of Colorado. *United States Geological Survey, Professional Paper*, no. 16, p. 1-544, pl. 1-14.

Haffer, J., 1959: Der Schlossbau früheterodonter Lamellibranchiaten aus dem rheinischen Devon. *Palaeontographica, Abteilung A*, vol. 112, p.133-192, pls. 11-14.

Ishii, K., 1966: Preliminary notes of the Permian fusulinids of H. S. Lee Mine no. 8 Limestone near Kampar, Perak, Malaysia. *Journal of Geosciences, Osaka City University*, vol. 9, article 4-VI, p. 145.

Kanmera, K., 1963: Fusulinids of the Middle Permian Kozaki Formation of Southern Kyushu. *Memoirs of the Faculty of Sciences, Kyushu University, Series D*, vol. 15, no. 2, p. 79-141, pls. 1-19.

Lea, I., 1853: On some new fossil molluscs in the anthracite seams of the Wilkes-Barre coal formation. *Philadelphia Academy of Natural Science, Journal*, vol. 2, p. 203-206, pl. 20.

Lee, C., 1980: Two new Permian ammonoids from Malaysia. *Geology and Palaeontology of Southeast Asia*, vol. 21, p. 63-72.

McAlester, A., 1962: Upper Devonian pelecypods of the New York Chemung Stage. *Bulletin of the Peabody Museum of Natural History*, no. 16, p. 1-88, pls. 1-32.

Nakazawa, K., 1991: Mutual relation of Tethys and Japan during Permian and Triassic time viewed from bivalve fossils. *In*, Kotaka, T. *et al.*,eds., *Shallow Tethys 3, Saito Ho-onkai Special Publicaiton*, no. 3, p. 3-20.

Nakazawa, K. and Newell, N. D.,1968: Permian bivalves of Japan. *Memoirs of the Faculty of Science, Kyoto University, Series Geology and Mineralogy*, vol. 35, no. 1, p. 1-106, pl. 1-11.

Newell, N. D., 1942: Late Paleozoic pelecypods: Mytilacea. *State Geological Survey of Kansas Bulletin*, vol. 10, part 2, p. 1-80, pls.1-15.

Newell, N. D., 1969: Superfamily Megalaodontacea. *In*, Moore, R.C.,*ed. Treatise on Invertebrate Paleontology, Part N*, vol. 2, *Mollusca 6, Bivalvia*, N742-749. The Geological Society of America and University of Kansas, Lawrence.

Runnegar, B. and Gobbett, D., 1975: *Tanchintongia* gen. nov., a bizarre Permian myalinid bivalve from West Malaysia and Japan. *Palaeontology*, vol. 18, no. 2, p. 315-322.

Sheng, J. C., 1963: Permian fusulinids of Kwangsi, Kueichou and Szechuan. *Palaeontologia Sinica, New Series*, vol. l0, p. 1-115, pls. 1c.-36.

Suntharalingam, T., 1986: Upper Palaeozoic stratigraphy of the area west of Kampar, Perak. *Geological Survey of Malaysia Bulletin*, vol.1, p. 1-15.

Wardlaw, B., 2000: Notes from the SPS Chair. *Permophiles*, 37, p.1-3.

Yancey, T. E., 1973: Apical characters of *Prodentalium* from the Permian of Malaysia. *Malaysian Journal of Science*, vol. 2 (B). p. 145-148.

Yancey, T. E., 1982: The alatoconchid bivalves: Permian analogs of modern tridacnid clams. *Third North American Paleontological Convention Proceedings*, vol. 2, p. 589-592.

Yancey, T. E., 1985: Bivalvia of the H. S. Lee Formation (Permian) of Malaysia. *Journal of Paleontology*, vol. 59, no. 5, p. 1286-1297.

Yancey, T. E. and Boyd, D. W., 1983: Revision of the Alatoconchidae: a remarkable family of Permian bivalves. *Palaeontology*, vol. 26, part 3, p. 497-520, pls. 62-64.

Yancey, T. E. and Ozaki, K., 1986: Redescription of the genus *Shikamaia*, and clarification of the hinge characters of the family Alatoconchidae (Bivalvia). *Journal of Paleontology*, vol. 60, no. 1, p. 116-125.

Paleontological Research, vol. 6, no. 1, pp. 73–83, April 30, 2002

Systematic position and palaeoecology of a cavity-dwelling trilobite, *Ityophorus undulatus* Warburg, 1925, from the Upper Ordovician Boda Limestone, Sweden

YUTARO SUZUKI

Department of Biology and Geosciences, Faculty of Sciences, Shizuoka University, 836 Ohya, Shizuoka, 422–8529, Japan.
(e-mail: sysuzuk@ipc.shizuoka.ac.jp)

Received 2 August 2001; Revised manuscript accepted 7 December 2001

Abstract. **The high level systematic position and autecology of the Upper Ordovician cavity-dwelling trilobite *Ityophorus undulatus* is discussed. The lectotype is here selected from syntypes. The Late Cambrian family Loganellidae Rasetti, 1959 appears to contain the ancestors of this species. *Ityophorus* is compared with the closely related Middle Ordovician trilobite *Frognaspis* to pick out the stable characters. These are the yoked free cheeks, the wide cephalic doublure in combination with a distinct narrow cephalic rim, pygidial pleural and interpleural furrows, and a smooth mesial part of the inner cephalic doublural margin (lack of an embayment of the hypostomal suture). Because of the presence of several characteristics unique to the two, they are best attributed to a subfamily Ityophorinae, which is interpreted as a relict group of the Loganellidae. The discussion of the autecology is based on the structural relationship of the mouth opening and position of basal podomeres in relation to the cephalic margin, and on the functional morphology of terrace lines on the brim margin. The appendages appear to have been long to reach the substrate. The cephalon appears to have held the body rigidly by means of the terrace lines. This made it possible for the animal to use its appendages freely, for instance, in scratching the substrate. Some cavities in the present study area show evidence of a gel-like consistency of the cavity walls, which best fits the behavior mentioned above. *Ityophorus* is interpreted to have been an animal adapted to cavities rich in bacterial mats, on which it may have fed.**

Key words: **cavity dwelling, *Ityophorus undulatus*, life habit, Loganellidae, structural relationship, Trilobita, yoked free cheeks.**

Introduction

The term "cryptic habit" denotes an adaptations into a buildup environment, which usually provides cohesive substrates with the potential to provide cavities. Caves in recent reefs, which offer spaces for cryptic modes of life, occasionally are dominated by sponges and cryptic bacteria (Reitner, 1993). With these, bivalves, gastropods and arthropods form cryptic biotopes. From a classificatory point of view, some cavity-dwelling metazoans appear to be phylogenetically relict groups (relict biota), or groups which retain primitive morphological characters (Hayami and Kase, 1996; Hobbs, 2001). This trend should have been characteristic also of ancient cavity dwellers in buildups, although no vagile metazoan fossil group has ever been recognised as a "relict group" so far.

The Upper Ordovician minute trilobite species *Ityophorus undulatus* Warburg, 1925, which is of uncertain position in high-rank systematics (Kaesler, 1997, p. 302), is commonly found in patches of internal sediment in autochthonous taphonomical conditions (Suzuki and Bergs tröm, 1999, fig. 10), commonly associated with microgastropods. The sediment is characteristic of the "stromatactis cavity" system which is a common sedimentary structure in Palaeozoic carbonate mud mounds. Thus Suzuki and Bergström (1999) concluded that the present species was a cavity dweller. This rare mode of occurrence, which is defined correctly as a cavity setting, offers us an unusual chance to examine if a fossil species of cryptic habit has a similar mode of adaptation to recent examples or not.

The aims of the present study are to examine the high-rank systematic position of *Ityophorus undulatus*, to present an example of morphological transformations in a trilobite caused by environmental pressure, and to discuss the autecology from functional and sedimentological points of view.

Geological setting

Ityophorus undulatus occurs in the Upper Ordovician Boda Limestone, Siljan district, Sweden. This unit

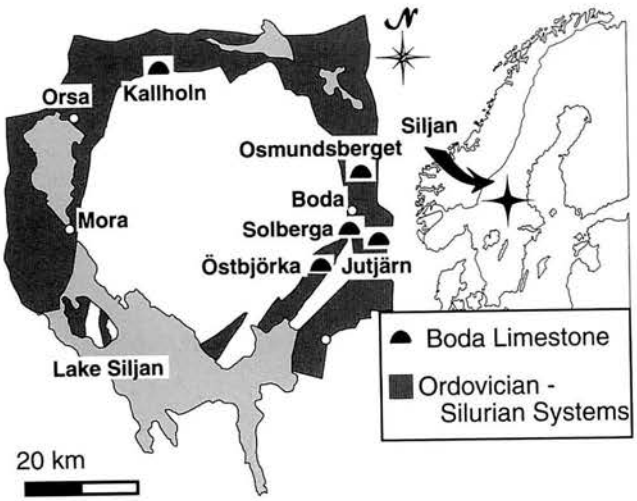

Figure 1. Locality map of some Boda Limestone bodies.

consists of a set of carbonate buildup masses of which now up to 20 are known in the Siljan district of Sweden (Figure 1; Jaanusson, 1979). The thickness and the diameter of an isolated Boda Limestone body are said to be about 100-140 m and up to over 1 km, respectively (Jaanusson, 1982). However, my own observations and calculations based on a topographic map indicate a maximum size more or less half the dimension mentioned. The facies is massive pure limestone without obvious bedding, but with frequent open space structures such as stromatactis cavities and synsedimentary dykes. *Ityophorus undulatus* is commonly found with internal sediment in relatively large open space structures. On the rim of these, a unique type of open space structure is often recognised, shown in Figure 2B. Microscopically, internal sediment is dominated by peloids, and the host sediment is micritic (Figure 2D). In case of the Boda Limestone, "normal" stromatactis structures differ considerably both macroscopically and microscopically (Figure 2A, D; or readers are referred to Pratt, 1995, p. 63, fig. 14G). The internal sediment in stromatactis cavities and host sediments of the cavity system is mostly microcrystalline, and peloids are rare. The transversely elongate cavity system with peloids which is similar in construction to that shown in Figures 2B and 2D is generally classified as "zebra cavity of laminoid or flat stromatactis type" (for definition, see Monty, 1995, p. 25), and is interpreted as originating by the decay of superposed thin sheet-like microbial mats (Pratt, 1982).

Systematic description

The present species was originally described in detail by Warburg (1925, p. 229). General characters and new observations are presented below.

Genus ***Ityophorus*** Warburg, 1925

Type species.—*Ityophorus undulatus* Warburg, 1925

Ityophorus undulatus Warburg, 1925

Figure 3

Ityophorus undulatus Warburg, 1925, p. 229, pl. 11, figs. 40–43; Moore, 1959, p. *O*430, fig. 333; Nikolaisen, 1965, p. 237.

Types.—3 syntypes, PMU D194 (Warburg, 1925, pl. 11, fig. 40), PMU D195 a, b (Warburg, 1925, pl. 11, fig. 41) and PMU D196 (Warburg 1925, pl. 11, figs. 42, 43), are housed in the Palaeontological Institute, University of Uppsala. PMU D196 is here selected as the lectotype.

Type locality.—Boda Limestone, a buildup mass in Kallholn, Dalarna, Sweden. The stratigraphic level within the mass is unknown. The range of the species is likely to correspond to the Cautleyan to Rawtheyan stage of the Ashigill series, and not the Hirnantian.

Repository.—All the specimens figured herein are housed in the Swedish Natural History Museum, Stockholm, with "RM" numbers.

Description.—The entire exoskeleton is ovate in outline (Figure 3A). Its entire length seldom exceeds 1 cm. The cephalon occupies about half of the length, sagittally. The axis is fairly convex, and almost half of a circle in cross-section.

The cephalon is horseshoe-shaped (Figure 3A) and strongly convex (Figure 3B). The maximum length including the genal spine is about twice the sagittal length and almost equal to the length of the entire body. The genal angle is acute. The long genal spine curves evenly posteriorly and adaxially. The width of the spine is almost constant throughout. Its posterior end is situated more or less at the level of the posterior end of the pygidium. The anterior cephalic rim, which is narrower and less convex than the posterior cephalic border, disappears where it meets the genal spine. Thus, the genal spine is seemingly an extension of the cephalic posterior border. The glabella is cylindroid in profile and expands slightly anteriorly. It is strongly convex transversely. Three pairs of glabellar furrows are recognised. The 2S and 3S furrows are short and extend more or less transversely. Their length is about one fourth the width of the glabella. The 1S furrow is longer than the 2S and 3S furrows. It is directed about 45° posteriorly from a transverse line. It becomes wider adaxially. Probably the furrow is bifurcated adaxially, but the specimens are too small for a definite observation. The eye ridge is short but strongly convex, and distinctly set off from the surroundings. It extends transversely in front of the level of the 3S glabellar furrows. The length of the eye ridge roughly equals the distance between the 2S

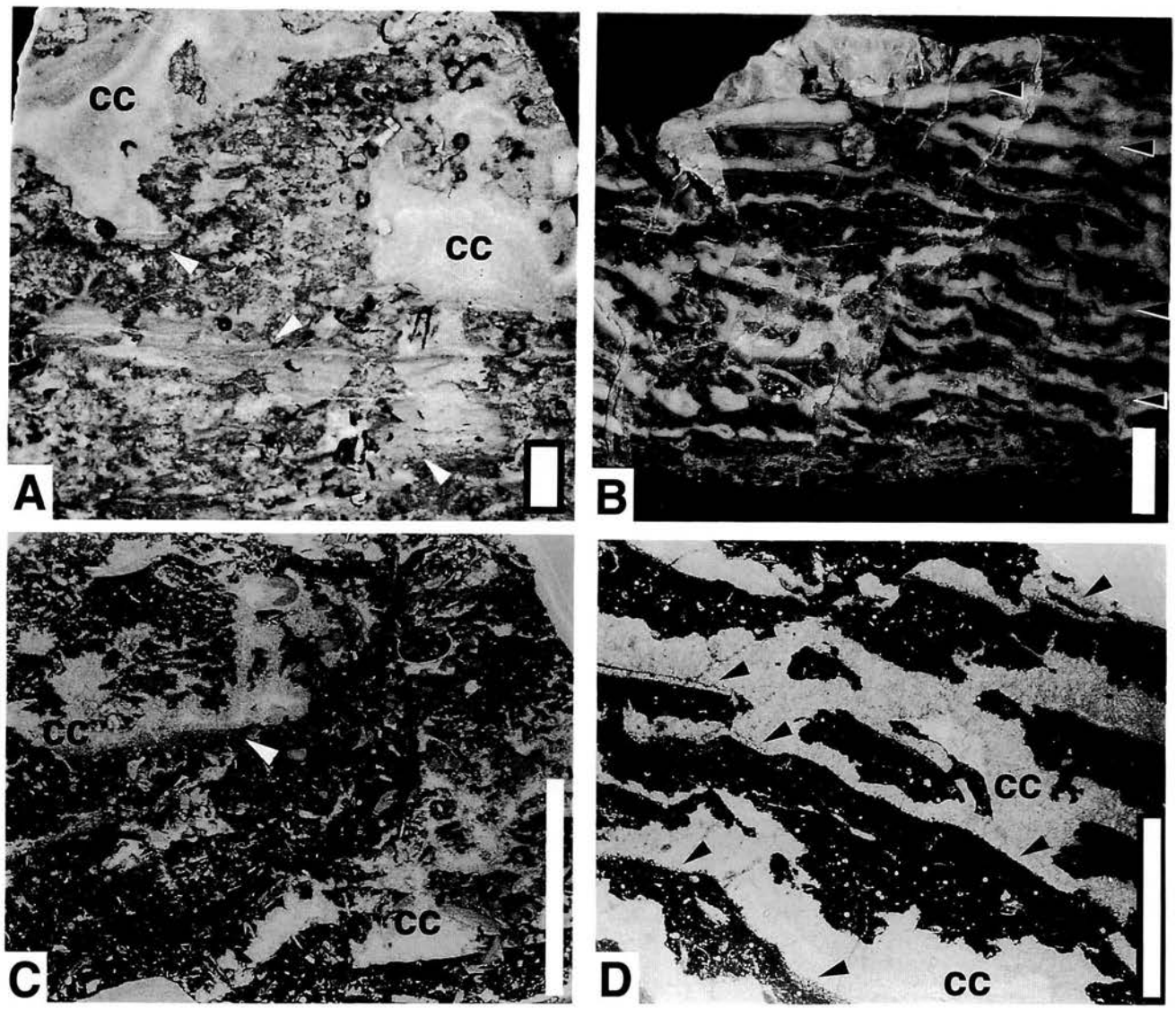

Figure 2. Macro- and microfacies of the Boda Limestone. **A.** Polished slab of the core facies, vertical section. White arrows indicate laminated internal sediment. **B.** Polished slab of the "zebra cavity", sampled from the rim of an open space structure. Vertical section. Transversely continued white area pointed by black arrows are cavity systems. **C.** Microfacies of the core facies. Matrix is rich in bioclasts. White arrow indicates microcrystalline internal sediment. **D.** Microfacies of the zebra cavities. Black arrows point to peloidal internal sediment. All white scales are 1 cm. CC stands for cavity filling cement.

and 3S furrow. There may be eyes, as described by Warburg (1925, p. 230). However, the structure described as the eye may be vestigial since it is not proven that there is a visual surface. The possible visual surface forms half a sphere. A median occipital tubercle is present anteriorly on the occipital ring. The peripheral genal area is steeply inclined. Five furrows extend in parallel with the narrow cephalic rim (Figure 3A). The outermost one is the furrow of the cephalic rim. The innermost one extends laterally and posteriorly from the anterior end of the glabella (Figure 3B, E; black arrows). The area between these furrows is moderately convex. The brim, here defined as the area outward of the fourth furrow described above, is broad. The undulating brim has a general dip sagittally from the inner to the outer margin of around 30° (Figure 3C). The dip gradually becomes steeper backwards to about 60° laterally. The facial sutures are of opisthoparian type. Their anterior branches enclose a parabolic anterior part of the cranidium (Figure 3E). The posterior branch extends obliquely backwards to cross the cephalic posterior border

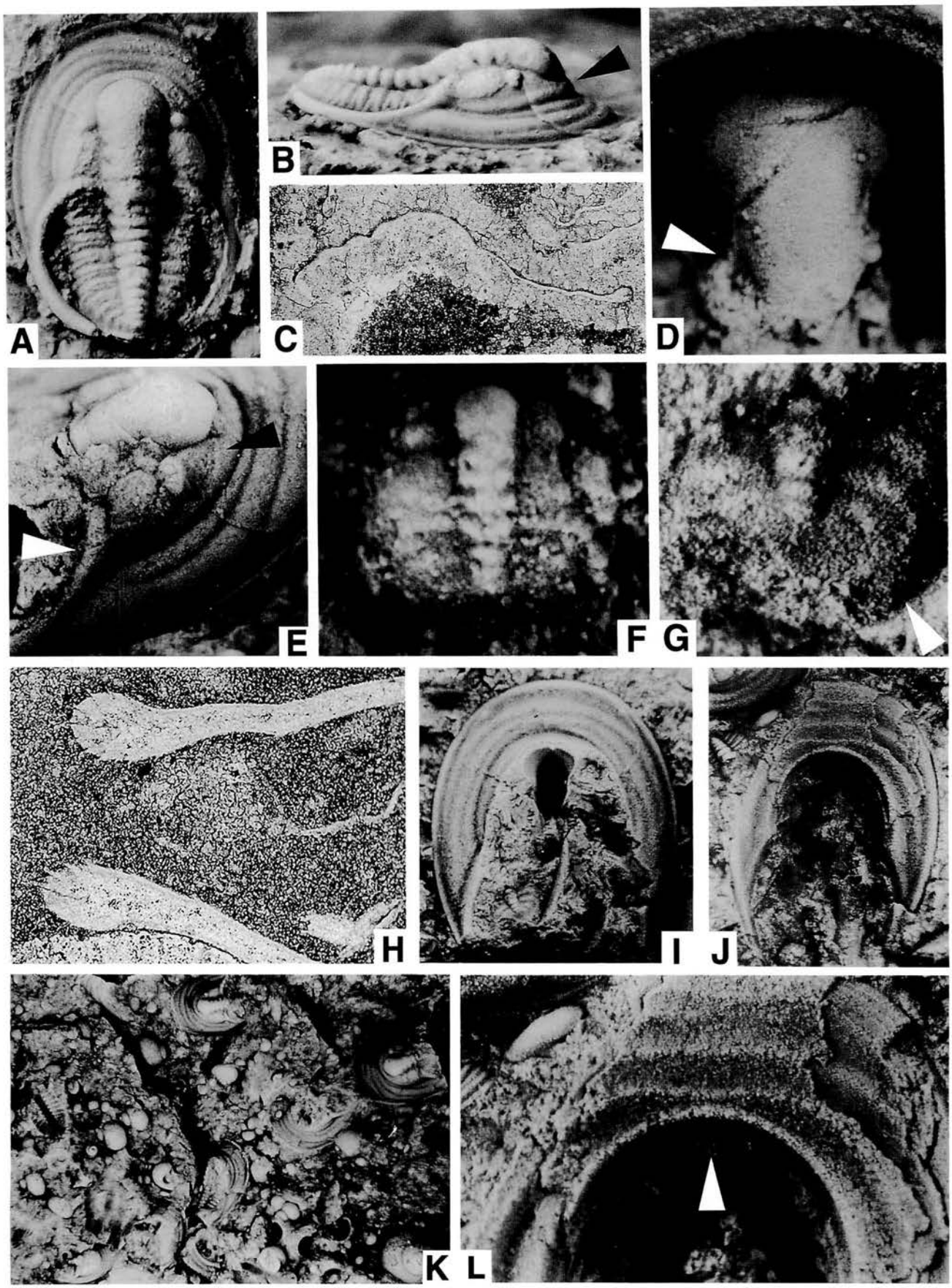
A
B
C
D
E
F
G
H
I
J
K
L

at a right angle (Figure 3E; white arrow). The free cheeks are fused into a single unit, because no furrows or gaps are recognised on the cephalic doublure (compare dorsal and ventral cephalic views in Figure 3I, J, respectively). The doublure closely follows the shape of the brim, and the space between the two is very narrow (Figure 3C). The doublure is wide (Figure 3C, J, L). The interior edge of the doublure (Figure 3L; white arrow) is situated below the innermost parabolic furrow in the cephalon, which is indicated by black arrows in Figure 3B, E. The cephalic doublure has three or four parabolic furrows which are almost parallel to the cephalic margin (Figure 3J). An interior part of the doublure, between the fourth and fifth parabolic furrow mentioned above, is steeply inclined and distinctly set off from the surrounding. Thus the cephalic doublural morphology is quite similar to the lower lamella of harpids.

In the cephalic rim, terrace lines with an asymmetrical cross-section are recognised on both the dorsal and ventral side (Figure 3H). The steep surfaces of the ventral terrace lines face dorsally, whereas they face ventrally in the dorsal ones (for detail, see Figure 5).

The hypostome is situated just below the glabella (Figure 3I). Its anterior margin must have been in contact with the cephalic doublure mesially. Three specimens among hundreds of cephala show the same position of the hypostome. Thus the described position of the hypostome should be original. The length of the hypostome is 55% of that of the glabella (Figure 3D). It is strongly convex transversely. The maximum length is about 1.3 times longer than the maximum width. An anterior wing is relatively long (exsag.) and evenly inclined dorsally. The distal part of the wing is broadly rounded. The anterior margin is slightly depressed medially. The lateral border is narrow and short. The border furrow extends from the level of the posterior end of the anterior wing to four-fifths of the anterior end of the hypostome. The shoulder is triangular in shape and horizontally extended (Figure 3D; white arrow). The posterolateral corner of the central body is angulate. The posterior margin is convex without a border. No distinct boundary separating the anterior and the posterior lobes is recognised. The central body is longitudinally elliptic in shape.

The thorax consists of six segments (Figure 3A). The axis gradually becomes narrower backwards. The ratio between axial and pleural widths ranges from 1 to 1.2 from in front to the rear. The pleurae extend almost straight transversely except for the posteriormost two segments, in which the pleurae distal to the geniculation curve moderately backwards. A distinct pleural furrow is present. It extends almost parallel to the anterior and posterior margins of the segment.

The pygidium is wide (Figure 3A). The maximum width/length ratio is about 1.9. Six axial rings and five pairs of pleural ribs are discernible. Distal to the fulcrum, pleural ribs and furrows curve gently backward. Pleural and interpleural furrows lie parallel with each other. The posterior end of the axis is obscure. It gradually dies out posteriorly. A narrow flattened border is present.

Specimens of a younger growth stage, a meraspid degree? (Figure 3F), and a transitory pygidium (Figure 3G) are available. Both specimens are found along with adult specimens in internal sediment. No other trilobite species is recognised in this sediment. The former specimen (Figure 3F) is most probably a moult, because it lacks the entire free cheek unit. The glabella is proportionally narrower than in the adult. The 2S furrow differs in its course from that of the adult. The abaxial end of the furrow does not reach to the axial furrow. The furrow is directed posteriorly and adaxially in the young specimen, but transversely in adults. The axial ring of the first thoracic segment is seen posterior to the cephalon. A distinct eye ridge is present. Its proportion and position in relation to the glabella is almost the same as in an adult specimen. A most notable feature is the facial suture course. The anterior branch is not parabolic as in adult specimens, but extends straight forwards. The transitory pygidium seems to have a spiny margin (Figure 3G; white arrow). The posterior extremity of the axis ends well in front of the margin. The preservation is not good enough to permit further observations.

Remarks. — Previously, Warburg (1925, p. 231) described the genal spine of the present species as being a short pointed spine. Because of the minute size of the species, it tends to be broken. In most of the cases the genal spine is recognised as a concave mould.

← **Figure 3.** *Ityophorus undulatus* Warburg, 1925. **A.** Complete exoskeleton, dorsal view. ×18. Jutjärn. RM Ar 56890. **B.** Same, lateral view. ×17. Black arrow points to the furrow, below which the inward edge of the doublure is situated. **C.** Exsagittal or sagittal section of the cephalon. ×39. Jutjärn. RM Ar 56891. **D.** Hypostome, ventral view. ×54. Jutjärn. RM Ar 56892. White arrow points to the posterior wing, which is partly broken. **E.** Cephalon, oblique lateral view showing curving facial suture course. ×15. Locality unknown. RM Ar 56893. White arrow points to the termination of the posterior branch of the facial suture. Black arrow to the furrow, below which the inward edge of the doublure is situated. **F.** Fairly young individual. ×70. Jutjärn. RM Ar 56894. **G.** Fairly young pygidium. ×65. Jutjärn. RM Ar 56895. White arrow points to pygidial spine. **H.** Magnified brim in cross section. ×150. The lower brim of the two is upside down. Jutjärn. RM Ar 56896. **I.** Ventral mould of hypostome and cephalic brim, dorsal view. ×16. Specimen is in the same slab as G. **J.** Cephalic doublure, ventral view. ×12. Same slab as E. **K.** Occurrence pattern with microgastropods. ×4. Same slab as E. **L.** Magnified cephalic doublure, ventral view. ×45. Specimen same as J. White arrow points to the inner edge of the cephalic doublure.

Systematic position of *Ityophorus undulatus*

Morphological characters of *Ityophorus* and *Frognaspis*

For more than a half century, opinion on the high-rank classification of the present genus was far from a clear consensus. First, Warburg (1925) made a new family Ityophoridae consisting of only the present genus. Later in Moore (1959), the species was doubtfully classified as a member of the Trinucleina Swinnerton, 1915, of the order Ptychopariida without any demonstrated evidence. It is clear that the convex cephalon with horseshoe outline is just a superficially similar to a trinucleid cephalon. Nikolaisen (1965) described a new species, *Frognaspis stoermeri*, which is closely related to the present species, from the Middle Ordovician of Norway, and classified it into the Ityophoridae. Furthermore, he implied a neotenic development of the present species from *Frognaspis stoermeri*. As will be discussed in a later paragraph, *Frognaspis stoermeri* shares fairly many characters with the present species. The suggestion of a close relationship between the two is therefore convincing. However, Nikolaisen did not tackle the problem of the position of Ityophoridae. Fortey (1997) also gave up and simply stated that the family belongs to the Ptychopariida Swinnerton, 1915.

Before examining the high-rank systematic position of the present species, we must understand how the unique morphology evolved in the phyletic lineage. Since *Ityophorus undulatus* preserves characters seen in young individuals of *Frognaspis stoermeri*, the heterochronic evolution of the former from the latter is worth consideration. After comparison of the two, we can sort out a "heterochr onic polish". Then we can define stable characters and infer the ancestral conditions of characters which differ between the two. In addition, one has to remember what kind of morphological changes would arise in a shift to cavity-dwelling habits in modern arthropods.

Characters shared between *Ityophorus undulatus* and *Frognaspis stoermeri* are as follows:

1) wide cephalic brim.
2) facial suture course.
3) distinct furrows in the cephalic doublure.
4) small eyes.
5) fairly wide cephalic doublure with distinct narrow cephalic rim.
6) free cheeks forming single unit.
7) distinct pleural furrow (known only from the pygidium in the latter species).
8) narrow flattened pygidial rim.
9) pygidial pleural ribs distal to the geniculation extend obliquely backwards.
10) hypostomal morphology.
11) directions of pleural tips in the thorax.
12) cephalic doublural margin smoothly rounded mesially (no embayment for the hypostomal suture). Since the mesial part of the inner margin of the doublure is below the anterior extremity of the glabella, the hypostome should be attached to the doublure medially.

Characters which are not shared by the two species are:

1) glabellar profiles (expanded in *Ityophorus*).
2) glabellar furrows (deepened adaxially and 1S furrows faintly connected over midline in *Frognaspis*).
3) number of segments in the pygidium.
4) ornaments on dorsal surfaces.

The characters 1) and 2) in *Ityophorus* are apparently derived from younger growth stages of *Frognaspis* (see Nikolaisen, 1965, pl. 3, fig. 4). The inferred ancestral conditions of the two characters should thus be represented in the adult stages of *Frognaspis*.

The ancestral glabellar character 1) should be preserved in the adult stage of *Frognaspis*. This is because the glabellar profile in *Ityophorus* is fairly similar to a younger stage of *Frognaspis* (Nikolaisen, 1965, p. 243). Thus the ancestral group should have had an anteriorly tapering glabella, and possibly the 1S furrows may have been connected mesially (non shared character 2). The latter situation is recognised in *Frognaspis*.

Determining the ancestral condition of character 3) is difficult. This is because the adult number of pygidial segments is, in general, related to the number of thoracic segments. Unfortunately, the exact number of thoracic segments is not known in *Frognaspis*. I can only say that the ancestral condition of the number of segments in the pygidium may vary between species in the high-rank group, in which the two species belong.

Concerning character 4), since the exoskeletal ornament pattern is unstable among the genera in some family groups (e.g., Styginidae), we should hesitate to use that character in determining the high-rank systematic position. In general, recent cavity-dwelling organisms are equipped with specialized sensory organs. Especially in cavity-dwelling arthropods, the appendages tend to be long, which increases the area for the number or the size of sense organs (Culver, 1982, p. 17). Coarse tubercles on the exoskeletal surface in trilobites are generally understood as sensory ducts (Osmólska, 1975, p. 203). As will be discussed in a later paragraph, *Ityophorus* must have had long appendages, so the animal had the potential to equip its appendages rather than the dorsal exoskeleton richly with sensory organs. Thus smoothing of the dorsal exoskeletal surface may be a result of adaptation inhabiting cavities.

Discussion of systematic position of *Ityophorus*

I first try to narrow down candidate ancestral groups of *Ityophorus* from other groups with yoked free cheeks.

Next, I judge the possible relationships based on other characters such as ventral morphology, facial suture type, and pygidial morphology.

Trilobite groups which possess yoked free cheeks are bathynotids and conocoryphids from the Lower to Middle Cambrian, Nileidae, Phacopida, Trinucleina, Harpina, Olenidae, Hypermecaspididae, some species of Dikelocephalidae such as *Dikelocephalus retrorsus*, Loganellidae, some species of Dikelokephalinidae (readers are referred to *Dactylocephalus latus* (Peng, 1990a, pl. 9, fig. 8) and *Ciliocephalus angulatus* (Peng, 1990b, pl. 17, fig. 3)), Harpididae and Entomaspididae. Of these, the Lower Cambrian groups are so different in several characters such as facial suture courses, pygidial morphology and ventral cephalic characters, that a phylogenetic relationship with *Ityophorus* or *Frognaspis* is most unlikely. Harpina and conocoryphids (marginal suture), Harpididae (marginal or characteristic proparian suture), Phacopida (proparian suture) are profoundly different in their facial suture types from that of *Ityophorus*. Among the rest, the Entomaspididae have a characteristic pygidial morphology (a narrow upturned (geniculated) border or stubby spines in front of a continuous pygidial rim: Ludvigsen *et al.* 1989, p. 47) which is unlikely of the ancestor of *Ityophorus*. Most of the Trinucleina do not have eyes with dorsal facial suture except some genera such as *Orometopus* which has opisthoparian facial sutures. However, the overall morphology, especially the pygidial morphology of trinucleid type is quite different from the *Ityophorus* pygidium with distinct border and posteriorly curved pleural and interpleural furrows. The Nileidae have a characteristic hypostome, cephalic and pygidial morphology, large eyes with no eye ridges, more or less straight pygidial furrows, all of which are unlikely in a relative of *Ityophorus*. The Olenidae and the Hypermecaspididae have yoked free cheeks. In the case of olenids and hypermecaspidids with a wide preglabellar field, the cranidium is similar in outline and the cephalic doublural margin smoothly rounded mesially as in *Ityophorus*, but the hypostomes become natant. Since the hypostome of *Ityophorus* and *Frognaspis* must have attached mesially to the cephalic doublural margin (shared character 12), their ancestor should have possessed this mode of hypostomal attachment. Moreover, the pleural and interpleural pygidial furrows of the Olenidae and the Hypermecaspididae extend obliquely posteriorly in a more or less straight way, which is different from the situation in *Ityophorus*. Therefore, a phylogenetic relationship between the Olenidae and *Ityophorus* is unlikely.

Other candidates are the Dikelocephalidae, Dikelokephalinidae and Loganellidae. Some species of the former two families, although not all, possess yoked free cheeks with a wide cephalic doublure. The pygidial morphology is also fairly similar between them. The Dikelocephalidae and the Loganellidae were extinct before the Cambrian-Ordovician transition, whereas the Dikelokephalinidae persisted beyond that boundary (Öpik, 1967, p. 254). One could therefore think that the third group, the Dikelokephalinidae, might contain the ancestor of *Ityophorus*. Classifying the Dikelokephalinidae is usually difficult, because most of the characters are too general to be diagnostic (Fortey and Chatterton, 1988, p. 209). However, the pygidium of Dikelokephalinidae has posteriorly curved pleural furrows but not interpleural furrows whereas *Ityophorus* has both. Thus, Dikelokephalinidae should not be related to *Ityophorus*. The Dikelocephalidae and the Loganellidae have interpleural furrows in their pygidia. However in the former, an embayment is present mesially in the cephalic doublure for an attachment of the hypostome. In contrast, the Loganellidae have a mesially smooth outline of the cephalic doublure (Moore, 1959, p. *O*333) which is concordant with the ventral cephalic morphology in *Ityophorus*. Below I discuss the phylogenetic relations between the Loganellidae, and *Ityophorus* and *Frognaspis*.

There are several shared characters between the Loganellidae and the two species such as the shared characters between *Ityophorus* and *Frognaspis* 1), 2), 5), 6), 7), 8), 9) and 11) listed above. Futhermore the characters of the inferred ancestral conditions which are listed as non-shared characters between *Ityophorus* and *Frognaspis* 1) and 2) fit well to this family. Generally, in species with the free cheeks in a single unit and a wide doublure, the cephalic rim [called a "border" in Fortey and Chatterton 1998: fig. 6, readers are referred to Whittington and Kelly (1997, p. 315) for the terminology of the "border" and "rim"] is of fairly low convexity (e.g., Fortey and Chatterton, 1988, fig. 6). Nikolaisen (1965, p. 237) stressed the differences in eye size and the hypostomal morphology in species between loganellids and *Frognaspis* or *Ityophorus*, but the reduction of eye size is a common feature in organisms adapted to cavities (Humphreys, 2000, p. 4). Anteriorly in the hypostome of *Ityophorus* and *Frognaspis*, there is a unique longitudinal median groove (Figure 3D; Nikolaisen, 1965, pl. 3, fig. 6). The groove structurally corresponds to the median longitudinal groove or depression (see Nikolaisen, 1965, pl. 2, figs. 1, 3; pl. 3, figs. 1, 2) anteriorly in the *Frognaspis* glabella. In general, species with yoked free cheeks (e.g., *Cloacaspis senilis*: see Fortey, 1974, pl. 10, fig. 6) may or may not possess a similar longitudinal glabellar groove or depression. If present, the longitudinal groove in the glabella tends to be more weakly impressed in older growth stages (Fortey, 1974, fig. 6). Thus the groove is more or less an embryonic character. Hence the two latter genera are most likely descended from a species of the Loganellidae. However, there are still several facts

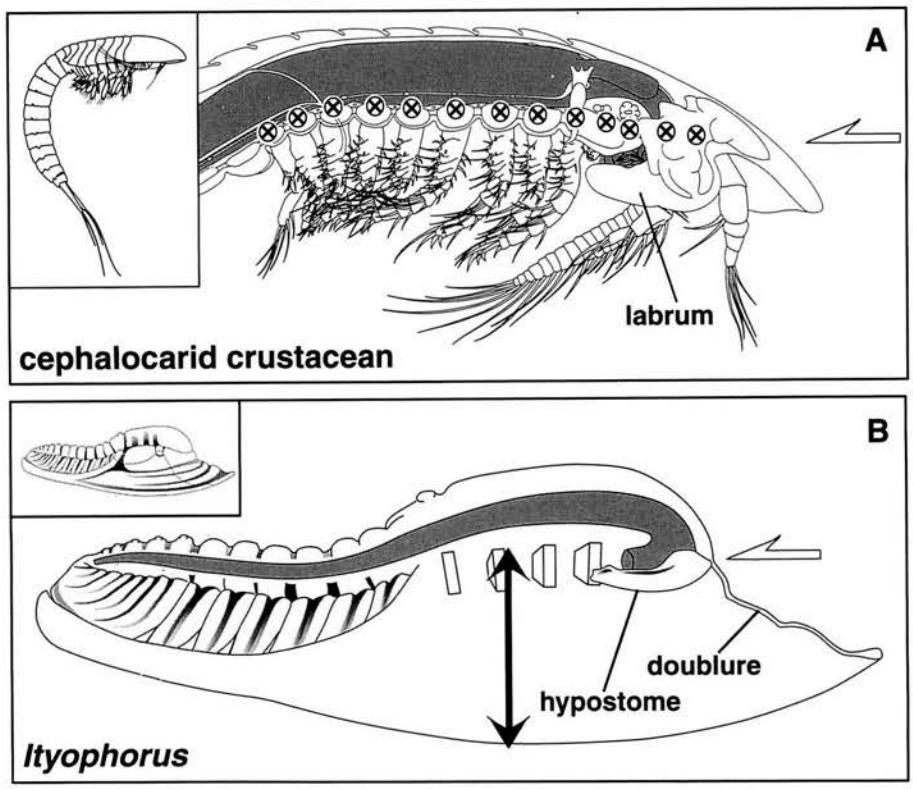

Figure 4. **A.** Schematic drawing of cephalocarid crustacean showing the structural relationship in basal appendage joints (represented as "X" in a circle), digestive tract (grey area), labrum and basal podomere. Positions of the joints are situated above the level of the mouth opening. Modified from Sanders (1963: fig. 4) and Hessler and Elofsson (1992: fig. 3). **B.** Schematic drawing of *Ityophorus undulatus* showing structural relationship in inferred digestive tract (grey tube), hypostome and basal podomeres (represented as bricks). White arrows indicate dorsoventral level of mouth openings. Black double arrow indicates minimum distance between basal joints of appendages and the substrate.

which may differentiate *Ityophorus* and *Frognaspis* from typical Cambrian loganellids: 1) the two are Middle to Late Ordovician trilobites, 2) the body size of the two has undergone considerable shrinking, 3) the presence of crescentic furrows in the doublure (shared character 3) in the two species, but not in Cambrian loganellids. Therefore, the two genera are best accounted for as a subfamilial group of the Cambrian Loganellidae. Ityophoridae Warburg, 1925, including *Frognaspis* and *Ityophorus*, is therefore downgraded to a subfamily Ityophorinae Warburg, 1925, of the family Loganellidae Rasetti, 1959.

The Ityophorinae now appears to be a relict of the Late Cambrian group. Since growth stages are unknown in most fossil arthropods, how the Ityophorinae had evolved from a loganellidae as becomes vague. Recent animals, "progenetic evolution" is quite common as part of a cryptic adaptation, and the considerable size decrease of the Ityophorinae in comparison with the Loganellidae may be one indication of "progenetic evolution".

Functional morphology of *Ityophorus undulatus*

The present species had attained a body with apparently a "snow-shoe" effect, which increases the area of the animal substrate interface and prevents the animal from sinking into the substrate. A parallel is seen in harpid trilobites, although previous functional studies of these were restricted to the function of their characteristic brim. Unfortunately, we have no data on appendages in *Ityophorus* or harpid trilobites. It may be worth trying to infer the length and use of the legs from the space relationships between the probable attachment of the legs and the head shield, particularly its margin. This may give some hint of the mode of life.

Elevation of leg insertion over substrate

The hypostome of *Ityophorus* is oriented horizontally (Figures 3I, 4). This means that the mouth opened backwards, and not downwards. Recent crustaceans such as cephalocarids and notostracans a structure similar to the trilobite hypostome plus associated soft tissue is present, al-

though it is not homologous. This is the "labrum". In a crustacean with a labrum the digestive tract first extends forwards from the mouth. The tract then flexes in the head and continues backwards (Figure 4; see grey area in the cephalocarid), extending more or less straight to the anus. The digestive tract in *Ityophorus* should have followed the same course as in the cephalocarid crustacean (Figure 4; *Ityophorus* with digestive tube in grey). Actual evidence on such a digestive course in trilobies is reported in phacopid (Stürmer and Bergström, 1973, pl. 20) and trinucleid trilobites (Šnadjr, 1987, fig. 3).

In case of a crustacean with the mouth opening backward, there is an important structural relationship between the dorsoventral positions between the labrum and the basal podomeres. Since the mouth is directed backwards, food particles have to be transported mechanically (handled by appendages) or indirectly (handled by food collecting wave created by appendages) from back to front *via* the midventral line. For transporting the food particles, the "labrum" and mouth must be situated below the level of the midventral line posterior to the labrum. Since the line is higher than the labrum and the mouth, the basal podomeres, which are attached to the axial body, automatically are at more or less the same horizontal level as the mouth opening. Such a relationship is seen in three-dimensionally preserved *Ceraurus* (Walcott, 1881, pl. 2, figs. 1–3). In *Ityophorus*, the spatial relationship between hypostome and basal podomeres appears to have been identical (see white arrow in Figure 4B). Therefore, the basal podomeres must have been situated fairly high relative to the cephalic margin (Figure 4). This configuration forced the animal to develop long appendages simply to reach the substrate. As discussed earlier, this condition is a common feature in cavity-dwelling arthropods, and *Ityophorus* could probably rest with the brim on the substrate without using its appendages. This means that the appendages were free to be used for different aims such as food collecting.

Relationship between brim and appendages

In general, the morphology of the arthropod appendages directly influences the method of feeding. The combination in *Ityophorus* of long legs surrounded by a brim forming a long "skirt" should have been of significance for the mode of life. As described above, the two sets of terrace lines are restricted to the edge of the brim, where the steep sides of each set face the other set (Figures 3H, 5). The lower set of terrace lines should have prevented the animal from sliding laterally outwards (Schmalfuss, 1981), while the inner set would hinder extensive sinking into the substrate.

When an appendage scratched the substrate in one direction (Figure 5; black arrow with A), the body would be subjected to a pull in the opposite direction (Figure 5; black arrow with R). This is determined by simple physical rules. Scratching or burrowing leg movements may also tend to pull animal downwards into the substrate. In *Ityophorus*, the terrace lines on the cephalic rim would hinder the head shield from sliding sidewards or downwards (Figure 5; see magnification in left rectangle). Thus, for as long as the animal kept scratching, it could presumably move along inclined walls in a cavity. This mode of behaviour would work on a gel-like or sticky substrate such as a bacterial mat, the existence of which is suggested by the geological setting. Such a mode of life must require one more important factor, a low weight of the animal. *Ityophorus* was indeed unusually small and light. Therefore, I conclude that *Ityophorus* was most probably adapted to cavities coated with microbial mats. Some examples are known from Recent cavity-dwelling arthropods such as isopods which feed directly on fungi and bacteria (Sarbu and Popa, 1992).

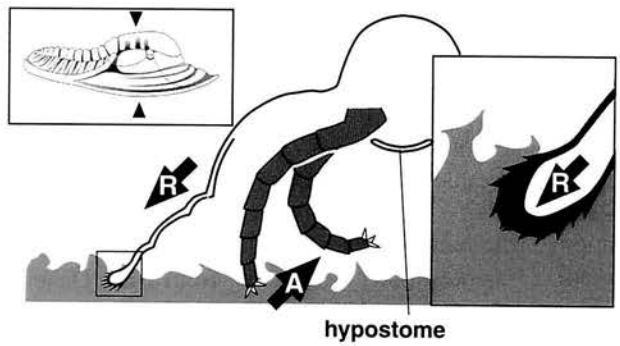

Figure 5. Schematic drawing of transversely sectioned cephalon (black arrow in top of the figure) with inferred appendage, showing the relationship of the action and reaction mechanics between the exoskeleton and the substrate when the animal was scratching. The rectangle shown in the right of the figure is the magnified cephalic rim with substrate. For more details, see text. Black arrow with A means the vector of action from exoskeleton to the substrate, black arrow with R of reaction from the latter to the former.

Epilogue

The Late Ordovician trilobite *Ityophorus undulatus* appears to have had a set of morphological characters characteristic of cavity dwellers, such as reduced eyes, long appendages relative to the body length, considerable dwarfing, and possible heterochronic development, which is most likely to be progenesis. The supposed ancestral group of the Ityophorinae, the Loganellidae, is thought to be extinct before the Cambrian-Ordovician transition. A relict group might have persisted into the Ordovician by "progenetic evolution", and later adapted into a cryptic life. This is the first report that tries to interpret a phylogenetically relict fossil group as cryptic animals.

A Devonian proetid genus, *Denemarkia* (see Moore, 1959, *O*397; Snajdr 1980, p. 146, pl. 37), was a possible cavity dweller (Alberti, 1969, p. 336) with an overall morphology similar to *Ityophorus*. Taphonomical evidence showing the entombment of *Denemarkia* specimens in a cavity is available (such an occurrence pattern is not illustrated so far but a slab showing such a situation is stored in National Museum, Czech Republic, museum number L 16634). *Denemarkia* is known from the Devonian Koněprusy Limestone in Czech Republic (Šnadjr, 1980) and the Kess Kess Limestone in Morocco (Alberti, 1969). Both limestone units are of the carbonate mud mound type of buildups. Interestingly, shared characters between *Denemarkia* and *Ityophorus*, such as fairly vaulted cephalon (see Moore, 1959, fig. 302-1b), distinct cephalic rim with wide cephalic doublure, lacking mesial embayment for the hypostomal suture (see Snadjr, 1980, pl. 27, fig. 9), a combination of which is quite rare in proetids, and less developed eye, are a fairly unique morphological combination in trilobites. A major morphological difference between the two is that the dorsal exoskeleton of *Denemarkia* is fairly rich in tubercles, whereas *Ityophorus* is smooth, and this can be explained as a result of adaptation to cavities as discussed previously. Repeated body modifications into ityophorid-like morphology from completely different clades means that there was a general capacity in the Trilobita to evolve in this direction.

Acknowledgements

I thank two reviewers, B. D. E. Chatterton (University of Alberta, Edmonton, Canada) and P. Ahlberg (Lund University, Sweden), for critically reading the manuscript and providing constructive suggestions. I am grateful to J. Bergström (Swedish Museum of Natural History, Stockholm) for thorough discussions and the permission to examine museum collections. Helpful discussions of cavity organisms were conducted with T. Kase and Y. Kano (National Science Museum, Japan). I thank S. Stuenes (Uppsala University) for access to the type specimens. I also thank J. Slavíčková (National Museum, Prague) for sending me latex casts of *Denemarkia*, and for access to the specimens. This study was financially supported by the Grant-in-Aid for JSPS Research Fellow (No. 04015 in 2001–2003) from the Ministry of Education, Science, Sports and Culture, Japan. A bilateral scholarship of the Swedish Institute, and a scholarship of the Mitsubishi Shintaku Yamamuro memorial Fund are greatly acknowledged.

References

Alberti, G., 1969: Trilobiten des jüngeren Siluriums sowie des Unter-und Mitteldevons. I. *Abhandlungen der Senckenbergischen Naturforschenden Gesellschaft*, no. 520. P. 1–692.

Culver, D. C., 1982: Adaptation. *In*, Culver, D.C. *ed.*, *Cave Life. Evolution and Ecology*, p. 8–36, Harvard University Press, Cambridge, Masachusetts and London, England.

Fortey, R. A., 1974: The Ordovician trilobites of Spitsbergen. I. Olenidae. *Norsk Polarinstitutt Skrifter*, no. 160, p. 1–181.

Fortey, R. A., 1997: Classification. *In*, Kaesler, R. L., *ed.*, *Treatise on Invertebrate Paleontology, Part O, Arthropoda 1, Trilobita, revised*, p. 289–302. Geological Society of America, Boulder, Colorado, and University of Kansas, Lawrence, Kansas.

Fortey, R. A. and Chatterton, B. D. E., 1988: Classification of the trilobite suborder Asaphina. *Palaeontology*, vol. 31, p. 165–222.

Hayami, I. and Kase, T., 1996: Characteristics of submarine cave bivalves in the northwestern Pacific. *American Malacological Bulletin*, vol. 12, p. 59–65.

Hessler, R. R. and Elofsson, R., 1992: Cephalocarida. *In*, Harrison, F. W. and Humes, A. G. *eds.*, *Microscopic Anatomy of Invertebrates*, vol. 9. *Crustacea*. p. 9–24, Wiley-Liss, Inc., New York.

Hobbs, H. H. III, 2000: Crustacea. *In*, Wilkens, H., Culver, D. C. and Humphreys, W. *eds.*, *Ecosystems of the World*, vol. 30, *Subterranean Ecosystems*, p. 95–107, Elsevier, Amsterdam.

Humphreys, W. F., 2000: Background and glossary. *In*, Wilkens, H., Culver, D.C. and Humphreys, W. *eds.*, *Ecosystems of the World*. vol. 30, *Subterranean Ecosystems*, p. 3–14, Elsevier, Amsterdam.

Jaanusson, V., 1979: Karbonatnye postrojki v ordovikye shvyetsii. [Carbonate mounds in the Ordovician of Sweden.]-*Izvestija Akademii Nauk Kazahstan.SSR, Ser. Geologiy*, vol. 4, p. 92–99. [In Russian with English summary]

Jaanusson, V., 1982: The Siljan district. *In*, Bruton, D. L. and Williams, S. H. *eds.*, *4th International Symposium on the Ordovician System. Field Excursion Guide*. p. 15–42. *Palaeontological Contributions from the University of Oslo*, vol. 279. University of Oslo, Oslo.

Ludvigsen, R., Westrop, S. R. and Kindle, C. H., 1989: Sunwaptan (Upper Cambrian) trilobites of the Cow Head Group, western Newfoundland, Canada. *Palaeontographica Canadiana*, no. 6, p. 1–175.

Monty, C. L. V., 1995: The rise and nature of carbonate mudmounds: an introductory actualistic approach. *In* Monty, C. L. V. *et al.*, *eds. Carbonate mud-mounds.Special Publication of the International Association of Sedimentologists*, no. 23, p. 11–48, Blackwell Science, Oxford.

Moore, R. C., 1959: *Treatise on Invertebrate Paleontology, Part O, Arthropoda 1*, 560 p. Geological Society of America and University of Kansas Press, Lawrence, Kansas.

Nikolaisen, F., 1965: The Middle Ordovician of the Oslo region, Norway. 18. Rare trilobites of the families Olenidae, Harpidae, Ityophoridae and Cheiruridae. *Norsk Geologisk Tidsskrift*, vol. 45, p. 241–247.

Osmólska, H., 1975: Fine morphological characters of some Upper Palaeozoic trilobites. *Fossils and Strata*, vol. 4, p. 201–207.

Öpik, A. A., 1967: The Mindyallan fauna of North-western Queensland. *Commonwealth of Australia, Bureau of Mineral Resources, Geology and Geophysics, Bulletin*, 74, vol. 1, p. 1–404.

Peng, S., 1990a: Tremadoc stratigraphy and trilobite faunas of northwestern Hunan. 1. Trilobites from the Nantsinkwan Formation of the Yangtze Platform. *Beringeria*, vol. 2, p. 3–53.

Peng, S., 1990b: Tremadoc stratigraphy and trilobite faunas of northwestern Hunan. 2. Trilobites from the Panjiazui Formation and the Madaoyu Formation in Jiangnan slope belt. *Beringeria*, vol. 2, p. 55–171.

Pratt, B. R., 1982: Stromatolitic framework of carbonate mud-mounds. *Journal of Sedimentary Petrology*, vol. 52, p. 1203-1227.

Pratt, B. R., 1995: The origin, biota and evolution of deep-water mud-mound. *In*, Monty, C. L. V. *et al., eds. Carbonate mud-mounds.Special Publication of the International Association of Sedimentologists*, no. 23, p. 49-123. Blackwell Science, Oxford.

Rasetti, F., 1959: Family Loganellidae. *In*, Moore, R. C. *ed., Treatise on Invertebrate Paleontology, Part O, Arthropoda 1*, p. *O*331-332, Geological Society of America and University of Kansas Press, Lawrence, Kansas.

Reitner, J., 1993: Modern cryptic microbialite/metazoan facies from Lizard Island (Great Barrier Reef, Australia) formation and concepts. *Facies*, vol. 29, p. 3-40.

Sarbu, S. M. and Popa, R., 1992: A unique chemoautotrophically based cave ecosystem. *In*, Camacho, A. I., *ed., The Natural History of Biospeleology*, p. 637-666, Monografías del Museo Nacional de Ciencias Naturales, CSIC Madrid.

Sanders, H. L., 1963: The Cephalocarida. Functional morphology, larval development, comparative external anatomy. *Memoirs of the Connecticut Academy of Arts and Sciences*, vol. 15, p. 1-80.

Schmalfuss, H., 1981: Structure, patterns and function of cuticular terraces in trilobites. *Lethaia*, vol. 14, p. 331-341.

Šnajdr, M., 1980: Bohemian Silurian and Devonian Proetidae (Trilobita). *Rozpravy Ústredního Ústavu Geologického*, vol. 45, p. 1-324.

Šnajdr, M., 1987: On the digestive system of *Denaspis goldfussi* (Barrande). *Casopis Narodniho Musea*, vol. 156, p. 8-16.

Stürmer, W. and Bergström, J., 1973: New discoveries on trilobites by X-rays. *Paläontologische Zeitschrift*, vol. 47, p. 104-141.

Suzuki, Y. and Bergström, J., 1999: Pocket taphonomy and ecology of carbonate mound trilobites of the Boda Limestone, Dalarna, Sweden. *Lethaia*, vol. 42, p. 159-172.

Walcott, C. D., 1881: The trilobite: New and old evidence relating to its organization. *Bulletin of the Museum of Comparative Zoölogy at Harvard University*, vol. 8, p. 191-224.

Warburg, E., 1925: Trilobites of the *Leptaena* Limestone in Dalarna. *Bulletin of the Geological Institution of the University of Upsala*, vol. 27, p. 1-446 p.

Whittington, H. B. and Kelly, S. R. A., 1997: Morphological terms applied to Trilobita. *In*, Kaesler, R. L., *ed., Treatise on Invertebrate Paleontology, Part O, Arthropoda 1, Trilobita, revised*, p. 313-329. Geological Society of America, Boulder, Colorado, and University of Kansas, Lawrence, Kansas.

Paleontological Research, vol. 6, no. 1, pp. 85–99, April 30, 2002

Changes in Holocene ostracode faunas and depositional environments in the Kitan Strait, southwestern Japan

MORIAKI YASUHARA[1], TOSHIAKI IRIZUKI[2], SHUSAKU YOSHIKAWA[1] AND FUTOSHI NANAYAMA[3]

[1]*Department of Biology and Geoscience, Graduate school of Science, Osaka City University, Osaka, 558-8585, Japan (e-mail: yassan@sci.osaka-cu.ac.jp)*

[2]*Department of Geosciences, Interdisciplinary Faculty of Science and Engineering, Shimane University, Matsue 690-8504, Japan*

[3]*Active Fault Research Center, National Institute of Advanced Industrial Science and Technology, Tsukuba, 305-8567, Japan*

Received 16 October 2001; Revised manuscript accepted 21 December 2001

Abstract. At least 106 species were identified from 36 samples obtained from two cores (T1 and T2), which were recovered from the Kitan Strait off Wakayama City, southwestern Japan. Q-mode cluster analysis of cores T1 and T2 revealed three biofacies (PL, PT and LS). Changes in depositional environments based on the observed distribution of ostracodes were analysed, and the following sequence is proposed. Before ca. 7,000 cal yr BP, the T1 site was a sandy coast, ranging from an outer bay to the open sea, close to a river mouth, at water depths of more than 15–20 m, while the T2 site ranged from a bay coast to an outer bay, close to a river mouth, at water depths of less than 15–20 m. During ca. 7,000–2,000 cal yr BP, the position of the sites fell within ranging an outer bay to the open sea at water depths of 30–40 m influenced by residual and/or tidal currents from the straits. After ca. 2,000 cal yr BP, the sites were situated on a sandy coast, ranging from an outer bay to the open sea, close to a river mouth, at water depths of more than 15–20 m. Two new species, *Trachyleberis ishizakii* and *Cytheropteron kumaii*, are also described.

Key words: depositional environments, Holocene, Kitan Strait, Ostracoda, Wakayama

Introduction

Fossil ostracodes have frequently been used to elucidate the way in which the environment of deposition changes with time (*e.g.*, Ishizaki *et al.*, 1993; Cronin *et al.*, 1994; Irizuki *et al.*, 1998b), because they are highly sensitive indicators of several environmental factors (e.g., Ishizaki and Irizuki, 1990; Ikeya and Suzuki, 1992; Yamane, 1998; Yasuhara and Irizuki, 2001). However, little studies of Japanese Holocene ostracodes have been carried out (Frydl, 1982; Ishizaki, 1984; Ota *et al.*, 1985; Ikeya *et al.*, 1987; Ikeya *et al.*, 1990; Iwasaki, 1992; Kamiya and Nakagawa, 1993; Irizuki *et al.*, 1998a; Miyahara *et al.*, 1999; Irizuki *et al.*, 2001). Many of these studies concentrate on temporal changes of Holocene ostracode assemblages in small drowned valleys and enclosed bays. Irizuki *et al.* (1998a) elucidated paleoenvironmental changes on the western coast of the Miura Peninsula, central Japan on the basis of numerical analyses of ostracode distributions. Miyahara *et al.* (1999) and Irizuki *et al.* (2001) used sedimentary facies from cores, containing fossil ostracodes and high density radiocarbon dating to construct a relative sea-level curve and to discuss paleoceanic changes in the Osaka area, southwestern Japan.

The Kitan Strait is situated between Osaka Bay and the open sea. The area provides an important record of the depositional environments of the Seto Inland Sea and Osaka Bay, and therefore yields key data for inferring paleoceanic conditions.

This study aimed to elucidate ostracode faunas and the temporal change in depositional environments off the western coast of Wakayama City, near the Kitan Strait. We also discuss the consequences of sea-level changes in Osaka Bay and the study area.

Locality, lithofacies and methodology

Drilling cores (T1 and T2) were excavated by the National Institute of Advanced Industrial Science and Technology from the Kitan Strait (T1: 34°14.7′ N, 135°5.2′ E, 19.61 m

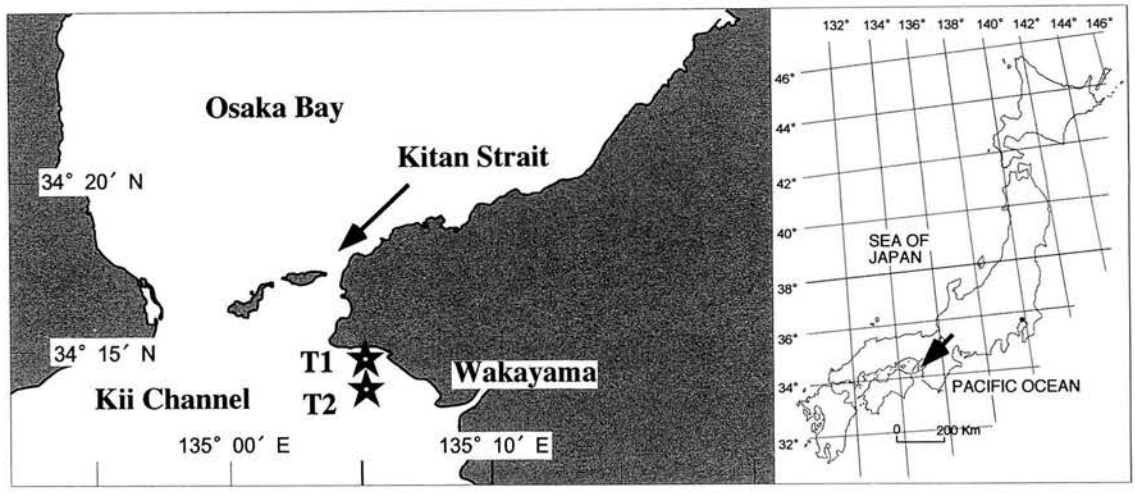

Figure 1. Index and locality maps.

water depth; T2: 34°14.5′ N, 135°5.2′ E, 24.78 m water depth) off Wakayama City, southwestern Japan (Figure 1). Nanayama *et al.* (1999) described in detail the Holocene and upper Pleistocene sequences in cores T1 and T2. We briefly mention those sequences here (Figure 2). Sediments at altitudes lower than −33.5 m in core T1 and −38.3 m in core T2 consist of sand and gravel, and the enclosing matrix is coarse sand. Sediments at altitudes between −19.6 and −33.5 m in core T1 and between −24.8 and −38.3 m in core T2 consist of alternating beds of fine to medium sand layers and silt layers with shell fragments, showing intensive bioturbation. Nanayama *et al.* (1999) reported two layers of debris flow deposits (Df1 and Df2). Df1 is situated at altitudes of approximately −24.1 to −24.3 m in core T1 and −29.3 to −30.4 m in core T2 (Figure 2). Df2 is situated at altitudes of approximately −27.2 to −27.7 m in core T1 and −34.5 to −35.7 m in the core T2 (Figure 2). Volcanic glasses are concentrated at an altitude of approximately −31 m in core T2. Nanayama *et al.* (1999) reported that these volcanic glasses are correlated with the Kikai-Akahoya (K-Ah) volcanic ash, dated at ca. 7,300 cal yr BP (Fukusawa, 1995).

Samples of the sediment core, each approximately 5 cm thick, were immersed in water, boiled for about one hour on a hot plate, washed through a 75 μm sieve and then dried. Dry weights were calculated from the original sample weight, scaled by the percentage water content of each sample. The fraction coarser than 200 μm was sieved to allow the ostracode fauna to be determined, and for specimens of each taxon to be obtained. Samples containing abundant ostracode specimens were divided using a sample splitter into workable aliquots of approximately 100–200 specimens. In the remaining samples, all the specimens present were picked. The number of specimens refers to the estimated minimum number of carapaces present in each sample, determined by taking the total number of left or right valves, whichever was the greater.

Ostracode biofacies

At least 106 ostracode species were identified from 36 samples obtained from cores T1 and T2 (Appendix). A selection of these species is illustrated in Figure 3.

Q-mode cluster analysis was used to examine vertical changes in ostracode faunas and to determine ostracode biofacies, which would closely reflect variations in the depositional environment. Taxa represented by three or more specimens in any one sample were used for analysis (some *Aurila* and *Pontocythere* species groups are expressed collectively as "spp."), and each sample contained more than 50 specimens. Horn's overlap indices (Horn, 1966) were used to assess similarities, and clustering was achieved by the unweighted pair-group arithmetic average method. The results revealed three biofacies (PL, PT and LS; Figure 4). To interpret these biofacies reflecting depositional environments, we referred to the distributions of present-day dead ostracode shells, because many studies of the distributions of present-day ostracodes have been based on dead ostracode shells.

Figures 5 and 6 show the stratigraphic positions of biofacies and percentages of 24 taxa dominating each of the biofacies in these cores.

*(1) Biofacies LS (*Loxoconcha viva -Spinileberis quadriaculeata biofacies*).*—Biofacies LS is composed of seven samples and lies in the middle part of cores T1 and T2. It is characterized by the dominance of *Loxoconcha viva* Ishizaki, *Spinileberis quadriaculeata* (Brady) and *Cytheropteron kumaii* sp. nov. (= *Cytheropteron miurense* of Ikeya

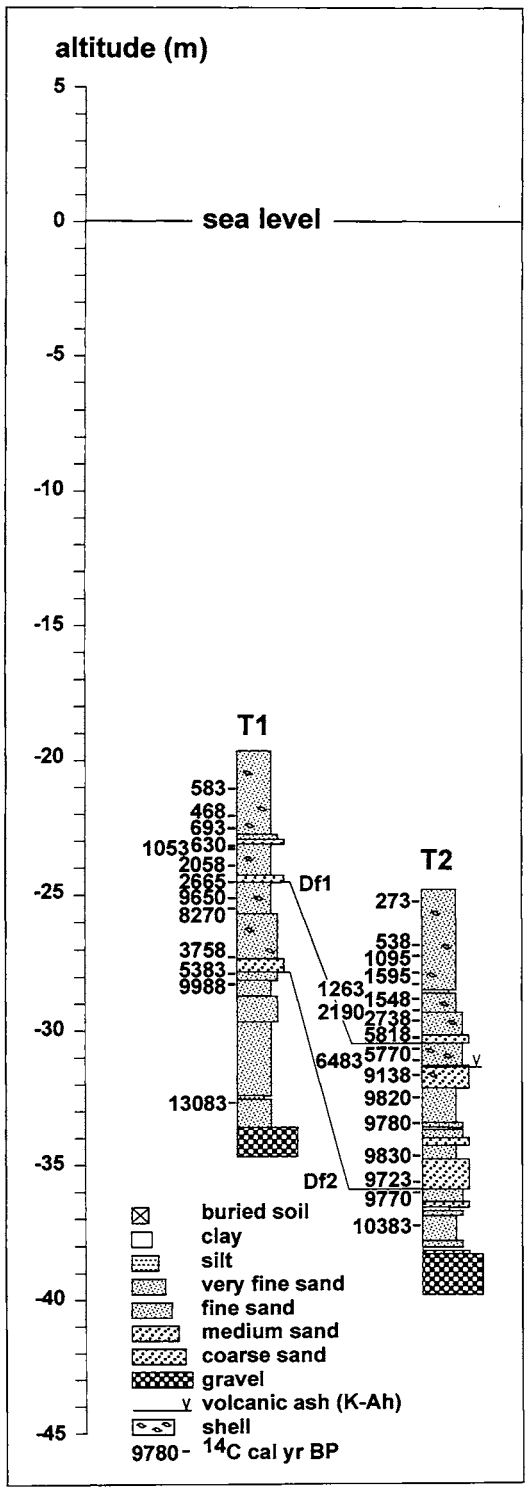

Figure 2. Columnar sections of T1 and T2 cores and horizons of radiocarbon age (cal yr BP). Radiocarbon ages calibrated and columnar sections modified from Nanayama *et al.* (1999).

and Itoh, 1991 and *Cytheropteron* sp. of Yasuhara and Irizuki, 2001). *Ambtonia obai* (Ishizaki), *Falsobuntonia hayamii* (Tabuki), "form A" (Abe and Choe, 1988) of *Bicornucythere bisanensis* (Okubo), *Aurila spinifera* Schornikov and Tsareva s.l., *Krithe japonica* Ishizaki, *Kobayashiina donghaiensis* Zhao and *Amphileberis nipponica* (Yajima) are also common.

L. viva is abundant at water depths of 15–37 m in Tateyama Bay, central Japan (Frydl, 1982). *S. quadriaculeata* is common in most areas of Osaka Bay and Hiuchi-nada Bay (Yasuhara and Irizuki, 2001; Yamane 1998). *C. kumaii* is reported from the outer part of Sendai Bay near the open sea at water depths of more than 50 m (Ikeya and Itoh, 1991) and from Osaka Bay at water depths of 37.2 m (Yasuhara and Irizuki, 2001). *Falsobuntonia* (*hayamii* and *taiwanica* Malz) is commonly found in the open sea off Shimane at water depths of more than 50 m (Ikeya and Suzuki, 1992). *A. obai* is abundant at water depths of 20–40 m (e.g., Ishizaki, 1971; Frydl, 1982; Bodergat and Ikeya, 1988). *A. spinifera* s.l. is reported from the sandy part of Hiuchi-nada Bay near the Kurushima Strait (Yamane, 1998) and from the sandy part of Osaka Bay at a water depth of 37.2 m, where the influence of residual and/or tidal currents from the Akashi Strait is apparent (Yasuhara and Irizuki, 2001). *K. japonica*, *Ko. donghaiensis* and *A. nipponica* are common at water depths of more than 15–20 m in shallow sea areas around Japan (e.g., Yasuhara and Irizuki, 2001; Yamane, 1998; Bodergat and Ikeya, 1988; Frydl, 1982; Ishizaki, 1971).

The distribution of species suggests that biofacies LS is interpreted as ranging from an outer bay to the open sea at a water depth of 30–40 m, under the influence of residual and/or tidal currents from the strait.

*(2) Biofacies PT (*Pontocythere *spp.*-Trachyleberis scabrocuneata *biofacies).*—Biofacies PT is composed of two samples and lies in the lower part of core T2. It is characterized by the dominance of *Pontocythere* spp., *Trachyleberis scabrocuneata* (Brady), *S. quadriaculeata* and *Loxoconcha uranouchiensis* Ishizaki, with smaller numbers of *Loxoconcha pulchra* Ishizaki and *Nipponocythere bicarinata* (Brady). Intertidal and phytal species (*Aurila* spp. except *A. munechikai* and *A. spinifera* s.l., *Australimoosella tomokoae*, *Cornucoquimba tosaensis*, *Hemicytherura* spp., *Loxoconcha* spp. except *L. optima*, *L. pulchra*, *L. tosaensis*, *L. uranouchiensis* and *L. viva*, *Neonesidea oligodentata*, Paradoxostomatidae spp., *Pseudoaurila japonica*, *Robustaurila* spp., *Sclerochilus* sp., *Semicytherura* spp. and *Xestoleberis* spp.) are also common.

Pontocythere spp. are found in a range of habitats, from the sandy coasts of outer bays to open sea areas and/or river mouths (e.g., Ishizaki, 1968; Ikeya and Hanai, 1982; Yamane, 1998). *T. scabrocuneata* is abundant in middle to outer bay regions (Yasuhara and Irizuki, 2001). *L.*

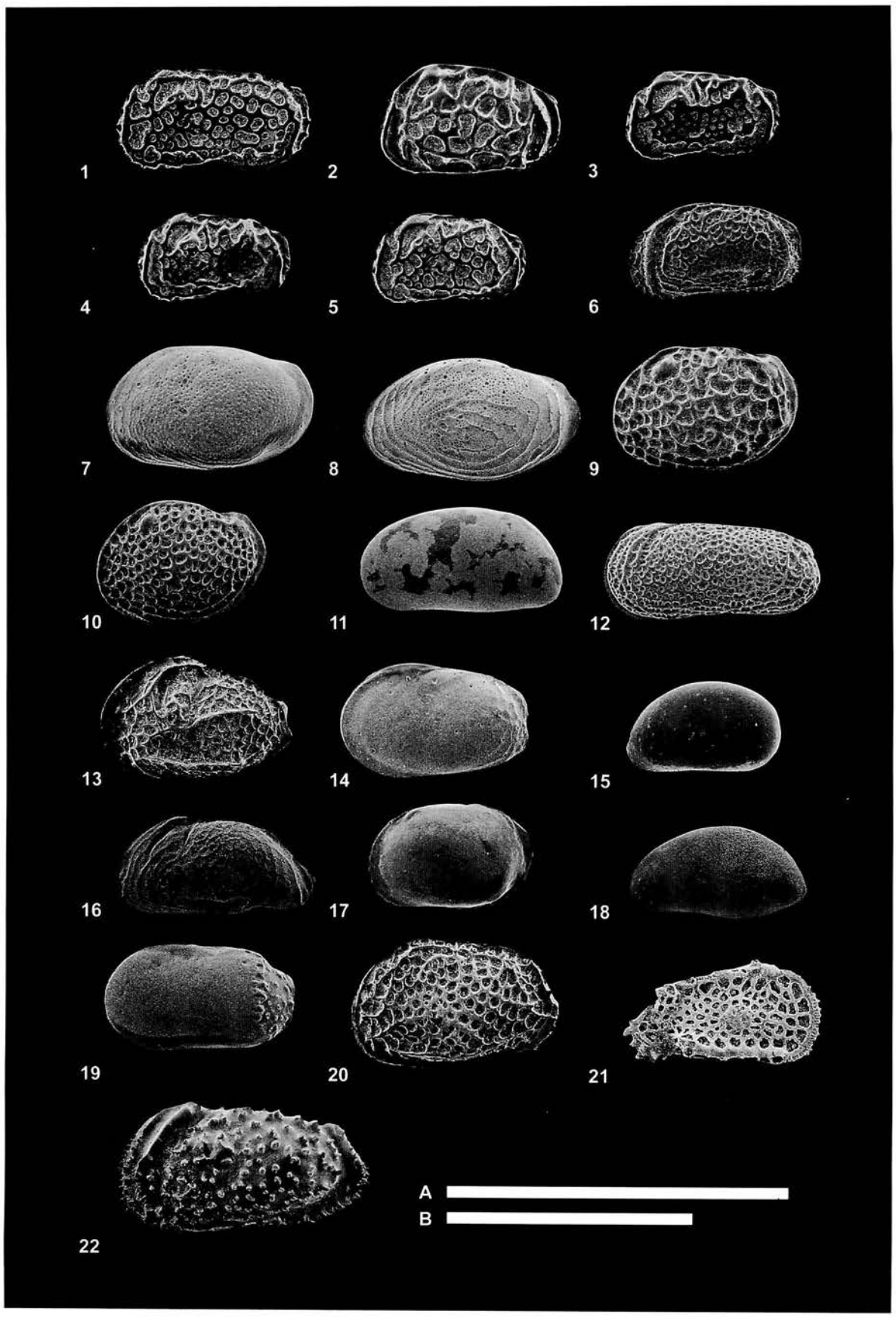
1
2
3
4
5
6
7
8
9
10
11
12
13
14
15
16
17
18
19
20
21
22
A
B

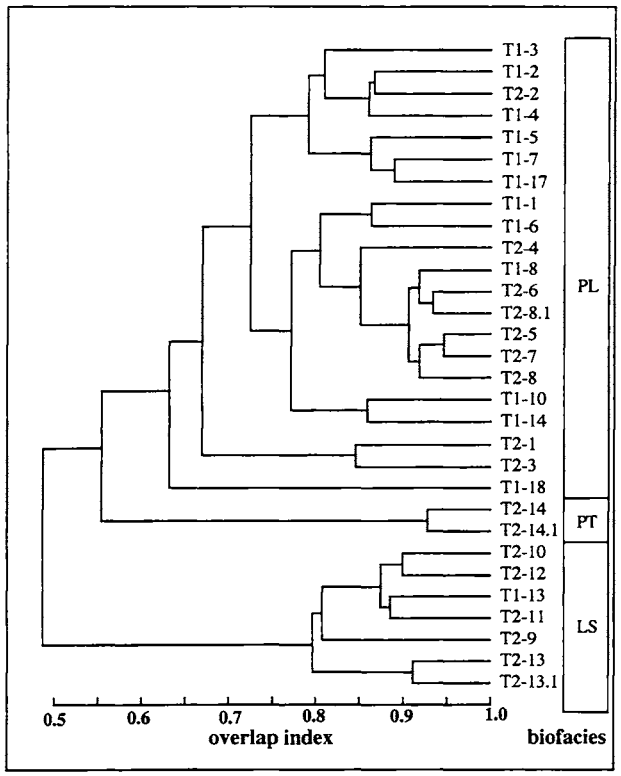

Figure 4. Dendrogram from Q-mode cluster analysis. PL, PT and LS represent the three biofacies found.

uranouchiensis is common in sandy bay coasts and abundant at water depths of less than 10 m (Frydl, 1982). *L. pulchra* is an estuarine inhabitant of Hiuchi-nada Bay, Seto Inland Sea, western Japan, that prefers low salinity and a water depth of less than 4 m (Yamane, 1998). *N. bicarinata* is common at water depths of more than 15 m in Osaka Bay (Yasuhara and Irizuki, 2001). However, species common at water depths of more than 15–20 m in shallow sea areas around Japan (e.g., *K. japonica*, *Ko. donghaiensis*, *A. nipponica*) are either rare or absent in this biofacies. Intertidal and phytal species could have been transported to this area by wave action or coastal currents.

Thus, biofacies PT is interpreted as ranging from a bay coast to an outer bay, near a river mouth, with water depths of less than 15–20 m.

(3) Biofacies PL (Pontocythere *spp.*—Loxoconcha optima *biofacies*).—Biofacies PL is composed of 21 samples and lies in the upper part of cores T1 and T2, and also in the lower part of the T1 core. It is characterized by the dominance of *Pontocythere* spp., *Loxoconcha optima* Ishizaki, *L. pulchra* and intertidal and phytal species. *K. japonica*, *Ko. donghaiensis* and *A. nipponica* also occur in this biofacies.

L. optima is reported from a sandy coast, ranging from an outer bay to the open sea (Ishizaki, 1968). Those species which are common in biofacies LS, such as *C. kumaii*, *A. obai* and *F. hayamii*, are either rare or completely absent.

Biofacies PL is therefore interpreted as a sandy coast, ranging from an outer bay to the open sea, near a river mouth at water depths of more than 15–20 m, but shallower than biofacies LS.

Temporal changes of depositional environments

Radiocarbon dating was conducted using 31 samples from cores T1 and T2 (Nanayama *et al.*, 1999). We calibrated these radiocarbon ages using INTCAL98 (Stuiver *et al.*, 1998), because this was not done in the original study. Many of the radiocarbon ages in core T1 were reversed (Figure 6): we therefore used the radiocarbon ages from core T2 to date temporal changes in depositional environments. Correlations between cores T1 and T2 are based on Nanayama *et al.* (1999).

Based on the results of Q-mode cluster analysis, vertical changes in depositional environments and associated ostracode faunas in these cores are distinguished as follows:

Before ca. 7,000 cal yr BP.—This period is represented by biofacies PT, composed of two samples in core T2 (T2-14 and 14.1), and the lower part of biofacies PL, composed of three samples in core T1 (T1-14, 17 and 18).

It is considered that during this period the T2 drilling site ranged from a bay coast to an outer bay, near a river mouth, with water depth shallower than 15–20 m. At the same time, the T1 site was on the sandy coast, ranging from an

← **Figure 3.** Scanning electron micrographs of fossil ostracodes from drilling cores in the Kitan Strait off Wakayama City. Scale bars = 1.0 mm (A for 1–19; B for 20–22). All specimens are adult left valves, except one specimen in Fig. 4.21 (an adult right valve). **1.** *Callistocythere hayamensis* Hanai (sample no. T1–8). **2.** *Callistocythere alata* Hanai (sample no. T1–6). **3.** *Callistocythere asiatica* Zhao (sample no. T2–3). **4.** *Callistocythere undata* Hanai (sample no. T2–4). **5.** *Callistocythere* sp. 1 (sample no. T2–8). **6.** *Ishizakiella miurensis* (Hanai) (sample no. T2–3). **7.** *Loxoconcha pulchra* Ishizaki (sample no. T1–8). **8.** *Loxoconcha optima* Ishizaki (sample no. T1–8). **9.** *Loxoconcha tosaensis* Ishizaki (sample no. T1–6). **10.** *Loxoconcha viva* Ishizaki (sample no. T2–8.1). **11.** *Parakrithella pseudadonta* (Hanai) (sample no. T1–6). **12.** *Cytheromorpha acupunctata* (Brady) (sample no. T1–6). **13.** *Spinileberis quadriaculeata* (Brady) (sample no. T2–13.1). **14.** *Falsobuntonia hayamii* (Tabuki) (sample no. T2–9). **15.** *Xestoleberis opalescenta* Schornikov (sample no. T2–3). **16.** *Perissocytheridea* sp. (sample no. T2–2). **17.** *Phlyctocythere japonica* Ishizaki (sample no. T2–14). **18.** *Neopellucistoma inflatum* Ikeya and Hanai (sample no. T2–2). **19.** *Ambtonia obai* (Ishizaki) (sample no. T2–12). **20.** *Aurila spinifera* s.l. Schornikov and Tsareva (sample no. T2–13). **21.** *Cletocythereis* sp. (sample no. T2–6). **22.** *Trachyleberis scabrocuneata* (Brady) (sample no. T1–7).

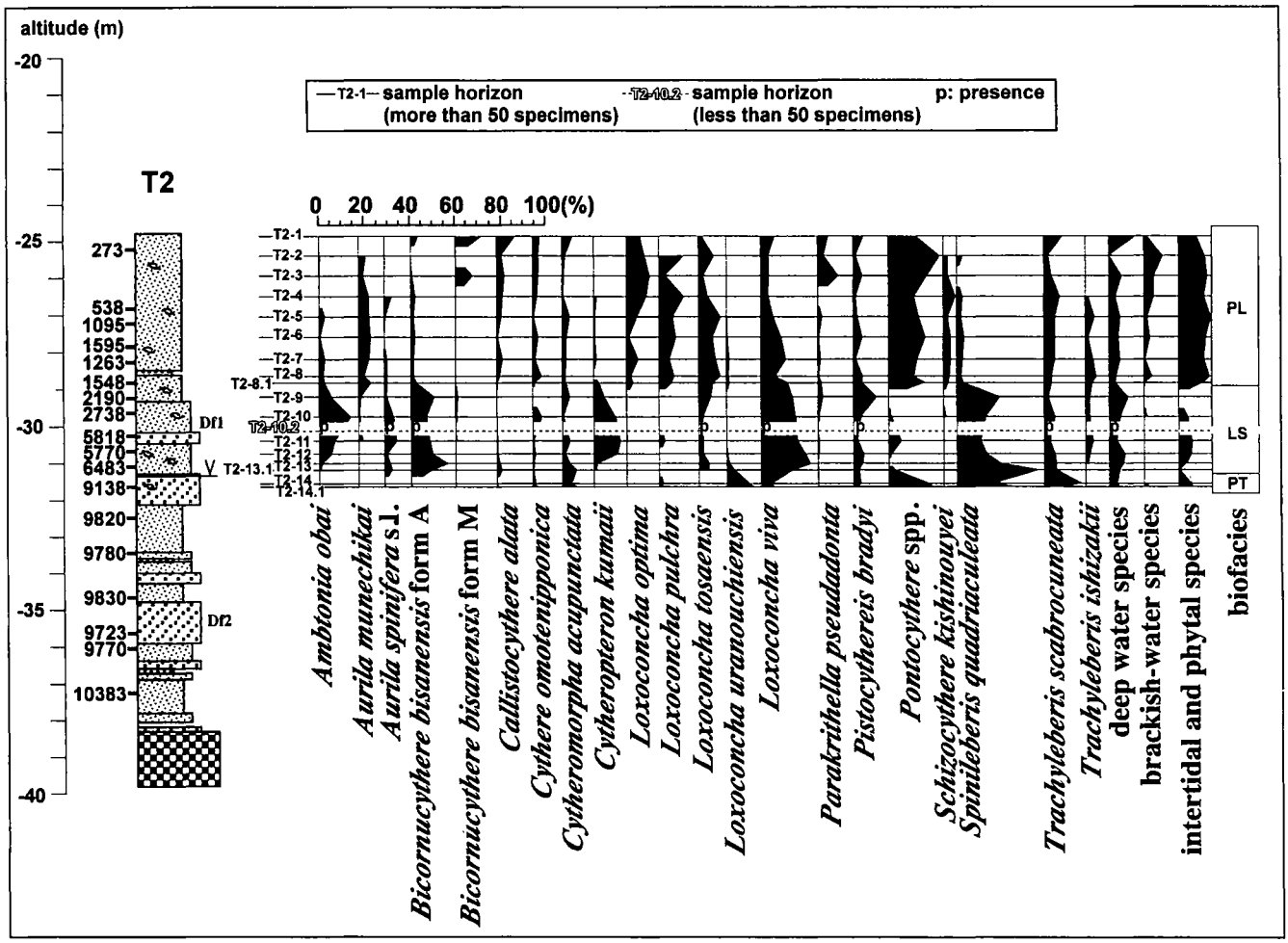

Figure 5. Columnar section of core T2, sample horizons, radiocarbon ages (cal yr B.P.), biofacies and percentages of dominant ostracode species. Deep-water species are *Amphileberis nipponica*, *Falsobuntonia hayamii*, *Kobayashiina donghaiensis*, *Krithe japonica* and *Nipponocythere bicarinata*. Brackish water species are *Cytherura miii*, *Darwinula* sp., *Ishizakiella miurensis*, *Perissocytheridea japonica*, *Perissocytheridea* sp., *Spinileberis furuyaensis* and *Spinileberis pulchra*. Intertidal and phytal species are *Aurila* spp. except *A. munechikai* and *A. spinifera* s.l., *Australimoosella tomokoae*, *Cornucoquimba tosaensis*, *Hemicytherura* spp., *Loxoconcha* spp. except *L. optima*, *L. pulchra*, *L. tosaensis*, *L. uranouchiensis* and *L. viva*, *Neonesidea oligodentata*, Paradoxostomatidae spp., *Pseudoaurila japonica*, *Robustaurila* spp., *Sclerochilus* sp., *Semicytherura* spp. and *Xestoleberis* spp.

outer bay to the open sea, near a river mouth, with water depths of more than 15–20 m. Species that are common at water depths of more than 15–20 m in shallow sea areas around Japan (e.g., *A. obai*, *K. japonica*, *Ko. donghaiensis* and *A. nipponica*) are, however, absent in samples T1-17 and T1-18. In these horizons, it is considered that water depths were shallower than the other horizons.

Ca. 7,000–2,000 cal yr BP.—This period is represented by biofacies LS, and is composed of six samples in core T2 (T2-9, 10, 11, 12, 13 and 13.1), and one sample in core T1 (T1-13).

These sites ranged from an outer bay to the open sea at water depths of 30–40 m, and were influenced by residual and/or tidal currents from the strait.

After ca. 2,000 cal yr BP.—This period is represented by biofacies PL and is composed of nine samples in core T2 (T2-1, 2, 3, 4, 5, 6, 7, 8 and 8.1), and also the upper part of biofacies PL, which is composed of nine samples in core T1 (T1-1, 2, 3, 4, 5, 6, 7, 8 and 10).

These sites were at the sandy coast, ranging from an outer bay to the open sea, near a river mouth, with water depths greater than 15–20 m, but shallower than biofacies LS. The percentage of those species that are common at water depths of more than 15–20 m in shallow sea areas around Japan (e.g., *A. obai*, *K. japonica*, *Ko. donghaiensis* and *A. nipponica*) are smaller in core T1 than in core T2. This indicates that the T1 site was in shallower water than the T2 site during this period.

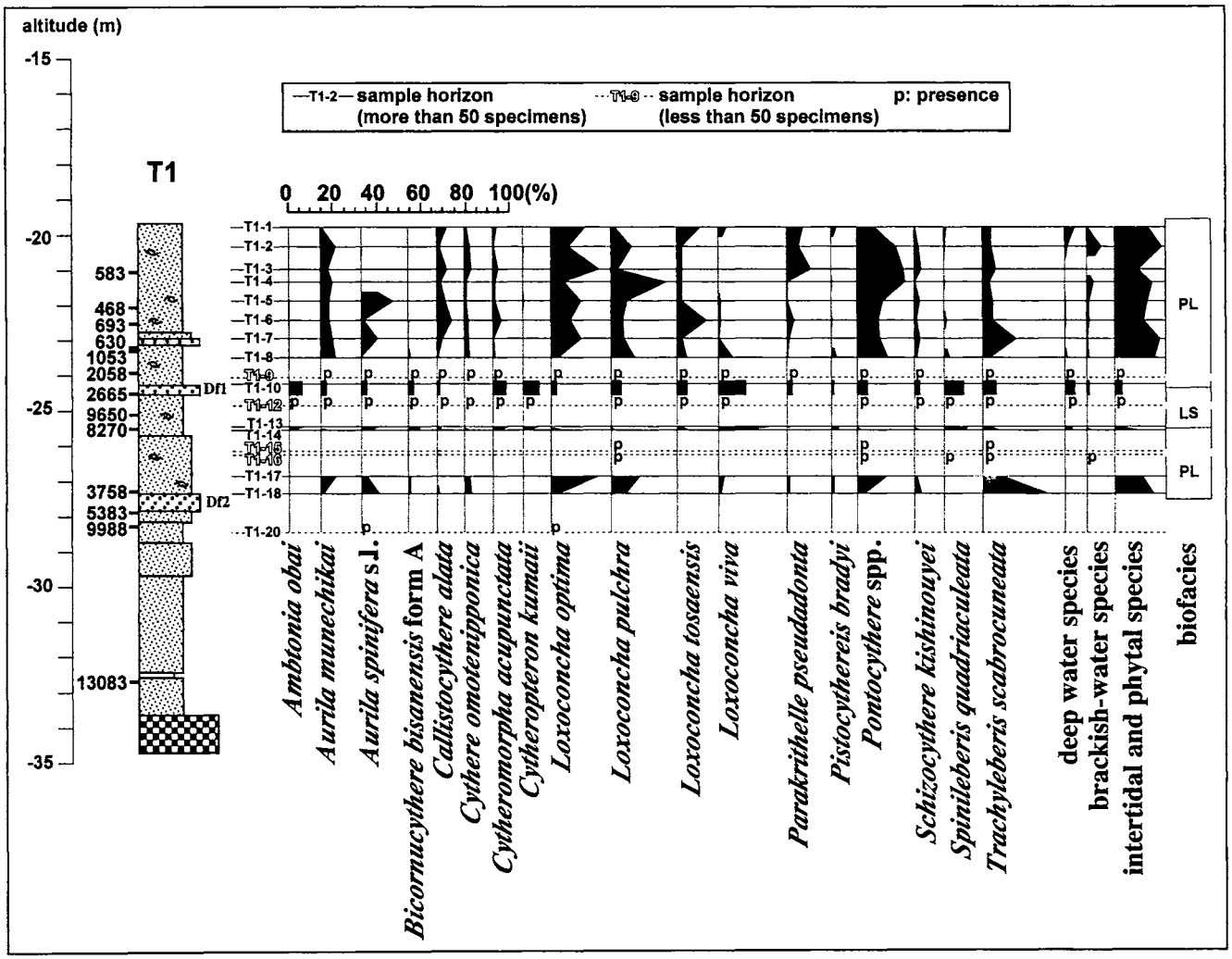

Figure 6. Columnar section of core T1, sample horizons, radiocarbon ages (cal yr B.P.), biofacies and percentages of dominant ostracode species. Deep-water, brackish, and intertidal and phytal species are similar to those in Figure 5.

In the Osaka Plain and the inner part of Osaka Bay, the relative sea-level change has been studied in detail on the basis of sedimentary facies, fossil ostracode faunas and high-density radiocarbon dating of molluscan shells (Miyahara *et al.*, 1999; Masuda *et al.*, 2000; Masuda and Miyahara, 2000; Irizuki *et al.*, 2001). These studies reported that the sea level rose rapidly from the period between ca. 11,000 cal yr BP to ca. 5,300–5,000 cal yr BP and from that time fell to the present sea level. The maximum sea level highstand was at ca. 5,300–5,000 cal yr BP in Osaka Bay (Masuda *et al.*, 2000). The historical changes in water depth at the two sites investigated in this study are similar to the relative sea-level changes proposed by Masuda *et al.* (2000), although the cores reveal areal differences in faunal changes during the same period. This result suggests that the relative sea-level curve of Masuda *et al.* (2000) lends itself to the standard for relative sea-level change not only in Osaka Bay but also in more wide areas.

Systematic descriptions

All the illustrated specimens are deposited in the collections of the Department of Biology and Geosciences, Graduate School of Science, Osaka City University (OCUCO).

Suborder Podocopina Sars, 1866
Superfamily Darwinuloidea Brady and Norman, 1889
Family Darwinulidae Brady and Norman, 1889
Genus ***Darwinula*** Brady and Robertson in Jones, 1885

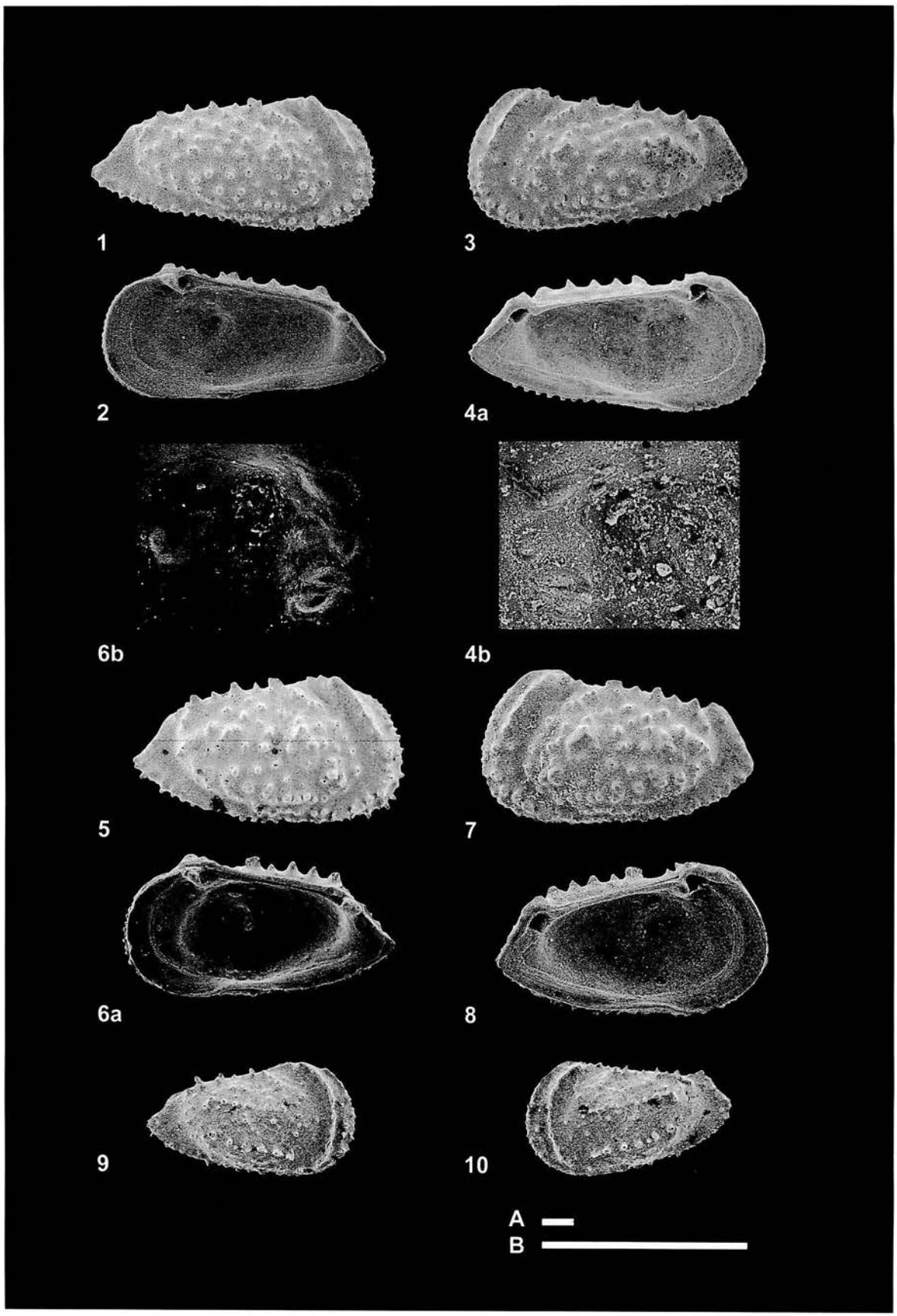
1
3
2
4a
6b
4b
5
7
6a
8
9
10
A
B

Darwinula sp.

Figure 8.5–8.8

Materials.—20 specimens.

Diagnosis.—*Darwinula* characterized by elongate and small carapace.

Occurrence.—T1–2, 4-6, 8, T2–2 to T2–4, 6, 8, 10.

Remarks.—This species has central muscle scars characteristic of darwinulids. This is the first fossil record of the genus from the Japanese Holocene. Ikeya and Hanai (1982) attributed a single broken valve from the Recent of Hamana-ko Bay, central Japan, to this genus. This genus has a freshwater habitat (Van Morkhoven, 1963).

Superfamily Cytheroidea Baird, 1850
Family Trachyleberididae Sylvester-Bradley, 1948
Subfamily Trachyleberidinae Sylvester-Bradley, 1948
Tribe Trachyleberidini Sylvester-Bradley, 1948
Genus ***Trachyleberis*** Brady, 1898

Trachyleberis ishizakii sp. nov.

Figure 7.1–7.10

Cythereis Yamigera [*sic*] (Brady). Kajiyama, 1913, p. 12, pl. 1, 64-66.

Trachyleberis scabrocuneata (Brady). Ishizaki, 1969, p. 221–222, pl. 26, fig. 8; Ishizaki, 1971, p. 92–93, pl. 4, fig. 16; Okubo, 1979, p. 156, fig. 7a, b; Ikeya and Compton, 1983, p.120, pl. 10–120, figs. 1a–4b, p. 126, pl. 10–126, figs. 1a–4b; Paik and Lee, 1988, p. 550, pl. 2, fig. 11; Ikeya and Itoh, 1991, p. 145, fig. 24, C; Kamiya and Nakagawa, 1993, p. 129, pl. 4, fig. 7; Ishizaki *et al.*, 1993, p. 329, fig. 7c; Irizuki *et al.*, 1998a, p. 7, fig. 2.13; Kamiya *et al.*, 2001, p. 103, fig. 18.18.

Cythere scabrocuneata Brady. Puri and Hulings, 1976, p. 289, pl. 26, figs. 6, 8.

Trachyleberis sp. 1. Ikeya and Suzuki, 1992, p. 137, pl. 9, fig. 4.

Actinocythereis sp. Kamiya and Nakagawa, 1993, p. 129, pl. 4, fig. 8.

Trachyleberis sp. Irizuki *et al.*, 2001, p. 109, fig. 3.8; Yasuhara and Irizuki, 2001, p. 95, pl. 12, figs. 9–13.

Etymology.—In honor of Dr. Kunihiro Ishizaki.

Materials.—86 specimens.

Diagnosis.—*Trachyleberis* characterized by subtriangular valve shape, tubercles on valve surface, large dorsal tubercles and anterior marginal ridge.

Description.—Carapace large, subtriangular, tapering posteriorly in lateral view, highest at anterior cardinal angle. Anterior margin broadly rounded and slightly extended below. Dorsal margin straight. Ventral margin broadly convex in female and straight in male. Posterior margin acuminate. Anterior, ventral and posterior margins fringed by spines and tubercles. Surface ornamented with tubercles, subcentral tubercle and anterior marginal ridge. Anterior marginal ridge running from anterior cardinal angle to midpoint of anterior margin. Eye and subcentral tubercles distinct. Pore canal openings moderate in number, scattered on most of valve surface. Pore canals with opening along edge of marginal contact zone of ventral marginal surface straight, numerous along anterior and posteroventral margins. Marginal infold moderate in width along anterior and posterior margins. No vestibule. Hinge holamphidont. Muscle scars consisting of one V-shaped frontal scar and a row of four adductor scars. Sexual dimorphism distinct; males more slender than females.

Types.—Holotype, sample no. T1–6, OCUCO 0005, male RV, L = 0.884 mm, H = 0.420 mm (Figure 7.1); 9 paratypes, sample nos. T2–8.1, OCUCO 0006, T2–7, OCUCO 0007, T2–8, OCUCO 0008, T2–7, OCUCO 0009, T2–8.1, OCUCO 0010, T2–8.1, OCUCO 0011, T2–8, OCUCO 0012, T1–6, OCUCO 0013 and T1–6, OCUCO 0014.

Type locality.—Holocene sediments off Wakayama City (34° 14.7′ N, E 135° 5.2′ E).

Occurrence.—T1-2, 5–10, 13, 14, 18, T2-4 to T2-8, 8.1, 9, 10, 11–13.

Remarks.—This species is similar to *Trachyleberis scabrocuneata* (Brady, 1880), but differs in having a shorter anterior marginal ridge, smaller carapace, straight margin broadly convex in male, larger dorsal tubercles, smaller number of surface tubercles and more slender shape. Also, this species is similar to *Trachyleberis niitsumai* Ishizaki, 1971, but differs in having a shorter anterior marginal ridge, more prominent and regular surface tubercles, larger dorsal tubercles and more slender shape.

← **Figure 7.** *Trachyleberis ishizakii* sp. nov. **1.** Lateral view of male RV, holotype, T1–6, OCUCO 0005, L = 0.884 mm, H = 0.420 mm. **2.** Internal view of male RV, T2-8.1, OCUCO 0006, L = 0.883 mm, H = 0.419 mm. **3.** Lateral view of male LV, T2–7, OCUCO 0007, L = 0.869 mm, H = 0.447 mm. **4a, b.** Internal view and muscle scars of male LV, T2–8, OCUCO 0008, L = 0.921 mm, H = 0.439 mm. **5.** Lateral view of female RV, T2–7, OCUCO 0009, L = 0.848 mm, H = 0.463 mm. **6a, b.** Internal view and muscle scars of female RV, T2–8.1, OCUCO 0010, L = 0.848 mm, H = 0.445 mm. **7.** Lateral view of female LV, T2–8.1, OCUCO 0011, L = 0.848 mm, H = 0.476 mm. **8.** Internal view of female LV, T2–8, OCUCO 0012, L = 0.852 mm, H = 0.480 mm. **9.** Lateral view of A-1 stage RV, T1–6, OCUCO 0013, L = 0.656 mm, H = 0.359 mm. **10.** Lateral view of A-1 stage LV, T1–6, OCUCO 0014, L = 0.641 mm, H = 0.362 mm. Scale bars are 0.1 mm: A for 1–4a, 5–6a and 7–10; B for 6b and 4b.

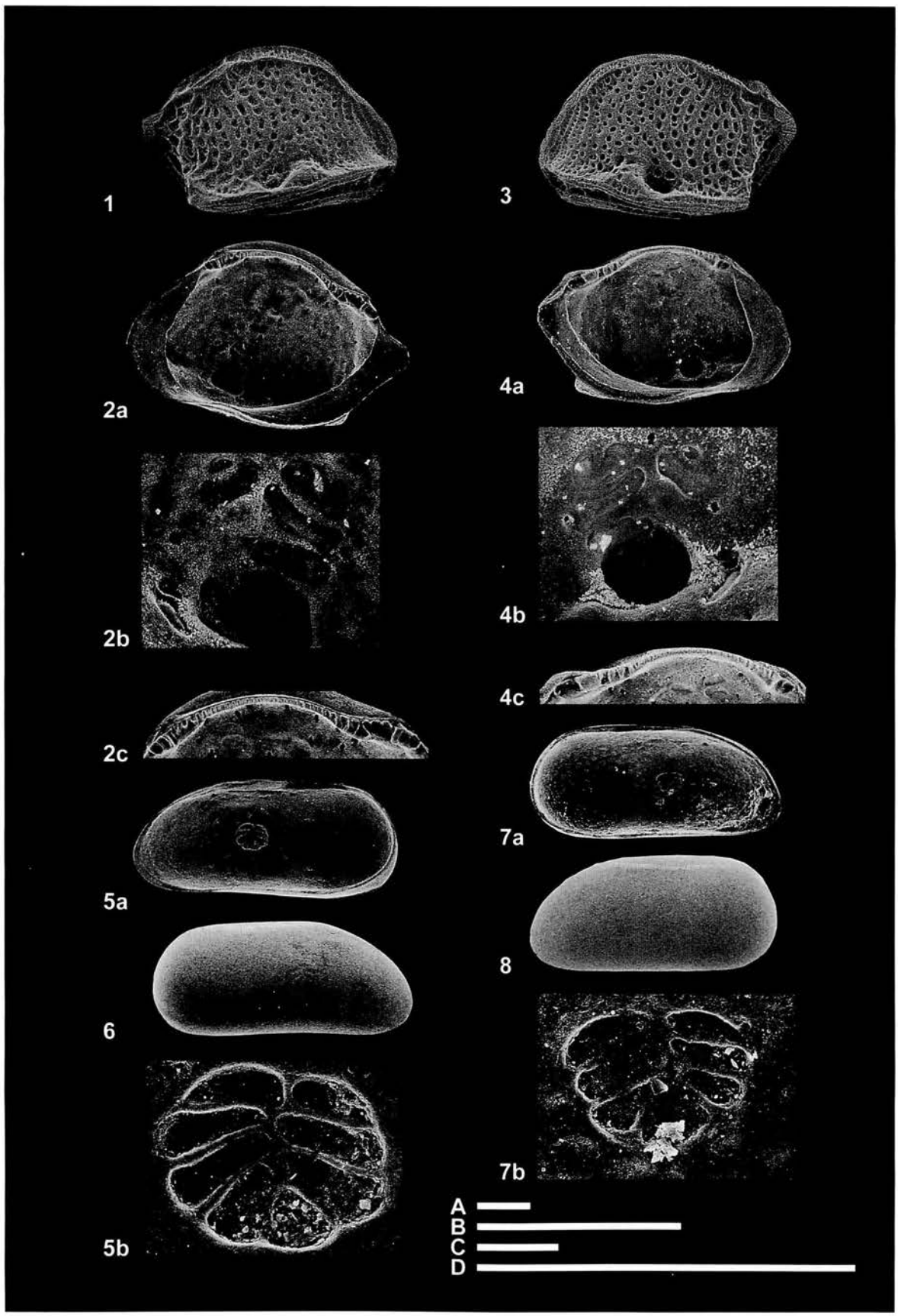
1
2a
2b
2c
5a
6
5b
3
4a
4b
4c
7a
8
7b
A
B
C
D

Family Cytheruridae G.W. Müller, 1894
Subfamily Cytheropterinae Hanai, 1957
Genus ***Cytheropteron*** Sars, 1866

Cytheropteron kumaii sp. nov.

Figure 8.1-8.4

Cytheropteron miurense Hanai. Ikeya and Itoh, 1991, p. 136, fig. 15, A.

Cytheropteron sp. Yasuhara and Irizuki, 2001, p. 79, pl. 4, fig. 10.

Etymology.—In honor of Prof. Hisao Kumai.

Materials.—80 specimens.

Diagnosis.—*Cytheropteron* characterized by subrhomboidal valve shape, small carapace and straight ventral alar process.

Description.—Carapace small, subrhomboidal in lateral view, highest at midlength. Anterior margin obliquely rounded. Dorsal margin strongly arched. Ventral margin sinuate, concave in middle, obscured in posterior third by alar process. Posterior margin protruding into a horizontally pointed caudal process. Surface ornamented with numerous reticula aligned more or less vertically, and dorsal and ventral marginal ridges. Reticula coarser in posterior half. Dorsal marginal ridge arcuate, very narrow, running along dorsal margin from anterior third to posterior terminal. Ventral marginal ridge starting from anterior end and running along ventral margin to form a prominent anterior edge of alar process. Eye tubercle indistinct. Pore canal openings moderate in number, scattered on most of valve surface. Pore canals with openings along edge of marginal contact zone of ventral marginal surface few, approximately ten along anterior margin. Marginal infold moderate in width along anterior and posterior margins. Vestibule poorly developed along anterior margin, broadest at anteroventral margin. Hinge line sinuous in interior view. Hinge of right valve consists of anterior and posterior teeth and an intermediate groove. Intermediate groove subdivided into three parts: short anterior part with three large crenulations, finely crenulate median part and concave posterior part with six small sockets, of which the anterior three are clearly separated and the posterior three are connected to each other. Hinge of left valve complementary of that of right valve. Muscle scars consist of two frontal scars, of which upper scar is smaller and lower scar is elongate, and a row of four elongate adductor scars. Sexual dimorphism indistinct.

Type and Dimensions.—Holotype, sample no. T2-12, OCUCO 0015, adult LV, L = 0.482 mm, H = 0.313 mm (Figure 8.3); 3 paratypes, sample nos. T1-12, OCUCO 0016, T1-12, OCUCO 0017 and T2-12, OCUCO 0018.

Type locality.—Holocene sediments off Wakayama City (34° 14.5′ N, 135° 5.2′ E).

Occurrence.—T1-2, 5, 10, 12-14, T2-4 to T2-7, 8.1, 9, 10, 11-13, 13.1.

Remarks.—This species is similar to *Cytheropteron miurense*, but differs in having a thinner alar process and finer and larger amount of surface ornamentation.

Conclusions

1. Before ca. 7,000 cal yr BP, site T2 ranged from a bay coast to an outer bay, near a river mouth, at water depths of less than 15-20 m, and site T1 was a sandy coast, ranging from an outer bay to the open sea, near a river mouth, at water depths of more than 15-20 m, but shallower than biofacies LS.

2. From ca. 7,000-2,000 cal yr BP, the two sites varied in condition from an outer bay to the open sea at water depths of 30-40 m, where they were strongly influenced by the residual and/or tidal currents from the strait.

3. After ca. 2,000 cal yr BP, the two sites were situated along a sandy coast, ranging from an outer bay to the open sea, near a river mouth, at water depths of more than 15-20 m, but shallower than biofacies LS. Site T1 was shallower than site T2 during this period.

Acknowledgements

We would like to thank Kunihiro Ishizaki of Ishinomaki Senshu University for critical reading of the manuscript, and Hisao Kumai of Osaka City University for advice and continuous encouragement throughout the course of the present study. We also thank Hisao Ishii and Yoko Ishii of the Osaka Museum of Natural History for permission and assistance to access the drilling core samples, and Takamoto Okudaira of Osaka City University for providing permission to use and instruction in the operation of the scanning electron microscope (JEOL JSM-5500) in his laboratory. Anonymous reviewers improved the paper considerably.

← **Figure 8. 1-4**, *Cytheropteron kumaii* sp. nov. **1**. Lateral view of adult RV, T1-12, OCUCO 0016, L = 0.482 mm, H = 0.326 mm. **2a-c**. Internal view, muscle scar and hinge of adult RV, T1-12, OCUCO 0017, L = 0.530 mm, H = 0.349 mm. **3**. Lateral view of adult LV, holotype, T2-12, OCUCO 0015, L = 0.482 mm, H = 0.313 mm. **4a-c**. Internal view, muscle scars and hinge of adult LV, T2-8, OCUCO 0018, L = 0.474 mm, H = 0.299 mm. **5-8**. *Darwinula* sp. **5a-b**. Internal view and muscle scars of adult RV, T2-8, OCUCO 0001, L = 0.494 mm, H = 0.226 mm. **6**. Lateral view of adult RV, T2-4, OCUCO 0002, L = 0.487 mm, H = 0.227 mm. **7a-b**. Internal view and muscle scars of adult LV, T1-2, OCUCO 0003, L = 0.469 mm, H = 0.222 mm. **8**. Lateral view of adult LV, T2-4, OCUCO 0004, L = 0.462 mm, H = 0.226 mm. Scale bars are 0.1 mm: A for 1-2a, 3-4a, 5a, 6, 7a and 8; B for 2b and 4b; C for 2c and 4c; D for 5b and 7b.

References

Abe, K. and Choe, K. -L., 1988: Variation of *Pistocythereis* and *Keijella* species in Gamagyang Bay, south coast of Korea. *In*, Hanai, T., Ikeya, N. and Ishizaki, K. *eds.*, *Evolutionary Biology of Ostracoda, its Fundamentals and Applications*, p. 367-373. Kodansha, Tokyo and Elsevier, Amsterdam.

Bodergat, A. M. and Ikeya, N., 1988: Distribution of recent Ostracoda in Ise and Mikawa Bays, Pacific Coast of Central Japan. *In*, Hanai, T., Ikeya, N. and Ishizaki, K. *eds.*, *Evolutionary Biology of Ostracoda, its Fundamentals and Applications*, p. 413-428. Kodansha, Tokyo and Elsevier, Amsterdam.

Cronin, T. M., Kitamura, A., Ikeya, N., Watanabe, M. and Kamiya, T., 1994: Late Pliocene climatic change 3.4-2.3 Ma: paleoceanographic record from the Yabuta Formation, Sea of Japan. *Palaeogeography, Palaeoclimatology, Palaeoecology*, vol. 108, p. 437-455.

Frydl, P. M., 1982: Holocene ostracods in the southern Boso Peninsula. *In*, Hanai, T. *ed.*, *Studies on Japanese Ostracoda. University Museum, University of Tokyo, Bulletin*, vol. 20, p. 61-140, 257-267.

Fukusawa, H., 1995: Non-glacial varved lake sediment as a natural timekeeper and detector on environmental changes. *The Quaternary Research (Daiyonki-kenkyu)*, vol. 34, p. 135-149. *(in Japanese with English abstract)*

Horn, H. S., 1966: Measurement of "overlap" in comparative ecological studies. *American Naturalist*, vol. 100, p. 419-424.

Ikeya, N. and Compton, E. E.,1983: On *Trachyleberis scabrocuneata* (Brady). *In*, Bate, R. H. *et al. eds.*, *A Stereo-atlas of Ostracod Shells*, vol. 10, p. 119-126.

Ikeya, N. and Hanai, T., 1982: Ecology of recent ostracods in the Hamana-ko region, the Pacific coast of Japan. *In*, Hanai, T. *ed.*, *Studies on Japanese Ostracoda. University Museum, University of Tokyo, Bulletin*, vol. 20, p. 15-59, 257-272.

Ikeya, N., Hasegawa, H. and Kashima, T., 1987: Analysis of the fossil ostracodes: Holocene ostracode assemblages in Kawasaki city, Kanagawa prefecture. *In*, Matsushima, Y. *ed.*, *Research of the Alluvial Formation in Kawasaki City*, p. 51-64. *(in Japanese)*

Ikeya, N. and Itoh, H., 1991: Recent Ostracoda from the Sendai Bay region, Pacific coast of northeastern Japan. *Reports of Faculty of Science, Shizuoka University*, vol. 25, p. 93-145.

Ikeya, N. and Suzuki, C., 1992: Distributional patterns of modern ostracodes off Shimane Peninsula, southwestern Japan Sea. *Reports of Faculty of Science, Shizuoka University*, vol. 26, p. 91-137.

Ikeya, N., Wada, H, Akutsu, H. and Takahashi, M., 1990: Origin and sedimentary history of Hamanako Bay, Pacific coast of central Japan. *Memoirs of the Geological Society of Japan*, vol. 36, p. 129-150. *(in Japanese with English abstract)*

Irizuki, T., Fujiwara, O., Fuse, K. and Masuda, F., 1998a: Paleoenvironmental changes during the last post glacial period on the western coast of the Miura Peninsula, Kanagawa Prefecture, Central Japan: Fossil ostracode fauna and event deposits in bore hole cores. *Fossils (Palaeontological Society of Japan)*, vol. 64, p. 1-22. *(in Japanese with English abstract)*

Irizuki, T., Ishizaki, K., Takahashi, M. and Usami M.,1998b: Ostracode faunal changes after the mid-Neogene climatic optimum elucidated in the Middle Miocene Kobana Formation, Central Japan. *Paleontological Research*, vol. 2, p. 30-46.

Irizuki, T., Masuda, F., Miyahara, B., Hirotsu, A., Ueda, S. and Yoshikawa, S., 2001: Vertical changes of Holocene ostracodes in bore hole cores from off Kobe, related to the opening of straits and relative sea-level change in western Japan. *The Quaternary Research (Daiyonki-kenkyu)*, vol. 40, p. 105-120.

Ishizaki, K., 1968: Ostracodes from Uranouchi Bay, Kochi Prefecture, Japan. *Science Reports of the Tohoku University, 2nd Series (Geology)*, vol. 40, p. 1-45.

Ishizaki, K., 1969: Ostracodes from Shinjiko and Nakanoumi, Shimane Prefecture, western Honshu, Japan. *Science Reports of the Tohoku University, 2nd Series (Geology)*, vol. 41, p. 197-224.

Ishizaki, K., 1971: Ostracodes from Aomori Bay, Aomori Prefecture, northeast Honshu, Japan. *Science Reports of the Tohoku University, 2nd Series (Geology)*, vol. 43, p. 59-97.

Ishizaki, K.,1984: Detailed survey on ostracods in the drilling No. 56-9 core samples at the Kansai International Airport in Osaka Bay. *In*, Nakaseko, K. *ed.*, *Geological Survey of the Submarine Strata at the Kansai International Airport in Osaka Bay, Central Japan*, p. 37-43. The Calamity Science Institute. *(in Japanese)*

Ishizaki, K. and Irizuki, T., 1990: Distribution of bathyal ostracodes in sediments of Toyama Bay, Central Japan. *Courier Forschungsinstitut Senckenberg*, vol. 123, p. 53-67.

Ishizaki, K., Irizuki, T. and Sasaki O., 1993: Cobb Mountain spike of the Kuroshio Current detected by Ostracoda in the lower Omma Formation (Early Pleistocene), Kanazawa City, central Japan: analysis of depositional environments. *In*, McKenzie, M. G. and Jones, P. J. *eds.*, *Ostracoda in the Earth and Life Sciences*, p. 315-334. A. A. Balkema, Rotterdam.

Iwasaki, Y., 1992: Ostracod assemblages from the Holocene deposits of Kumamoto, Kyushu. *Kumamoto Journal of Science (Geology)*, vol. 12, p. 1-12. *(in Japanese with English abstract)*

Kajiyama, E., 1913: The Ostracoda of Misaki, Part 3. *Zoological Magazine (Dobutugaku-zasshi)*, vol. 25, p. 1-16. *(in Japanese)*

Kamiya, T. and Nakagawa, T., 1993: Ostracode fossil assemblages in the Holocene shell bed found in Takahama-Cho, Fukui Prefecture, Central Japan. *Monograph of the Fukui City Museum of Natural History*, vol. 1, p. 115-133. *(in Japanese with English abstract)*

Kamiya, T., Ozawa, H. and Obata, M., 2001: Quaternary and Recent marine Ostracoda in Hokuriku district, the Japan Sea coast. *In*, Ikeya, N. *ed.*, *Guidebook of Excursions, 14th International Symposium on Ostracoda*, p. 73-106.

Masuda, F. and Miyahara, B., 2000: Depositional facies and processes of the Holocene Marine Clay in the Osaka Bay Area, Japan. *The Quaternary Research (Daiyonki-kenkyu)*, vol. 39, p.349-355. *(in Japanese with English abstract)*

Masuda, F., Miyahara, B., Hirotsu, J., Irizuki, T., Iwabuchi, Y. and Yoshikawa, S., 2000: Temporal variation of Holocene Osaka Bay conditions estimated from a core in off-Kobe. *The Journal of the Geological Society of Japan*, vol. 106, p. 482-488. *(in Japanese with English abstract)*

Miyahara, B., Masuda, F., Irizuki, T., Fujiwara, O. and Yoshikawa, S., 1999: Holocene sea level curve and paleoenvironments reconstructed from a core in Osaka, Japan. *In*, Saito, Y., Ikehara, K. and Katayama, H. *eds.*, *Land-sea Link in Asia, Proceedings of Prof. Kenneth O. Emery Commemorative International Workshop, (International Workshop on Sediment Transport and Storage in Coastal Sea-Ocean System, Tsukuba, 1999)*, p. 415-420.

Nanayama, F., Tsukuda, E., Mizuno, K., Ishii, H., Kitada, N. and Takemura, K., 1999: Paleoseismological study of the

Tomogashima-suido fault, Median Tectonic Line active fault system, during the Holocene, at the eastern side of the Kitan Straits,central Japan. *Geological Survey of Japan Interim Report no. EQ/99/3 1999, Interim Report on Active Fault and Paleoearthquake Researches in the 1998 Fiscal Year, Geological Survey of Japan*, p. 235-252.

Okubo, I., 1979: Six species of Marine Ostracoda from the Inland sea of Seto. *Research Bulletin of Shujitsu Women's College and Okayama Shujitsu Junior College*, vol. 9, p. 143-157.

Ota, Y., Matsushima, Y., Miyoshi, M., Kashima, K., Maeda, Y. and Moriwaki, H., 1985: Holocene environmental changes in the Choshi Peninsula and its surroundings, Easternmost Kanto, Central Japan. *The Quaternary Research (Daiyonki-Kenkyu)*, vol. 24, p. 13-29. *(in Japanese with English abstract)*

Paik, K. -H. and Lee, E, -H.,1988: Plio-Pleistocene ostracods from the Sogwipo Formation, Cheju Island, Korea. *In*, Hanai, T., Ikeya, N. and Ishizaki, K. *eds., Evolutionary Biology of Ostracoda, its Fundamentals and Applications*, p. 541-556. Kodansha, Tokyo and Elsevier, Amsterdam.

Puri, H. S. and Hulings, N. C., 1976: Designation of lectotypes of some ostracods from the Challenger Expedition. *Bulletin of the British Museum (Natural History), Zoology*, vol. 29, p. 249-315.

Stuiver, M., Reimer, P., Bard, E., Beck, J. W., Burr, G. S., Hughen, K. A., Kromer, B., McCormac, G., van der Plincht, J. and Spurk, M.,1998: INTERCAL98 radiocarbon age calibration, 24,000-0 cal BP. *Radiocarbon*, vol. 40, p. 1041-1083.

Van Morkhoven, F. P. C. M., 1963: *Post-Paleozoic Ostracoda, their Morphology, Taxonomy and Economic Use, Volume 2, Generic Description*, 478 p. Elsevier, Amsterdam.

Yamane, K., 1998: Recent ostracode assemblages from Hiuchi-nada Bay, Seto Inland Sea of Japan. *Bulletin of the Ehime Prefectural Science Museum, Ehime Prefectural Science Museum*, vol. 3, p. 19-59. *(in Japanese with English abstract)*

Yasuhara, M. and Irizuki, T., 2001: Recent Ostracoda from north-eastern part of Osaka Bay, southwestern Japan. *Journal of Geosciences, Osaka City University*, vol. 44, p. 57-95.

Appendix. List of fossil Ostracoda recovered from cores T1 and T2.

sample number	T1-1	T1-2	T1-3	T1-4	T1-5	T1-6	T1-7	T1-8	T1-9	T1-10	T1-12	T1-13	T1-14	T1-15	T1-16	T1-17	T1-18	T1-20	T2-1	T2-2	T2-3	T2-4	T2-5	T2-6	T2-7	T2-8	T2-8.1	T2-9	T2-10	T2-10.2	T2-11	T2-12	T2-13	T2-13.1	T2-14	T2-14.1
species																																					
Ambocythere japonica																																				
Ambtonia obai																																				
Amphileberis nipponica																																				
Anchistrocheles yamaguchii																																				
Aurila corniculata																																				
Aurila disparata																																				
Aurila hataii s.l.	1	1	1	4	3	3	4	5	1		1													4												
Aurila munechikai	1	11	3	14	9	13	15	25	3			2				5	1					9	10	11	9	5	3	1	1	5	6	1	2	5	23	15	9
Aurila spinifera s.l.		1	1		33	4	22		1	5	5	5				2	1		1	1	1	7	2	1	3	1	1	5	1	1	1	2	4	2	14	9
Aurila tosaensis s.l.	2	1			1	2	2	4								1	1		1	5	1	2	1	1	1	1	1	1	1	1	1	1	1	1	1	1
Aurila sp. 1					1		1																													
Aurila sp. 2																																				
Aurila spp.						1																														
Australimoosera tomokoae	2	6	2	10	4	3	10	1	2	1	3	3	1	3	2	4	1		1	3	1	1	2	2	2	1	7	3	1	1	8	2	1	4	1	1
Bicornucythere bisanensis form A	6	2	4	5	9	2	1	5	2	2	3	3	3	2	3	1	4	1	7	2	9	4	3	3	1	2	1	1	1	1	2	1	1	1	1	1
Bicornucythere bisanensis form M	2	1	1	1	2	2	1	1	1	2	1	1	1	2	1	1	1	1	2	1	1	1	1	1	1	1	1	1	1	1	1	1	1	1	1	1
Bythoceratina hanaii					2																															
Bythoceratina sp. 1							1	4																												
Bythocythere ishizakii								2																												
Callistocythere alata	6	2	4	5	9	22	7	3	1	1	2	1	1	1			1																			
Callistocythere asiatica	2	1	2		2	3		1	2																											
Callistocythere hayamensis								2	1																											
Callistocythere hotaru						1		1	1																											
Callistocythere reticulata								1	1																											
Callistocythere undata				1	2																															
Callistocythere undulatifacialis																																				
Callistocythere sp. 1		2	4	5	9	22	7	3	1	1	2	1	1	1			1																			
Callistocythere sp. 2		1	3	4	2	3		1	2																											
Cletocythereis sp.							1																													
Coquimba ishizakii						1		2	1		1																									
Coquimba rugosa					1			1	1																											
Cornucoquimba tosaensis						1	1	1	1																											
Cythere omotenipponica	2	4	3	4	3	7	5	9	1	1		1	2			2		1																		
Cytherois nakanoumiensis		2						1	1																											
Cytherois uranouchiensis				1	4	13	2	5	1	4			4																							
Cytheromorpha acupunctata	3	1		2	3	1		1	1				2						3	1	1	1	1	1	1	3	2	1	1	1	1	1	1	1	4	1
Cytheropteron miurense										4	1	1								1	1	1	2	7	2	4	3	6	1	3	4	2	1	9	4	9
Cytheropteron uchioi											1	1										1	1	2		4	3	1	2	1	1	1				
Cytheropteron subuchioi																											1	2	1							
Cytheropteron kumaii		1			1					5	3											3	1	1	3	1	1	7	1	5	1	1				
Cytherura miii		1		2	3			2				4	2		1			1						1	1	1	1	3	1	1	1	1	1	1	1	1
Darwinula sp.		3		3	1			1					1																						
Falsobuntonia hayamii																																				
Hemicytherura cuneata	2			1	1	1																														
Hemicytherura kajiyamai	1			2	1	2																														
Hemicytherura tricarinata																																				
Ishizakiella miurensis		3		2		2																2	1	2	1	1	2	1	1	2	1	2	1	1	1	1
Kobayashiina donghaiensis	4																					4	1	1	1	2	1	1	1	2	2	2	2	5		
Krithe japonica												1	2									1	2	1	3	1	1	2	1	1	2	1	2	1	5	1
Loxoconcha epeterseni	2	1		2	3	7	3	7	1	1	1	1	2				1	1	2	1	1	2	2	1	3	1	4	1	4	1	1	1	1	1	1		
Loxoconcha harimensis																																				
Loxoconcha japonica	4	1	1	1	1	7		8	1	1	1	1	1			1	1	1	1	1	1	1	1	4	1	1	4	4	1	1	1	1	1	1		
Loxoconcha kattoi	1	1	1	1	1		1	3	1	1	1	1	1			1	1	1	1	1	1	1	1	1	1	1	1	1	1	1	1	1	1	1		
Loxoconcha optima	21	13	18	16	68	7	32	17	7	2	3	2	2	3		2	3	1	4	11	15	12	3	2	3	16	13	4	12	17	3	1	3	7		
Loxoconcha pulchra	3	15	3	2	7	43	17	8	3	3	3	2	1	3		16	9	2	1	9	2	3	2	8	22	18	17	15	9	18	20	5	1	2	3	6
Loxoconcha tosaensis	14	4	2	7	17	8	3	18	8	3	2	3	1	3		2	4	3	1	2	3	2	8	21	13	16	13	9	15	13	5	2	7	3	6	2

Appendix. Continued.

sample number / species	*Loxoconcha uranouchiensis*	*Loxoconcha viva*	*Loxoconcha* sp. 1	*Loxoconcha* sp. 2	*Loxoconcha* sp. 3	*Loxocrniculum mutsuense*	*Microcythere* sp.	*Munseyella japonica*	*Munseyella oborozukiyo*	*Munseyella* sp.	*Neonesidea oligodentata*	*Neopellucistoma inflatum*	*Nipponocythere bicarinata*	*Paracathaycythere costaereticulata*	*Paradoxostoma* sp.	*Parakrithella pseudadonta*	*Perissocytheridea japonica*	*Perissocytheridea* sp.	*Phlyctocythere japonica*	*Pistocythereis bradyformis*	*Pistocythereis bradyi*	*Pontocythere miurensis*	*Pontocythere* spp.	*Pontocythere* ? sp.	*Propontocypris* sp. 1	*Propontocypris* sp. 2	*Pseudoaurila japonica*	*Robustaurila ishizakii*	*Robustaurila kianohybridus*	*Robustaurila salebrosa*	*Schizocythere kishinouyei*	*Schizocythere* sp.	*Sclerochilus* sp.	*Semicytherura henryhowei*	*Semicytherura* sp. 1	*Semicytherura* sp. 2	*Spinileberis furuyaensis*	*Spinileberis pulchra*	*Spinileberis quadriaculeata*	*Stigmatocythere* sp.	*Trachyleberis scabrocuneata*	*Trachyleberis* cf. *scabrocuneata*	*Trachyleberis ishizakii*	*Trachyleberis* sp.	*Xestoleberis hanaii*	*Xestoleberis opalescenta*	*Xestoleberis* sp. 1	*Xestoleberis* sp. 2	gen. et sp. indet. 1	gen. et sp. indet. 2	Total number of specimens	Total number of species	Number of specimens per 10g
T1-1	2	5				1					4	1			1	10				4	4		11		1								1																		127	37	10.4
T1-2	3										7	3	2			9		2					27				1				3								6	5											154	36	12.3
T1-3											2	2				9							17								3																				80	19	7.6
T1-4	1		2								9	7				1				1	1	1	57							2	2	1																		261	40	37.1
T1-5		3				1	1				4	13	1										27				1																								228	44	68.9
T1-6	4	4	1								9	8	1			10					3		29					2		2	3	6																		299	47	37.6
T1-7	2	1				1					19	2				3	1				2		30						1	2	3	7																		279	38	98.4
T1-8	7	25			1						7	2	2			3					1	9	48						1	1	3	5																		343	61	87.3
T1-9	1	2				2				1	1					2						1	10								1																			43	20	5.4
T1-10		8									1		1			2							3						1	2																					64	24	8.0
T1-12		7																					1																											45	21	5.6
T1-13		14									2					1						2										1																		54	16	8.0
T1-14	1	7									2											2	1									1																		53	27	6.7
T1-15																							1																											5	4	2.2
T1-16																							1																											24	7	4.2
T1-17		2									4	1				1							9																											69	21	8.1
T1-18		1									2											1	3	2								1																		59	23	6.1
T1-20																																			1																6	6	1.7
T2-1		4									1		1			3						3	7								2																			60	22	6.9
T2-2		5									2	2				4					3		30					1				3																		133	32	14.6
T2-3		4									2	1				10					2		19									2																		112	36	13.1
T2-4		7	1				1				3		3								1	5	22	1					2	2																			192	43	21.0
T2-5	2	12				1					3	1									1	4	29						2	2																			214	44	74.2
T2-6	2	18	1								6		6			4						9	32						1	2	3	5	1																200	46	55.2
T2-7	3	21									3	2	4			2						9	23					1		2	2	7	1															186	41	69.5
T2-8	2	11						1			2	3	5			2						3	20						1	1	1	5																	176	48	71.8
T2-8.1	5	38								1	2	1	2			5						13	51							1	6	7																	321	52	75.8
T2-9		12						2				1	2			2						9	2																											84	20	8.4
T2-10		19														1						4	1	2																											123	29	24.2
T2-10.2		2																				2	2																											10	8	3.8
T2-11		18						1								1				1		2	1	6																											111	31	25.2
T2-12	1	29									1		1			1					1	7	1	2																											148	36	53.1
T2-13	2	30										1	3									6																													138	23	107.6
T2-13.1	5	21														1							4																											146	20	45.6
T2-14	10	4		1									3									3	17																											93	23	44.8
T2-14.1	16	7	2										5									6	27																											136	24	20.1

Paleontological Research, vol. 6, no. 1, pp. 101-120, April 30, 2002

Taphonomy of the bivalve assemblages in the upper part of the Paleogene Ashiya Group, southwestern Japan

NORIHIKO SAKAKURA

Department of Geology and Mineralogy, Kyoto University, Kyoto 606-8502, Japan
(E-mail: sakakura@kueps.kyoto-u.ac.jp)
Present address: Research Institute for Integrated Science, Kanagawa University, 2946 Tsuchiya, Hiratsuka, 259-1205, Japan

Received 18 August 2000; Revised manuscript accepted 30 November 2001

Abstract. **The Paleogene Ashiya Group, in which molluscan fossils are abundant (= Ashiya fauna), consists mainly of shallow marine deposits that exhibit sedimentary cycles especially in the Waita Formation (upper part of the Group). Each cycle is redefined as a thin transgressive basal sandstone (transgressive systems tract) overlain by a progradational coarsening-upward interval (highstand systems tract). The depositional environment varies from a shallower condition influenced by strong wave action (shoreface?) to a deeper condition below the storm wave base, which is followed by next shallower conditions such as lower shoreface or intertidal zone. Molluscan fossils occur only from the thin lower part of each cycle, namely the transgressive basal sandstone and from the mudstone of the earliest progradational phase. The fossils occur both as shell concentrations and more dispersed fossiliferous deposits. Bed-by-bed sampling based on taphonomic, sedimentologic and paleoecologic observations distinguishes four fossil assemblages, (a) *Glycymeris-Phacosoma*, (b) *Venericardia-Crassatella*, (c) *Venericardia* and (d) *Yoldia-Nucula*. These assemblages occur successively in each cycle, and their taphonomic features also change upward from a wave-generated allochthonous shellbed on the basal ravinement surface to autochthonous shell patches. The successive change accompanies a decreasing wave-influence during a transgressive period. Epibionts, such as epifaunal byssally attached bivalves and barnacles, occur abundantly as associated species of the *Venericardia-Crassatella* assemblage from the middle part of the transgressive basal sandstone. Epibiontic colonization probably reflects taphonomic feedback, with shelly substrates avoiding burial by the winnowing of sediments during transgression. Autochthonous shellbeds dominated by *Venericardia subnipponica* are intercalated in the glauconitic sandstone beds (surface of maximum transgression) at the top of the transgressive basal sandstone. The shellbeds probably represent an attritional accumulation with dead shells of *Venericardia* supplied continuously *in situ* during a phase of low sediment supply.**

Key words: **Ashiya Group, bivalves, paleoecology, Paleogene, sedimentary cycle, transgression**

Introduction

The Ashiya Group is the uppermost sequence of coal-bearing Paleogene deposits in the northern limb of Kyushu. It consists of shallow marine sandstones and mudstones, and is biostratigraphically assigned to the latest Early Oligocene age by calcareous nannoplankton and foraminifera (Saito and Okada, 1984; Tsuchi *et al.*, 1987). It was lithostratigraphically subdivided into the Yamaga, Sakamizu, and Waita Formations in upward sequence (Nagao, 1927a, 1928a; Okabe and Ohara, 1972 etc.). Recently the stratigraphic division was revised by Ozaki *et al.* (1993), in which the Yamaga, Norimatsu, Jinnobaru, Honjo and Waita Formations were redefined. Hayasaka (1991) investigated the group sedimentologically, distinguished 23 coarsening-upward sedimentary cycles, and gave their environmental interpretations.

Abundant molluscan fossils from the Group are called the Ashiya Fauna and represent the typical molluscan fauna of Oligocene age in west Japan (Nagao, 1927a, 1928a; Otsuka, 1939; Oyama *et al.*, 1960 etc.). The molluscan fossils have been taxonomically and biostratigraphically studied by several authors (Nagao, 1927b, 1928b; Mizuno, 1963 etc.). In addition, the molluscan fauna from the Jinnobaru Formation was studied paleoecologically (Shuto and Shiraishi, 1971).

However, little is known about the precise relation between sedimentary cycles and the molluscan assemblages, which exhibit characteristic modes of occurrence by facies. Taphonomic features of the molluscan assemblages also re-

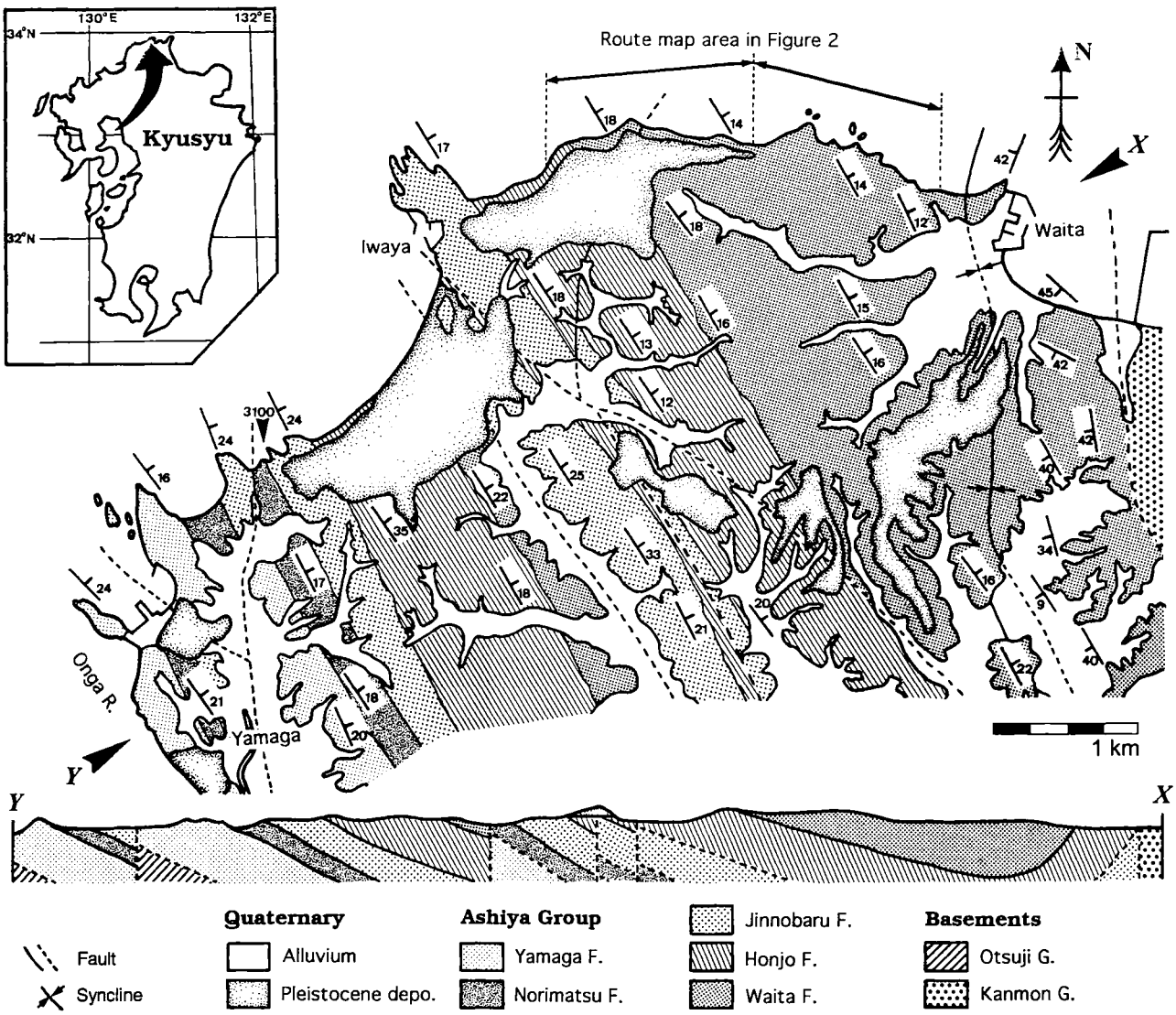

Figure 1. Geologic map of the Wakamatsu area, Kitakyushu, northern Kyushu. Route-mapped area in Figure 2 indicated by thick arrows and Locality 3100 are shown.

main largely to be investigated.

To clarify these problems, I closely examined the sedimentary features and modes of fossil occurrence of the Ashiya Group bed-by-bed. Through detailed observations, particularly in the Waita Formation (the upper part of the Group), I discovered a close relationship between the sedimentary cycle and the composition and mode of occurrence of bivalve assemblages. These changes are commonly repeated in every cycle of the Waita Formation.

This paper aims to reconstruct the sedimentological and paleoecological processes in the Ashiya Group based on detailed observations of its sedimentological and taphonomic features. My aims here are to: (1) redefine the sedimentary cycles in the Waita Formation and describe its lithofacies, (2) describe modes of occurrence and the succession of the molluscan assemblages in the cycle, and (3) discuss the formative process of the sedimentary and paleoecological succession.

Geological setting

The Ashiya Group in the study area is bounded on the east by a fault of NNW-SSE trend, and on the west by the Onga River. The strata of the group strike N 20–45° W and dip 10–30° gently northeastward except for those in the eastern limb of the syncline (Figure 1). In the eastern limb, the strata steeply strike N 10–50° W and dip 45° W. At least seven faults of similar NW-SE trend are observed

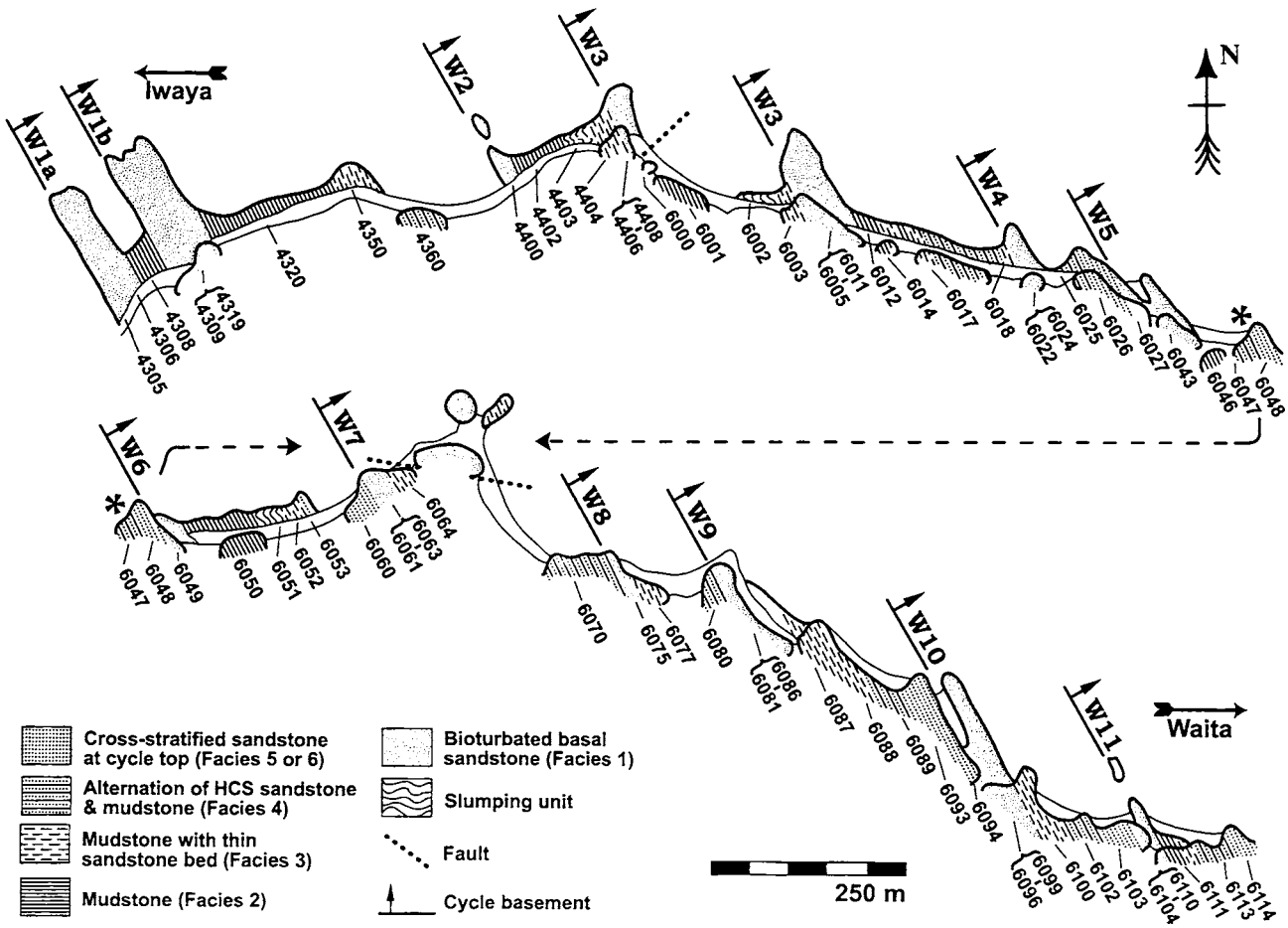

Figure 2. Route map from the Iwaya to Waita coast (Figure 1). The left section connected to the right at the asterisks (*). Localities and redefined sedimentary cycles are shown.

or estimated.

The Ashiya Group is subdivided into the Yamaga, Norimatsu, Jinnobaru, Honjo and Waita Formations in ascending order (Ozaki *et al.*, 1993). The lowermost Yamaga Formation is characterized by bioturbated fine sandstones. The formation is more than 170 m thick, although the basal part is unexposed. The succeeding Norimatsu Formation consists of the alternating sandstone and mudstone, and is 50–70 m thick. Both formations crop out in the western part of the study area (Figure 1).

The Jinnobaru Formation consists of sandstones in which hummocky cross-stratification is occasionally observed, and is 140–260 m thick. The Honjo Formation consists of sandstones and mudstones, exhibits sedimentary cycles, and is about 230 m thick. Both formations crop out in the central part of the area from north to south (Figure 1).

The Waita Formation (uppermost of the Group) exhibits clear sedimentary cycles composed of sandstones and mudstones (Figure 2). It is widely distributed in the eastern part of the area, and is more than 450 m thick, although the top part is unexposed (Figure 1).

Sedimentary cycles

The upper part of the Ashiya Group (Honjo and Waita Formations) consists of coarsening-upward sedimentary cycles (Hayasaka, 1991; Ozaki *et al.*, 1993). Each cycle is 30–100 m thick (Figure 3), and consists of various sandstones and mudstones. At least 11 sedimentary cycles, named W1–W11 in ascending order, are recognized in the Waita Formation (Hayasaka, 1991; Ozaki *et al.*, 1993). Previous studies defined the sedimentary cycles as coarsening-upward lithologic change, which begins with a mudstone interval and ends with a sandstone interval (Hayasaka, 1991, p. 617, fig. 5; Figure 3).

However, close examination indicates that the definition of the cycles must be revised. Specifically, there is a sharp erosional surface within the upper sandstone interval of

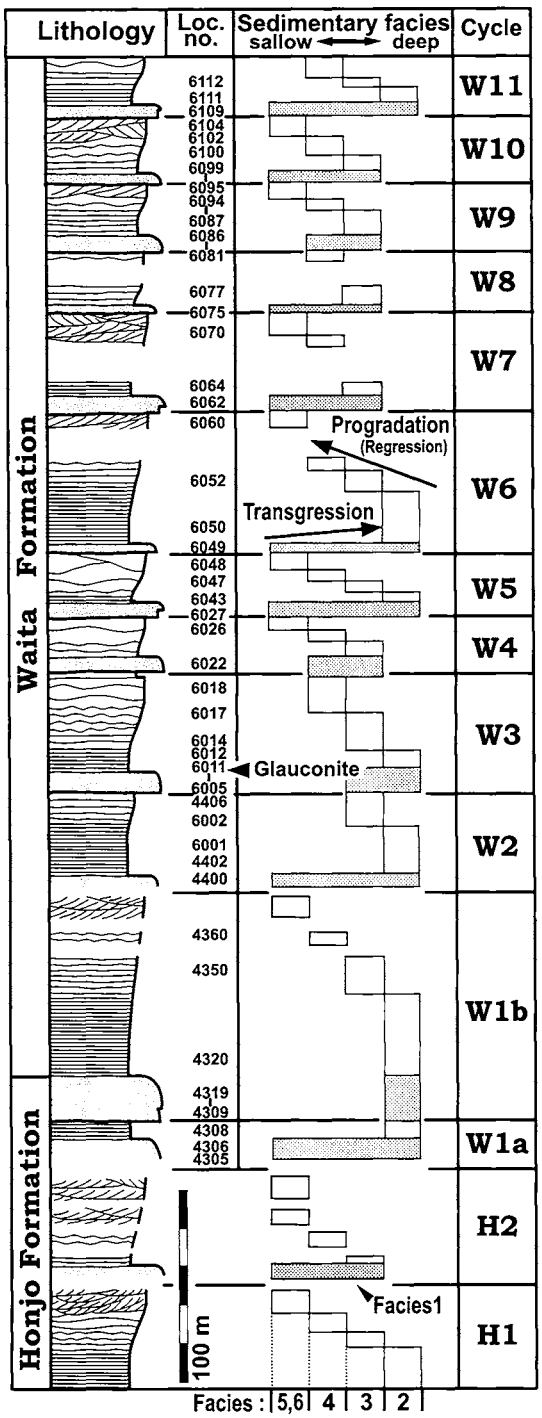

each previous "cycle" (Figure 4A). This surface marks a distinct depositional boundary between the stratified sandstone and the mottled sandstone (Figure 3), whereas the transition from the burrowed sandstone to the overlying mudstone is continuous and gradational, as well as from the mudstone to the stratified sandstone. Therefore, it is much better to define the erosional surface as the base of each cycle. I use the names of W1-W11 to denote cycles defined in this way.

Following this revision, each cycle consists of a transgressive basal sandstone (Facies 1), which fines usually from medium sandstone upward to very fine sandstone, and the overlying progradational coarsening-upward interval (Facies 2-6; Figures 4B and 5). The latter is lithologically subdivided into five sedimentary facies: mudstone (Facies 2), mudstone interbedded with very thin sandstone beds (Facies 3), alternated HCS (hummocky cross-stratification) sandstone and mudstone (Facies 4), amalgamated HCS sandstone (Facies 5), and tabular cross-stratified sandstone (Facies 6; Figure 5). As examples, successions of the cycle W3 and W10 are shown in Figure 5.

Transgressive basal sandstone (Facies 1)

The transgressive basal sandstone (Facies 1) rests on a distinctive erosional surface truncating the upper part of the underlying cycle (Figures 3, 5), and fine upward from medium sandstone to very fine sandstone (Figure 5). This basal sandstone facies is conformably capped with mudstone of the Facies (2) or (3) (Figures 3, 5). The thickness of the basal sandstone attains 5-20 m, and is thin compared with the overlying coarsening-upward interval in each sedimentary cycle (30-100 m).

The basal sandstone is gray to greenish gray in color and includes lithic granules, grains of green smectite, and pum-

Figure 3. Columnar section of the Waita Formation exposed along the Iwaya to Waita coast. At least 11 sedimentary cycles, W1-W11 in ascending order, are recognized in the Waita Formation. Facies 1-6 indicate sedimentary facies in a cycle: transgressive basal sandstone (Facies 1), mudstone (Facies 2), mudstone interbedded with very thin sandstone beds (Facies 3), alternation of HCS sandstone and mudstone (Facies 4), amalgamated HCS sandstone (Facies 5), and tabular cross-stratified sandstone (Facies 6) in order. Glauconite sandstone bed is intercalated at the top of the transgressive basal sandstone of the Cycle 3. Facies 2-4 compose the progradational coarsening-upward interval.

➡ **Figure 4.** Lithofacies of the cycles in the Waita Formation. **A.** Erosional basement of the sedimentary Cycle W3, Loc.6005 A shellbed showing a wave dune covers the erosional surface. Hammer is 30 cm long. **B.** Up-coarsening interval (Facies 2-5) in Sedimentary Cycle W5, Loc. 6047. The cliff is 15 m in height. **C.** Vertical profile of the basal sandstone (Facies 1) bioturbated by *Thalassinoides* ichnosp, Loc. 6006. (Natural size.) **D.** Vertical profile of the basal sandstone. Light-colored grains are pumice, dark-colored grains green smectite. Loc. 6098a. (Natural size) **E.** Photomicrograph of top part of basal sandstone (Facies 1), Loc. 6011a. Glauconite grains, gray in the photograph, are abundant. Scale is 0.5 mm long. **F.** *Phycosiphon* ichnosp. in vertical profile of the mudstone with thin sheet sandstone (Facies 3), Loc. 6017. (Natural size.) **G.** *Planolites* ichnosp. in vertical profile of alternation of HCS sandstone and mudstone (Facies 4), Loc. 6102. (Natural size) **H.** Amalgamated HCS sandstone (Facies 5), Loc. 6026. Hammer is 30 cm long.

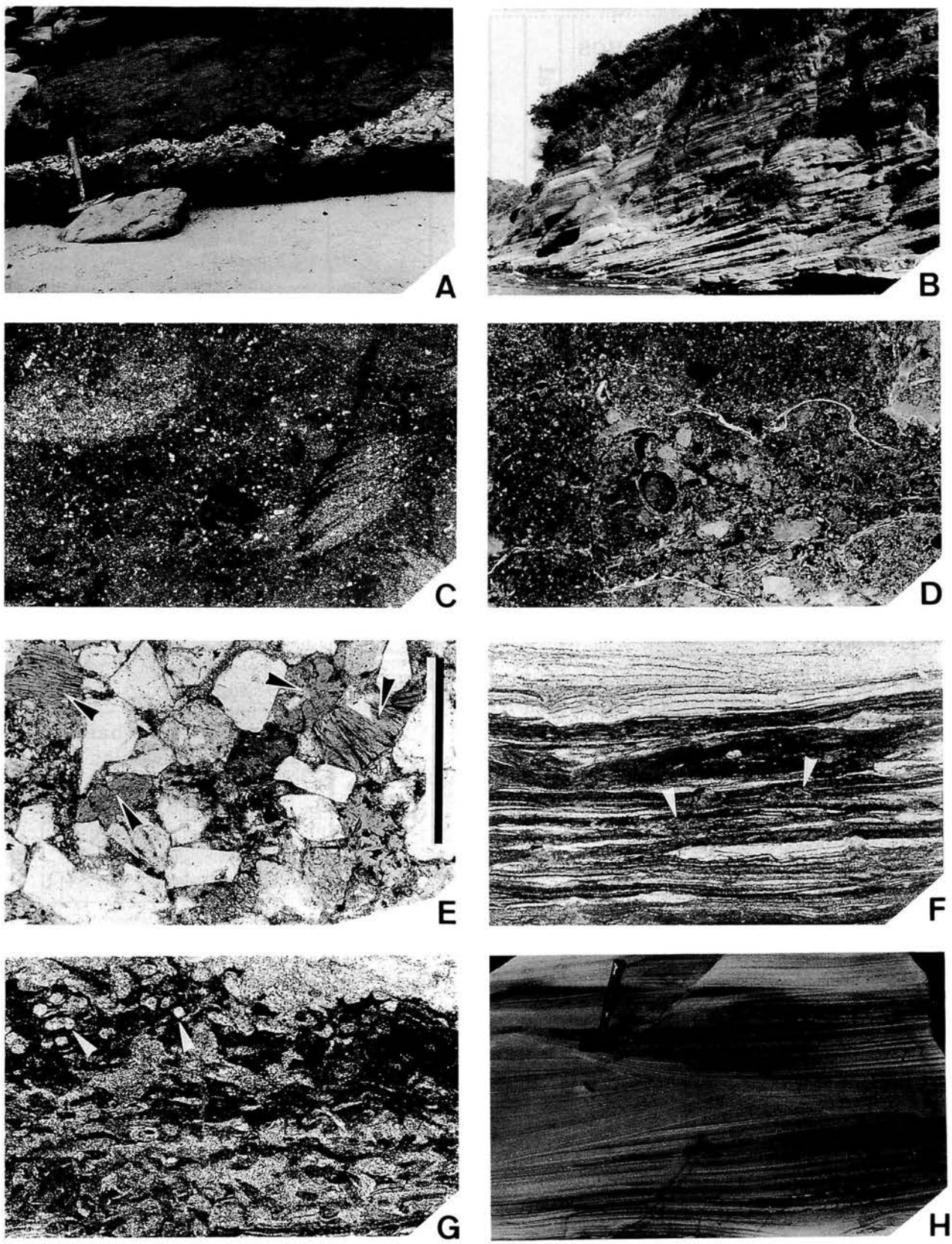
A
B
C
D
E
F
G
H

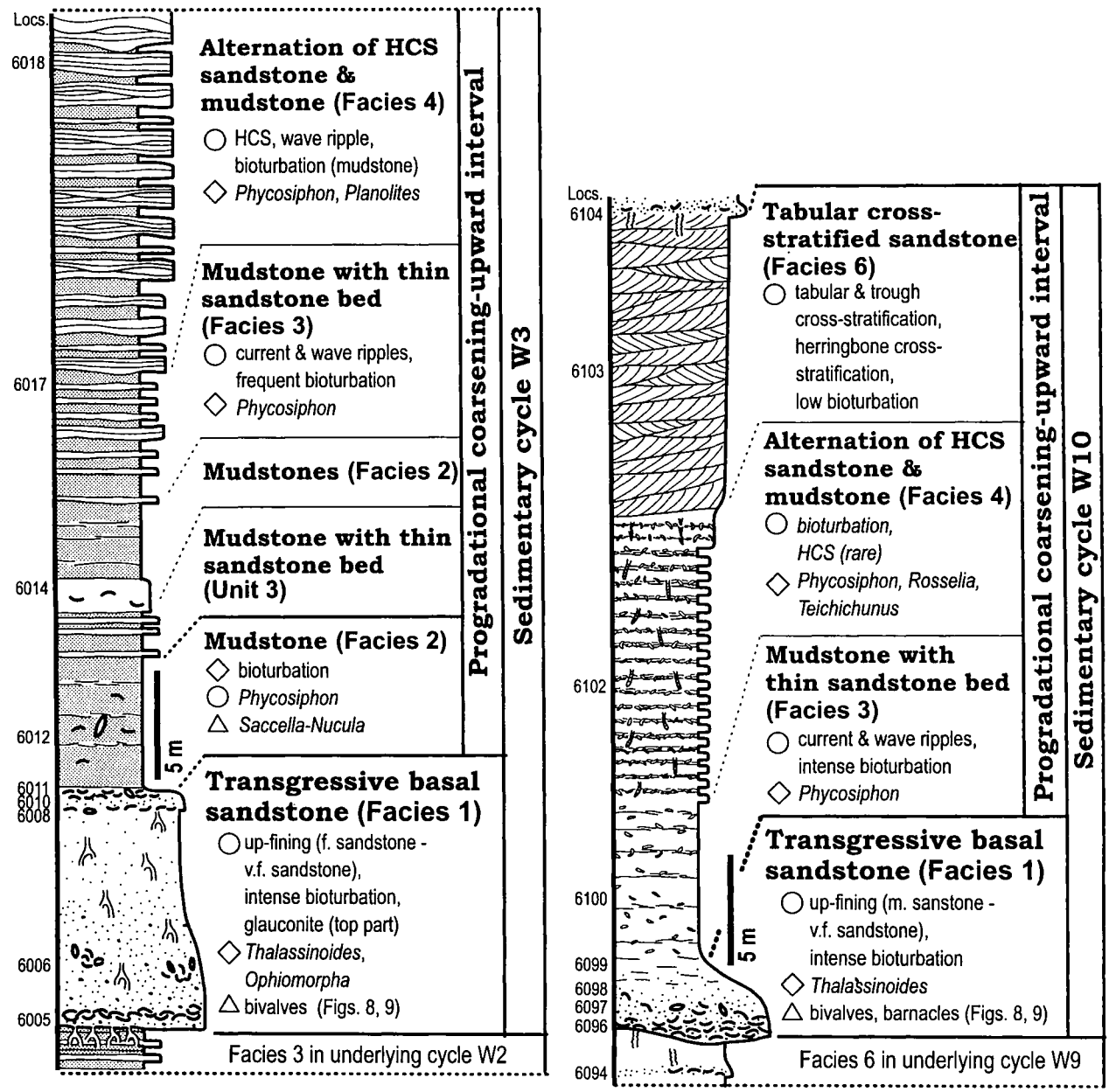

Figure 5. Sedimentary cycles and the lithological facies in the Waita Formation. Each cycle is subdivided into the basal sandstone (Facies 1) and the up-coarsening interval (Facies 2–5 or 6).

➡ **Figure 6.** Modes of fossil occurrence. **A.** Bidirectional imbrications (arrows) of shell fragments of the *Glycymeris-Phacosoma* Assemblage (a) in the basal sandstone (Facies 1) of cycle W3, at Loc. 6005. This sedimentary structure is characteristic of a wave dune.Sscale bar is 2 cm long. **B.** Epifaunal bivalves, *Chlamys* sp. and barnacles of *Venericardia-Crassatella* Assemblage (b2) in the basal sandstone (Facies 1) of cycle W11, at Loc. 6109. Barnacles attach to shell surface. Lens cap is 5.5 cm in diameter. **C.** Matrix of the host sediment of the *Venericardia-Crassatella* Assemblage with abundant epifauna (b2; same as in figure 6B). The shell fragments are concentrated and imbricated in the vertical profile. (X 0.9). **D.** Articulated shells showing geopetal of the *Venericardia-Crassatella* Assemblage (b2; same as in figure 6B). Scale bar is 2 cm long. **E.** Shell replaced by clay minerals of the *Venericardia-Crassatella* Assemblage (b2) in the basal sandstone (Facies 1) of cycle W10, at Loc. 6098a. Scale bar is 1mm long. **F.** Horizontal view of shell clumps (*Venericardia subnipponica*) of the *Venericardia* Assemblage in the middle part of the basal sandstone of cycle W3, at Loc. 4407. Articulated shells are observed. Lens cap is 5.5 cm in diameter. **G.** Profile of the matrix deposits of the *Yoldia-Nucula* Assemblage (d) in the mudstone of the cycle W2, at Loc. 6001a. (Natural size.) **H.** Apices-oriented shells on minor erosional surface of the *Yoldia-Nucula* Assemblage (d; same as in figure 6G). Lens cap is 5.5 cm in diameter. Loc. 6001a.

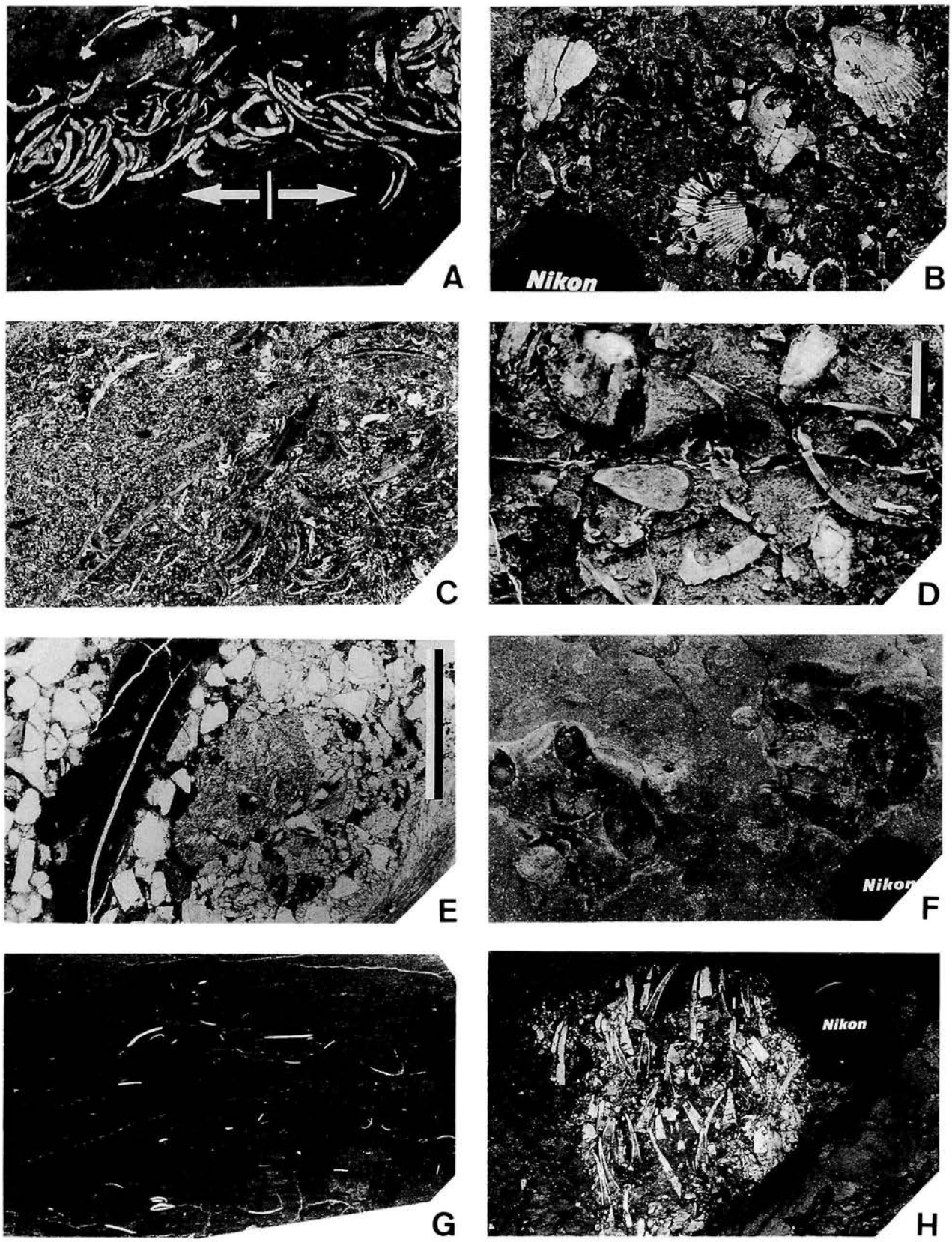
A
Nikon
B
C
D
E
F
G
Nikon
H

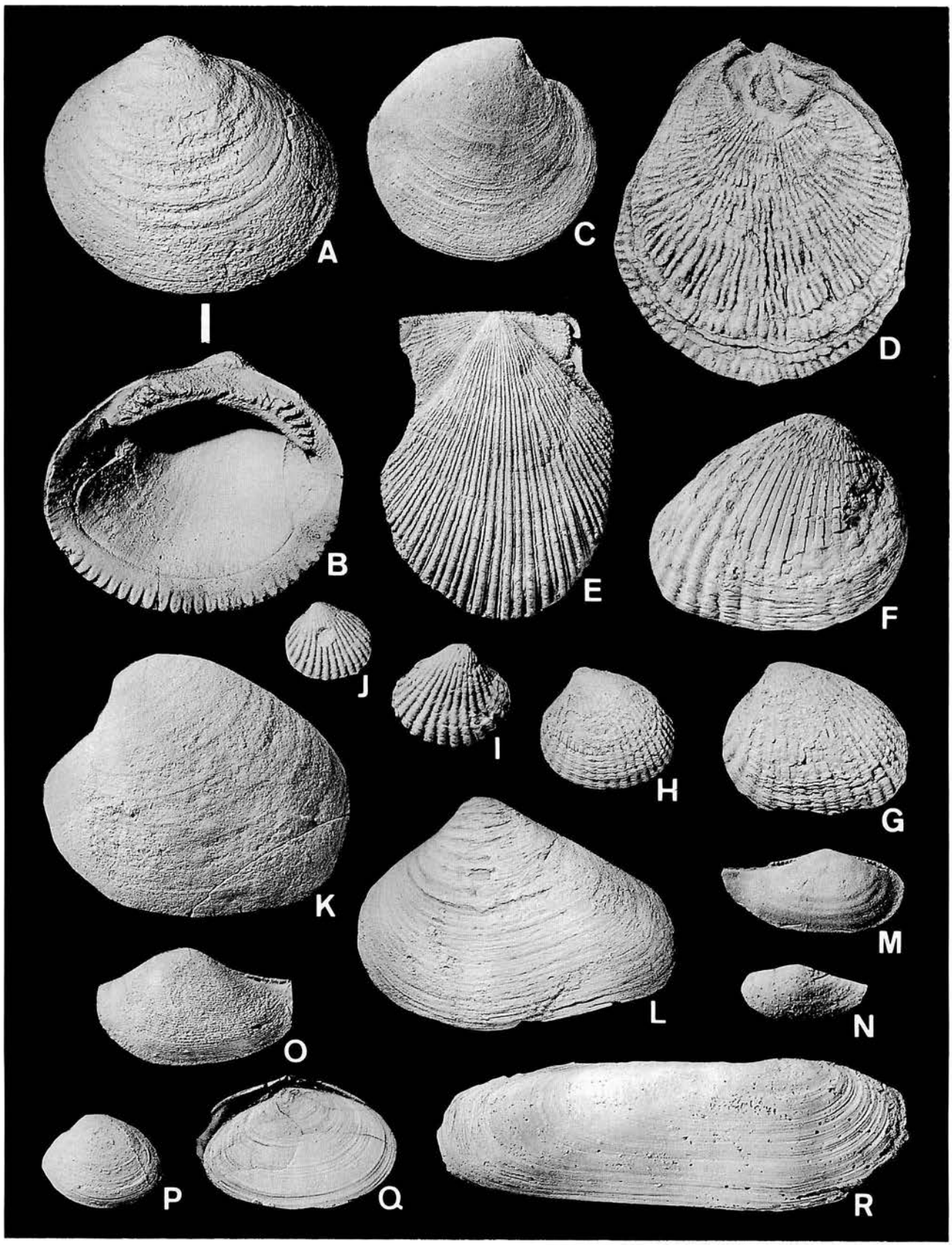
A
C
D
B
E
F
J
I
H
G
K
L
M
O
N
P
Q
R

ice (Locs. 6006, 6082, 6098a; Figure 4D). In cycle W3, many glauconite grains occur, especially from the top part of the transgressive basal sandstone just below the mudstone of Facies (2) (Figures 4E, 5). The basal sandstone is mottled and intensely bioturbated; *Thalassinoides* and *Ophiomorpha* burrows are abundant (Figure 4C). The basal erosional surface is burrowed occasionally by these ichnospecies (Loc. 6005).

In addition to the basal surface, several minor erosional surfaces are recognized, usually within the lower part of the sandstone. These erosional surfaces undulate with relief of up to 30 cm, and are usually overlain by allochthonous shellbeds or pumice layers (Figures 4A, 5). The basal shellbed locally forms small shell mounds on the wavy erosional surface. These shells show bidirectional imbrications (Loc.6005; Figure 6A). Such sedimentary structure characterizes a wave dune (Cheel and Leckie, 1992). Articulated bivalve shells are dispersed as patches in the upper part of the basal sandstone (Figures 5, 6F), in contrast to the allochthonous shellbeds in the lower part of the facies.

Molluscan fossils are abundant (Figure 7). Assemblages of (a) *Glycymeris-Phacosoma*, (b) *Venericardia-Crassatella*, and (c) *Venericardia* occur from this facies (Figure 8; described later).

Progradational coarsening-upward interval (Facies 2–6)

Two types of progradational coarsening-upward intervals are recognized in the Honjo and Waita Formations. The first type is composed of mudstone (Facies 2), mudstone interbedded with very thin sandstone beds (Facies 3), alternated HCS sandstone and mudstone (Facies 4), and amalgamated HCS sandstone (Facies 5) in ascending order. Another type of the coarsening-upward intervals is also composed of the Facies (2–4) capped by tabular cross-stratified sandstone (Facies 6). That is, Facies (6) replaces Facies (5) in the uppermost part of the interval. Facies (5) and (6) do not coexist within a single cycle.

Mudstones (*Facies 2*).—This facies conformably covers the basal sandstone (Facies 1), and characterizes the lowermost part of the progradational coarsening-upward interval (e.g., Cycle W3; Figure 5). It consists of dark gray laminated or bioturbated mudstone 5–40 m thick. Very fine sandstone beds (less than 5 cm thick) are occasionally intercalated in the mudstone (Locs. 4402, 6001a, 6050). *Yoldia-Nucula* Assemblage (Figure 8; described later) and *Phycosiphon* ichnosp. are abundant in the bioturbated parts (Figure 6G).

Mudstone interbedded with very thin sandstone beds (*Facies 3*).—This facies changes transitionally from the underlying mudstone (Facies 2) (Loc. 6012 etc.), or directly covers the basal sandstone (Facies 1) (Locs. 6012 and 6100). It attains 3–10 m thickness (Locs. 4404, 6003, 6052 etc.), and is characterized by mudstone interbedded with very thin sandstone bed of less than 15 cm thickness. The sheet sandstone is very fine, and shows parallel, current and wave ripple laminations.

Primary sedimentary structures are sometimes disturbed by *Phycosiphon* ichnosp. (Figure 4F). The intensely bioturbated part which directly covers the basal sandstone yields various types of ichnofossils (*Planolites*, *Paleophycus*, *Rosselia*, *Skolithos* etc.; Locs. 6088, 6100), and molluscan fossils such as *Acila ashiyaensis* and *Dentalium* sp. etc. (Figure 8).

Alternation of HCS sandstone and mudstone (*Facies 4*).—This facies overlies Facies 3, and is capped with the Facies (5) or (6). It is 3–20 m thick and consists of alternations of sandstone and mudstone (Locs. 6017, 6047, 6101 etc.). The sandstone beds are 15–150 cm thick and tend to thicken upward, and each bed has a slight erosional base. Hummocky cross stratification, parallel lamination and wave ripples are well observed in the sandstone without remarkable signs of bioturbation. In contrast, the interbedded mudstone is commonly bioturbated by *Phycosiphon* ichnosp. (e.g., Cycle W3 at Loc. 6017). In Cycles W9 and W10, both sandstone and mudstone are exceptionally intensely bioturbated by *Phycosiphon* and *Planolites* ichnospp. (Locs. 6089, 6102: Figure 4G), and also yield *Teichichnus* and *Rosselia* ichnospp. *Rosselia* burrows show the upward removal trails to escape from rapid burial (Nara, 1997).

Amalgamated HCS sandstone (*Facies 5*).—This facies consists of amalgamated HCS sandstone, 10 m thick, at the top part of the cycle (Locs. 6026, 6048; Figure 4H). The sandstone is clean, well-sorted and very fine-grained. Primary sedimentary structures, such as hummocky cross-stratification, are well preserved. Mudstone and wave rippled sandstone beds, 20 cm thick, are rarely intercalated in the sandstone. The top of this facies yields many *Ophiomorpha* burrows (Loc. 6027).

Tabular cross-stratified sandstone (*Facies 6*).—Some cycles have tabular cross-stratified sandstone (6) at the top,

← **Figure 7.** Bivalve fossils from the Waita Formation (D, R X0.9; I, M, 0, Q X2; N X2.5; J, P X3; others X1). **A, B.** *Glycymeris cisshuensis* Makiyama, Cycle W5 at loc. 6043. **C.** *Phacosoma chikuzenensis* Nagao, Cycle W9 at loc. 6083. **D.** *Monia* sp. Cycle W3 at loc. 6008. **E:** *Chlamys* sp. Cycle W10 at loc. 6098a. **F–J.** *Venericardia subnipponica* Nagao, F, G, H; Cycle W1 at loc. 4309. I, J; Cycle W2 at loc. 6001a. **K.** *Pitar matsumotoi* (Nagao), Cycle W10 at loc. 6083. **L.** *Crassatella yabei* (Nagao), Cycle W5 at loc. 6043. **M, N.** *Yoldia* sp., Cycle W2 at loc. 6001a. **O.** *Saccella* sp., Jinnobaru F. at loc. 3100. **P.** *Nucula* sp., Cycle W2 at loc. 6001a. **Q.** *Angulus maximus* (Nagao), Cycle W2 at loc. 6001a. **R.** *Cultellus izumoensis* (Yokoyama), Jinnobaru F. at loc. 3100. All specimens in this figure are housed in the Kyoto University Museum.

Sedimentary cycle	Locality. no.	Bivalvia																							Gastropoda						others				
		Glycymeris cisshuensis	*Phacosoma chikuzenensis*	*Pitar matsumotoi*	*Meretrix* sp.	*Spisula* sp.	*Crassostrea* sp.	*Crassatella yabei*	*Venericardia subnipponica*	*Chlamys* sp.	*Monia* sp.	*Arca sakamizuensis*	*Clinocardium* sp.	*Felaniella* sp.	*Lucinoma nagaoi*	*Cultellus izumoensis*	*Solamen subformicatum*	*Periplomya* sp.	*Angulus maximus*	*Saccella* sp.	*Yoldia* sp.	*Acila ashiyaensis*	*Nucula* sp.	"*Diloma*" sp.	*Phyllonoyus ashiyaensis*	*Euspira ashiyaensis*	*Turritella infralirata*	*Turritella karatsuensis*	*Fulgoraria* sp.	*Dentalium* sp.	barnacles	Spatangoida	*Echinodiscus ashiyaensis*	calcareous tube of Serpulid warm
W11	6109	12	5	4				25 (4)	2	27	29													5	2						15		2	2
W10	6098 a		5					33 (6)	37 (12)	31 (2)	8 (4)	2 (2)													4	4			2	2	15			
	6097		14 (2)	16				8	17																									
	6096	58	34					3	7	6																								
W9	6094			5																										6				
	6087																		2 (2)			36 (10)								6				
	6086								53 (8)							14 (8)				42 (2)	4	1	6											
	6083		54	12					26 (4)																					5				
	6082		25 (4)	18 (4)				27	11 (4)																									
W7	6062	10	12	2				8	23																									
W6	6049			5 (2)																														
W5	6043	72	12	2				14																		10								
	6027	6	26	15	1	4																			4									
W4	6022						15																											
W3	6014															10 (8)			10 (4)										12					
	6012															14 (8)			2 (2)		5		8						8					
	6011 a								98 (8)								9 (4)	4 (4)	7	10														
	6010 a		27 (4)	21 (8)				12 (4)	102 (8)	2	3		5	8						5							3							
	6008	3	9 (4)	15 (6)					73 (58)	1	9 (4)															3	6							
	6006								72 (52)																									
	6005	36	33																															
W2	6001 a								4 (2)						4 (2)	23 (22)			16 (10)		35 (8)	1	14			6		4		18				
W3	4407								87 (18)																									
	4406	36	55																															
W2	4402								3							8 (8)			20 (12)		12 (4)	2	8				4		10					
W1b	4217								57 (4)						4 (4)												20		30					
	4315														10											2	34		90					
	4312			1					48 (20)																									
	4310 a								27 (12)						2 (2)	98 (80)										8	50		18	4	1			
	4309								77 (60)							2 (2)				6						2			2					
W1a	4308 a								14 (2)						1						42 (8)													
	4306																				5													

Figure 8. Fossil list in the Waita Formation (route map area). Numbers of articulated bivalve shells is parenthesized.

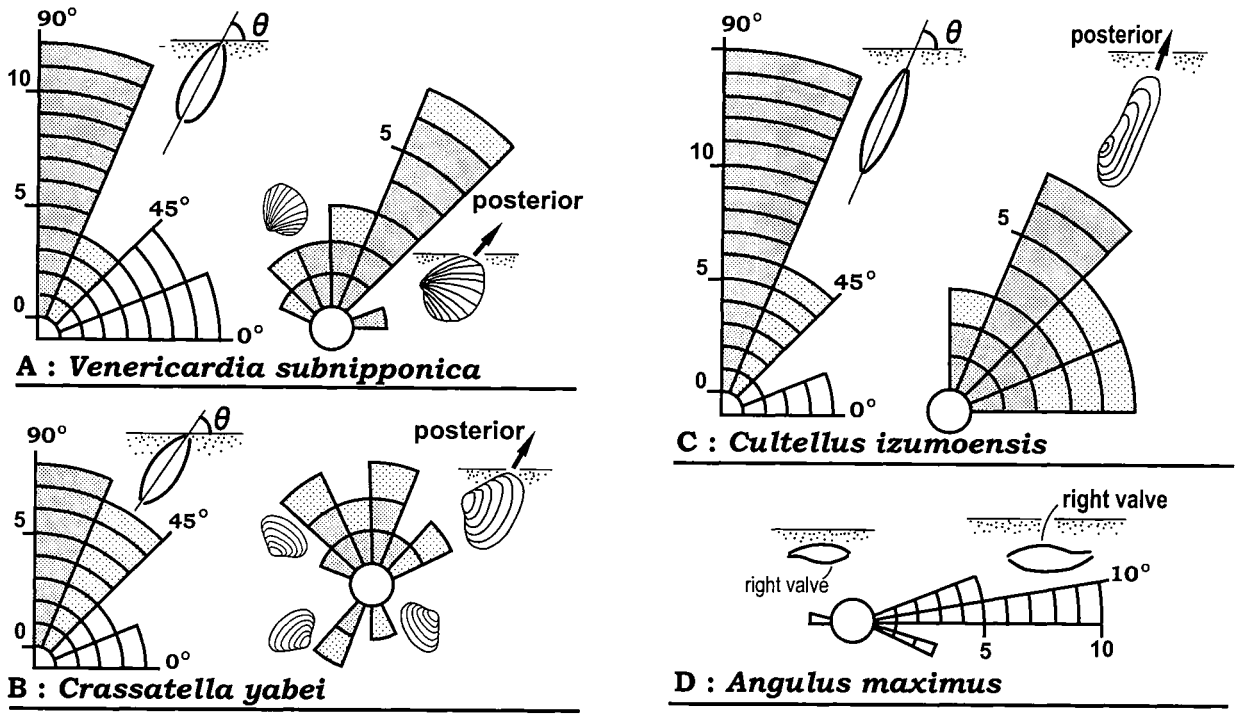

Figure 9. Diagrams showing orientation of articulated bivalve shells in outcrop. **A.** *Venericardia subnipponica* at Loc. 6097, **B.** *Crassatella yabei* at Loc. 6097, **C.** *Cultellus izumoensis* at Loc. 6001a, **D.** *Angulus maximus* (tellinine bivalve) at Loc. 6001a. Left diagrams in A-C show total modes of lateral inclination of commissure planes. Lateral inclinations MORE THAN 45° are stippled by dark or light. Right diagrams in A-C show posteriorwardl direction of selected specimens maintaining their standing positions in the left diagrams (lateral inclinations more than 45° are stippled samples of left diagrams). These articulated shells mainly are elevated in the posterior direction of shell length at angles of about 60°. Darkly or lightly stippled blocks correspond to those areas in left diagrams. D indicates dips of commissure planes and upper valve either left or right. Most articulated *Angulus maximus* lie keeping their right valve up.

instead of Facies (5). Facies (6) consists of tabular and trough cross-stratified fine sandstone 10 - 15 m thick. Single sets of tabular and trough cross-stratified beds range from 20 to 40 cm thick. Herringbone cross-bedding, tidal-bundle sequences and reactivation surfaces are well observed in the facies (Locs. 6060, 6092, 6102; Sakakura and Masuda, 2001). Lenticular and flaser bedding, 20-30cm thick, is rarely intercalated in the tabular and trough cross-stratified sandstone (Loc. 6070). As in Facies (5), the top of this facies yields many *Ophiomorpha* burrows (Locs. 6094, 6104).

Interpretation of sedimentary environments

Sedimentary environments of transgressive basal sandstone (Facies 1)

The transgressive basal sandstone can be interpreted as the deposits of relative sea level rises during transgression, because signs of wave influence clearly decrease upward. At the base of the basal sandstone (Facies 1), the wave dune is observed on the erosional surface. Such wave dunes strongly suggest deposition under the intense influence of waves in shallow environments (Cheel and Leckie, 1992). No sedimentary structures formed by waves are observed in the upper part of the basal sandstone. Therefore, the upper part of this facies is interpreted to having been deposited below the storm wave base. The view is supported by the fining-upward features of these deposits and the bivalve assemblages whose contents and modes of occurrence differ clearly between the lower and upper parts (discussed later).

Sedimentary environments of coarsening-upward intervals (Facies 2-6)

Progradation of wave-dominated shoreline (Facies 2-5).—The progradational coarsening-upward intervals composed of Facies (2-5) shows wave-influenced sedimentary structures such as wave ripples and hummocky cross-stratification increasing upward.

Facies (2) is the lowermost part of this coarsening-upward interval, and shows no signs of wave-influenced sedimentary structures. It gradually changes upward into

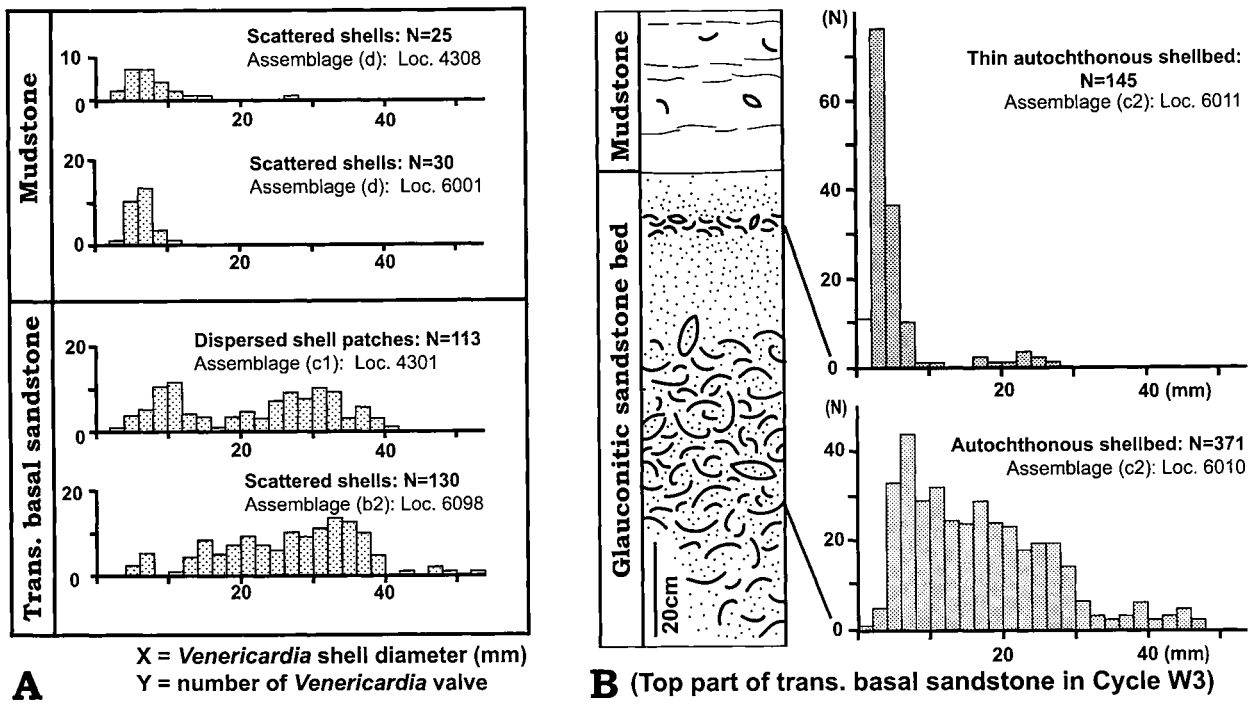

Figure 10. A. Size distribution patterns of *Venericardia subnipponica* shells that occur as scattered shells or dispersed shell patches from the basal sandstone (Facies 1) and mudstone (Facies 2). In the basal sandstone, *Venericardia* shells vary in size from less than 10 mm diameter to up to 50 mm. The size-distributional patterns show wide level-curves rather than polymodal ones. In contrast, only small shells, less than 15 mm, occur from the overlying mudstone (Facies 2). B. Size-distribution patterns of *V. subnipponica* shells accumulated into autochthonous shellbeds at the top of the basal sandstone. The shell size-distribution pattern in the lower shellbed has a broad range from 2 mm to 48 mm and a gentle and inclined "peak" at 6–8 mm. In contrast, the pattern in the upper shellbed has a very strong mode at 2–4 mm for about 50% of the total number of valves, and with 85% concentrated in the 0–6 mm range.

the overlying Facies (3) in which wave ripple are observable. These features suggest that Facies (2) was deposited below the storm wave base in an outer shelf environment.

Facies(3) and (4) are usually intercalated between the hemipelagic Facies (2) and the amalgamated HCS sandstone (Facies 5). They are characterized by alternation of sandstones that exhibit wave ripples and hummocky cross-stratification, and mudstone. Hummocky cross-stratification is well known in episodic storm deposits (e.g. Dott, Jr. and Bourgeois, 1982). On the other hand, the mudstone represents hemipelagic deposition during fair-weather conditions. Thus, the alternation of sandstones and mudstone (Facies 3 and 4) may suggest deposition above storm wave base and below fair-weather wave base.

The amalgamated HCS sandstone (Facies 5) is the uppermost part of the coarsening-upward interval. This facies is characterized by amalgamated HCS sandstones with few intercalations of hemipelagic mudstone, and indicates deposition above fair-weather wave base. These characters of this facies are typically found in lower shoreface deposits (Walker and Plint, 1992).

The coarsening-upward interval composed of Facies (2–5) may record a successional environmental change from below storm wave base to lower shore face. Such a successional change reflects the progradational processes of a wave-dominated shoreface (*e.g.*, Walker and Plint, 1992).

Progradation of a wave- and tide-influenced shoreline (Facies 2–4 and 6).—Another coarsening-upward interval similarly consists of Facies (2–4) in its lower and middle parts. However, the uppermost part of the interval is replaced by the tabular cross-stratified sandstone (Facies 6), instead of amalgamated HCS sandstone (Facies 5).

The tabular cross-stratified sandstone (Facies 6) overlies inner shelf deposit (Facies 4) and exhibits many tide-influenced sedimentary structures such as herringbone cross-stratification, tidal-bundle sequences, reactivation surfaces, and lenticular and flaser bedding (Nio and Yang, 1989). Based on these features, Facies (6) is interpreted to have accumulated in subtidal or intertidal environments.

The progradational coarsening-upward interval with tidal deposits (Facies 6) at the top also reflects progradational process. In contrast to the coarsening-upward interval of a wave-dominated shoreface, however, it was deposited in a tide- and wave-influenced shelf. Such progradational

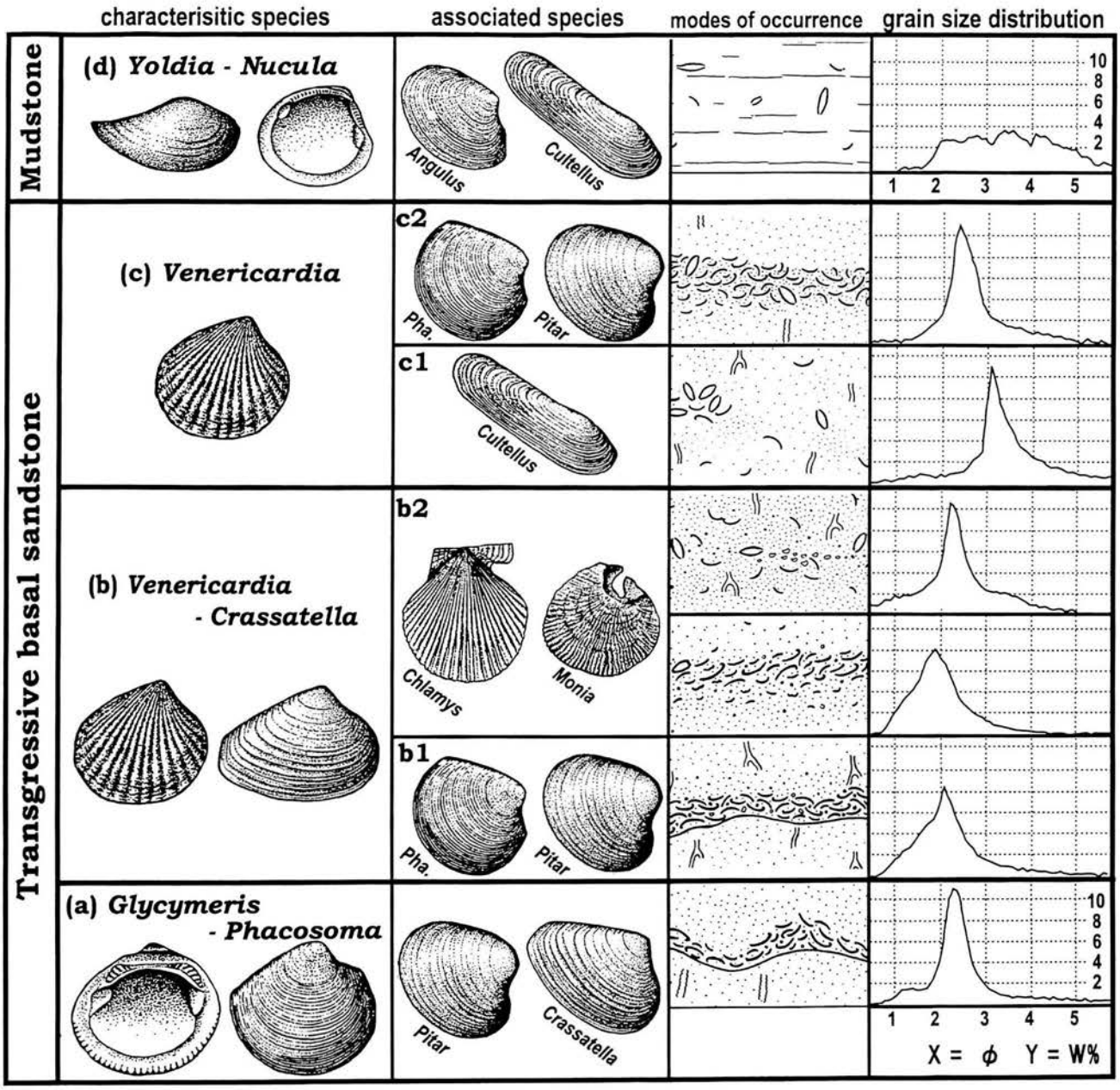

Figure 11. Schematic diagram of bivalve assemblages, showing their compositions, typical modes of occurrence and grain size distributions of the host sediments. The lowermost *Glycymeris-Phacosoma* Assemblage (a) occurs from the well-sorted medium-grained sandstone (Facies 1) as an allochthonous shellbed on the basal erosional surface. On the other hand, the *Yoldia-Nucula* Assemblage (d) indigenously occurs from poorly sorted siltstone (Facies 2). The *Venericardia-Crassatella* and *Venericardia* Assemblages (b, d) show intermediate taphonomic features between the erosional phase and the muddy quiet phase in each cycle.

deposits on a tide- and wave-influenced shelf was reported from the Devonian of the central Appalachian and upper Precambrian of Scotland (Prave *et al.*, 1996; Kessler and Gollop, 1988).

Meaning of redefined sedimentary cycle by sequence stratigraphy

After revision of the cycle boundaries, every cycle can be redefined as a pair of the transgressive basal sandstone that exhibits the decreasing of wave influence, and the progradational coarsening-upward interval of the regressive phase. The new definition seems quite consistent with a

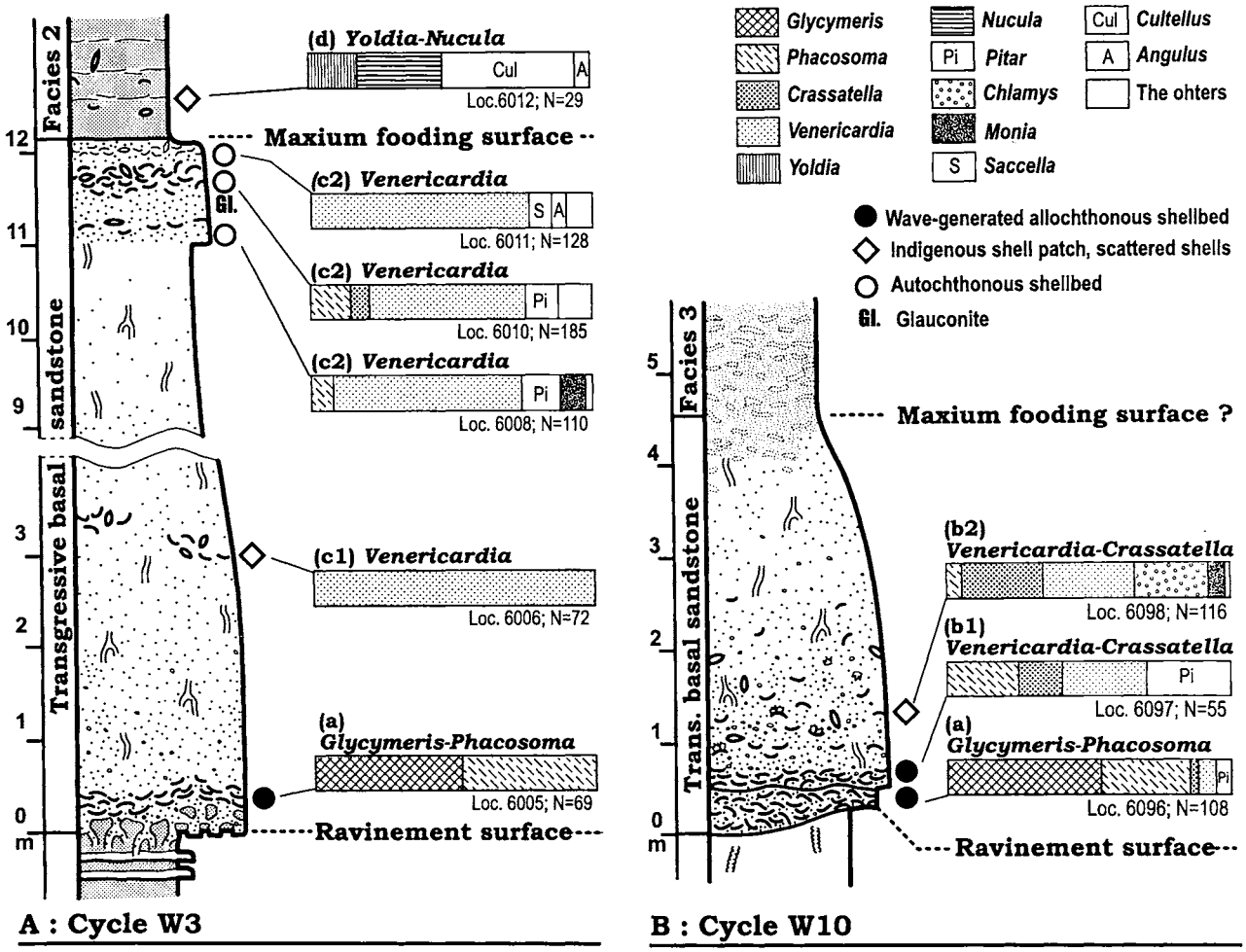

Figure 12. Successive change of fossil bivalve composition in the transgressive basal sandstone (Facies 1) and the lower part of the overlying mudstone (Facies 2). **A.** Cycle W3 and **B.** Cycle W10 are the most typical examples. Four assemblages can be discriminated. *Glycymeris-Phacosoma* Assemblage (a) is replaced upward by the *Yoldia-Nucula* Assemblage (d) via the *Venericardia-Crassatella* (b) and *Venericardia* Assemblages (c). Although all of these assemblages are not always observable in a cycle, the successive change is widespread in every cycle in the Waita Formation.

framework of sequence stratigraphy. The basal sandstone and the coarsening-upward interval reflect the transgressive and high-stand systems tracts, respectively (Posamentier and Vail, 1988). The distinct erosional surface at the base of every cycle probably corresponds with the ravinement surface (transgressive surface; Swift, 1968; Nummedal and Swift 1987), and the glauconitic sandstone beds in the top part of the transgressive basal sandstone in the Cycle W3 (Figure 6E) is regarded probably as the condensed section (Loutit *et al.*, 1988) at maximum flooding surface, which is generated by low sediment supply and slow deposition. Revision of the sedimentary cycles provides a simple but more reasonable paleoenvironmental framework for further studies on paleoecology.

Succession of molluscan assemblages

Molluscan assemblages

Molluscan fossils occur abundantly in, and are stratigraphically restricted to, the transgressive basal sandstone (Facies 1) and the overlying mudstone (Facies 2 and 3) in the lower part of each cycle (Figures 3, 5 and 7). Four different fossil assemblages are distinguished from the viewpoints of faunal composition and modes of occurrence. These four assemblages occur successively within a section, appear repeatedly in every cycle in the same order, and show characteristic taphonomic features. I have examined their modes of occurrence, paying particular attention to articulation and burial position of the shells, shell fabric and fragmentation in shellbeds, articulated bivalve fossils still in life position, and shell size distribution

(Figures 6, 9 and 10). Figure 11 summarizes the contents and modes of occurrence of the four assemblages. The grain size distribution of their host sediments was investigated in detail by a settling tube system. The settling distance was 150 cm, and the cumulative sediment weight was automatically logged by computer.

(*a*) *Glycymeris-Phacosoma Assemblage.*—This assemblage is characterized by *Glycymeris cisshuensis* and *Phacosoma chikuzenensis*, and is associated with *Pitar matsumotoi*, *Crassatella yabei* etc. (Figures 8, 11, 12).

The assemblage (a) characteristically occurs in clean sandstone, which rests directly on the erosional basement (ravinement surface) of the transgressive basal sandstone (Figure 12). The occurrence interval is 50–100 cm thick above the base. The host sandstone is massive or sometimes mottled by bioturbation (Figure 4C, D), and is fine- to medium-grained.

The shells are densely concentrated as an allochthonous shellbed of 20–50 cm thick, on an erosional surface at the base of the cycle (Locs. 6005, 6043, 6096; Figure 4A). The erosional surface shows wavy undulation, whose relief is up to 20 cm high. Bivalve shells are usually disarticulated and somewhat fragmented. They are sometimes piled up and imbricated bidirectionally along both slopes on the crest (Loc. 6005; Figure 6A). These features are characteristic of wave dunes (Cheel and Leckie, 1992).

The assemblage consists mainly of medium- to large-sized shells (30–100 mm). Their calcareous shell tests are occasionally replaced by clay minerals (Figure 6E).

A grain-size distributional pattern of the sandstone matrix is highly concentrated, and the mode lies on fine-grained sand size (ϕ = 2.3 ; Figure 11). Very fine sand or finer grains ($\phi > 3$) do not contribute much (Figure 11).

(*b*) *Venericardia-Crassatella Assemblage.*—The assemblage consists mainly of *Venericardia subnipponica* and *Crassatella yabei* (Figures 11, 12). It is subdivided into two subtypes by differences of the associated species. The first subtype (b1) is associated with *Phacosoma chikuzenensis* and *Pitar matsumotoi* which are common in the *Glycymeris-Phacosoma* Assemblage (a) (Locs. 6082, 6097: Figures 8, 11, 12). The second subtype (b2) is characteristically associated with epibionts represented by epifaunal byssally attached bivalves, *Chlamys* sp. and *Monia* sp., and by barnacles, which attach to molluscan shell surfaces (Locs. 6098a and 6109: Figures 6B, 8, 11, 12).

The first subtype assemblage with *Phacosoma* and *Pitar* (b1) occurs from medium to fine-grained sandstone in the lower to middle parts of the transgressive basal sandstone (Figure 12). The shells occur as allochthonous shellbeds of 20 cm thick on wavy erosional surfaces (Locs. 6082, 6097 etc.), much as those of the *Glycymeris-Phacosoma* Assemblage (a). Green smectite and pumice grains are common in the sandstone. Grain-size distribution of the sandstone matrix shows a moderately concentrated curve (Figure 11). The mode lies on fine-grained sand size (ϕ = 2.2). Silt-size or finer grains, less than 4 ϕ in diameter, do not amount to much.

The second subtype with epifaunal byssally attached bivalves (b2) occurs from medium to fine-grained sandstone 1–2 m thick in the middle part of the basal sandstone (Figure 12). The second subtype assemblage (b2) includes articulated individuals of *Venericardia subnipponica*, *Crassatella yabei* and *Chlamys* sp. (Figures 11, 12). The shells are scattered about the bioturbated sandstone which includes smectite and pumice grains, and which has also little silt or finer grains ($\phi > 4$). The grain-size distributional pattern is similar to that of the first type (b1; Figure 11).

Articulated shells account for 32% of total *V. subnipponica* and 18% of total *C. yabei* shells (Loc. 6098a; Figure 8). Some of them are still in their living position. For example (see Figure 9), twelve among 29 articulated individuals of *V. subnipponica* stand with their commissure plane almost vertical. In this case, most of the standing ones raise their posterior part upward with angles around 60° (Loc. 6098c; Figure 9A). *C. yabei* also exhibits trend similar to that of *V. subnipponica* but the burial pattern is much more dispersed (Loc. 6098c; Figure 9B).

Some disarticulated and articulated bivalve shells are occasionally encrusted by barnacles. Epifaunal byssally attached bivalves such as *Chlamys* sp. and *Monia* sp. are typical examples. They are encrusted not only on the outer side of shells but also on the inner side (encrustation on the inner side indicates that it occurred after the death of the host bivalves). The barnacles keep their attaching colony on the encrusted shell, and the large barnacles shells are consecutively attached by small individuals of new generations. Barnacles also occur as dislocated colonies and disarticulated shell fragments.

The shells of the assemblage (b2) are sometimes accumulated as shellbeds, however, no erosional surface is observed at the base (Loc. 6109). The matrix of the shellbed consists of a mixture of many shell fragments showing imbrications, articulated shells filled by geopetal, and medium- to fine-grained sands (Figure 6C and D). Shell fragments are variously abraded (Figure 6C). Encrustation by barnacles is common on disarticulated bivalve shells (Figure 6B).

In both subtypes (b1 and b2), medium- and large-sized shells of *V. subnipponica* (20–40 mm) are abundant (Locs. 6083, 6095, 6098b). In contrast, small shells less than 10 mm in diameter are few. Figure 10A shows a size-distributional pattern of *V. subnipponica* shells that are scattered about the middle interval of the basal sandstone at Loc 6098b. The smaller-shell portion might have been trimmed off the original thanatocoenosis by fragmentation and winnowing out by wave currents or the replacement of

shell tests by clay minerals (Figure 6E).

(*c*) *Venericardia Assemblage.*—The assemblage is characterized by abundant *Venericardia subnipponica* (Figures 11, 12). The assemblage can be subdivided into two subtypes, c1 and c2, by difference of the associated species (Figure 11). The subtype (c1) consists mostly of *V. subnipponica*, and has very few associated species except for *Cultellus izumoensis* in places (Locs. 4310a, 4313, 6006 etc; Figures 8, 12). The subtype (c2) is characterized by a great quantity of *V. subnipponica*, and associated *Phacosoma chikuzenensis*, *Pitar matsumotoi*, *Monia* sp. and *Crassatella yabei* (Locs. 6009–6011a; Figures 8, 12).

The subtype (c1) occurs commonly from very fine sandstone 8–20 m thick in the middle to upper part of the transgressive basal sandstone (Figure 12). The sandstone yields many *Thalassinoides* burrows (Figure 4C). The *Venericardia* Assemblage (c1) occurs from much more fine-grained deposits than the assemblages (a) and (b). The grain-size distribution curve shifts fineward, and the mode lies on very fine sand size (ϕ = 3). Coarse and medium-grained sands are few.

The subtype (c1) occurs as indigenous shell-patches (Figure 11) or scattered shells. *Venericardia subnipponica* sometimes forms a shell clump composed of tens of articulated individuals (Locs. 4313, 6006; Figure 6F). They frequently keep their living position in bioturbated very fine sandstone. Size distribution pattern of *V. subnipponica* in the subtype (c1) has a wide range (4–40 mm) and polymodal curve (Loc. 4310b; Figure 10A). These features might result from overprinting of indistinguishable populations because of sampling from the thick interval of bioturbated and mottled sandstone.

On the other hand, Subassemblage (c2) is restrictedly found only from a glauconitic sandstone bed at the top of the transgressive basal sandstone in the cycle W3 (successive Locs. 6008, 6010a and 6011a; Figure 12). The shells of the Subtype (c2) accumulated as an autochthonous shellbed (Figures 10B, 11, 12), which contained articulated large *Monia* sp. that probably attached to other shells with a byssus, particularly in their early growth stage (Loc. 6008; Figure 7D). The grain-size distribution curve of the host rock has a mode at very fine sand (ϕ = 2.4; Loc. 6010a; Figure 11), which is slightly coarser than the host rock of the subtype (c1).

A great quantity of disarticulated *V. subnipponica* shells constructs a shellbed 40–60 cm in thickness (Loc. 6010b, Figure 10B). The shellbed starts with a gradual increase of shell content in the lower 20 cm interval, and ends at a sharp top. The shells are oriented at random, and are occasionally attacked by boring polychaetes. The shellbed also yields articulated individuals of *V. subnipponica* and *P. matsumotoi* (Figure 8), some still in their living positions. A quantity of *V. subnipponica* shells has a broad range in shell diameter from less than 2 mm to 48 mm. The histogram of the shell size distribution shows a mode at 6–8 mm for 44 valves of 317; it forms a broad and inclined "peak" that rises swiftly from the smallest shells then declines gradually to the largest ones (Figure 10B lower).

In the transitional zone from glauconitic sandstone to mudstone (Facies 2), the subtype (c2) is composed particularly of many small *V. subnipponica* shells accompanied with *Angulus maximus*, an associated species of the *Yoldia-Nucula* Assemblage (d) at Loc. 6011a (discussed below; Figures 8, 12). Many small *V. subnipponica* shells are concentrated into a thin shellbed 2–5 cm in thickness. The histogram of the shell diameter distribution shows a high mode at the 2–4 mm; range, in which about 50% of the total of 145 valves are included. More than 85% of the valves fall in the range of 0–6 mm, and otherwise medium-sized shells (10–30 mm) account for only about 7% (Loc. 6011b; Figure 10B). A similar distributional tendency of *V. subnipponica* shell diameters is represented in the *Yoldia -Nucula* Assemblage (d) (described immediately below).

(*d*) *Yoldia-Nucula Assemblage.*—The assemblage consists mainly of *Yoldia* sp., *Nucula* sp., *Angulus maximus*, *Cultellus izumoensis*, *Venericardia subnipponica*, *Dentalium* sp. (Locs. 6001a and 6012; Figures 8, 11, 12). Unlike the other assemblages, the *Yoldia-Nucula* assemblage occurs from the bioturbated mudstone (Facies 2; Figure 6G) which overlays the basal sandstone (Facies 1) at Locs. 4308a and 6012 (Figure 10), and the grain size distributional pattern shows a broad curve extending from fine sand size (ϕ = 2) to silt size (ϕ = 5; Figure 11) without an obvious peak.

Usually, the molluscan fossils are scattered about the mudstone (Figure 6G). Some bivalve shells of *Yoldia* sp. and *Nucula* sp. are articulated and arranged at random. Most *Cultellus izumoensis* shells are articulated (Loc. 6001a; Fgiure 8). Among 26 articulated individuals, fifteen *C. izumoensis* stand with their commissure plane subvertical, and frequently the posterior part is raised upward at angles around 60° (Loc. 6001c; Figure 9C). The shells of *Angulus maximus* (= tellinine bivalve) are also articulated in high numbers (Loc. 6001a; Figure 8), and retain their living position, in which their right-warped siphonal gape is oriented upward. Their articulated shells lie horizontally in the matrix still keeping their right valve uppermost. (Loc. 6001c; Figure 9D).

Shells of *Dentalium* sp. and *Turritella karatsuensis* occur occasionally as allochthonous shell stringers (Kidwell *et al.*, 1986) on minor erosional surfaces (Loc. 6001a). The horn- or drill-shaped shells are concentrated in parallel and arranged into a scar 50 cm long and 20 cm wide, and their apices are unimodally pointed (Figure 6H).

Venericardia subnipponica occurs not only from the basal sandstone (Facies 1) but also from the mudstone

(Facies 2). In the *Yoldia-Nucula* Assemblage (d), *V. subnipponica* is a subordinate species, and is represented only by small individuals. It accounts only for 4.1% of in total 97 individuals in the assemblage (b) at Loc. 6001a (Figure 8). Figure 10A show two shell diameter distributional histograms at localities 6001b and 4308b. The pattern at Loc. 6001b has a mode at 6–8 mm, and shells larger than 12 mm diameter are scarce.

Successive occurrences of molluscan assemblages

The molluscan assemblages change successively in upward sequence within the transgressive basal sandstone and the overlying mudstone in each cycle. The successive occurrences are similarly made up of, in ascending order, the (a) *Glycymeris-Phacosoma* Assemblage, (b) *Venericardia-Crassatella* Assemblage, (c) *Venericardia* Assemblage and (d) *Yoldia-Nucula* Assemblage (Figure 11). Their successive occurrence is never reversed in order, and is uniformly repeated in every sedimentary cycle, though all the four assemblages are not always completely observable within a cycle. Related to the faunal change, their typical modes of occurrence shift upward from allochthonous shellbed into indigenous shell clumps and patches.

The most typical examples of the Cycles W3 and W10 are summarized in Figure 12. In cycle W3 (Locs. 6005–6012; Figure 12A), the faunal succession starts with the *Glycymeris-Phacosoma* Assemblage (a), which occurs only as the basal allochthonous shellbed with wave dunes at the base of the cycle (Locs.6005). The *Venericardia-Crassatella* Assemblage (b) is skipped there. The lowermost assemblage (a) is replaced upward directly by the *Venericardia* Assemblage (c) at the 3 m-level above the base. The top part of the occurrence range of the assemblage (c) intercalates with *V. subnipponica* shellbeds in glauconitic sandstone bed that indicates the surface of maximum transgression (11–12 m level in figure 12A). The shellbeds also yield a few *Phacosoma chikuzenensis* and *Pitar matsumotoi*, both of which are associate species of the Subassemblage (c2). The indigenous *Yoldia-Nucula* Assemblage (d) appears at the 12.5 m-level as the lithology changes quickly from sandstone to the overlying mudstone (Facies 2).

The faunal succession is almost identical in the Cycle W10, but is condensed within a thin basal interval (0–2 m level in Figure 12B). The *Glycymeris-Phacosoma* Assemblage (a) is also dominant on the basal erosional surface, and is similarly replaced upward by the *Venericardia -Crassatella* Assemblage (b1) on the erosional surface at the level of 0.5 m above the base (Loc.6096–6097; Figure 12B). The latter assemblage (b1) is immediately succeeded by another subtype (b2) of the *Venericardia-Crassatella* Assemblage with abundant epibionts, such as *Chlamys* sp., *Monia* sp. and barnacles, at the level of 0.7 m above the base (Loc. 6097, 6098a: Figure 12B). The occurrence range of Assemblage (b2) encompasses 1.5 m in thickness, and is terminated with an increase of mud content in the host rock (Figure 12B).

Discussion

Taphonomic implication of faunal change in cycles

Molluscan fossils mostly occur from the lower part of each cycle, i.e., the transgressive basal sandstone (Facies 1) and the mudstone (Facies 2) that had been deposited during the earliest regressive phase (Figure 12). Four distinctive fossil assemblages are preserved in this relatively thin part. Close taphonomical observation can "decode" the hidden paleoenvironmental and paleoecological changes condensed in this transgressive interval in high resolution.

The lowermost *Glycymeris-Phacosoma* Assemblage (a) occurs only as allochthonous shellbeds on the erosional base of the transgressive basal sandstone (Figures 11, 12). Most of the shells are disarticulated completely and fragmented considerably there, and often form wave dunes (Cheel and Leckie, 1992: Figure 6A). The matrix of the host rock is well-sorted, fine-grained sandstone, and the mud content is small (Figure 11). These features strongly suggest deposition under intensely wave-influenced conditions, in which the sea bottom is frequently eroded and shells are easily winnowed. The molluscan shells in this assemblage might be reworked repeatedly even if they were not transported horizontally far from their habitats. The succeeding *Venericardia-Crassatella* Assemblage associated with *Phacosoma* and *Pitar* (b1) occurs also as wave-influenced shellbeds on additional minor erosional surfaces (Figure 11)

In contrast, no signs of bottom erosion and shell reworking by wave currents are observable in the upper part of Facies (1) and, also in Facies (2). The *Venericardia* Assemblage (c) consists partly of autochthonous or indigenous shell patches. in the upper part of the basal sandstone (Facies 1), whose grain size distributional pattern shifts fineward ($\phi > 3$: Figure 11).

The uppermost *Yoldia-Nucula* Assemblage (d) occurs mostly as indigenous scattered shells in the overlying mudstone (Facies 2; Figure 12). Their shells are often articulated and found in their living positions (Figure 10). These are no signs of bottom erosion and shell reworking. The host rock contains very fine sand ($2 < \phi < 3$) but is dominated by muds (Figure 11). Allochthonous shells of *Dentalium* sp. and *Turritella karatsuensis* are sometimes accumulated in depressions on the bedding plane of the mudstone, and show preferred orientation (Facies 2; Figure 6H). The cause of such apex-oriented shell stringers is not attributable to waves but to unidirectional currents (Nagle, 1967; Figure 6H).

The successional change of these taphonomic features suggests that the faunal succession is closely associated with the upward decreasing of wave influence. The *Glycymeris-Phacosoma* Assemblage (a) is replaced upward by the *Yoldia-Nucula* Assemblage (d) via the *Venericardia-Crassatella* and *Venericardia* Assemblages (b, c), while the strong wave influence declines from the erosional and winnowing phase to the quiet muddy phase through the transgression period.

Successive faunal change within a sedimentary cycle is widespread and exhibited repeatedly in the Waita Formation. The *Glycymeris-Phacosoma* Assemblage always occurs as the allochthonous shellbed, which corresponds to an onlap shellbed (Kidwell, 1991) on the ravinement surface that indicates early transgression. The other assemblages also retain the autochthonous or indigenous occurrences above this onlap shellbed. Besides the Ashiya Group, similar faunal change in and above onlap shellbeds is observable in the other Paleogene deposits (e.g., the Nishisonogi Group and Hioki Group). Therefore, it seems one of the basic sedimentological and paleoecological features of the Paleogene deposits in west Japan.

Epibionts-enriched fauna

The successive faunal records are sometimes condensed within a very short interval in a cycle, for example, within an interval of 2 m thick from the base in the cycle W10 (Figure 12). Intermittent and limited deposition of this interval is suggested by abundant occurrence of epibionts. Epifaunal byssally attached bivalves: *Chlamys* sp. and *Monia* sp., and barnacles occur commonly as associated species of the *Venericardia-Crassatella* Assemblage (b) from the lower middle part of the transgressive basal sandstone (Figure 12). Some of them are found in the attaching position *in situ* (Figure 6B), while others are fragmented, abraded, and finally assimilated into the shellbed matrices showing imbrications (Figure 6C). Scarcity of fine-grained sediments in the matrix also implies that this component was winnowed out and swept away by currents (Subassemblage b2; Figure 11).

These epifaunal byssally attached bivalves and barnacles require the peculiar condition that their attachment to shelly ground avoids burial by the winnowing out of sediments. A number of shells have been attached by plural generations of barnacles (Loc. 6098a). Some other shells have repeatedly settled by epibionts after death. *Chlamys* and *Monia* probably attached to other shells by their byssus at least in the early ontogenetic stage, although the attachment position is not observable in the fossil record since the byssus is missing. The line of evidence converges to an argument that the shelly ground, which lifts the restriction on the migration of the epibionts, was exposed for a long time. The signs of taphonomic feedback , by which the skeletal remains of dead organisms impact on the next living community (Kidwell and Jablonski 1983), are observable in places (Locs. 6008, 6098a and 6109). The epifaunal byssally attached bivalves cannot survive on the seafloor in which sediments are rapidly and continuously deposited; the same is true of the cemented barnacles, because they have neither a foot to escape rapid burial nor a siphon (Stanley, 1970; Kranz, 1974). The epibiont-rich shellbeds at least in three cycles might indicate strong or gentle current-influenced conditions in which sedimentation was intermittent, and probably, relatively slow.

Autochthonous shellbed in glauconitic sandstone

The glauconitic sandstone bed at the top of the transgressive basal sandstone intercalates with autochthonous shellbeds composed of a great quantity of *Venericardia subnipponica* shells (Subassemblage c2; Locs. 6010 and 6011). Unlike the allochthonous shellbed on the ravinement surface at the base of the cycle, the shellbed at the top is autochthonous because bivalve fossils often keep their living position (Figures 10B, 12). Abundant glauconite grains in matrices (Figure 4E), which develop in areas characterized by low sedimentation (Chamley, 1989), imply condensation as a process of shell accumulation *in situ* during a relatively long period. This view is also supported by the occurrence of epifaunal byssally attached bivalves such as *Monia* sp.

The shell diameter distributional pattern of *V. subnipponica* in this shellbed is shown in Figure 10B (lower). These shells range in length from 2 to 48 mm, with a low mode at 6–8 mm. This may suggest a continuous and stable supply of dead shells of all growth stages *in situ*, which consist of many juveniles and a few mature specimens, except for very small juveniles that have little fossilization potential. As noted above in the sequence stratigraphic interpretation of the sedimentary cycle, the glauconitic sandstone where the autochthonous shellbed lies is regarded as a condensed section associated with the maximum-flooding surface (Figures 5, 12B).

The autochthonous shellbed in the glauconitic sandstone probably reflects attrition from a normal population or "cemetery" (Ager, 1963; Dodd and Stanton, Jr., 1990). It is produced by repetitive colonization of *Venericardia subnipponica* populations *in situ* under low sedimentation rate during the maximum-flooding period. Such a shellbed at the top of a transgressive deposit is classified as a backlap shellbed by Kidwell (1991).

On the other hand, another autochthonous shellbed is intercalated in the transitional zone from the glauconitic sandstone to overlying mudstone (Facies 2) (Figure 10B, upper).

It is composed mostly of small shells of *Venericardia*

subnipponica, some of which are articulated (Figure 10B). In contrast to the *Venericardia* Assemblage in the glauconitic sandstone, the size-distributional pattern of the present species shifts strongly to the smallest portion (Figure 10B upper). The mode of the histogram lies at 2–4 mm, in which more than 50% of the total individuals are concentrated. These features probably suggest that a mass mortality of juvenile shells occurred after an opportunistic larval settlement, and that these shells represent a census population (Ager, 1963; Dot and Stanton Jr., 1990).

Venericardia is a typical infaunal nonsiphonate suspension feeder having limited mantle fusion. They are usually shallow and slow burrowers (Stanley, 1970), and have low escape ability from rapid burial (Kranz, 1974). Consequently, the mass mortality may be involved with the incidental deposition of soupy muds that caused an obrution. The population of *Venericardia* juveniles might be smothered by the obrution event in the transitional phase between condensed glauconitic and muddy. It should be noted that *Venericardia* populations in the overlying mudstone (Facies 2; *Yoldia-Nucula* Assemblage) are also restricted to small-diameter shells.

Conclusion

Based on detailed observations, 11 sedimentary cycles in the upper part of the Ashiya Group (upper Oligocene) were revised and redefined here (Figure 5). Each cycle consists of a basal erosional surface overlain by a transgressive basal sandstone and a progradational-interval of mudstones and sandstones. In this revision, every cycle is bordered by an erosional surface at the base of a fossiliferous sandstone. Four molluscan fossil assemblages are distinguished. They exhibit similar successive occurrences accompanied with transitions of sedimentological and taphonomical features. These are a key to understanding the Paleogene stratigraphy and paleoecology, because similar successive occurrences of bivalve fossils are widespread in other Paleogene deposits in western Japan (i.e., Nishisonogi and Hioki Groups). The successive occurrence of bivalve fossil faunas is interpreted to result from transgressive-regressive shifts in sedimentary regimes (variable wave influence and sediment supply).

Paleoecological aspects of Paleogene bivalves, for example *Venericardia*, still remain obscure. Unlike Neogene or Quaternary fauna, direct analogies from the ecology of modern relatives should not be simply drawn for Paleogene bivalves. On the other hand, taphonomic and sedimentologic aspects can be directly read from the strata. Sedimentary regime seems to be a factor in defining the habitats of bivalves, and is regarded as the most important environmental factor controlling morphologic adaptations of bivalves (Stanley, 1970), owning to their benthic habitat, which not only is closely related to the depositional substrate, but also contains many infaunal styles of burrowing into deposits. Therefore, taphonomic and sedimentologic observation will be a key to understanding the paleoecology of Paleogene bivalve fauna.

Acknowledgments

I would like to express my gratitude to H. Maeda (Kyoto University) for his critical reviews and kind guidance of the manuscript. I am deeply indebted to F. Masuda and T. Sakai (Kyoto University) for their sedimentological cooperation in the field and laboratory, and to Y. Kondo (Kochi University) for his helpful suggestions and encouragements. I am also grateful to S. M. Kidwell (University of Chicago) and an anonymous referee for their helpful comments to improve the manuscript. Thanks are also extended to T. Komatsu (Kumamoto University) and B. Tojo (Kyoto University) for their valuable comments, and staff of Tsuyazaki Fishery Research Laboratory of Kyushu University for their help during fieldwork. This study has been partly supported by a grant-in-aid from the Fukada Geological Institute.

References

Ager, D. V., 1963: *Principles of Paleoecology*, 371 p. McGraw-Hill Co., New York.

Cheel, R. J. and Leckie, D. A., 1992: Coarse-grained storm beds of the Upper Cretaceous Chungo Member (Wapiabi Formation), southern Alberta, Canada. *Journal of Sedimentary Petrology*, vol. 62, no. 6, p. 933–945.

Chamley, H., 1989: *Clay Sedimentology*, 623 p. Springer-Verlag Berlin.

Dott, J. R. and Stanton, Jr., R. J., 1990: *Paleoecology, Second Edition*, 502 p. A Wiley-Interscience Publication John Wiley and Sons, New York.

Dott, Jr., R. H. and Bourgeois, J., 1982: Hummocky stratification: Significance of its variable bedding sequences. *Geological Society of America Bulletin*, vol. 93, p. 663–680.

Hayasaka, R., 1991: Sedimentary facies and environments of the Oligocene Ashiya Group in the Kitakyushu-Ashiya area, Southwest Japan. *The Journal of Geological Society of Japan*, vol. 97, p. 607–619. (*in Japanese with English abstract*)

Loutit, T.S., Hardenbol, J., and Vail, P.R., 1988: Condensed sections: the key to age determination and correlation of continental margin sequences. *In*, Wilgus, C. K. *et al. eds.*, *Sea-level Changes—an Integrated Approach*, SEPM, Special Publication, no. 42, p. 183–213.

Kessler, L.G. and Gollop, Ian.G., 1988: Inner shelf/shoreface-intertidal transition, Upper Precambrian, Port Askaig Tillite, of Islay, Argyll, Scotland. *In*, de Boer, P.L., van Gelder, A. and Nio, S.D. *eds.*, *Tide-influenced Sedimentary Environments and Facies*, p. 341–358. D. Reidel Publishing Company, Boston.

Kidwell, S. M., 1991: Condensed deposits in siliciclastic sequences: expected and observed features. *In*, Einsele, G., Ricken, W. and Seilacher, A. *eds.*, *Cycles and Events in Stratigraphy*, p. 182–195. Springer-Verlag, Berlin Heidelberg.

Kidwell, S. M. and Jablonski, D., 1983: Taphonomic feedback: ecological consequences of shell accumulation. *In*, Tevesz, M. J. S. and McCall, P. L. *eds.*, *Biotic Interaction in Recent and Fossil Benthic Communities (Topics in Geobiology 3)*, p. 195-248. Plenum Press, New York.

Kidwell, S. M., Fürsich, F. T. and Aigner, T., 1986: Conceptual framework for the analysis and classification of fossil concentrations. *Palaios*, vol. 1, p. 228-238.

Kranz, P. M., 1974: The anastrophic burial of bivalves and its paleoecological significance. *Journal of Geology*, vol. 82, p. 237-265.

Mizuno, A., 1963: Paleogene and Lower Neogene biochronology of West Japan (III. Stratigraphic and geographic distributions of molluscan faunas in West Japan). *The Journal of Geological Society of Japan*, vol. 69, p. 38-49. *(in Japanese with English abstract)*

Nagao, T., 1927a: The Palaeogene stratigraphy of Kyushu (Part 17). *Journal of Geography*, vol. 39, p. 665-674. *(in Japanese)*

Nagao, T., 1927b: Palaeogene fossils of the Island of Kyushu, Japan, Part 1. *Science Reports of Tohoku Imperial University*, vol. 9, no. 3, p. 97-128.

Nagao, T., 1928a: The Palaeogene stratigraphy of Kyushu (Part 20). *Journal of Geography*, vol. 40, p. 143-155. *(in Japanese)*

Nagao, T., 1928b: Palaeogene fossils of the Island of Kyushu, Japan, Part 2. *Science Reports of Tohoku Imperial University*, vol. 12, no. 1, p. 1-140.

Nagle, J. S., 1967: Wave and current orientation of shells. *Journal of Sedimentary Petrology*, vol. 37, no. 4, p. 1124-1138.

Nara, M., 1997: High-resolution analytical method for event sedimentation using *Rosselia socialis*. *Palaios*, vol. 12, p. 489-494.

Nio, S. D. and Yang, C. S., 1989: Diagnostic criteria for recognized tidal dominance in shallow marine clastic deposits. *Short Course Note Series #61*, p. 25-75. International Geoservices BV, Leiderdorp.

Nummedal, D. and Swift, D. J. P., 1987: Transgressive stratigraphy at sequence-bounding unconformities: some principles derived from Holocene and Cretaceous examples. *In*, Nummedal, D., Pilkey, O. H. and Howard, J. D. *eds.*, *Sea-level Fluctuation and Coastal Evolution. SEPM, Special Publication*, no. 41, p. 241-259.

Okabe, M. and Ohara, J., 1972: Variation of heavy mineral assemblage from the Otsuji Group to the Ashiya Group, Chikuho Coal-field, northern Kyushu. *Reports of Earth Science College of General Education, Kyushu University*, vol. 17, p. 59-71.

Otsuka, Y., 1939: Tertiary crustal deformation in Japan—with short remarks on Tertiary paleogeography. *Jubilee Publication in the Commemoration of Professor H. Yabe, M. I. A., 60th Birthday*, vol. 1, p. 481-519. Yabe Kyoju Kanreki Kinen Kai, Sendai.

Oyama, K., Mizuno, A. and Sakamoto, T., 1960: *Illustrated Handbook of Japanese Paleogene Molluscs*, 224 p. Geological Survey of Japan.

Ozaki, M., Hamada, S. and Yoshii, M., 1993: *Geology of the Orio District. with Geological Sheet Map at 1: 50,000*, 121 p. Geological Survey ofJapan. *(in Japanese with English abstract)*

Posamentier, H. W. and Vail, P. R., 1988: Eustatic controls on clastic deposition II—Sequence and systems tract models. *In*, Wilgus, C. K. *et al. eds.*, *Sea-level Changes—an Integrated Approach, SEPM, Special Publication*, no. 42, p. 183-213.

Prave, A. R., Duke, W. L. and Slattery, W., 1996: A depositional model for storm- and tide-influenced prograding siliciclastic shorelines from the Middle Devonian of the central Appalachian foreland basin, USA. *Sedimentology*, vol. 43, p. 611-629.

Sakakura, N. and Masuda, F., 2001: Macro-tidal deposits showing semi-diurnal with a diurnal inequality of low water in Paleogene Kyusyu, Japan. *In*, Park, Y. A. and Davis, R. A., Jr. *eds.*, *Proceedings of Tidalites 2000*, p. 87-96. The Korean Society of Oceanography, Special Publication, Seul.

Saito, T. and Okada, H., 1984: Oligocene calcareous plankton microbiostratigraphy of the Ashiya Group, North Kyushu: *In*, Saito, T., Okada, H. and Kaiho, K. *eds.*, *Biostratigraphy and International Correlation of the Paleogene System in Japan*, p. 85-87. Faculty of Science, Yamagata University,

Shuto, T. and Shiraishi, N., 1971: A note on the community-paleoecology of the Ashiya Group. *Science Reports of Faculty of Science, Kyushu University, Ser. D, Geology*, vol. 10, no. 3, p. 253-270.

Stanley, S.M., 1970: Relation of shell form to life habit in the Bivalvia (Mollusca). *Geological Society of America, Memoir 125*, p. 1-296.

Swift, D. J. P., 1968: Coastal erosion and transgressive stratigraphy. *Journal of Geology*, vol. 76, p. 444-456.

Tsuchi, R., Shuto, T. and Ibaraki, M., 1987: Geologic ages of the Ashiya Group, North Kyushu from a viewpoint of planktonic foraminimera. *Reports of Faculty of Science, Shizuoka University*, vol. 21, p. 109-119.

Walker, R. G. and Plint, A. G., 1992: Wave and storm dominated shallow marine systems. *In*, Walker, R. G. and James, N. P. *eds.*, *Facies Models: Response to Sea Level Change*, p. 219-238. Geological Association of Canada, St. John's, Newfoundland.

Paleontological Research, vol. 6, no. 1, pp. 121-124, April 30, 2002

SHORT NOTES

Revision of an Ordovician cephalopod *Ormoceras yokoyamai* (Kobayashi, 1927)

SHUJI NIKO

Department of Environmental Studies, Faculty of Integrated Arts and Sciences, Hiroshima University, Higashihiroshima, 739-8521, Japan (e-mail: niko@hiroshima-u.ac.jp)

Received 27 August 2001: Revised manuscript accepted 20 November 2001

Key words: Llanvirn, Proteoceratidae, *Treptoceras yokoyamai*

Introduction

Systematic position of an Ordovician cephalopod *Ormoceras yokoyamai* (Kobayashi, 1927) is reconsidered on the basis of type specimens kept in the University Museum of the University of Tokyo (prefixed UMUT) and the new material from the type stratum Jigunsan Formation, Choson Supergroup in Gangwon-Do, South Korea. The Jigunsan Formation, named by Yamanari (1926), is a relatively thin (45-100 m in thickness) fossiliferous sequence of interbeded shale and subordinate limestone. On the basis of studies primarily of trilobites and cephalopods, Kobayashi (1966) assigns the principal part of the formation to Llanvirn (upper Middle Ordovician). This correlation is in agreement with conodont biochronology by Lee (1977, 1980). The newly collected specimens come from float blocks of shale at (1) locality G90075, latitude 37° 10′ 39.5″ N, longitude 128° 42′ 7.1″ E, in a field on the southwestern slope of Mt. Jigun, Jikdongri, Jungdong-myeon, Yeongwol-gun (UMUT PM 27827), and (2) locality J89105, latitude 37° 5′ 42.4″ N, longitude 129° 0′ 52.6″ E, on the northern flank of a small tributary of the Hwangji River in Jangseong, Taebaek-city (UMUT PM 27828).

Systematic paleontology

? Subclass Actinoceratoidea Teichert, 1933
? Order Actinocerida Teichert, 1933
Family Proteoceratidae Flower, 1962
Genus ***Treptoceras*** Flower, 1942

Type species.—*Orthoceras duseri* Hall and Whitfield, 1875.

Treptoceras yokoyamai (Kobayashi, 1927)

Figure 1

Loxoceras yokoyamai Kobayashi, 1927, p. 186, 187, pl. 18, figs. 9a-c.
Sactoceras yokoyamai (Kobayashi). Kobayashi, 1934, p. 439, 440, pl. 27, figs. 1-6, pl. 28, fig. 2.
Ormoceras yokoyamai (Kobayashi). Yun, 1999, p. 214.

Emended diagnosis.—Small species of *Treptoceras* with low angle (approximately 5°) of shell expansion, oval cross section with form ratio (lateral/dorsoventral diameter) 1.2-1.5; siphuncle submarginal with siphuncular position ratio (minimum distance of central axis of siphuncle from shell wall per dorsoventral shell diameter) approximately 0.2 in adoral shell; septal necks cyrtochoanitic to suborthochoanitic; cameral deposits weak for genus.

Description.—Small-sized orthocones for genus with gradual shell expansion indicating approximately 5° in dorsoventral plane (Figure 1.1); apical shell may be curved on the basis of a specimen (UMUT PM 0686 figured by Kobayashi, 1934, pl. 27, fig. 6); details of shell surface not observed in all examined specimens, but annulations and conspicuous ornamentation not detected; cross section of shell dorsoventrally depressed, oval with form ratio of 1.2-1.5 (Figure 1.2); largest known specimen (UMUT PM 0685 figured by Kobayashi, 1934, pl. 27, figs. 3-5) attains 11.0 mm in dorsoventral diameter and 15.5 mm in lateral diameter, whose adoral part represents apical body chamber; sutures transverse to slightly oblique, nearly straight or weakly sinuate to form very shallow ventral and dorsal lobes in rare cases (Figure 1.1); camerae very short, giving width/length ratios which ranges from 4.6 to 10.9+, with shallow septal curvature (Figure 1.3); no septal furrow detected; adoral siphuncle stenosiphonate and submarginal in position, with siphuncular position ratio approximately 0.2 (Figure 1.3); septal necks cyrtochoanitic to suborthochoanitic, not recumbent (Figure 1.4-1.7); well-preserved dorsal septal neck attains 0.27 mm in length at dorsoventral shell diameter of approximately 7 mm; adnation area usually

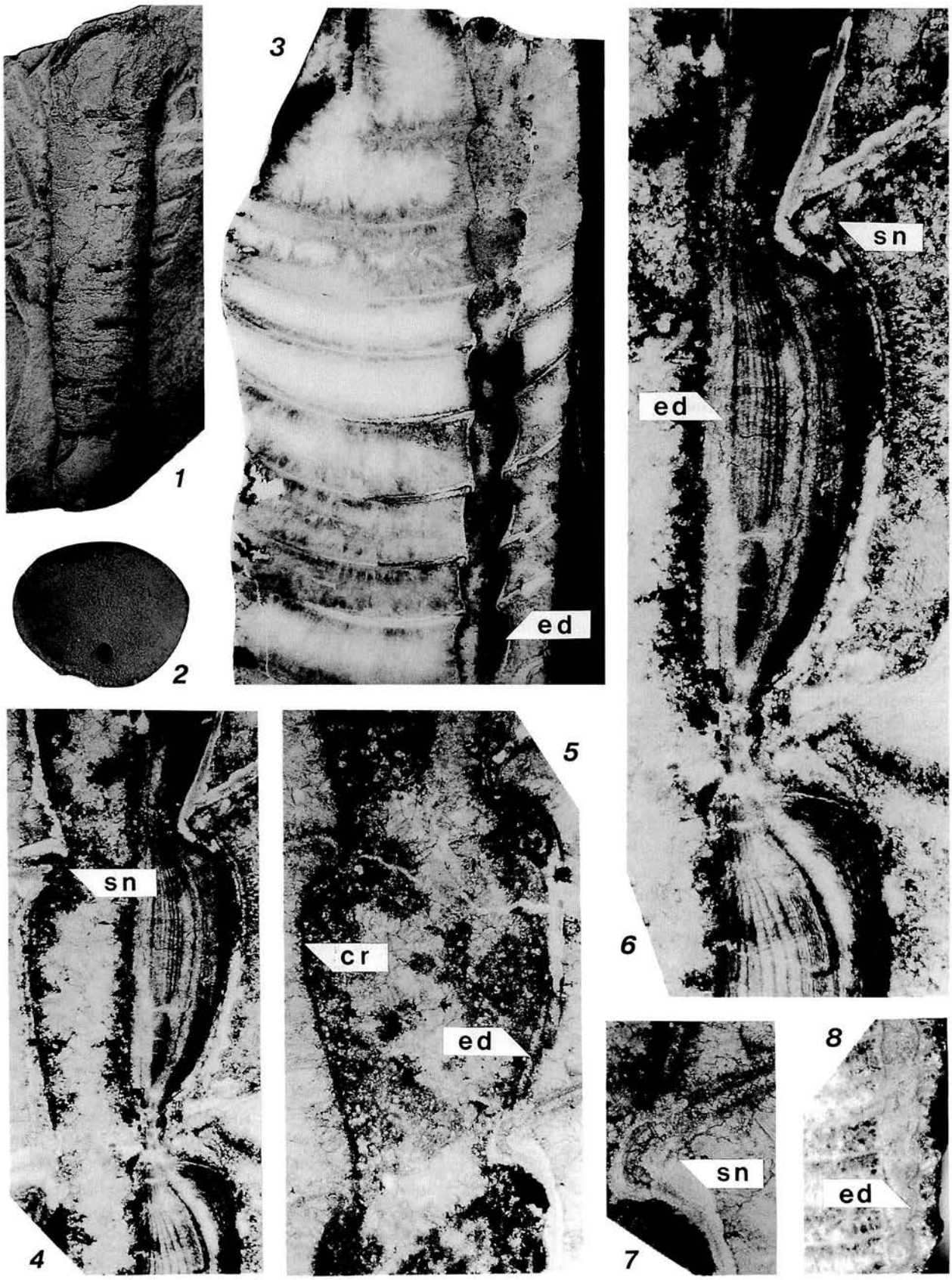
1
2
3
ed
sn
ed
4
sn
5
cr
ed
6
7
sn
8
ed

absent; connecting rings relatively thick, 0.05–0.07 mm, and undifferentiated (Figure 1.5), forming subglobular profile in apical dorsoventral section of a specimen (UMUT PM 0686) with maximum diameter/length ratio of siphuncular segments approximately 1.3, inflation then rapidly decreases, creating fusiform to pyriform (and subglobular in rare cases) profile in adoral dorsoventral section with ditto ratio 0.6–0.9 (Figure 1.4, 1.5); curvature of septal brims and inflation of connecting rings are slightly stronger on ventral siphuncular side than on dorsal one (Figure 1.4, 1.5); cameral deposits weak for genus, restricted in apical camerae, composed of thin episeptal-mural and hyposeptal deposits (Figure 1.3). Endosiphuncular deposits are also restricted to apical siphuncle (Figure 1.3); laminated parietal deposits to form thick lining on ventral siphuncular wall (Figure 1.4, 1.6); thickness of ventral lining decreases at septal foramen and its surface usually linear in profile in longitudinal section (Figure 1.4, 1.6); parietal deposits rarely developed on dorsal connecting rings, which interrupted at septal foramen (Figure 1.4); canal system and perispatium not developed.

Discussion.— Morphologically, the most diagnostic feature of this species is the structure of the endosiphuncular deposits that is observable in Kobayashi's specimen UMUT PM 0687 (Figure 1.8), and a section from the new material, UMUT PM 27827 (Figure 1.3–1.6). Its combination of the characteristic parietal deposits that form the ventral lining and lack of a canal system (Figure 1.4, 1.6) confirm systematic placement of the species in the Proteoceratidae rather than the Pseudactinoceratidae (*Loxoceras* M'Coy, 1844; Doguzhaeva and Shkolin, 1999) or the Ormoceratidae (*Ormoceras* Stokes, 1840 and its subjective junior synonym *Sactoceras* Hyatt, 1884). In addition, the species does not exhibit an exogastric cyrtocone, surface annulations and strongly bulging sutural elements, which features are diagnostic only for two closely related genera, i.e., *Treptoceras* (some emendations to the generic diagnosis were added by Aronoff, 1979, and Frey, 1988) and *Proteoceras* (Flower, 1955; type species *Ooceras*(?) *perkinsi* Ruedemann, 1906). These genera can be distinguished by the degree of the siphuncular changes which are less drastic in *Treptoceras duseri* and the present Korean species (Figure 1.3) than in *Proteoceras perkinsi*. The siphuncular segments of *Proteoceras* shift from a subglobular form to a nearly cylindrical one in the space of 6–8 camerae. Accordingly, *Ormoceras yokoyamai* is attributed to *Treptoceras*.

Although confident determination of the proteoceratid's higher taxonomic position is pending until the apical shell form is clarified, it is herein proposed that a possible origin of the Proteoceratidae was derived from the subclass Actinocerida. Flower (1962) placed the Proteoceratidae in the order Orthocerida of the subclass Nautiloidea, and his assertion was followed in the Treatise (Sweet, 1964) and by Aronoff (1979) and Frey (1988). However, the rapid decrease of the siphuncular inflation of *Proteoceras perkinsi*, *Treptoceras duseri*, and *T. yokoyamai* is exceedingly unusual for the subclass Nautiloidea, and it seems rather suggestive of a phylogenetic relationship with some actinocerids including *Paractinoceras* (Hyatt *in* Zittel, 1900), *Leurorthoceras* (Foerste, 1921) and *Kobayashiceras* (Niko, 1998). Endosiphuncular lining deposits lacking radial canal and perispatium are also known in the adoral siphuncle of *Kobayashiceras*. This indicates that presence or absence of the canal system in the adoral shell is not always essential for Actinoceratoidea.

Material examined.—The holotype, UMUT PM 0016. The five specimens, UMUT PM 0683–0687, also identified as this species by Kobayashi (1934). In addition, the two new specimens of the imperfect phragmocones of UMUT PM 27827, 44.8 mm in length, and UMUT PM 27828, approximately 31 mm in length, have been examined.

Acknowledgments

I gratefully acknowledge my debt to the late Teiichi Kobayashi, for his helpful comments on the Ordovician stratigraphy and fauna of South Korea and encouragement when the author was a graduate student. Thanks also are due to Kan-San Ahn for aid in conducting field work and Tamio Nishida for providing locality information. The help of Takeo Ichikawa in examination of the type specimens, deposited in the University Museum of the University of Tokyo, is appreciated. I also thank Cheol-Soo Yun and an anonymous reviewer for their useful comments.

References

Aronoff, S. M., 1979: Orthoconic nautiloid morphology and the case of *Treptoceras* vs. *Orthonybyoceras*. *Neues Jahrbuch für Geologie und Paläontologie, Abhandlungen*, vol. 158, p. 100–122.

Doguzhaeva, L. A. and Shkolin, A. A., 1999: Sifon "*Loxoceras*" (Pseudactinoceratidae) iz nizhnego karbona tsentral'noi Rossii: mikrostruktura, taksonomicheskoe znachenie i funktsional'naya interpretatsiya (Siphuncle of "*Loxoceras*" (Pseudactino-

← **Figure 1.** *Treptoceras yokoyamai* (Kobayashi). **1**, **3–7**, UMUT PM 27827. **1**, dorsal view, × 2; **3**, dorsoventral thin section, venter on right, × 8; **4**, details of apical siphuncle, × 30; **5**, details of adoral siphuncle, × 30; **6**, details of endosiphuncular deposits, × 50; **7**, details of adoral septal neck, × 50. **2**. UMUT PM 27828, septal view of adoral end, venter down, silicon rubber replica, × 4. **8**. UMUT PM 0687, dorsoventral polished section, venter on right, × 5.5. Abbreviations: **cr**, connecting ring; **ed**, endosiphuncular deposits; **sn**, septal neck.

ceratidae) from the Lower Carboniferous of Central Russia: Ultrastructure, Phylogenetic implication and functional morphology). p. 271-287. *In*, Rozanov A. Yu. and Shevyrev A. A. *eds.*, *Iskopaemye Tsefalopody: Noveishie Dostizhenii' v Ikh Izuchenii* (*Fossil Cephalopods: Recent Advances in their Study*), Rossiiskaya Akademiya Nauk Paleontologicheskii Institut, Moscow. (*in Russian with English abstract*)

Flower, R. H., 1942: An arctic cephalopod faunule from the Cynthiana of Kentucky. *Bulletins of American Paleontology*, vol. 27, p. 1-50, pls. 1-4.

Flower, R. H., 1955: New Chazyan orthocones. *Journal of Paleontology*, vol. 29, p. 806-830, pls. 77-81.

Flower, R. H., 1962: Part 2. Notes on the Michelinoceratida. *New Mexico Bureau of Mines and Mineral Resources, Memoir 10*, part 2, p. 19-42, pls. 1-6.

Foerste, A. F., 1921: Notes on Arctic Ordovician and Silurian cephalopods. *Denison University Bulletin, Journal of the Scientific Laboratories*, vol. 19, p. 247-306, pls. 27-35.

Frey, R. C., 1988: Paleoecology of *Treptoceras duseri* (Michelinoceratida, Proteoceratidae) from Late Ordovician of southwestern Ohio. *New Mexico Bureau of Mines and Mineral Resources, Memoir 44*, p. 79-101.

Hall, J. and Whitfield, R. P., 1875: Section 1. Descriptions of invertebrate fossils, mainly from the Silurian System. Fossils of the Hudson River Groups. (Cincinnati Formations). *Geological Survey of Ohio*, vol. 2, part 2, p. 65-110, pls. 1-4.

Hyatt, A., 1883-1884: Genera of fossil cephalopods. *Proceedings of the Boston Society of Natural History*, vol. 22, p. 253-272 [1883], 273-338 [1884].

Kobayashi, T., 1927: Ordovician fossils from Corea and South Manchuria. *Japanese Journal of Geology and Geography*, vol. 5, p. 173-212, pls. 18-22.

Kobayashi, T., 1934: The Cambro-Ordovician formations and faunas of South Chosen. Palaeontology. Part 1. Middle Ordovician faunas. *Journal of the Faculty of Science, Imperial University of Tokyo, Section 2*, vol. 3, p. 329-519, pls. 1-44.

Kobayashi, T., 1966: The Cambro-Ordovician formations and faunas of South Korea. Part 10. Stratigraphy of the Chosen Group in Korea and South Manchuria and its relation to the Cambro-Ordovician formations of other areas. Section A. The Chosen Group of South Korea. *Journal of the Faculty of Science, University of Tokyo, Section 2*, vol. 16, p. 1-84.

Lee, H. Y., 1977: Conodonten aus den Jigunsan- und den Duwibong-Schichten (Mittelordovizium) von Kangweon-Do, Südkorea. *The Journal of the Geological Society of Korea*, vol. 13, p. 121-150.

Lee, H. Y., 1980: Lower Palaeozoic conodonts in South Korea. *In*, Kobayashi, T. *et al. eds.*, *Geology and Paleontology of Southeast Asia*, vol. 21, p. 1-9, pls. 1, 2. University of Tokyo Press, Tokyo.

M'Coy, F., 1844: *A Synopsis of the Characters of the Carboniferous Limestone Fossils of Ireland*, 274 p. Privately published. (reissued by Williams and Norgate, London, 1862)

Niko, S., 1998: *Kobayashiceras gifuense*, a new actinocerid cephalopod from the Lower Devonian of Japan. *Journal of Paleontology*, vol. 72, p. 36-38.

Ruedemann, R., 1906: Cephalopoda of the Beekmantown and Chazy Formations of the Champlain Basin. *New York State Museum, Bulletin 90*, p. 393-611.

Stokes, C., 1840: On some species of Orthocerata. *Transactions of the Geological Society of London, Ser. 2*, vol. 5, p. 705-714, pls. 59, 60.

Sweet, W. C., 1964: Nautiloidea-Orthocerida. p. K216-K261. *In*, Moore, R. C. *ed.*, *Treatise on Invertebrate Paleontology*. The Geological Society of America, New York and the University of Kansas Press, Lawrence, Kansas.

Teichert, C., 1933: Der Bau der actinoceroiden Cephalopoden. *Palaeontographica, Abteilung A*, vol. 78, p. 111-230, pls. 8-15.

Yamanari, F., 1926: Scale structure in Kogendo. *Geographical Review of Japan*, vol. 2, p. 572-590. (*in Japanese*)

Yun, C. S., 1999: Ordovician cephalopods from the Maggol Formation of Korea. *Paleontological Research*, vol. 3, p. 202-221.

Zittel, K. A. von, 1900: *Text-book of Paleontology* (translated and edited by Eastman, C. R.), vol. 1, 706 p., Macmillan and Co., Limited, London, New York.

The Palaeontological Society of Japan has revitalized its journal. Now entitled **Paleontological Research,** and published in English, its scope and aims have entirely been redefined. The journal now accepts and publishes any international manuscript meeting the Society's scientific and editorial standards. In keeping with the journal's new target audience the Society has established a new category of membership (**Subscribing Membership**) which, hopefully, will be especially attractive to new and existing overseas members. The Society looks forward to receiving your applications. Thank you.

APPLICATION FOR OVERSEAS MEMBERSHIP TO THE PALAEONTOLOGICAL SOCIETY OF JAPAN

1. NAME: _____
   Last (Surname) First (Given name) Middle Initial
2. POSTAL ADDRESS: _____
   _____
   _____
3. TELEPHONE AND FAX (please include country code if known):
   TEL _____
   FAX _____
   country code area code number
4. E-MAIL: _____
5. MEMBERSHIP CATEGORY (please check one):
   ☐**Full Member** receives four issues of **Paleontological Research** ····· **8,500 JP Yen**
   and two issues of **Kaseki** (a Japanese language journal of paleontology)
   in a year and all privileges of the Society including voting rights and
   conference programs
   ☐**Subscribing Member of PR** receives four issues of ····· **6,000 JP Yen**
   Paleontological Reasearch in a year (Current JP Yen is 0.008 U.S. $)
6. METHOD OF PAYMENT (Please check one box):
   ☐I enclose a bank draft made payable to the PSJ.
   ☐I will remit/have remitted the above amount on_____JP Yen through my bank to the account of JPS, a/c #062-0211501, The Bank of Tokyo-Mitsubishi, Kasuga-cho Branch, Tokyo.
   ☐I agree to pay the amount of_____JP Yen by my credit card.
   ☐Master ☐VISA ☐American Express
   ☐Diners Club ☐Access ☐Euro
   Card Account Number ☐☐☐☐ ☐☐☐☐ ☐☐☐☐ ☐☐☐☐
   Signature (required) _____ Card Expiration _____
7. SIGNATURE _____ DATE _____
8. MAIL TO: Palaeontological Society of Japan
   c/o Business Center for Academic Societies, Japan
   5-16-9 Honkomagome, Bunkyo-ku, Tokyo, 113-8622 Japan

A GUIDE FOR PREPARING MANUSCRIPTS

PALEONTOLOGICAL RESEARCH is decicated to serving the international community through the dissemination of knowledge in all areas of paleontological research. The journal publishes original and unpublished articles, normally not exceeding 24 pages, and short notes, normally less than 4 pages, without abstract. Manuscripts submitted are subject to review and editing by reviewers and a language editor. Manuscripts accepted for publication will generally be published in order of submission. Authors submit three copies of their manuscript to: Dr. Kazushige Tanabe, Editor of Paleontological Research, Department of Earth and Planetary Science, University of Tokyo, Hongo 7-3-1, Tokyo 113-0033, Japan. After review, two copies of the revised manuscript are to be returned for copy editing.

Text: Paleontological Research is intended to be read by an international audience, therefore it is particularly critical that language be clear and concise. Manuscripts should be written in English. Either British or American usage style is acceptable. The editors strongly recommend the author(s) whose mother language is not English to ask critical reading and stylistic corrections of the manuscript before submission by specialist(s) who are familiar with English. Use SI (Systeme International d' Unités) units wherever possible.

Text should be typed always in double space on one side of white paper of not less than either 210×280 mm (A4 size) or 8 1/2×11 inches in the following order.

Cover sheet. Cover sheet should contain (1) full name, address, phone and fax numbers, and e-mail address of the author taking responsibility for the galley proofs, (2) running title composed of less than 40 characters, and (3) the numbers of tables and figures.

Title page. Title of the paper, names of authors and their professional affiliations with postal and e-mail addresses (or residential address, if an author is unaffiliated). Tities are to be brief and simple. Spell out one or more of the authors' first names.

Abstract. Abstract should be a condensation and concentration of the essential qualities of the paper. All the papers, excluding Short Notes, are to be accompanied by an abstract not exceeding 500 words. New taxonomic or stratigraphic names should be mentioned in the abstract.

Key words. Select keywords (not more than six words or phrases) which identify the most important subjects covered by the paper and arrange them in alphabetical order.

Main text. Use three or fewer levels of heading. No footnotes are to be used. Bibliographical references are to be identified by citing the authors' names, followed, in parentheses, by the date of publication, with a page number if desired. All citations must have a corresponding entry in the reference list. Acknowledgments should be placed at the end of the text, before References. Do not use honorifies such as Dr., Prof., Mrs., etc. Footnotes should be avoided. Stratigraphic nomenclature must follow the International Stratigraphic Guide.

The typical format for arrangement of systematic paleontology can be learned from current issues of the Journal. All descriptions of new taxa must include a diagnosis, and, as appropriate, stratigraphic and geographic indications, designation of a type or types, depository information, and specification of illustrations. In synonymies use an abbreviated form of the reference, consisting only of authors of reference, date of publication, and number of pages, plates, figures and text-figures referring to the organism or organisms in question.

References. Heading for the bibliography can be "References." Entries are to be listed alphabetically. No abbreviations will be used in article and book titles. Journal titles are written out, not abbreviated. Series, volume, and number or part are to be given, with the appropriate word abbreviated in each case("ser.", "vol.", etc.; see the examples).

Illustrations. All illustrations, including maps, geologic sections, and half-tone illustrations (including "plates") are to be called figures and must be numbered in the same sequence as they are first cited in the text. Citations of illustrations in the text are to be spelled out in full (e. g., Figure 2 or Figure 2.1). Figure captions are to be typed separately. Plan the illustrations so that they take up either the entire width of the printed page (170 mm) or the width of one column (80 mm). Originals should not be smaller than the final intended size for printing. No foldouts will be accepted. Mark all originals clearly with authors' names and figure number. Photographs of all specimens except sections must be illuminated from the upper left side, as is conventional.

Manuscripts on disk. Authors are encouraged to deliver final, revised manuscript copy on disk, but disks should be sent only after the paper has been accepted. 3.5 inch disk with the RTF file (not the text file) written by a recent version of Word Perfect or Microsoft Word (ver. 5.1 or higher) for Windows 3.1 or higher, or Mac OS is acceptable. Be sure to specify, in a covering note, the hardware and the word-processing package used.

Galley proofs and offprints. Galley proofs will be sent to authors about one month before the expected publication date and should be returned to the editors within 3 days of receipt. The authors are responsible for reading the first galley proof. Minor changes submitted by the author will be permitted while a paper is in galleys, but a charge will be made for substantial alterations.

The authors receive 50 free of charge offprints without covers. Additional copies and covers can be purchased and should be ordered when the proofs are returned.

Charges. If a paper exceeds 24 printed pages, payment of page charges for the extra pages is a prerequisite for acceptance. Illustrations in color can also be published at the authors' expense. For either case, the editors will provide infomation about current page charges.

Return of published figures. The manuscripts of the papers published will not be returned to the authors. However, figures will be returned upon request by the authors after the paper has been published.

Ager, D. V., 1963: *Principles of Paleoecology*, 371p. McGraw-Hill Co., New York.

Barron, J. A., 1983: Latest Oligocene through early Middle Miocene diatom biostratigraphy of the eastern tropical Pacific. *Marine Micropaleontology*, vol. 7, p. 487-515.

Barron, J. A., 1989: Lower Miocene to Quaternary diatom biostratigraphy of Leg 57, off northeastern Japan, Deep Sea Drilling Project. *In*, Scientific Party, *Initial Reports of the Deep Sea Drilling Project*, vols. 56 and 57, p. 641-685. U. S. Govt. Printing Office, Washington, D. C.

Burckle, L. H., 1978: Marine diatoms. *In*, Haq, B. U. and Boersma, A. *eds., Introduction to Marine Micropaleontology*, p. 245-266. Elsevier, New York.

Fenner, J. and Mikkelsen, N., 1990: Eocene-Oligocene diatoms in the westem Indian Ocean: Taxonomy, stratigraphy, and paleoecology. *In*, Duncan, R. A., Backman, J., Peterson, L. C., *et al., eds.Proceedings of the Ocean Drilling Program, Scientific Results*, vol. 115, p. 433-463. College Station, TX (Ocean Drilling Program).

Kuramoto, S., 1996: Geophysical investigation for methane hydrates and the significance of BSR. *Journal of the Geological Society of Japan*, vol. 11, p. 951-958. (*in Japanese with English abstract*)

Zakharov, Yu. D., 1974: Novaya nakhodka chelyustnogo apparata ammonoidey (A new find of an ammonoid jaw apparatus). *Paleontologicheskii Zhurnal* 1974, p. 127-129. (*in Russian*)

行 事 予 定

◎2002年年会・総会は2002年6月21日（金），22日（土），23日（日）の3日間にわたり福井県立恐竜博物館（福井県勝山市）で開催されます．6月21日（金）には国際シンポジウム「環日本海地域における白亜系層序と国際対比 —手取層群を中心として—： 世話人，平野弘道・長谷川卓・佐野晋一・東洋一」が開催されます．また，総会と懇親会はシンポジウムに続いて開催します．一般講演の申し込み締切は2002年5月7日（火）です．

◎第152回例会は2003年1月25日（土），26日（日）に横浜国立大学教育人間科学部にて開催の予定です．

◎第153回例会を含め，これ以後の例会は熊本県天草御所浦の白亜紀資料館から開催申し込みがありました．

◎古生物学会では，小人数で実施されるワークショップやショートコースを主催しております．学会から金銭を含む援助を行うことができますので，企画をお持ちの方は行事係りまでお問い合わせ下さい．

個人講演・シンポジウム案の申し込み方法

個人講演の申し込みは予稿原稿を下記まで直接お送り下さい．E-mail やファックスでの申し込みは原則として受け付けておりません．また行事全般に関するお問い合わせも行事係か行事係幹事までお寄せください．

〒305-8571 つくば市天王台 1-1-1
筑波大学地球科学系（古生物学会行事係）
小笠原 憲四郎
Tel: 0298-53-4302（直通） Fax: 0298-51-9764
E-mail: ogasawar@arsia.geo.tsukuba.ac.jp

本山 功（行事係幹事）
〒305-8571 つくば市天王台 1-1-1
筑波大学地球科学系
Tel: 0298-53-4212（居室）or 53-4465（実験室） Fax: 0298-51-9764
E-mail: isaomoto@sakura.cc.tsukuba.ac.jp

本誌の発行に要する費用は，会員の会費以外に，賛助会員からの会費が当てられています．現在の賛助会員は下記の通りです．

神奈川県立生命の星・地球博物館　北九州市立自然史博物館　国際石油開発株式会社
石油資源開発株式会社　帝国石油株式会社　兵庫県立人と自然の博物館
ミュージアムパーク茨城県自然博物館　(アイウエオ順)

2002年4月25日　印　刷
2002年4月28日　発　行
ISSN　1342-8144
Paleontological Research
第6巻，第1号
2,500円

発 行 者　日本古生物学会
〒113-8622 東京都文京区本駒込5-16-9
日本学会事務センター内
電話 03-5814-5801
編 集 者　棚部一成・加瀬友喜
編集幹事　遠藤一佳・重田康成・佐々木猛智
印 刷 者　学術図書印刷株式会社　富田 潔
〒176-0012 東京都練馬区豊玉北2の13の1
電話 03-3991-3754

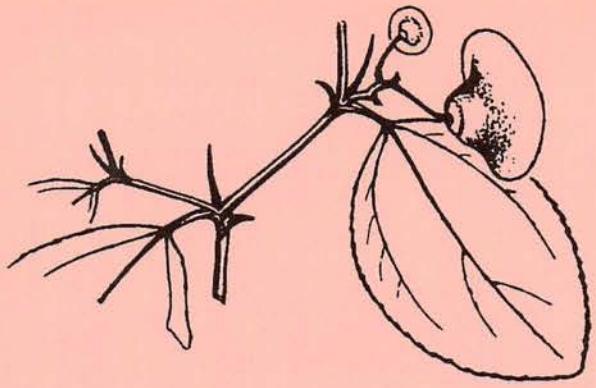

ISSN 1342-8144

Paleontological Research

Vol. 6, No. 1 April 30, 2002

CONTENTS

ARTICLES

SHORT NOTES